Lincoln University
Te Whare Wānaka o Aoraki
CHRISTCHURCH•NEW ZEALAND

Lincoln University Digital Thesis

Copyright Statement

The digital copy of this thesis is protected by the Copyright Act 1994 (New Zealand).

This thesis may be consulted by you, provided you comply with the provisions of the Act and the following conditions of use:

- you will use the copy only for the purposes of research or private study
- you will recognise the author's right to be identified as the author of the thesis and due acknowledgement will be made to the author where appropriate
- you will obtain the author's permission before publishing any material from the thesis.

Mitigating N_2O emissions from pasture soils by optimising irrigation scheduling based on relative gas diffusivity.

A thesis

submitted in partial fulfilment

of the requirements for the Degree of

Doctor of Philosophy

at

Lincoln University

by

Camille Rousset

Lincoln University

2021

Abstract

Mitigating N_2O emissions from pasture soils by optimising irrigation scheduling based on relative gas diffusivity.

By
Camille Rousset

It is projected that the World's average temperature could rise by 0.2 ^oC over each of the next two decades, and by 1.1 up to 6.4 ^oC this century. Grazed pasture irrigation practices play a vital role in meeting the global food demand of a growing population, are keys for the efficient use of water, and conjointly, could be used to meet the climate change targets by decreasing greenhouse gas emissions levels. Grazed pasture systems are a significant source of nitrous oxide (N_2O), a potent greenhouse gas and ozone-depleting-substance. In pastures, N_2O emissions are driven by changes in soil inorganic-N substrate supply following urine and/or fertiliser inputs. Increasing soil moisture as a result of irrigation and rainfall events potentially increases N_2O production via nitrifier-denitrification and denitrification, since these are hypoxic and anaerobic processes, respectively, and increasing soil moisture reduces oxygen (O_2) supply.

Net surface emissions rely on subsurface gas transfer which is controlled mainly by diffusion. Soil relative gas diffusivity (D_p/D_o) is the predominant parameter that describes O_2 transport in soils and has been shown to be a promising integrator of soil physical conditions to better understand and mitigate N_2O emissions. The value of D_p/D_o is a function of the soil air content and gaseous phase tortuosity, both of which vary with soil physical properties including soil texture, soil structure and water content.

Abstract

The principal outcomes of this project were:

- The confirmation that D_p/D_o can be used as a useful measure to predict soil physical conditions where N_2O emissions occur and that recent observations of a critical diffusivity window under 0.02, and especially close to 0.006, need to be avoided when managing pastures if excessive N_2O emissions are to be prevented.
- Soil texture and structure were shown to have an effect on drainage rate which in turn directly affected D_p/D_o, and thus N_2O emissions following irrigation events.
- Optimised irrigation minimised soil anaerobic conditions when compared to standard irrigation, identified through higher soil D_p/D_o, which, in turn, was shown to increase plant growth and N uptake in a lysimeter study.
- Lower N_2O emissions were also measured under optimised irrigation in field trials, but conversely, higher emissions were observed in the lysimeter study with optimal irrigation. It was hypothesised that this may have resulted from the "Birch effect" being enhanced due to rewetting after extended drying periods (reduced in the standard irrigation) that in turn could promote hypoxia and N_2O generating processes.

The first laboratory experiment (Chapter III) examined the consistency of D_p/D_o across different soil types to predict peaks of N_2O emissions. It was hypothesised that regardless of soil type, the N_2O emissions would peak at the previously reported D_p/D_o value of 0.006. Increasing soil bulk density and soil matric potential caused D_p/D_o to decline. As D_p/D_o declined to a value of 0.006 N_2O fluxes increased, peaking at a D_p/D_o value of ≤ 0.006. This experiment shows that the elevation of N_2O fluxes as a D_p/D_o threshold of 0.006 is approached, holds across soil types. However, the variability in the magnitude of the N_2O flux as D_p/D_o declines is not explained by D_p/D_o and is likely to be dependent on factors affecting the N_2O:(N_2O+N_2) ratio.

Abstract

In Chapter IV, the effect of successive wetting-drainage cycles on both D_p/D_o dynamics and associated N_2O and N_2 emissions in two soils; a pallic silt loam and an allophanic sandy-silt, with the later also having a higher organic matter content was determined. For both soils each wetting-drainage cycle induced N_2O fluxes but with 5-fold lower fluxes in the allophanic soil. Greater aggregation and sand content in the allophanic soil generated higher porosity and D_p/D_o values that were almost always greater than recognised anaerobic limits ($D_p/D_o < 0.02$). While wetting-drainage events induce N_2O emissions by altering D_p/D_o and the soil aeration status, the drainage of soils, especially soils high in organic matter, may enhance O_2 demand generating anaerobic zones conducive to denitrification. Low N_2 emissions were potentially due to pH and high nitrate concentration effects in the pallic soil.

Chapter V evaluated the potential for managing soil N_2O emissions by altering irrigation timing based upon modelled D_p/D_o using repacked lysimeters, sown with perennial ryegrass (*Lolium perenne*), that received either a standard irrigation treatment (15 mm every three days), or an optimised irrigation treatment where irrigation was applied when soil D_p/D_o was 0.085 (equivalent to 50% of plant available water) and top up below $D_p/D_o = 0.02$ (based on the previous results). Emission factors over the first 39 days of the experiment for optimised and standard irrigation treatments with urine were 1.26 and 0.12%, respectively, with an increase of N_2O emissions in the optimised irrigation possibly due to the "Birch effect". Cumulative pasture dry matter production and N uptake were higher in the optimised irrigation treatment. Macropores flow of urine derived N was lower under optimised irrigation.

Finally, Chapter VI re-evaluated the effect of irrigation scheduling (standard and optimised), using soil gas diffusivity as a decision tool to mitigate N_2O emissions, in the field using automatic chambers. The optimised irrigation treatment was favoured as there was a significant decrease in cumulative N_2O emissions compared to the standard irrigation. Despite growth

rates lower than the summer average for fertilised irrigated pastures, dry matter production for both irrigation treatments with urine were not significantly different.

It was concluded that D_p/D_o appears to be a relevant parameter to predict N_2O emissions and future implementation into models is conceivable. Moreover, this study demonstrates the need to adjust irrigation cycles to prevent excessive drying of the soil profile between water events while anticipating the rain events and keeping $D_p/D_o > 0.02$. Further detailed studies are needed to: (i) examine the interaction between soil structure and soil organic matter content and their effect on N_2O emissions under wetting-drainage events, with measures of soil O_2 (ii) consider avoiding intra-aggregate disruption through irrigation management which might minimise the Birch effect while also helping to minimise N_2O emissions through reducing the increase of C supply for denitrifiers.

Keywords: nitrous oxide, ruminant urine, soil bulk density, relative gas diffusivity (measured and modelled), water-filled pore space, irrigation frequency, plant N uptake and inorganic-N leaching.

This project (number SOW14-GPLER-SP198-LIN) was funded by the New Zealand Fund for Global Partnerships in Livestock Emissions Research (GPLER), an international research fund set up by the New Zealand Government in support of the Global Research Alliance on Agricultural Greenhouse Gases (GRA).

Graphical abstract with D_p/D_o values based on the field experiments (Chapter VI).

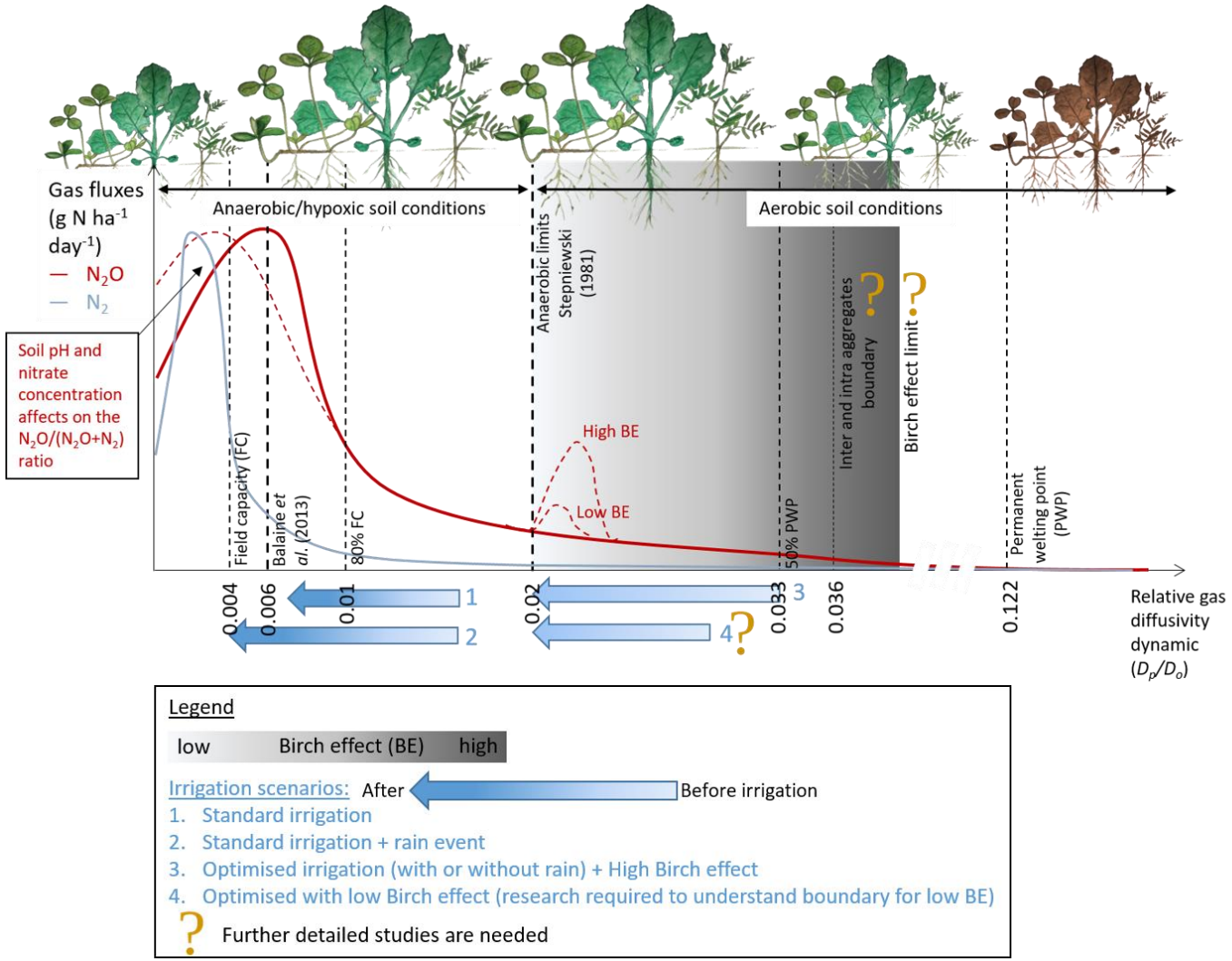

Acknowledgements

Thank you first and foremost to my main supervisor, Professor Tim Clough, for his guidance throughout this PhD. I am really grateful for all the time he spent mentoring me through these three intense years, for all his advice, his generous sharing of scientific and technical knowledge, his support, and his patience. It was my pleasure to work with Tim and I admire him greatly. Thanks Tim for making my PhD experience a rewarding journey.

I would also like to thank my co-supervisors, Dr David Rowlings and Dr Clemens Scheer, for their time, spent on Skype, to discuss concepts and experimental design details but also for their writing suggestions on my papers and their tremendous help on the automatic chamber experiments. Their visits to the experiment site location at Lincoln University were always fruitful for my progress. Thanks to Dr. Henry Chau for his guidance on the irrigation practices and Dr. Jim Moir who was my proof-reader during this PhD.

I appreciate the help of Prof. Peter Grace for his efforts to secure funding for this project. Consequently, I would like to thank the primary financial supporter for this PhD, the New Zealand Fund for Global Partnerships in Livestock Emissions Research (GPLER), an international research fund set up by the New Zealand Government in support of the Global Research Alliance on Agricultural Greenhouse Gases (GRA).

I also owe a special thanks to all of the technical and analytical staff at Lincoln University, namely, the "2nd floor crew", Neil Smith and Trevor Hendry who helped make all of this work possible. I would like to specifically thank the incredible secretary of the Soil and Physical Sciences Department, Amal Torky, for all her administration help, friendship and cooking! A special thanks also goes to Roger Cresswell, manager of the technical team in the department,

who, as well as excelling in the laboratory, is also a legendary friend and a fantastic mountain biking buddy.

This PhD would not have been successful without the continuous support from my friends and my family's love and support, which is by far the best I could wish to have. To my kiwi buddies, non-kiwis buddies (Brazilian, American, French, Colombian, Scottish, Mexican, Chinese, Japanese, Indian, Swedish, German and Danish, to name a few) living on the Māori land, and to Marie, Cyprien and Victor who crossed the globe to visit me, thanks for all the epic adventures (short and long, dangerous and harmless) spent in your company which helped me maintain my sanity while writing this thesis. I am “enchantée” and lucky to have met and have in my life such wonderful people.

Camille

Contents

ABSTRACT I

ACKNOWLEDGEMENTS VI

CONTENTS VIII

LIST OF TABLES XII

LIST OF FIGURES XIV

LIST OF ABBREVIATIONS XXVI

CHAPTER I INTRODUCTION 1

I.1 Background and research objectives 1

I.2 Thesis structure 3

CHAPTER II LITERATURE REVIEW 5

II.1 Nitrous oxide, an environmental and agronomic issue 6
- II.1.1 Brief History 6
- II.1.2 Nitrous oxide, a major threat to the planet with a focus on New Zealand emissions 8
- II.1.3 Sources and impacts of N_2O on the agrosystem 10

II.2 The processes responsible for N_2O emissions from soil 16
- II.2.1 An overview on the N cycle in the soil 16
- II.2.2 Denitrification 19
  - II.2.2.a Nitrogen substrates influence on the denitrification rate 20
  - II.2.2.b Carbon and other factors influence on the denitrification rate 21
- II.2.3 Nitrification 23
  - II.2.3.a Nitrogen substrates influence on nitrification and N_2O emissions through nitrifier denitrification 27
  - II.2.3.b Other factors affecting nitrification rate 28
- II.2.4 Coupled nitrification-denitrification 29
- II.2.5 DNRA-denitrification 30
- II.2.6 Chemodenitrification 31

II.3 The balance between saturation and aeration in the soil and its impact on N_2O production pathways 34
- II.3.1 Soil aeration and water content, and their effects on N_2O emissions 35
- II.3.2 How useful is WFPS for predicting N_2O emissions? 38
- II.3.3 A promising indicator: D_p/D_o 41

II.3.4 Physical and mechanical soil characteristics affecting water content and O_2 diffusion in the soil 46

II.4 Irrigation systems; an option to reduce agricultural N_2O emissions? 48
II.4.1 World's need for irrigation 48
II.4.2 Impacts of irrigation systems on N_2O emissions 49
II.4.3 Development opportunities to reduce N_2O production from agriculture with a focus on irrigation management 52

II.5 Scope of this thesis 56

CHAPTER III SOIL TYPE, BULK DENSITY AND DRAINAGE EFFECTS ON RELATIVE GAS DIFFUSIVITY AND N_2O EMISSIONS 58

III.1 Abstract 59

III.2 Introduction 60

III.3 Materials and methods 63
III.3.1 Soil collection and experimental design 63
III.3.2 Nitrous oxide and relative gas diffusivity measurements 67
III.3.3 Soil analyses 71
III.3.4 Statistical analyses 72

III.4 Results 73
III.4.1 Soil chemical and physical properties 73
III.4.2 Soil N_2O fluxes and relationships with soil physical parameters 80

III.5 Discussion 85
III.5.1 Soil chemical and physical characteristics 85
III.5.2 Soil N_2O Fluxes and relationships with soil physical parameters 86

III.6 Conclusion 88

CHAPTER IV **:** SOIL WETTING AND DRAINAGE CYCLES: EFFECTS ON RELATIVE GAS DIFFUSIVITY, N_2O EMISSIONS AND DENITRIFICATION RATE 90

IV.1 Abstract 90

IV.2 Introduction 92

IV.3 Materials and Methods 94
IV.3.1 Soil collection, Experimental Design, and Setup 94
IV.3.2 Determination of D_p/D_o, N_2O and N_2 fluxes. 97
IV.3.3 Destructive soil analyses 100
IV.3.4 Statistical analyses 101

IV.4 Results 102
IV.4.1 Soil physical conditions 102
IV.4.2 N_2O and N_2 emission trends during the two cycles 108

IV.5 Discussion 119

IV.6 Synthesis of the data from the previous two chapters 126

CHAPTER V CAN PASTURE IRRIGATION BE SCHEDULED USING SOIL GAS DIFFUSIVITY: IMPLICATIONS FOR URINARY-N DERIVED N_2O FLUXES, LEACHING AND PLANT N UPTAKE. 130

V.1 Abstract 131

V.2 Introduction 132

V.3 Materials and methods 135
V.3.1 Lysimeter design 135
V.3.2 Experimental design 137
V.3.3 Nitrous oxide fluxes 141
V.3.4 Soil, pasture biomass, root biomass, leachate sampling and ^{15}N recovery 142
V.3.5 Statistical analyses 146

V.4 Results 147
V.4.1 Soil water content and gas diffusivity 147
V.4.2 N_2O fluxes 149
V.4.3 Root characteristic, dry matter production and N uptake 152
V.4.4 Drainage and inorganic-N leaching 156
V.4.5 Soil pH, DOC and inorganic-N concentrations 159

V.5 Discussion 161

V.6 Conclusion 166

CHAPTER VI EFFECT OF IRRIGATION SCHEDULING, USING SOIL GAS DIFFUSIVITY AS A DECISION TOOL TO MITIGATE N_2O EMISSIONS FROM A URINE-AFFECTED PASTURE (2 FIELD TRIALS) 167

VI.1 Abstract 169

VI.2 Introduction 170

VI.3 Materials & methods 173
VI.3.1 Experimental site 173
VI.3.2 Experimental design 174
VI.3.2.a Field trial 1 174
VI.3.2.b Field trial 2 177
VI.3.3 Sample collection and analysis 178
VI.3.3.a Automatic chambers for N_2O fluxes 178
VI.3.3.b Pasture biomass and soil samples 181
VI.3.4 Statistical analyses 183

VI.4 Results 184
VI.4.1 Rainfall, soil temperature and irrigation cycles 184
VI.4.1.a Field trial 1 184

VI.4.1.b Field trial 2 186
VI.4.2 Soil water content and gas diffusivity evolution 188
VI.4.2.a Field trial 1 188
VI.4.2.b Field trial 2 191
VI.4.3 Dry matter production, inorganic-N, DOC and N_2O fluxes 194
VI.4.3.a Field trial 1 194
VI.4.3.b Field trial 2 198

VI.5 Discussion 204
VI.5.1 Field trial 1 204
VI.5.2 Field trial 2 208
VI.5.3 Conclusion 210

CHAPTER VII CONCLUSION 211

VII.1 The current problematic 211

VII.2 Summary of findings and conclusion 213

VII.3 The next steps to improving our knowledge on N_2O production in soils and future direction for irrigation management 216

APPENDICES 219

REFERENCES 223

List of Tables

Table 1 New Zealand's gross emissions by gas in 1990 and 2017 (Ministry for the Environment 2018) 10

Table 2: Soil (0-10 cm) texture, particle density and carbon contents. Texture analyses were performed using a laser diffraction particle analyser (Mastersizer 3000, Malvern Panalytical) 65

Table 3: Results of the general accuracy and tendency test comparing WLR-Marshall model and Moldrup et al. (2013) SWLR model for Wakanui and Otorohanga soils. 99

Table 4: Soil pH, dissolved organic carbon (DOC), ammonium-N (NH_4^+-N) and nitrate-N (NO_3^--N) concentrations at destructive sampling times. Days 12 and 25 are at the end of the first and second drainage cycles, respectively. 104

Table 5: Soil (0-10 cm) characteristics before urine application. Texture analyses were performed using a laser diffraction particle analyser (mastersizer 3000, Malvern Panalytical). IUSS stand for International Union of Soil Science (clay 0-2 µm, silt 2-63 µm, and sand 63-2000 µm). 136

Table 6: ^{15}N recovery (%) among the herbage, leachate and soil. Values are means (n = 4) at the end of the experiment and errors are standard error of the mean (s.e.m). 155

Table 7: Mass of inorganic-N collected in the leachates and concentration of inorganic-N at collection time for both NO_3^--N and NH_4^+-N. Values are means (n = 4) and errors are standard error of the mean (s.e.m). 158

Table 8: Field trial 1 concentration of inorganic-N for both NO_3^--N and NH_4^+-N and dissolved organic carbon measured in the soil (0–7.5 cm) per treatments. Values are means (n=3) and errors are standard error of the mean (s.e.m) 196

List of tables

Table 9: Field trial 2 concentration of inorganic-N for both NO_3^--N and NH_4^+-N and dissolved organic carbon (DOC) measured in the soil (0–7.5 cm) per treatments. The values with a pink background were sampled in the spare chambers (2 cores mixed in a zip bag for each / date / chamber). The last line of the table (no pink background) represents the data from the autosampling chamber samples. For the last date, values are means (n=4) and errors are standard error of the mean (s.e.m). 203

List of Figures

Figure 1: From left to right; Joseph Priestley (1733-1804), Humphry Davy (1778-1829) and cartoon of the Horace Wells (1815-1848) tooth extraction with Gardner Quincy Colton (1814-1898) standing in front. (source: Wikipedia) 7

Figure 2: Global natural versus anthropogenic N_2O emissions in 2005. (Davidson and Kanter 2014) 11

Figure 3: The relationship between nitrogen (N) application rate (Nrate, kg N ha^{-1}) and the replicate nitrous oxide (N_2O) fluxes accumulated over 67 days (kg N ha^{-1}). Linear regression yielded N_2O flux = (0.0122 ± 0.0006) * Nrate + 0.8352 ± 0.0626, a statistically significant relationship ($P < 0.05$) accounting for 92% of the variability. 12

Figure 4: Sources of N_2O emissions from agricultural soils, showing the contribution of each source to emissions through both direct and indirect pathways in New Zealand (Ministry for Primary Industries 2020) 14

Figure 5: Figure from Hallin et al. (2018) of "the microbial pathways in the nitrogen (N) cycle. Background colors differentiate between processes occurring under oxic or anoxic conditions. The compounds are positioned according to the oxidation state of N. Solid colored lines indicate microbial pathways, and the genes encoding the respective enzymes that catalyse each step in the pathway are indicated as follows: amo, ammonia monooxygenase; hao, hydroxylamine oxidoreductase; hdh (also known as hzo), hydrazine dehydrogenase; hzs, hydrazine synthase, nar/nap, cytoplasmic and periplasmic dissimilatory nitrate reductases, respectively; nas, assimilatory nitrate reductase; nif, nitrogenase; nas/nirB, assimilatory nitrite reductase; nirS/nirK, cytochrome-cd1 and copper-based dissimilatory nitrite reductases,

respectively; ‘nor’, any of the multi-heme or heme–copper nitric oxide reductases; nosZ, nitrous oxide reductase; nrf, formate-dependent dissimilatory nitrite reductase; nxr, nitrite oxidoreductase. Dotted lines indicate the contributing pathways to atmospheric loading of gaseous nitrogen compounds, whereas dashed gray lines indicate biotic/abiotic processes generating gaseous N compounds that also feed into the overall N-cycle. DNRA, dissimilatory nitrate reduction to ammonium”. 18

Figure 6: Denitrification steps including the different enzymes involved..... 19

Figure 7: Nitrification pathways undertaken by ammonia-oxidizing bacteria (AOB), nitrite oxidizing bacteria (NOB) and comammox bacteria. (Stein 2019) 24

Figure 8: Pathways for N_2O production by AOB and AOA. Reactions with red arrows are catalysed by enzymes and only by AOB. Reactions with blue dashed arrows are abiotic, or biotic via partnering microorganisms, and occur for both AOB and AOA from intermediates produced during active ammonia oxidation. (Stein 2019)..... 26

Figure 9: Likely occurrence of N_2O releasing pathways as a function of substrate type and NO_2^- concentration. Note that the circles are drawn to indicate proximate optimal conditions. Occurrence in soil (microsites) might differ and substrate pools are not uniform. (Wrage-Mönnig et al., 2018)..... 28

Figure 10: “Cause and effects of nitrite- and nitrate-induced (chemo) denitrification-based N_2O formation in coastal marine sediment. When Fe(II) and nitrite/nitrate was added to the marine sediment, Fe(III) was formed among different process by chemodenitrification which is stimulating Fe(III)-reducing bacteria (FeRed). The FeRed bacteria then produce Fe(II) and stimulate Fe(II)-oxidizing bacteria. Therefore chemodenitrification has a significant impact on Fe-cycling in general. Simultaneously, nitrite/nitrate was reduced to NO and further to N_2O by chemodenitrification and denitrifying bacteria. In addition, the presence of high nitrite/nitrate

concentration leads to a high typical nosZ gene expression in denitrifying bacteria which is responsible for the reduction of N_2O into N_2." From Otte et al. (2019) 32

Figure 11: Possible ecological niches for the different microbial processes involved in the N_2O emissions (Wrage et al. 2001) 33

Figure 12: Spatial distribution of N_2O emissions in a field plot experiment (n=36). (Mathieu et al. 2006) 35

Figure 13: Diagram of the two different type of water held in soil pores between or within aggregates (left). Drainage process of water in soil (right) from Chen et al. (2019) 39

Figure 14: Variations in the volume fraction of air and WFPS for soils at different bulk densities. Erratum corrected (2009) from Farquharson and Baldock (2007). 41

Figure 15: Gas diffusivity models: landmarks and their authors. 43

Figure 16: Results obtained by Balaine et al. (2013) showing the relationship of measured N_2O-N flux with water-filled pore space (left) and relative soil gas diffusivity (right) at varying soil ρ_b (Mg m^{-3}). 45

Figure 17: Changes (mean, minimum maximum) in N_2O emissions under irrigation compared with non-irrigated conditions, based on six investigations (Trost et al., 2013). 50

Figure 18: Stoppered bottles used in the pycnometer method to determine particle density (left) and the vacuum chamber setup used to remove the air from the soil and the water (right). ... 64

Figure 19: Tension table setup 66

Figure 20: Gas sampling setup showing soil cores inside gas-tight 1 L jars. 67

Figure 21: Diffusion chambers apparatus made O_2 free containing a soil core and a KE-25 O_2 sensors connected to a datalogger (not present in the picture). 69

Figure 22: Example of ln (Cr) vs time graph plotted to measure the diffusion coefficient (D_p) in the soil cores. The black line was obtained by fitting linear regressions to the data. The linear slope of the line (= – 0.0144) corresponded to $-D_p \alpha_1^2/\varepsilon$ 70

Figure 23: Mean soil pH versus soil matric potential. Numerals in the legend indicate soil bulk density treatments applied (Mg m^{-3}). Error bars = s.e.m, n=4. 74

Figure 24: Mean dissolved organic carbon concentration (mg g–1) versus soil matric potential. Numerals in the legend indicate soil bulk density treatments applied (Mg m^{-3}). Error bars = s.e.m, n = 4. 75

Figure 25: Soil nitrate concentrations versus soil matric potential for the four soils. Numerals in the legend indicate soil bulk density treatments applied (Mg m^{-3}). Error bars = s.e.m, n=4. 76

Figure 26: Water-filled pore space (WFPS, %) versus soil matric potential for the four soils. Numerals in the legend indicate soil bulk density treatments applied (Mg m^{-3}). Error bars = s.e.m, n= 4. 78

Figure 27: Relative gas diffusivity (D_p/D_o) at varying soil bulk density and soil matric potential. Numerals in the legend indicate soil bulk density treatments applied (Mg m^{-3}). Error bars = s.e.m., n= 4. 79

Figure 28: Soil relative gas diffusivity (D_p/D_o) versus soil air-filled porosity (cm^3 cm^{-3}). 80

Figure 29: Relationship between measured N_2O-N fluxes and measured matric potential (-kPa) for each soil separately and at varying soil ρ_b (Mg m^{-3}). Numerals in the legend indicate soil ρ_b treatments applied (Mg m^{-3}). Error bars = s.e.m, n = 4. 81

Figure 30: Relationship between measured N_2O-N fluxes and measured D_p/D_o for each soil separately and at varying soil bulk density. Numerals in the legend indicate soil bulk density treatments applied (Mg m^{-3}). Error bars = s.e.m., n=4. The vertical red lines show the 0.006 threshold from Balaine et al. (2013) 82

Figure 31: Relationship between measured N_2O-N fluxes and WFPS (%) for each soil at varying soil bulk density. Numerals in the legend indicate soil bulk density treatments applied (Mg m^{-3}). Error bars = s.e.m, n = 4. 83

Figure 32: Relationship between measured N_2O-N fluxes and volumetric water content (m^3 m^{-3}) for each soil at varying soil ρ_b (Mg m^{-3}). Numerals in the legend indicate soil ρ_b treatments applied (Mg m^{-3}). Error bars = s.e.m, n= 4. 84

Figure 33: Soil cores saturated with 50 atom% ^{15}N solution just before putting them on the tension tables. 96

Figure 34: Test of two D_p/D_o models against D_p/D_o observed data for Otorohanga soil. SWLR, structure-dependent water induced; WLR, water induced linear reduction; Cm, media complexity factor. The observed D_p/D_o data have been collected in the diffusion chambers and are presented in Chapter II. The black line represents the identity line (y=x). 100

Figure 35: Picture of the Shimadzu TOC analyser used to measure the DOC concentrations from soil extraction samples. Chain loop of the samples on the left picture. 101

Figure 36: Percentage of soil mass passing through sieves at a given particle size for the Wakanui and Otorohanga soils. The black and orange lines were obtained by fitting a polynomial regression to the data. 103

Figure 37: Mean dissolved organic carbon content (DOC) for the Wakanui and Otorohanga soils at the beginning of the experiment (Day 0), after the end of the first wetting-drainage cycle (Day 12) and at the end of the second wetting-drainage cycle (Day 25). Numerals in the legend indicate the soil bulk density treatments applied (Mg m^{-3}). Error bar = s.e.m; n=4. . 105

Figure 38: Mean nitrate (NO_3^-) concentrations for the Wakanui and Otorohanga soils at the beginning of the experiment (Day 0), after the end of the first wetting-drainage cycle (Day 12) and at the end of the second wetting-drainage cycle (Day 25). Numerals in the legend indicate the soil bulk density treatments applied (Mg m-3). Error bar = s.e.m; n=4 106

Figure 39: Soil air content (Ɛ), as a function of relative matric potentials (-kPa) for the Wakanui soil and the Otorohanga soil. Numerals in the legend indicate the soil bulk density treatments applied (Mg m^{-3}). Error bar = s.e.m; n=4. Note the different scales for the y-axis. 107

Figure 40: Soil-gas diffusivity (D_p/D_o), as a function of relative air-filled porosity (ε/Φ) for the Wakanui soil and the Otorohanga soil. Also shown are the previously reported gas diffusivity values for peak N_2O fluxes at D_p/D_o = 0.006 (– – – –; Balaine et al. 2013) and anaerobic conditions D_p/D_o = 0.02 (------; Stepniewski 1981). Numerals in the legend indicate the soil bulk density treatments applied (Mg m^{-3}).Note the different scales for the y-axis.....108

Figure 41: Mean daily N_2O fluxes from soil cores and gas diffusivity (D_p/D_o) over time for the Wakanui soil. The 2 wetting-draining cycles are represented with the first cycle from day 0 to 12 and the second from day 13 to 25. The solid red line represent D_p/D_o = 0.006. Numerals in the legend indicate the soil bulk density treatments applied (Mg m^{-3}). Error bars = s.e.m, n=4. The vertical yellow lines are here to show the days where D_p/D_o = 0.006.....110

Figure 42: Mean daily N_2O fluxes from soil cores and gas diffusivity (D_p/D_o) over time for the Otorohanga soil. The 2 wetting-drainage cycles are represented with the first cycle from day 0 to 12 and the second from day 13 to 25. The solid red line represent D_p/D_o = 0.006. Numerals in the legend indicate the soil bulk density treatments applied (Mg m-3). Error bars = s.e.m, n=4. Note D_p/D_o scale is greater than in Figure 8.....111

Figure 43: Mean daily N_2O fluxes from soil cores and WFPS over time for the Wakanui soil. The 2 wetting-draining cycles are represented with the first cycle from day 0 to 12 and the second from day 13 to 25. Numerals in the legend indicate the soil bulk density treatments applied (Mg m^{-3}). Error bars = s.e.m, n=4. 112

Figure 44: Mean daily N_2O fluxes from soil cores and WFPS over time for the Otorohanga soil. The 2 wetting-draining cycles are represented with the first cycle from day 0 to 12 and the second from day 13 to 25. Numerals in the legend indicate the soil bulk density treatments applied (Mg m^{-3}). Error bars = s.e.m, n=4. 113

Figure 45: Cumulative N_2O fluxes (% of applied N) for days 1, 12 and 24 for the Wakanui soil and the Otorohanga soil. Day 12 was the last day of the 1st cycle and 24 the last day of the 2nd

cycle. Numerals in the legend indicate the soil bulk density treatments applied (Mg m-3). Error bars = s.e.m, n=4. 115

Figure 46: Cumulative N_2O fluxes over time for the Wakanui soil and the Otorohanga soil. Also are shown the 2 saturation events (vertical dashed lines). Numerals in the legend indicate the soil bulk density treatments applied (Mg m^{-3}). Error bars = s.e.m, n=4. 116

Figure 47: Mean daily N_2O ^{15}N enrichment (atom %) over time for the Wakanui soil and the Otorohanga soil. Also are shown the 2 saturation events (vertical dashed lines). Numerals in the legend indicate the soil bulk density treatments applied (Mg m^{-3}). Error bars = s.e.m, n=4. 118

Figure 48: Mean daily N_2 fluxes over time for the Wakanui soil and Otorohanga soil. Also shown are the 2 saturation events (dashed vertical lines). Numerals in the legend indicate the soil bulk density treatments applied (Mg m^{-3}). Error bars = s.e.m, n=4. 119

Figure 49: Data distribution graphs showing the general distribution of N_2O fluxes over gas diffusivity (A) and the density estimates of D_p/D_o for the 4 different soil types (B) and bulk densities (C) in the first lab experiment (Chapter II). The dashed lines represent the 0.006 threshold (Balaine et al. 2013) and 0.02 threshold (Stepniewski 1981). 128

Figure 50: Data distribution graphs showing the general distribution of N_2O fluxes over WFPS (A) and the density estimates of the WFPS for the 4 different soil types (B) and bulk densities (C) in the first lab experiment (Chapter II). 129

Figure 51: A schematic of the lysimeter setup 136

Figure 52: Tim helping out at the farm to collect cow's urine during the milking 138

Figure 53: Diagrammatic soil water response to irrigation events and rainfall with field capacity (solid black line), trigger point (solid red line), permanent wilting point (dashed red line) and 80% of PAW-plant available water (dashed black line). 139

Figure 54: Daily temperatures being measured for the gas sampling period. Urine was applied on day 1 (yellow dashed line), the standard irrigation applications are shown by the blue triangles and the optimised irrigation by the blue highlighted areas. The red highlighted areas show the two periods where both irrigation treatments were withheld. 141

Figure 55: Leachates collected on the 31st of July 2019 (day 14). The darker leachates came from the lysimeters under the standard irrigation treatment. 143

Figure 56: Picture taken during harvesting of ryegrass. 144

Figure 57: Lysimeter soil destructive sampling day (26/09/2019-day 71). Left: whole lysimeters out of PVC cylinder. Top right: incision in the middle to take pH measurements and soil samples. Bottom right: two views from the bottom of lysimeters number 8 (urine on) with few roots and number 9 (urine off) with greater root density. 146

Figure 58: Water-filled pore space (WFPS) dynamics over time for optimised (Opt) and standard (Std) irrigation treatments with urine applied (on) or no urine applied (off). Data points are means of four replicates ± s.e.m. Urine has been applied on day 1 (yellow dashed line), the standard irrigation applications are shown by the blue triangles and the optimised irrigation by the blue highlighted areas. 148

Figure 59: Modelled soil gas diffusivity dynamics over time for optimised (Opt) and standard (Std) irrigation treatments with urine applied (on) or no urine applied (off). Data points are means of four replicates ± s.e.m. Urine has been applied on day 1 (yellow dashed line), the standard irrigation applications are shown by the blue triangles and the optimised irrigation by the blue highlighted areas. The 0.006 red dashed line is based on the study from Balaine et al. (2013). 149

Figure 60: Daily average N_2O-N fluxes over time for optimised (Opt) and standard (Std) irrigation treatments with urine applied (on) or no urine applied (off). Data points are means of

four replicates ± s.e.m. The standard irrigation applications are shown by the blue triangles and the optimised irrigation by the blue highlighted areas. 151

Figure 61: Cumulative average N_2O-N fluxes over time for optimised (Opt) and standard (Std) irrigation treatments with urine applied (on) or no urine applied (off). Data points are means of four replicates ± s.e.m. The standard irrigation applications are shown by the blue triangles and the optimised irrigation by the blue highlighted areas. The red highlighted areas show the two periods where both irrigation treatments were withheld. 152

Figure 62: Cumulative dry biomass collected 12 times over the total period of the experiment for optimised (Opt) and standard (Std) irrigation treatments with urine applied (on) or no urine applied (off). Data points are means of four replicates ± s.e.m. The red highlighted areas show the two periods where both irrigation treatments were withheld. 153

Figure 63: Root biomass (0-5 cm) per treatments at the end of the experiment. 154

Figure 64: pH averages at different depths in the lysimeters (low = 18 cm, middle = 9 cm and top = soil surface) during the destructive sampling (day 71) for optimised (Opt) and standard (Std) irrigation treatments with urine applied (on) or no urine applied (off). The red dashed line represents the pH at the beginning of the experiment before applying urine. Values are means (n = 4) ± s.e.m 159

Figure 65: A schematic of the field trial 1 with the 12 chambers locations randomised per treatments with optimised (Opt) and standard (Std) irrigation treatments with urine applied (on) or no urine applied (off). Photo of the final result on the field taken from the shed is shown on the right corner. 174

Figure 66: Soil cores taken in the field to determine field capacity by saturation method. ... 175

Figure 67: Application of urine in the chamber. The FDR probes is placed in the middle of the chamber to measure the volumetric water content for the subsurface soil (first 10cm) 176

Figure 68: A schematic of the field trial 2 with the 12 chambers locations randomised per treatments with optimised (Opt) and standard (Std) irrigation treatments with urine applied (on) or no urine applied (off). Photo of the final result on the field taken from the side is shown on the right. 178

Figure 69: A twelve chamber sampling sequence. 179

Figure 70: The complete Sampling Unit setup in the shed including the top view of the sample unit. The computer is not present on the picture but was connected to the left of the sample unit. The calibration gas and carrier gas were on the right. 181

Figure 71: Pasture harvest in one chamber (left) and dry biomass weigh taken (right). 182

Figure 72: Soil samples taken on the last day of the experiment for the field trial 2 (left) and the filtering step during the KCL extraction in the lab (right). 183

Figure 73: Daily rainfall (blue bar), potential evapotranspiration (PET; yellow bar) and soil average temperature (black line) of a ryegrass pasture in Lincoln from the 15 November 2018 to 13 December 2018 following ruminant urine application (red bar). Blue and yellow arrows denote standard and optimised irrigation events, respectively. The error bars represent the night and day variations (s.d) 185

Figure 74: Daily rainfall (blue bar), potential evapotranspiration (PET; yellow bar) and soil average temperature (black line) of a ryegrass pasture in Lincoln from the 10 February 2020 to 24 March 2020 following ruminant urine application (red bar). Blue and yellow arrows denote standard and optimised irrigation events, respectively and the dashed blue line the rain simulation (6.7mm) on the 24th March 2020. The error bars represent the night and day variations (s.d) 187

Figure 75: Field trial 1 daily average in situ WFPS (%) from the 15 November 2018 to 13 December 2018 with or without urine and under standard (STD) or optimised (OPT) irrigation.

The data are represented per replicates. The red bar shows the date of the urine application event. Error bars = s.e.m. with n = the number of sample per day per chamber (24). 189

Figure 76: Field trial 1 modelled, daily average soil relative gas diffusivity (D_p/D_o) from the 15 November 2018 to 13 December 2018. The vertical red bar shows the date of the urine application event. Blue and yellow arrows denote the standard (STD) and optimised (OPT) irrigation applications, respectively. Error bars = s.e.m, n=3.The black dashed horizontal line represents 80% FC while diffusivity values are shown by red dotted/dashed lines. 190

Figure 77: Field trial 2 daily average WFPS (%) from the 12/02/2020 to the 24/03/2020. The red bar represents the urine application, blue triangles and yellow horizontal lines denote the standard (Std) and optimised (Opt) irrigation applications, respectively. Error bars = s.e.m, n=4. Treatment with urine applied (on) or no urine applied (off).The blue vertical dashed line on the 22/02/2020 represent the rain event (12.8mm) and the one at the end the rain simulation. 192

Figure 78: Field trial 2 modelled daily average relative gas diffusivity (D_p/D_o) from the 12/02/2020 to the 24/03/2020. The red vertical bar represents the urine application, blue triangles and yellow horizontal lines denote the standard (Std) and optimised (Opt) irrigation applications, respectively. The blue vertical dashed line on the 22/02/2020 represents a major rain event (12.8mm) and the one at the end the rain simulation. Error bars = s.e.m, n=4. Treatment with urine applied (on) or no urine applied (off).....193

Figure 79: Field trial 1 daily N_2O emissions (g N $ha^{-1}day^{-1}$) from the 15/11/2018 to the 13/12/2018 for the four treatments. The red bar represents the urine application, blue arrows and yellow arrow denote the standard (STD) and optimised (OPT) irrigation applications, respectively. Error bars = s.e.m, n=3. 197

Figure 80: Field trial 1 cumulative N_2O emissions (g N ha^{-1}) from the 15/11/2018 to the 13/12/2018 for the four treatments. The red bar represents the date of urine application. Blue

and yellow arrows denote standard (STD) and optimised (OPT) irrigation events, respectively. Error bars = s.e.m, n=3. 198

Figure 81: Field trial 2 dry biomass and cumulative dry biomass collected 3 times over the total period of the experiment for optimised (Opt) and Standard (Std) irrigation treatment with urine applied (on) or no urine applied (off). Data points are means of four replicates ± S.E.M. ...199

Figure 82: Field trial 2 daily N2O emissions (g N ha-1day-1) from the 11/02/2020 to the 25/03/2020. The red bar represents the urine application, blue triangles and yellow horizontal lines denote the standard (STD) and optimised (OPT) irrigation applications, respectively. Error bars = s.e.m, n=4. Treatment with urine applied (on) or no urine applied (off). The blue vertical dashed line on the 22/02/2020 represents a major rain event (12.8mm) and the one at the end the rain simulation. 200

Figure 83: Field trial 2 cumulative N_2O emissions (g N ha^{-1}) from the 11/02/2020 to the 25/03/2020 for the optimised (Opt) and standard (Std) irrigation treatments with urine applied (on) or no urine applied (off). Data points are means of four replicates ± s.e.m. 201

List of abbreviations

AOA	Ammonium-oxidising archaea
AOB	Ammonium-oxidising bacteria
ATP	Adenosine triphosphate
C	Carbon
CH_4	Methane
C_m	Media complexity factor
CO_2	Carbon dioxide
COMMAMOX	Complete ammonia oxidation
DI	Deionised water
DNA	Deoxyribonucleic acid
DNRA	Dissimilatory nitrate reduction to ammonia
D_o	Gas diffusion coefficient in air (cm^3 air s^{-1})
DOC	Dissolved organic content
D_p	Gas diffusion coefficient in soil (cm^3 soil air cm^{-1} soil s^{-1})
D_p/D_o	Relative gas diffusivity
EF	Emission factor
EF	Emission factor (%)
EPA	Environmental pollution agency
Ɛ	Air-filled porosity (cm^3 air cm^{-3} soil)
Fe (II)	Ferrous iron
Fe (III)	Ferric iron
FIA	Flow injection analysis
GHG	Greenhouse gas
HFCs	Hydrofluorocarbons
hv	High voltage
IPCC	Intergovernmental panel on climate change
N	Nitrogen
N_2	Dinitrogen
N_2O	Nitrous oxide
NH_2OH	Hydroxylamine

List of abbreviations

NH_3	Ammonia
NH_4^+	Ammonium
NI	Nitrification inhibitors
NO	Nitric oxide
NO_2^-	Nitrite
NO_3^-	Nitrate
NOB	Nitrite-oxidising bacteria
NO_x	Nitrogen oxides
Nr	Reactive nitrogen
NUE	Nitrogen use efficiency
NZ	New Zealand
O^1D	Excited oxygen atom
O_2	Oxygen
O_3	Ozone
OM	Organic matter
P	P-value
PFCs	Perfluorocarbons
q_d	Diffusivity flux
s.e.m	Standard error mean
s.d	Standard deviation
SF_6	Sulphur hexafluoride
SWLR	Structure-dependent water-induced linear reduction
U.K.	United Kingdom
U.S.	United States
WFPS	Water-filled pore space (%)
WLR	Water-induced linear reduction
θ_g	Gravimetric water content (g water g^{-1} dry soil)
θ_v	Volumetric water content (m^3 water m^{-3} soil)
ρ_b	Soil bulk density (g cm^{-3})
ρ_d	Soil particle density (g cm^{-3})
Φ	Total porosity (m^3 air m^{-3} soil)
ψ	Matric potential (-kPa)

Chapter I Introduction

I.1 Background and research objectives

Nitrous oxide (N_2O) is a potent greenhouse gas (GHG) involved in stratospheric ozone depletion (Ravishankara *et al.* 2009). It is the third most significant GHG after carbon dioxide (CO_2) and methane (CH_4) (Ritchie and Roser 2017). The atmospheric concentration of N_2O has increased since the preindustrial era by 20%, from 271 to 333 ppb in 2020 (NOAA 2020). This is the result of land use and land use change (NOAA 2020). Agriculture accounts for approximately 60% of anthropogenic N_2O emissions because agricultural soils provide an optimal environment for microorganisms involved in the N_2O producing processes, the mineralisation of soil organic matter and because of the high availability of nitrogen (N) substrates resulting from fertilisation of agriculture fields (Thompson *et al.* 2019). An improved understanding of N_2O emission processes and factors influencing these in pastoral soils is vital to develop mitigation strategies and develop accurate prediction models of emissions. The understanding of processes is notoriously difficult since diverse microbial species are capable of generating N_2O via numerous coexisting pathways that each respond differently to various environmental and soil factors. Nitrous oxide emissions are known to be highly variable both spatially and temporally (Butterbach-Bahl *et al.* 2013).

In general, N_2O production and its reduction product, dinitrogen (N_2), and their ratio ($N_2O/(N_2O+N_2)$) depend on: i) Proximal factors, such as N and carbon (C) supply to ensure the presence of acceptor/ donor electrons and the spatial extent of oxygen (O_2) conditions in soil, given that the two major biological pathways involved; nitrification and denitrification, are respectively aerobic and anaerobic pathways, and ii) Distal factors, which can be biological

(microbial community abundance), physical (soil structure, soil texture, water saturation) or chemical (temperature, pH). These distal factors also affect the proximal factors (Groffman *et al.* 1988). Improving field management practices to control these proximal and distal factors has the potential to mitigate N_2O emissions. Numerous studies have demonstrated that N_2O emissions can be reduced by improving application of N fertilisers (suitable rate and timing of application), thus increasing N use efficiency of crops (Eagle *et al.* 2012) or using nitrification inhibitors (Ruser and Schulz 2015). In addition, Eagle *et al.* (2012) reviewed several studies showing that irrigated lands produced more N_2O emissions than drylands. Scheer *et al.* (2008) determined that reducing irrigation intensity; irrigating cotton when soil moisture was at 65% instead of 75% of field capacity (FC), reduced N_2O emissions by almost 50%. Hence optimising irrigation could be a strategic key to reduce N_2O emissions in farming systems, besides being crucial to the world's food supplies. Irrigation will directly impact the soil water status and determine the pathway through which gaseous and dissolved O_2, but also N substrates and dissolved organic C content, may diffuse toward the location of their consumption, as will the soil structure. However, the use of water-filled pore space (WFPS) for irrigation models across soils, that vary in bulk density, is not ideal (Farquharson and Baldock 2007). Instead, it has been shown that soil gas diffusivity (D_p/D_o) can be used to predict the interaction of soil moisture and bulk density on soil O_2 supply and the resulting N_2O and N_2 emissions (Andersen and Petersen 2009; Balaine *et al.* 2016; Rousset *et al.* 2020). This raises the question "Can pasture N_2O emissions from irrigated lands be mitigated by considering irrigation management using D_p/D_o?"

This thesis aims to better understand the effect of soil O_2 supply, as determined by D_p/D_o, on N_2O emissions in the context of irrigated pastoral soil. The research focuses on how irrigation can be effectively managed to maximise D_p/D_o to minimise periods of anaerobic soil conditions that generate agricultural N_2O emissions, mainly via denitrification. Using both laboratory and

field-based studies, the impact of soil type and soil physical conditions were investigated to i) understand the robustness of D_p/D_o as a driver of N_2O emissions across soil types and as a decision tool for timing irrigation application, ii) understand the significance of wetting and draining cycles on N_2O emissions in irrigated soil and iii) investigate an optimal irrigation practice to minimise N_2O losses from intensely managed pastures.

I.2 Thesis structure

This PhD thesis is divided into seven chapters. Chapter I and Chapter II provide an overview of the thesis topic and a review of the relevant literature, respectively. The thesis objectives are detailed in the II.5 section. The next four chapters (Chapter III - Chapter VI) are organised as papers; with an abstract, an introduction, materials and methods sections and the presentation and discussion of the results, for the five experiments conducted. The final chapter summarises the overall findings of the thesis and provides suggestions for future research.

Chapter I — This chapter gives a general overview of this thesis's topic, the research objectives, and an outline of the thesis structure.

Chapter II — This chapter summarises the relevant background knowledge as a literature review and provides the reasoning and justification for the research conducted in this PhD thesis

Chapter III — This chapter presents the first laboratory experiment, which evaluated the consistency of D_p/D_o across different soil types to predict peaks of N_2O emissions.

Chapter IV Another laboratory experiment was presented in this chapter, using a ^{15}N enriched NO_3^- solution to visualise the N_2O:(N_2O+N_2) ratio in regards of D_p/D_o dynamics through wetting and draining cycles.

Chapter V This chapter presents a lysimeter experiment which evaluates the effects of soil perturbations with ruminant urine and D_p/D_o manipulation, and their interaction on temporal N_2O flux dynamics, N leaching and plants uptake.

Chapter VI The last experimental chapter presents two field trial experiments using automatic chambers to continue to evaluate the efficacy of using D_p/D_o as a trigger point for optimised irrigation in order to reduce N_2O emissions from intensely managed pastures.

Chapter VII This chapter summarises the results from Chapter III to Chapter VI and provides recommendations for future research.

Chapter II Literature review

The purpose of this chapter is to provide an overview of the nitrogen (N) cycle and the role irrigation systems play in agricultural pasture soils and the implications for nitrous oxide (N_2O) emissions, with an emphasis on how soil physical conditions impact upon those emissions.

II.1 Nitrous oxide, an environmental and agronomic issue

II.1.1 Brief History

It was not until late in the 18th century that the history of nitrous oxide (N_2O) began; starting with its discovery by the English chemist Joseph Priestley (Encyclopedia Britannica, 2019). At that time, it was not the history of N_2O as a greenhouse gas which was told but, on the contrary, the history of N_2O as an anaesthetic gas beneficial for surgical medicine. Humphry Davy (Figure 1) played a pioneering role in experimenting with the 'N_2O effect' on himself in 1799, declaring: "As nitrous oxide in its extensive operation appears capable of destroying physical pain, it may probably be used with advantage during surgical operations in which no great effusion of blood takes place" (Goerig and Schulte am Esch, 2001). Nevertheless, mankind was to suffer for another 40 years before Humphry's theory was considered in earnest. In the 1850s, Americans, Gardner Quincy Colton and Horace Wells, chemist and dental surgeon, respectively, re-appropriated the idea and experimented during a tooth extraction on Wells (Figure 1). A success! Wells proclaimed "A new era in tooth pulling. It did not hurt me as much as the prick of pain. It is the greatest discovery ever made" (Colton, 1886), and thus "painless dentistry" was born. Unfortunately, a clinical demonstration from Wells in 1845 failed and the N_2O disappeared from the anaesthetic scene for nearly two decades, until Colton revived its use in 1863 (Lew *et al.* 2018). The use of N_2O in dentistry then spread to Europe, particularly in France and Germany.

Figure 1: From left to right; Joseph Priestley (1733-1804), Humphry Davy (1778-1829) and cartoon of the Horace Wells (1815-1848) tooth extraction with Gardner Quincy Colton (1814-1898) standing in front. (source: Wikipedia)

Thereupon, scientists' names intertwined; with Jean Babtiste Rottenstein and Paul Bert in France, Edward Andrews in America, Theodor Hillischer in Austria, Frederic William in the UK, Carl Sauer in Germany and Stanislaw Klikovich in Russia. All proclaimed to use the anaesthetic in combination with air or oxygen (O_2) to prevent hypoxic side effects (Goerig and Schulte am Esch 2001). The publications came in rapid succession, as did the different anaesthetic apparatus, until a new device with a carbon dioxide (CO_2) absorber became available in the mid-1920s and this was produced by the Draeger Company. Thus, this manufacturer became a protagonist of N_2O anaesthesia apparatus all over the globe. Nowadays, N_2O is still the No. 1 inhaled worldwide anaesthetic in the medical profession, always administered as a 50/50 blend with pure O_2 (Roos, 2015).

Meanwhile, since the late 18th century, the inhalation of N_2O also became a popular form of public entertainment due to its euphoric and relaxant properties (Randhawa and Bodenham 2016). Later, N_2O was also found in the food industry as a highly effective propellant for dispensing fatty liquids like oil and heavy cream. Even the automotive industry adopted the gas for use as a fuel additive in car racing (Roos, 2015).

Despite its multiple uses (especially its use as a drug) and omnipresence for nearly 200 years, N_2O's future seems less certain than its illustrious past. Environmental concerns are at the fore.

II.1.2 Nitrous oxide, a major threat to the planet with a focus on New Zealand emissions

It is within this environmental crisis that this study stands, with the focus on N_2O as a potent greenhouse gas (GHG) and currently the most dominant ozone-depleting substance in the Earth's atmosphere (Ravishankara *et al.* 2009). Carbon dioxide (CO_2), methane (CH_4) and N_2O, are all GHGs that trap heat energy in the atmosphere. The concept of "greenhouse gas" is not recent and started with Svante Arrhenius, in 1896, who was the first to calculate GHG effects based on increasing CO_2 in the atmosphere. However, in 1988, GHGs were finally acknowledged as causing a rise in the global annual mean temperature; the greenhouse effect theory was named, and the Intergovernmental Panel on Climate Change (IPCC) was founded. Since the late 20th century, scientists have redoubled their efforts to warn that GHG impacts on the environment are of increasing concern to the climate (IPCC 2007). Scientific evidence demonstrates that climate change has been occurring and is mainly caused by human activities, posing significant risks to a broad range of both human and natural systems; the planet is heating up and fast! Most of the increase in atmospheric CO_2, and the associated warming, is attributed to the burning of fossil fuels due to the global shift towards motorised vehicle use in transportation and the automation systems adopted during the industrial revolution, and other anthropogenic activities which have been some of the greatest contributions to the release of CO_2 and other dangerous heat-trapping GHGs into the atmosphere. As indicated by a plethora of peer-reviewed journal publications, systematic reviews, and government reports, CO_2 has earned the prominent position of the most studied GHG (US EPA 2015). Carbon dioxide also remains in the atmosphere much longer than other major GHGs (US EPA, 2015). However, CO_2 should not be the sole focus: atmospheric concentrations of N_2O have also increased by 23% since pre-industrial times, from 271 ppb to 333 ppb in 2020 (NOAA 2020). Although this

is significantly lower than the absolute concentrations of the other major offending GHGs such as CO_2 and CH_4, its greater heat trapping potential means that its overabundance in the atmosphere has an important role to play in our weather system (Myhre *et al.* 2013): the IPCC reported a precipitous rise of 6% for the global radiative forcing of N_2O from 2005 to 2011. As a long-lived gas, N_2O has a lifespan of 116 years in the atmosphere (Prather *et al.* 2012) and the time-integrated radiative forcing resulting from a mass unit of N_2O is approximately 265–298 times larger than that of CO_2, for a 100-year time horizon (Tian *et al.* 2018).

In addition, N_2O remains and is expected to continue to be the dominant ozone-depleting substance emitted by humans (Revell *et al.* 2015). When N_2O is produced at the surface, it is relatively inert in the troposphere (first-atmosphere layer). But, when it is transported to the stratosphere, where the ozone (O_3) layer can be found, N_2O is broken down. It can either be photolyzed (1) or undertake reaction with the excited oxygen atoms (O^1D) (2). This latter process produces nitric oxides (NO), which catalyse O_3 destruction (3) (Revell *et al.* 2015).

1) $N_2O + h\nu \rightarrow N_2 + O(^1D)$

2) $N_2O + O(^1D) \rightarrow N_2 + O_2$ & $N_2O + O(^1D) \rightarrow 2NO$

3) $NO + O_3 \leftrightarrow NO_2 + O_2$

The N_2O molecule is the largest anthropogenic emission of an O_3-depleting compound (Portmann *et al*. 2012). Life as we know it would not be possible without this protective O_3 layer absorbing the ultraviolet radiation from the sun.

In New Zealand, there has been a 23% increase in total GHG emissions since 1990 (Table 1) (Ministry of the Environment New Zealand 2019). In 2017, New Zealand's GHG emissions inventory comprised of long-lived CO_2 that accounted for 44.5% of the total GHG emissions, CH_4 and N_2O. Collectively CH_4 and N_2O account for 53.5% of New Zealand's total GHG emissions (Table 1). However, the figures show a distinct increase in N_2O emissions since 1990

with increases of 27.8% compared to only a 6.17% increase for CH_4 (Table 1) in 2017. Nitrous oxide made up 21% of all agricultural GHG emissions in New Zealand in 2015 (Ministry of the Environment New Zealand 2019). N_2O is an omnipotent GHG and therefore, it requires mitigation.

Table 1 New Zealand's gross emissions by gas in 1990 and 2017 (Ministry for the Environment 2018)

Material removed due to copyright compliance				

II.1.3 Sources and impacts of N_2O on the agrosystem

Nitrous oxide is a long-lived GHG with both natural and anthropogenic sources (Davidson and Kanter 2014). Globally, naturally emitted N_2O emissions are estimated at 11 Tg N_2O-N per year, including terrestrial, marine and atmospheric sources, while net anthropogenic emissions account for 5.3 Tg N_2O-N per year (Figure 2) and are dominated by the agriculture sector contributing 77% of these emissions (Davidson and Kanter, 2014). Soil ecosystems constitute

the largest source of N_2O emissions and microbial nitrogen (N) transformations in the soil are the main cause of N_2O production (Ussiri and Lal 2013). New Zealand is atypical because the country has a relatively unique emissions profile, relative to other developed countries, with a higher proportion of CH_4 and N_2O, due to agriculture dominating land-based industries (Ministry for the Environment 2018).

Figure 2: Global natural versus anthropogenic N_2O emissions in 2005. (Davidson and Kanter 2014)

To support the increasing global population, it is conceivable that crop and stock numbers will increase, as well as the use of N fertilisers. The invention of the Haber–Bosch process gave rise to the introduction of synthetic N-based fertilisers, the availability of which has enabled the expansion of intensive farming (Thomson *et al.* 2012). This also has been the case in New Zealand where the amount of N fertiliser applied to agricultural soils was ~6–fold higher in 2013 than in 1990, 359kt and 59kt, respectively, with urea representing more than 80% of all synthetic N fertiliser applied (Ministry for the Environment, 2015). Despite the positive feature of using N fertilisers on farmlands, such as the increase of plant production, the fraction of applied N that is absorbed and used by plants, also called N use efficiency (NUE), is generally low. The fraction not used by the plants will be stored as organic N in the soil, lost to the atmosphere, or leached to ground and surface waters. In a grazed pasture system, which

converts plant biomass into human edible animal products, less than 50% of the N applied in fertiliser and manure is removed by the plants. Nitrogen use efficiency is also predominately influenced by fertilization with NUE significantly larger in unfertilised (NUE calculation including N mineralisation of the soil and N deposition rate) than fertilised plots (Keuter *et al.* 2013). Thus, greater N availability from fertilisers leads to increasing emissions of N_2O in the agriculture sector. Generally, for every 1000 kg of applied N fertilisers, it is estimated that around 10–50 kg of N will be lost as N_2O from soil, with the amounts of N_2O emitted increasing exponentially relative to the increasing N inputs (Shcherbak *et al.* 2014). A study by Kelliher *et al.* (2014) also showed that changing N application rate could significantly and proportionally change the soil NO_3^-–N concentrations, and with soil NO_3^-–N concentrations up to 891 mg kg^{-1} (1500 kg N ha^{-1} applied) linear increases in N_2O emissions were observed (Figure 3).

*Figure 3: The relationship between nitrogen (N) application rate (Nrate, kg N ha^{-1}) and the replicate nitrous oxide (N_2O) fluxes accumulated over 67 days (kg N ha^{-1}). Linear regression yielded N_2O flux = (0.0122 ± 0.0006) * Nrate + 0.8352 ± 0.0626, a statistically significant relationship ($P < 0.05$) accounting for 92% of the variability.*

(Kelliher et al. 2014)

Nitrous oxide emitted directly from the soils to which N has been added are called direct N_2O emissions. In contrast indirect N_2O emissions result from the volatilisation of N and leaching of N. A fraction of the volatilised N returns to the ground as wet or dry deposition and is then transformed and re-emitted as N_2O. Indirect emissions from leached N occur as dissolved inorganic-N is transformed resulting in N_2O emissions from ground waters, drains, streams and other water bodies in the landscape (IPCC 2007).

In grazed soils, synthetic N-based fertilisers are not the only source of N substrate for direct N_2O emissions. New Zealand's greenhouse gas inventory (2019) reported that in 2017, urine and dung deposited by grazing animals comprised 63.5% of N_2O emissions from the agricultural soils category, far ahead of the synthetic N fertilisers that comprised 15.9%. Ruminant urine is randomly deposited onto pasture in "patches" and the N rate is related to animal type with the rate of N deposited in a urine patch as high as 2000 kg N/ha (Selbie *et al.* 2015). Thus, grazed pasture systems are typically rich in N, with the urine patches creating "hot-spots" for N_2O production. In addition, some studies refer to the urine-N application effect on N_2O emissions as lasting for longer than 30 days (Baggs *et al.* 2006). It is well documented that urine additions to grassland soils result in significant quantities of N_2O production and emission, mainly due to the soil microbial processes of nitrification and denitrification (Selbie et al., 2015), following the addition of readily available N and carbon (C), and the effects of significantly increased soil water-filled pore space (WFPS) within the urine patch (Van der Weerden *et al.* 2017). Estimated denitrification losses from grasslands grazed for dairy cows in New Zealand have been estimated to be ~ 10 kg N ha^{-1} y^{-1} (Parfitt *et al.* 2006). The emission factor (EF) is, according to U.S. Environmental Pollution Agency (EPA), "a representative value that attempts to relate the quantity of a pollutant released to the atmosphere with an activity associated with the release of that pollutant". The EF is also higher for ruminant urine than the EF for ruminant dung, with values in New Zealand set at 1% and 0.25%, respectively (Ministry of the Environment 2019). A study in the United Kingdom (U.K.) (Chadwick *et al.* 2018) showed similar results with a significantly greater average for the N_2O EF for urine (0.69%) than dung (0.19%).

Plants may also be a source of N input to the soil, through N-fixing legumes such as clovers (e.g. *Trifolium sp.)*, or through decomposition of plant litter and crop residues (Figure 4). Crop residues are materials left in an agricultural field after the crop has been harvested. The current

U.K. Greenhouse Gas Inventory (2018) identifies crop residues as the third largest source of direct N_2O emissions from agricultural soil after synthetic N fertilisers and grazing returns (urine and dung). Consequently, the increases of N losses from N_2O emissions from the agriculture sector were and are no longer surprising.

Figure 4: Sources of N_2O emissions from agricultural soils, showing the contribution of each source to emissions through both direct and indirect pathways in New Zealand (Ministry for Primary Industries 2020)

Summary of the subsection:

Life on Earth depends on a temperature range controlled by the greenhouse effect. Changes in the concentration of GHGs have occurred in the past decades and have been related to the increase in global temperature. Among these GHGs, N_2O is of great importance because it remains in the atmosphere for more than 114 years and has a warming potential 298 times greater than CO_2. Most of the N_2O emissions take place from soils and are related to agricultural activities. The next subsection is aiming at presenting the main mechanisms of N_2O formation and emission in agricultural soils.

II.2 The processes responsible for N_2O emissions from soil

II.2.1 An overview on the N cycle in the soil

Nitrogen (N) is an essential nutrient for plant growth, development and reproduction (Lambers and Oliveira 2019). Despite N being one of the most abundant elements on earth, plant N deficiency is one of the most common problems affecting plants worldwide (Lambers and Oliveira 2019). Nitrogen is involved in many vital plant processes such as photosynthesis (N is a component of chlorophyll), the production of proteins (N is a component of the amino acids), energy-transfer (N is a component of adenosine triphosphate; ATP) and transfer of genetic material (N is a component of nucleic acids e.g. deoxyribonucleic acid; DNA).

Non-reactive N occurs as N_2 while reactive N (Nr) comprises all the inorganic oxidised (nitrate ion; NO_3^--, nitrogen oxides; NO_x, N_2O) and reduced forms (ammonia; NH_3, ammonium ion; NH_4^+) as well as the organic N compounds (Galloway *et al.* 2003). In the soil, N is most likely to be found as organic N compounds, or inorganic N such as NH_4^+ and NO_3^- (Fowler *et al.* 2013). In the plant/soil/atmosphere system, N is transformed from one form to another through reduction-oxidation reactions mediated by microbial communities in a complex biogeochemical N cycle (Figure 5). Among these many N transformation processes, N fixation and NO_3^- assimilation are the only pathways that are not directly involved in the production of N_2O. It is important to stress that this N cycle (Figure 5) includes only those pathways contributing to atmospheric loading of gaseous N compounds (excluding NH_3) and does not show the biotic losses (plant uptake of NH_4^+ or NO_3^-) and abiotic losses (N leaching) that are also part of the N cycle. Indeed, under high rainfall or irrigation, soil NO_3^- can move below the plant roots with drainage, a process termed 'leaching'. Ammonium (NH_4^+) is a positively

charged molecule that is held on the negatively charged sites on soil organic matter and mineral surfaces, thus it is retained in the soil and is not susceptible to being leached or volatilised. Volatilisation is the gaseous loss of ammonia (NH_3) from the soil surface after its conversion from NH_4^+, a process driven by the soil having a high pH (> ~7.0). Significant amounts of NH_3 can be lost from manure, urine or fertiliser via NH_3 volatilisation. The conversion of organic N sources to NH_4^+ by soil microorganisms in the soil (Figure 5) is called mineralisation (Schimel and Bennett 2004).

It follows that the N cycle is complex and indispensable for the "agrosystem" and plant development. Nevertheless, an unbalanced N cycle can have devastating consequences for the natural environment. The microorganisms' activity regulates the retention or loss of N from the system, and determines in which form N is lost. Reactive N is lost from agricultural soils mainly via the gaseous release of N_2O, NH_3 and NOx (Kasper *et al.* 2019), and via NO_3^- leaching, the latter will enter surface and ground waters, causing water eutrophication (Gruber and Galloway 2008). Several concurrent processes are responsible for N_2O emissions in agricultural soils (Signor and Cerri 2013; Hallin *et al.* 2018) and the relative contribution to net N_2O emissions of the different processes varies considerably and is influenced by the microbial community and environmental condition. However, the majority of N_2O (approximately 70%) is produced through the biological processes of nitrification and denitrification (Butterbach-Bahl *et al.* 2013). The following subsections discuss the details of these processes responsible for N_2O emission.

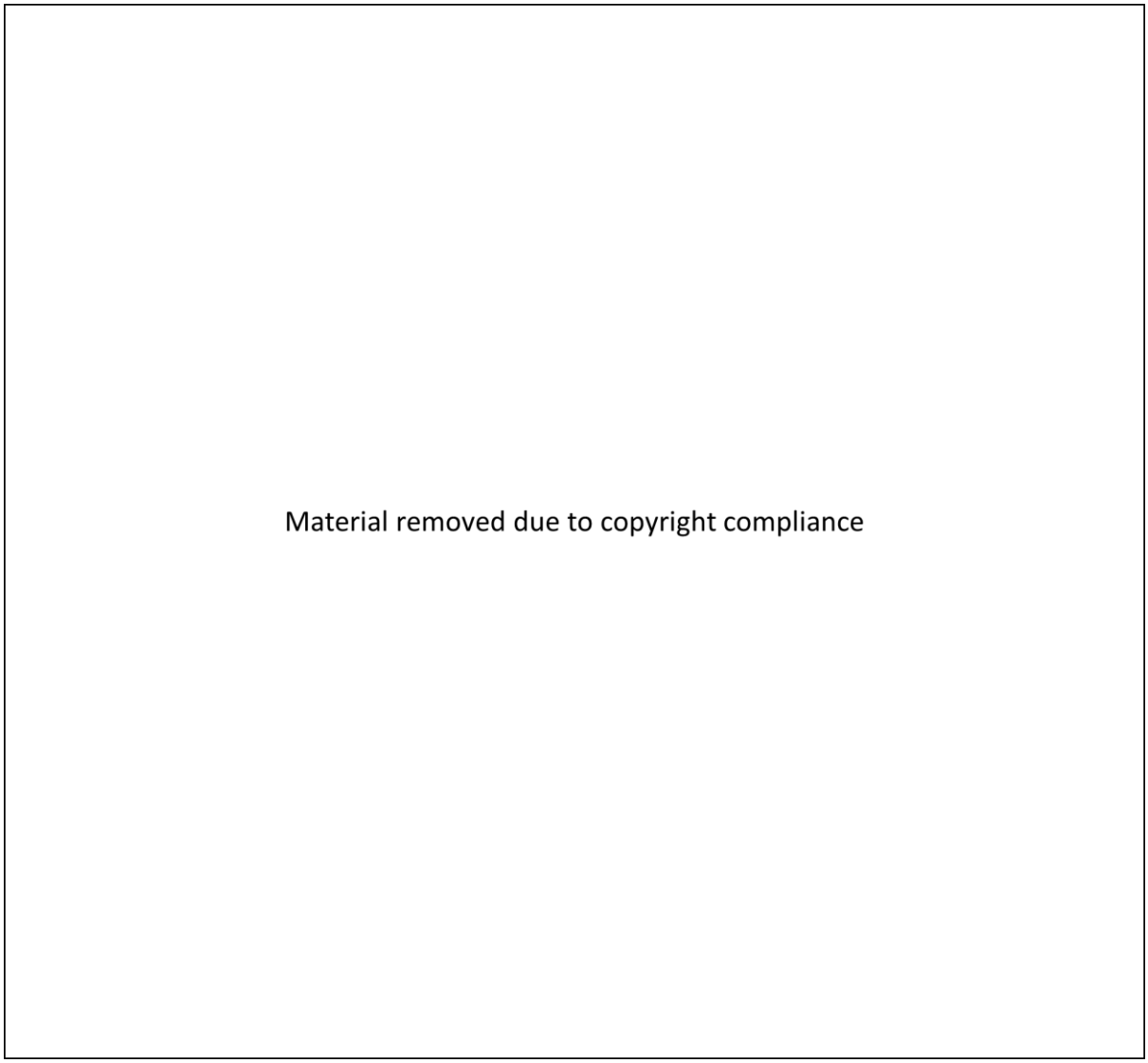

Figure 5: Figure from Hallin et al. (2018) of "the microbial pathways in the nitrogen (N) cycle. Background colors differentiate between processes occurring under oxic or anoxic conditions. The compounds are positioned according to the oxidation state of N. Solid colored lines indicate microbial pathways, and the genes encoding the respective enzymes that catalyse each step in the pathway are indicated as follows: amo, ammonia monooxygenase; hao, hydroxylamine oxidoreductase; hdh (also known as hzo), hydrazine dehydrogenase; hzs, hydrazine synthase, nar/nap, cytoplasmic and periplasmic dissimilatory nitrate reductases, respectively; nas, assimilatory nitrate reductase; nif, nitrogenase; nas/nirB, assimilatory nitrite reductase; nirS/nirK, cytochrome-cd1 and copper-based dissimilatory nitrite reductases, respectively; 'nor', any of the multi-heme or heme–copper nitric oxide reductases; nosZ, nitrous oxide reductase; nrf, formate-dependent dissimilatory nitrite reductase; nxr, nitrite oxidoreductase. Dotted lines indicate the contributing pathways to atmospheric loading of gaseous nitrogen compounds, whereas dashed gray lines indicate biotic/abiotic processes generating gaseous N compounds that also feed into the overall N-cycle. DNRA, dissimilatory nitrate reduction to ammonium".

II.2.2 Denitrification

Denitrification rates in agricultural soils are thought to be approximately one order of magnitude larger than in natural soils (Butterbach-Bahl and Dannenmann, 2013). Denitrification is the reduction of NO_3^- to N_2, with N_2O being an obligate intermediary compound. When this process is complete N_2 is formed and when it is incomplete a variable fraction of N will be emitted as NO and N_2O (Pilegaard 2013). Emissions of NO are typically low, probably due to coupled regulation of NO_2^- and NO reductase preventing toxic accumulation (Zumft 1997). Denitrification represents a significant source of N_2O emission from soils (Boyer *et al.* 2006; Butterbach-Bahl *et al.* 2013) and it is often considered a cause of the low N use efficiency in agriculture, since it can interfere in soil-plant relationships, competing for mineral N and leading to N loss from the system both as N_2O and N_2 (Galloway *et al.* 2004). Complete denitrification plays a pivotal role in the N cycle as it favours the conversion of N_2O into N_2 and returns N to the atmosphere. Hence, denitrification is the only terrestrial sink for N_2O.

The sequential reduction involved in the denitrification process can be summarised as follows in Figure 6:

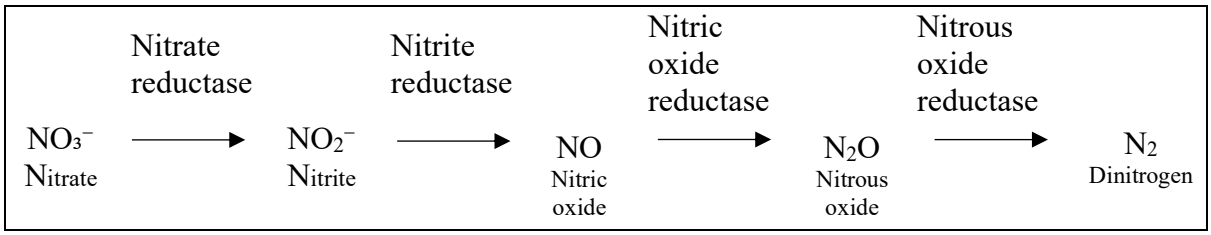

Figure 6: Denitrification steps including the different enzymes involved

Denitrification occurs under anaerobic conditions when facultative anaerobic bacteria use N-oxides as an electron acceptor instead of the O_2 molecule (Wrage-Mönnig *et al.* 2018). Facultative anaerobic bacteria represent 0.1-5.0% of the total bacteria population in the soil

(Signor and Cerri 2013). Anaerobic bacteria, mainly heterotrophic, are the stereotypical denitrifiers but the process is phylogenetically diverse (Graf *et al.* 2014), also occurring in fungi and archaea. Recent studies increasingly highlight the importance of fungal denitrification as a source of N_2O emissions (Maeda *et al.* 2015) potentially because fungi do not encode an N_2O reductase to completely reduce produced N_2O into N_2. The existence of microaerophilic and oxic denitrifiers, which emit N_2O emissions from aerobic soil, have also recently been discovered (Ji *et al.* 2015) but there significance is unknown. Thereby, the major requirements for denitrification to occur are the presence of microorganisms in the soil having the appropriate metabolic pathway, the availability of suitable reductants (NO_3^-, NO_2^-, NO or N_2O) and anaerobic soil conditions (0% O_2). Soils in New Zealand are generally not frozen in winter, and N_2O emissions are likely to be high both in wet winters when soils are saturated, and for poorly drained soils.

N_2O production is often described in terms of either: i) N_2O quantity emitted and/or accumulated, and ii) the $N_2O/(N_2O+N_2)$ ratio. The first is self-explanatory and implicitly the most relevant variable used to describe the release of N_2O to the atmosphere. The second variable ($N_2O/(N_2O+N_2)$ ratio) is relevant when highlighting the process generating N_2O emissions. The fraction of N_2O or N_2 emitted during the denitrification process is influenced by various soil and environmental factors.

II.2.2.a *Nitrogen substrates influence on the denitrification rate*

Nitrogen oxanions/oxides (NO_3^-, NO_2^-, NO and N_2O) are the substrates for the denitrification process (Figure 6), therefore, their availability clearly impacts the amount of gaseous products produced (NO, N_2O and N_2). An increase in the N inputs will give rise to an increase in N outputs, all things being equal, given appropriate anaerobic conditions for denitrification.

An increased availability of NO_3^- in the soil is known to shift the $N_2O/(N_2O+N_2)$ ratio towards N_2O (Senbayram *et al.* 2012), as NO_3^- is favoured over N_2O as electron acceptor during denitrification and due to the suppression of N_2O reductase activity (Giles *et al.* 2012). Moreover, NO_3^- is one of the most mobile of the Nr species in the soil, thus it may rapidly diffuse into anaerobic soil compartments where it may promote biological denitrification. Therefore, the application of N fertilisers or manures increases denitrification rates, especially when there is an ample supply of C (Bhandral *et al.* 2007; Fangueiro *et al.* 2008). Soil NO_3^- concentrations in the range 1–10 mg NO_3^-–N kg $soil^{-1}$ have been reported to limit denitrification (Barton *et al.* 1999). However, studies conducted on pastoral soils in New Zealand, report soil NO_3^- concentrations often > 50 mg NO_3^-–N kg $soil^{-1}$ for control sites without N-urea application (Kelliher *et al.* 2014). Consequently, this suggests that NO_3^- will not be a limiting factor for denitrification in New Zealand pastoral soils.

As for NO_3^-, the presence of NO_2^- can also impair the reduction of N_2O resulting in increased N_2O emissions in soils. During denitrification, there is electron competition between each reductase enzyme in the denitrification chain, competing for a restricted pool of electron carriers which are normally provided by C oxidation (Pan *et al.* 2013). Nitrous oxide reductase is known to have a lower affinity to the electron carriers than the preceding reductases involved in the denitrification process. Consequently, the N_2O reduction activity to N_2 is reduced in the presence of low concentrations of C, NO_3^- and NO_2^- (Pan *et al.* 2013).

II.2.2.b *Carbon and other factors influence on the denitrification rate*

Plant residues and animal manures represent the main inputs of C compounds to agricultural soils. Organic fertilisers are also a source of readily-decomposable organic C compounds. This

addition of C may trigger denitrification by enhancing respiration (through creation of anoxic micro-sites) and by providing energy for denitrifiers (Weier *et al.* 1993).

The electron supply per mole of C from different substrates may be a factor determining their efficiency in denitrification and nitrification. Denitrifying and nitrifying bacteria use a wide variety of organic acids, carbohydrates, and other organic compounds as C and energy sources when growing under aerobic conditions (Beauchamp *et al.* 1989). Denitrification rates may differ depending on the C sources. This has been seen in the experience of De Catanzaro and Beauchamp, (1985) where alfalfa-amended soil produced a significantly higher rate of denitrification than the same amount of added straw. Low C availability in the soil will reduce the denitrification rate and then reduce soil N_2O emissions and increase the opportunity for N to be lost by alternative processes such as leaching. However, higher denitrification rates do not always lead to higher N_2O losses from soil as denitrifying bacteria produce mainly two gases, N_2O and N_2. A decrease of the $N_2O/(N_2O+N_2)$ ratio can also be observed with a high C concentration in the soil leading potentially to an increase of N_2O reduction to N_2 (Senbayram *et al.* 2012) due to the lack of electron competition. As mentioned before, N_2O reductase has a lower propensity to bind to electron acceptors compared to other N-reductases (Pan *et al.* 2013). Hence, when C supply is high, electron supply is high, thus competition is minimised and N_2O reduction to N_2 increases. Moreover added C can simulate aerobic respiration in which C is oxidised to CO_2 with the release of energy. Respiration by microorganisms decomposing organic matter in soil consumes O_2 faster than it can penetrate the soil mass, and hence the creation of anoxic micro-sites in the soil occurs (Boyd 1995).

In general, the effect of available C compounds on the amounts of N_2O and N_2 produced in and emitted from the soils, as well as their ratio, is reported to vary with soil NO_3^- concentration and WFPS (Zaman *et al.* 2007).

Other additional factors that influence denitrification include soil temperature, with an optimal temperature reported to be 25°C (Canion *et al.* 2014). It has been shown that increasing temperature results in higher rates of N_2O emissions (Farquharson and Baldock 2007). Recently, a microcosm study carried out by Venterea et al., (2020) showed an unexpected increase in N_2O emissions as soil temperatures declined. This phenomena was explained by an accumulation of NO_2^- at cold temperatures (5 and 10 ºC), resulting from an increase in the first steps of nitrification (NH_3 oxidation, Figure 7). This increase of NO_2^- was then associated with increased production of NO, and to a lesser extent an increase in N_2O emissions.

Soil pH impacts upon denitrifiers abundance, $N_2O/(N_2O+N_2)$ ratios and denitrification rate. Bergaust *et al*. (2010) demonstrated that for highly acidic soil the formation of the N_2O reductase enzyme is impaired and therefore the ratio of N_2O to N_2 produced from denitrification is increased at low pH (acidic). In general, pH is also considered as an important determinant of microbial community composition in soils (Kaminsky *et al.* 2017).

Soil depth is also important with respect to surface soil N_2O emissions as there will be more opportunity for further reduction of N_2O via denitrification, if N_2O is generated deep within the soil (e.g. Clough *et al.* 2005).

II.2.3 Nitrification

Nitrification is an aerobic process where NH_3 is oxidised to NO_2^-or NO_3^- for the generation of energy by microorganisms, and joins N fixation and denitrification (Figure 5) as a major pathway within the N cycle (Stein and Klotz 2016). This process can produce N_2O directly, via chemical decomposition of hydroxylamine, and indirectly, via nitrifier denitrification. As seen in Figure 5, nitrification occurs in an oxic environment and the presence of O_2 is essential for this process to occur.

Nitrification in soils is classified into heterotrophic nitrification or autotrophic nitrification (more prevalent). The latter is mainly carried out by chemoautotrophic ammonia-oxidizing bacteria (AOB) and archaea (AOA), and nitrite-oxidizing bacteria (NOB). Heterotrophic nitrification is carried out by certain heterotrophic fungi and bacteria with the potential to oxidise both organic and inorganic N compounds (Hayatsu *et al.* 2008). Nitrification was historically considered a pathway to nitrate with 2 distinct stages. AOB (or AOA) were thought to produce only nitrite from their metabolism which was then released as a substrate for NOB to produce NO_3^- (Figure 7). However in 2015, two studies from Daims *et al.* (2015) and Van Kessel *et al*. (2015) found the existence of a bacterium that performed complete ammonia oxidation (COMAMMOX) from NH_3 to NO_3^-. The nitrification pathway, whether it is performed by one microorganism or divided into two phases, is described in Figure 7.

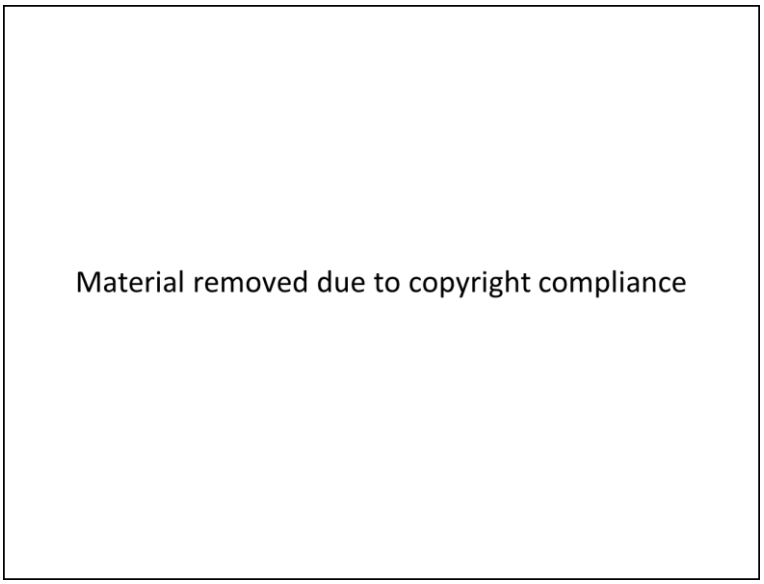

Figure 7: Nitrification pathways undertaken by ammonia-oxidizing bacteria (AOB), nitrite oxidizing bacteria (NOB) and comammox bacteria. (Stein 2019)

Ammonia in agricultural soils can be provided by NH_3 fertilisers or be derived from NH_4^+. The mechanism of N_2O production by nitrification is not completely elucidated but several studies suggest the following hypotheses:

1. A constant proportion of NH_4^+ can be converted to N_2O during nitrification, resulting from biotic or abiotic reactions of nitrification intermediates. A study led by Kozlowski *et al*. (2016) using microelectrodes, showed that AOA generated and rapidly consumed NO, but were incapable of nitrifier denitrification and produced N_2O via abiotic reactions of metabolic intermediates with media components. Consequently, N_2O is thought to be produced during abiotic NH_2OH decomposition and as a by-product of AOB or AOA nitrification of NH_3 (Stein 2019).

2. The partial oxidation of NH_4^+ into NO_2^- under aerobic conditions, followed by NO_2^- diffusion to hypoxic regions and its subsequent reduction to NO. This process is better known as nitrifier denitrification. This process occurs in AOB in order to maintain an intracellular redox balance and is not a respiratory pathway. Figure 8 shows that AOB encode and express Nir and Nor enzymes which reduce NO_2^- to NO and N_2O. Nitrifier denitrification is a process that is active under increasingly O_2 limited conditions but ceases under complex anoxia, where denitrification occurs. Nitrifying bacteria lack the nosZ gene (Stein 2019), therefore the obligate end product is N_2O which explains the high contribution rate of nitrifier denitrification.

3. The final mechanism for N_2O generation by AOB is the anaerobic oxidation of hydroxylamine by the enzyme cytochrome P460 (Caranto *et al.* 2016).

Stein (2019) reports that production of N_2O by nitrifier denitrification in AOB is significantly greater than N_2O from abiotic pathways. Regardless of the mechanism, N_2O as a by-product during the ammonia oxidation process accounts for around 1% of the total NH_3 consumed (Prosser *et al.* 2019).

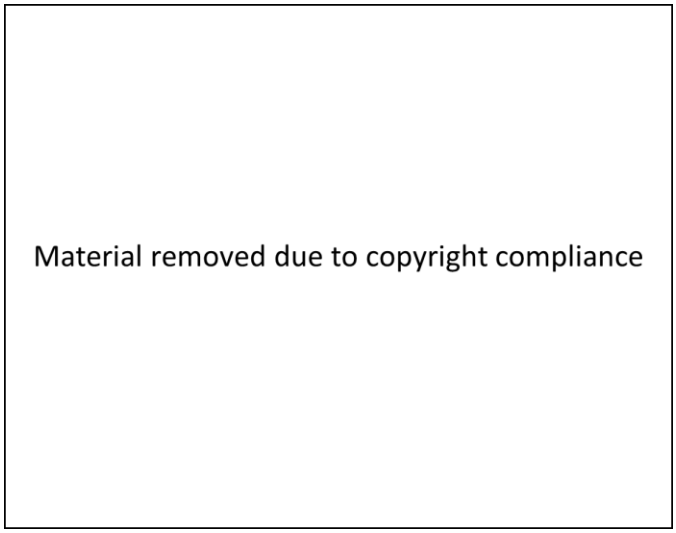

Figure 8: Pathways for N_2O production by AOB and AOA. Reactions with red arrows are catalysed by enzymes and only by AOB. Reactions with blue dashed arrows are abiotic, or biotic via partnering microorganisms, and occur for both AOB and AOA from intermediates produced during active ammonia oxidation. (Stein 2019)

Nitrous oxide production via NH_3 oxidation pathways increases as O_2 concentrations decrease (Zhu *et al.* 2013a). Nitrifier denitrification can account for up to 100% of N_2O emissions from NH_4^+ in soils and the process is more significant than classical denitrification under some conditions (Wrage-Mönnig *et al.* 2018). Zhu *et al*. (2013) showed that, hypoxic O_2 concentrations, 0.5% and 3%, resulted in nitrifier-denitrification generating between 34% and 66% of total N_2O emissions. This rate was higher than the heterotrophic denitrification rate (between 34% and 50%) for the same O_2 concentrations which, in the absence of oxygen (0%) was responsible for 100% of N_2O production. By comparison, the study of Mathieu *et al.* (2007), involving the use of ^{15}N isotope tracers ($^{15}NH_4^+$ or $^{15}NO_3^-$) to compare nitrification and denitrification, showed that under unsaturated and saturated conditions, both processes were significantly involved in N_2O production. Under unsaturated conditions, 60% of N_2O came from nitrification, while denitrification contributed around 85-90% under saturated conditions.

II.2.3.a *Nitrogen substrates influence on nitrification and N_2O emissions through nitrifier denitrification*

The rate of nitrification depends on various factors. The process will be indubitably influenced by the substrate abundance in the soil (NH_4^+, NH_3 or NO_2^-). Studies have shown that the addition of fertiliser or urea (adding NH_3 and NH_4^+ in the soil) stimulates an increase in AOB populations (Hermansson and Lindgren 2001; Okano *et al.* 2004; Cavagnaro *et al.* 2008). To reduce N_2O emissions from applied urea, NH_4^+-based fertilisers or urine-N, researchers have developed different mitigation technologies including the use of N inhibitors to reduce the entry of mineral N from applied fertiliser/urine into the available inorganic-N pool. The use of nitrification inhibitors (NI) has been pointed out as an efficient strategy to reduce N_2O emissions without yield penalties (Clough *et al.* 2007; Chen *et al.* 2010; Misselbrook *et al.* 2014). The basic premise of NI techniques is to delay either urea hydrolysis (urea fertiliser and ruminant urine patches) or the rate of NH_3 oxidation (fertilisers, ruminant urine patches). Reducing NH_3 oxidation by blocking the AMO gene activity (Figure 7) reduces the potential for abiotic generation of N_2O, the potential for nitrifier denitrification, and reduces the amount of NO_3^- subsequently available for denitrification. Urease inhibitors (UI) retard the hydrolysis of soil-applied urea and delay the entry of urea-N into the NH_4^+ pool (Liu 2012), which is likely to produce less N_2O via nitrification due to the limited availability of NH_4^+. However, this extended retention of N in form of NH_4^+ after NI application in soils may increase the risk of NH_3 volatilization and thus the risk of NH_3 deposition which is an indirect source of N_2O emissions via nitrification (Ministry for Primary Industries, 2020, Figure 4).

Both AOB and NOB are sensitive to NH_3 toxicity, but it is generally believed that NOB are more sensitive than AOB (Van Cleemput and Samater 1995); thus, soil NO_2^-accumulates in the presence of sufficiently high NH_3 levels because NOB are unable to fully process the NO_2^- produced by AOB leading to increased N_2O production via nitrifier denitrification in an attempt

to detoxify the NO_2^- (Venterea *et al.* 2015). Similar conditions, with large NH_3 concentrations leading to accumulating NO_2^-, are found after application of urea, urine, or manure (Elliot and Fox 2014; Breuillin-Sessoms *et al.* 2017; Norton and Ouyang 2019). This increase in NO_2^- concentration will favour the production of N_2O through codenitrification, nitrifier denitrification and denitrification/DNRA (Figure 9).

Figure 9: Likely occurrence of N_2O releasing pathways as a function of substrate type and NO_2^- concentration. Note that the circles are drawn to indicate proximate optimal conditions. Occurrence in soil (microsites) might differ and substrate pools are not uniform. (Wrage-Mönnig et al., 2018)

II.2.3.b *Other factors affecting nitrification rate*

As mentioned earlier the majority of nitrifiers found in the soil are autotrophic and gain energy to fix CO_2 into organic C compounds by oxidizing the N compounds in the NH_3 and NO_2^- molecules. Nitrifying bacteria use a wide variety of organic acids, carbohydrates, and other organic compounds as C and energy sources when growing under aerobic conditions (Beauchamp *et al.* 1989). However, a C limited environment could simulate N_2O production by increasing N oxidation, triggering favourable conditions for nitrification/nitrifier

denitrification pathways. For example, Köster *et al*. (2011) revealed that in an environment where all added labile C substrates had been consumed, nitrification gained in importance, reaching roughly the same N_2O production rate compared to the denitrification pathway. A high C:N ratio is also known to lead to the immobilization of NH_4^+ (Sahrawat 2008) which will affect the nitrification rate.

Let us not forget that plants take up and assimilate both NH_4^+ and NO_3^-, and this could also exert differential effects on nitrifiers. Some plants are also capable of producing nitrification suppressing chemicals (Skiba *et al.* 2011). Plants will also stimulate soil N transformation by releasing C into the rhizosphere as a consequence of root exudation. However, Thion *et al*. (2016) showed that AOB abundance in the rhizosphere and bulk soil depended on pH, rather than plant traits.

Finally, during the first phase of nitrification, hydrogen ions (H^+) are released which results in acidification of the soil. Optimum pH has been found to be approximately 7.8 to 9.0 and reductions in nitrification rate have been found outside this range (Amatya *et al.* 2011).

II.2.4 Coupled nitrification-denitrification

As seen above, denitrification and nitrification processes occur in the soil when the conditions are optimal for denitrifiers and nitrifiers, respectively.

Despite the fact that nitrification is an aerobic process and denitrification is an anaerobic process these processes may coexist within the same soil. When it occurs; when NO_3^- or NO_2^-, derived from nitrification, diffuses to sites of denitrification, the terminology "coupled nitrification-denitrification" (CND) is used (Wrage *et al.* 2001). In this process, nitrifiers and denitrifiers 'cohabit' in adjacent anaerobic and aerobic zones with nitrification products diffusing into the zone for denitrification. Unlike the nitrifier denitrification process, carried

out solely by ammonia oxidisers, CND is the result of the coupling of nitrification and denitrification with the denitrifiers using the nitrification products (Wrage-Mönnig *et al.* 2018). Marchant *et al.* (2016) show that nitrification fuels denitrification by providing an additional source of nitrate, and as such masks true N losses.

This suggests that the production of N_2O is highest at conditions that are sub-optimal for both nitrifiers and denitrifiers.

II.2.5 DNRA-denitrification

Dissimilatory nitrate reduction to ammonia (DNRA) is considered as one of the least understood processes in the N cycle (Kuypers *et al.* 2018). DNRA converts soil NO_3^- to NO_2^-, as in some denitrifiers, but involves a further fermentative step converting NO_2^- to NH_4^+ (Friedl *et al.* 2018). Thus, the principal importance of DNRA is that NO_3^- is transferred into another mineral N form which is less mobile and therefore conserves N in the ecosystem. Recent studies have suggested competition for NO_3^- exists between DNRA and denitrification under anaerobic conditions (Rütting *et al.* 2011).

Thus, the soil oxidation state is a principal factor that determines the importance of DNRA compared to denitrification (Friedl *et al.* 2018) with DNRA by bacteria and fungi occurring under more reducing (anoxic) conditions (Yin *et al.* 2002). In addition, DNRA is assumed to occur under NO_3^- limiting conditions and high C availability, with DNRA favoured over denitrification when the C to NO_3^- ratio is > 12 (Yin *et al.* 2002). Friedl et al. (2018) examined the effect of a wetting and drying cycle on denitrification and DNRA, and the results showed an exponential increase in both processes correlated with increasing WFPS and both processes responded to NO_3^- availability, demonstrating both processes as N-substrate driven. However, they did not see any correlation with NO_3^- concentration and DNRA but their findings suggest

that the high labile C availability under perennial pastures, together with the increase of labile C upon rewetting, drives heterotrophic soil respiration, which reduces the soil redox potential and ultimately shifts NO_3^- consumption from denitrification to DNRA.

Conditions required for DNRA are similar to those required for denitrification including available NO_3^- or NO_2^- and organic C availability. Thus increased NO_3^- availability also increases the potential for production of N_2O through DNRA.

II.2.6 Chemodenitrification

With reference to the five previous processes (denitrification, nitrification, coupled nitrification-denitrification, nitrifier-denitrification and DNRA-denitrification), N_2O production is generally thought to predominately arise from microbial enzymatic processes. However, iron, manganese and organic compounds readily undergo redox reactions with intermediates in the N cycle that produce N_2O abiotically under relevant environmental conditions at alkaline pH (Zhu-Barker *et al.* 2015). Chemodenitrification is the term used to describe abiotic reactions of NO_2^- with ferrous (Fe(II)) ions causing N_2O emissions (Figure 10) (Van Cleemput 1998). Similarly, decomposition of the nitrification intermediate NH_2OH to N_2O may occur through redox reactions with Fe (III) (Zhu-Barker *et al.* 2015). It has been suggested that chemodenitrification can account from 6.8 to 67.6% of the total N_2O production in paddy soil depending on the concentrations of Fe(II), N and C substrates (Wang *et al.* 2020).

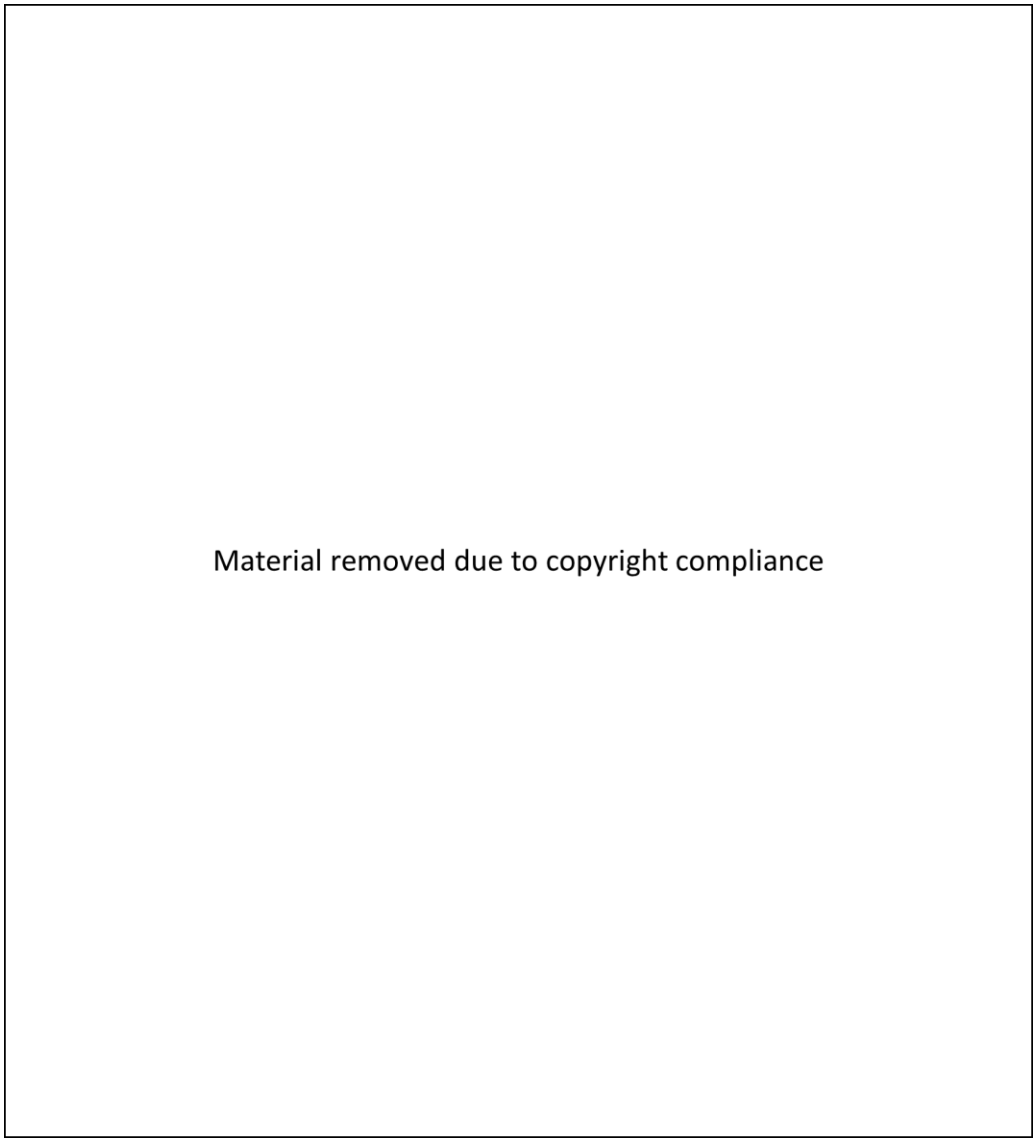

Figure 10: "Cause and effects of nitrite- and nitrate-induced (chemo) denitrification-based N_2O formation in coastal marine sediment. When Fe(II) and nitrite/nitrate was added to the marine sediment, Fe(III) was formed among different process by chemodenitrification which is stimulating Fe(III)-reducing bacteria (FeRed). The FeRed bacteria then produce Fe(II) and stimulate Fe(II)-oxidizing bacteria. Therefore chemodenitrification has a significant impact on Fe-cycling in general. Simultaneously, nitrite/nitrate was reduced to NO and further to N_2O by chemodenitrification and denitrifying bacteria. In addition, the presence of high nitrite/nitrate concentration leads to a high typical nosZ gene expression in denitrifying bacteria which is responsible for the reduction of N_2O into N_2." From Otte et al. (2019)

Summary of the subsection

In nature, microorganisms form complex networks that link N-transforming processes. They produce and consume N_2O. Denitrification has been shown to be the main source of the initial N_2O pulse after fertilisation (or urine deposition) and irrigation from subtropical pastures (Friedl *et al.* 2016). *Multiple pathways are involved in the production and consumption of N_2O that can occur simultaneously in different micro-environments within the same soil. There exists a considerable challenge in allocating their relative contributions. Furthermore, these processes, are 'soil factor' dependent (Figure 11). In order to reduce N_2O emissions, there is a need to better understand the factors influencing those processes. The next subsection is aiming at presenting the main soil factors influencing nitrification and denitrification processes.*

Figure 11: Possible ecological niches for the different microbial processes involved in the N_2O emissions (Wrage et al. 2001)

II.3 The balance between saturation and aeration in the soil and its impact on N_2O production pathways

The previous subsection highlights the importance of the microorganisms' pathways and more specifically the denitrification and nitrification processes in the soil for the production of N_2O emissions. Spatial variability of N_2O production in soils is high, varying with climate, soil type, and farming systems, all of which lead to an increasing challenge in terms of estimating the contribution of soil N_2O emissions to global warming. The challenge is all the greater given that this high spatial variability can be observed in the scale of a field or even an experimental plot (Figure 12). Oxygen availability, soil redox potential (electron acceptor/donor), and availability of substrates are the main drivers and regulators of the microbial processes involved in N_2O production (Senbayram *et al.* 2009) and potentially explain these observed spatial variabilities in the soil. The soil redox potential and substrate (mainly C and N compounds) influences on denitrification and nitrification have been discussed above. This section will examine the importance of O_2 availability in controlling N_2O production in farming systems.

Figure 12: Spatial distribution of N_2O emissions in a field plot experiment (n=36). (Mathieu et al. 2006)

II.3.1 Soil aeration and water content, and their effects on N_2O emissions

"Soil systems provide integrated functions that are greater than the sum of their parts" (Needelman, 2013). As noted above (Section II.2, Figure 5) different microbial pathways produce N_2O in the soil depending on the soil's oxic, hypoxic or anoxic status (Hallin *et al.* 2018). Therefore, O_2 supply is a key determinant of the biological pathways producing and consuming N_2O in soils (Wrage-Mönnig *et al.* 2018). Nitrification and denitrification respond differently to soil water status, largely due to the effect of soil water content on O_2 diffusion in soil and on the gaseous and aqueous diffusion of substrates and products associated with these biological processes (Farquharson and Baldock 2007).

Soil is a material composed of five ingredients: minerals, soil organic matter, living organisms, gas, and water. The soil system consists of three basic phases: solid, liquid and gas. When subjected to closer scrutiny, the soil is a complex network with half the volume being inorganic mineral particles of different sizes. The other half, the pores holding water or gas, that which

is not water is gas and vice versa, hence there is a relationship between soil air content (Ɛ, cm^3 air cm^{-3} soil) and soil water content (θ_v, cm^3 water cm^{-3} soil) as follows:

$$\varepsilon = \Phi - \theta_v \quad (1)$$

Where Φ (cm^3 pores cm^{-3} soil) is the soil total porosity.

The pore system is essential for drainage, aeration and root growth (McLaren and Cameron 1996). The proportion of O_2 and water in the pore space is altered by soil management and climate as a result of rainfall and irrigation events and will depend on the soil structure. The storage and movement of water and O_2 in any particular void of the porosity of a soil is related to the size of that void and also to its generally irregular geometry (Beven and Germann 1982). Well-structured aggregated pasture soils will typically have two distinct pore regions: the inter-aggregate regions which include the pore space between the aggregates, and intra-aggregates regions which include the pore spaces within individual soil aggregates (Ghezzehei 2012). These aggregates, as the pores, follow a hierarchical order of size and the smaller order particles do not contain the larger pores that exist in higher order particles. Elliott and Coleman (1988) proposed the following pore categories: (a) macropores (radii > 75 μm), (b) intermacroaggregate pores, (c) intramacroaggregate or intermicroaggregate pores, and (d) intramicroaggregate pores (radii < 30 μm).

Only the larger pores (macropores) also called transmission pores are effective in drainage (McLaren and Cameron 1996). The smaller pores, micropores, are effective to store water. They are generally found within, rather than between, the soil aggregates.

Water-filled pore space (WFPS), the ratio of volumetric moisture content to total porosity, has been widely used as a key parameter to describe the degree of moisture available in soil, and as a predictor of N_2O fluxes. Emissions of N_2O have been reported to result from denitrification over a range of 70–80% WFPS depending on soil type (Butterbach-Bahl *et al.* 2013). At higher

soil moistures, the major end product of denitrification favours N_2. Indeed, Friedl et al. (2018) show in their rewetting study that at 95% and 80% WFPS, denitrification was dominated by N_2 emissions, with the $N_2/(N_2+N_2O)$ ratio ranging from 0.5 to 0.9 while at 60% and 40% WFPS, the $N_2/(N_2+N_2O)$ ratio ranged from 0.2 to 0.3, showing that N_2O was the main product of denitrification. Similar results were reported by Guo *et al.* (2013). The production of N_2 at high WFPS is further facilitated by the associated decrease in gas diffusion that occurs under pronounced moisture conditions, which increases the retention time of N_2O and thus provides further time for N_2O to be denitrified to N_2 (Klefoth *et al.* 2014).

While N_2O emission from nitrification, occurs when the soil is between 35 and 60% WFPS (Bateman and Baggs 2005). Optimum WFPS for nitrification has been reported to be ~55% for fine textured soils and ~40% WFPS for coarse textured soils (Parton *et al*., 2001). Under high soil moisture, most of the soil pore spaces are occupied by water, and this negatively affects soil aeration and nitrification because of the lack of O_2. Indeed, Sexstone *et al*. (1985) measured an average intra-aggregate O_2 diffusion coefficient of 8.5 x 10^{-6} cm^2 s^{-1} for water-saturated aggregates. Diffusion of O_2 in water is slower than the diffusion in air by a factor of 10^4 times (Thorbjørn *et al.* 2008) so when O_2 is forced to diffuse through water saturated pores, this restriction on O_2 transport quickly leads to anaerobic conditions; unsuitable for nitrification. Moreover, slow rates of gaseous diffusion within soil micropores can also result in the development of anaerobic conditions favourable for some N_2O production pathways (i.e. denitrification, DNRA). The difference in the concentration of a particular gas in one zone compared with any other zone (i.e. pores/ atmosphere) in the soil results in the movement of that gas by a process called diffusion (McLaren and Cameron 1996). Soil moisture strongly influences not just the N_2O production but also its diffusion to the atmosphere (Davidson and Swank, 1986). The process of diffusion can be presented by a flow equation; Fick's law, in which the driving force is the gas concentration gradient:

$$q_d = -D_g \times \frac{dc}{dx} \quad (2)$$

Where q_d is the diffusive flux (mass diffusing across a unit area per unit of time), D_g the gas diffusion coefficient and *dc/dx* is the concentration gradient of the gas.

Soil gas diffusion governs a number of key soil ecosystem services including soil aeration and related crop productivity, and the uptake and emission of GHGs like CO_2, CH_4 and N_2O from soils. There is an increasing awareness that soil-gas dynamics and soil diffusion processes play an equally important role for soil ecosystem services (Rolston and Moldrup 2002). Soil gas diffusion is, by extension, controlled by soil water and soil structure. Soil structure is the combined effect of factors that include pore size structure, soil bulk density, tortuosity, pore connectivity, organic matter content and texture. Higher θ_v in the soil generates a decrease in soil gas diffusion, specifically due to the water bridges between soil particles causing water blockage for gas transport (Moldrup *et al.* 2000). The diffusion of a gas in soil is controlled by the magnitude of the soil-gas diffusion coefficient (D_p, cm^3 air cm^{-1} soil s^{-1}), typically represented by relative soil-gas diffusivity (D_p/D_o), the ratio between gas diffusion coefficient in soil and pure air (D_o, cm^2 air s^{-1}).

II.3.2 How useful is WFPS for predicting N_2O emissions?

When water is applied to a dry soil, a certain amount will be absorbed or stored before drainage starts. Water is held in soil pores and on the surface of soil materials. Water molecules are polar. From this polarity results the attraction of water molecules for each other (cohesion) and for other surfaces (adhesion) such as negatively charged soil mineral surfaces (Figure 13). The principle of 'capillarity' explains why soil is able to hold water against the force of gravity (McLaren and Cameron 1996). The smaller the pore diameter the greater the rise of water due

to capillarity. The soil particles are randomly arranged in the soil and as a result the pore-size distribution is also in a random distribution. The pore-size distribution will impact the drainage process of water through soil with drainage of water in micropores requiring the most suction (Chen *et al.* 2019). As showed in Figure 13 on the water retention curve, the water from inter-aggregate regions and between soil particles (silt or sand grains) will be the first to drain, followed by the meniscus water and finally the water in micropores (intra-aggregates).

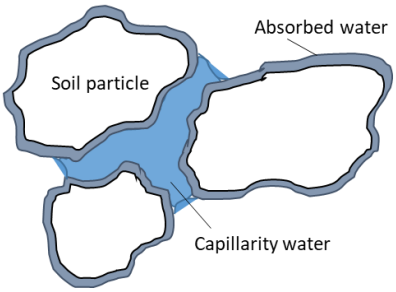

Material removed due to copyright compliance

Figure 13: Diagram of the two different type of water held in soil pores between or within aggregates (left). Drainage process of water in soil (right) from Chen et al. (2019)

A commonly used indicator to describe the soil water content in the soil is: WFPS. Expressed as a percentage, WFPS is the ratio of volumetric soil water content to total soil porosity, as follows:

$$WFPS\ (\%) = \frac{\theta_v\ (cm^3\ water\ cm^{-3}\ soil)}{\phi\ (cm^3\ voids\ cm^{-3}\ soil)} \times 100 \qquad (3)$$

Where θ_v, the volumetric water content is the volume of liquid water per volume of soil; Φ, is the soil porosity related to soil bulk density (ρ_b) and particle density of the soil's solid fraction (ρ_d) with the latter often approximated by the value 2.65 g cm^{-3}.

As mentioned above (Section II.3.1), soil WFPS has been used to describe microbial pathways and their correlated N_2O emissions, for many years (Linn and Doran 1984). WFPS has also been used as an indicator in various models, e.g. SPACSYS model (Wu *et al.* 2015) or NOE model (Hénault *et al.* 2005), to estimate the influence of environmental properties and soil management practices on N_2O emissions. However, Farquharson and Baldock (2007) state that "WFPS does not quantify the entire fraction of the soil volume filled with water or air and hence is not directly proportional to the diffusion of gases and solutes regulating process rates across soils with different total porosity". Studies have demonstrated that the use of WFPS to describe processes in a soil with different bulk densities are inadequate (Farquharson and Baldock 2007; Balaine *et al.* 2013) because soils with different soil ρ_b will have different volumes of air and water at any given value for WFPS (Figure 14). At constant WFPS (e.g. 60%, Figure 14), the air filled pore space will vary depending on the soil bulk density with values decreasing while bulk density increases (Figure 14, orange arrows). Moreover, studies (e.g. Sexstone *et al*. 1985) have shown significant rates of denitrification in unsaturated soil (medium WFPS) which can be explained by slow O_2 diffusion caused by an unappropriated pore connectivity or tortuosity, and/or by fast O_2 consumption by microorganisms.

Consequently, aerobic or anaerobic environments are ultimately determined by O_2 concentration rather than water content directly.

Figure 14: Variations in the volume fraction of air and WFPS for soils at different bulk densities. Erratum corrected (2009) from Farquharson and Baldock (2007).

II.3.3 A promising indicator: D_p/D_o

Soil gas diffusivity is a function of porous media characteristics facilitating diffusive gas migration, namely the air-filled porosity, and the tortuosity of the functional gaseous pore network. Soil gas diffusivity is generally represented as relative gas diffusivity (D_p/D_o). The soil-gas diffusion coefficient (D_p) is generally arduous to measure as it requires particular equipment in laboratory or under *in situ* conditions (Rolston and Moldrup 2002). Taylor (1950) used a Beckman O_2 analyser, Ball (1981) used radioactive krypton-85 as a trace gas and Currie (1984) used a hot wire sensor to measure D_p/D_o in the soil. In 1986, the first gas diffusion chamber was used by Rolston (1986) based on an N_2 diffusion apparatus. For this study specific diffusion chambers were used and accurate determination of the O_2 concentration in the chambers was critical to the success of the diffusion measurement.

Historically, predictive models have also been used to determine D_p/D_o. Buckingham in 1904 pioneered the research on soil gas diffusion. Since then, many models have been developed to relate D_p/D_o with Ɛ and Φ, the main ones are listed in Figure 15.

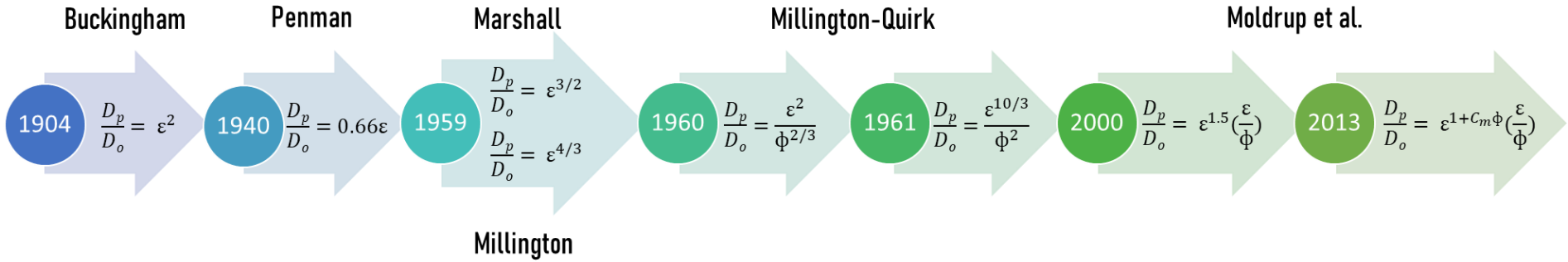

Figure 15: Gas diffusivity models: landmarks and their authors.

Until 1960, the models depended only on one parameter, Ɛ, and were obtained by fitting equations to the experimental data. The next generation of models included soil Φ along with Ɛ starting in 1960 with the Millington and Quirk models. However, these models were developed and based on assumed, ideal pore networks mostly resembling uniform sand or gravel. It was not until 2013 that Moldrup *et al.* (2013) found a flexible and easily applicable model that was successfully applied across soil types and conditions (repacked and intact soil) with the ability to express pore network complexity and water blockage effects for D_p/D_o. By including the water blockage effects in their models, Moldrup *et al.* (2013) were able to predict D_p/D_o for a range of soil ρ_b.

Existing predicted models for D_p/D_o as a function of Ɛ and Φ can be written in a general form as:

$$\frac{D_p}{D_o} = P\varepsilon^x \left(\frac{\varepsilon}{\Phi}\right)^{Ta} \quad (4)$$

With D_p the gas diffusion coefficient in soil (cm^3 air cm^{-1} soil s^{-1}), D_o the gas diffusion coefficient in free air (cm^2 air s^{-1}), Ɛ soil air content (cm^3 air cm^{-3} soil), Φ soil total porosity (cm^3 soil pore space cm^{-3} soil), and *P, x and* T_a model parameters. Moldrup *et al.* (2013) tested different models for D_p/D_o against observed D_p/D_o data and concluded that the SWLR (Structure dependent Water-induced Linear Reduction) model was best at predicting D_p/D_o for repacked and intact soils. SWLR uses $P = 1$, $x = 1+C_m\Phi$ and $T_a = 1$. This model is the only one that introduces a porous media complexity factor (C_m) that is assumed to be related to soil density and thus total porosity. This complexity factor is designated to equal 1 or 2.1 for repacked or intact soil, respectively.

Because D_p/D_o accounts for pore connectivity and continuity of the functional gaseous pore phase, while WFPS does not (Farquharson and Baldock 2007), recent studies have recognised

that D_p/D_o can be a better predictor of N_2O fluxes than WFPS. For example, Van der Weerden *et al.* (2012) demonstrated a strong correlation between D_p/D_o and log N_2O emissions from NO_3^- applied to soil cores and found that there was a 4.8 fold decrease in N_2O emissions with a small increase in D_p/D_o. Using repacked soil cores, Balaine *et al.* (2013) found that while peak N_2O emissions occurred at a given value of WFPS, this peak WFPS value varied markedly when comparing the same soil across a range of soil ρ_b. However, D_p/D_o range variation was significantly narrower for the same different soil ρ_b values and all N_2O peak emissions aligned with a value of D_p/D_o of 0.006 (Figure 16).

Figure 16: Results obtained by Balaine et al. (2013) showing the relationship of measured N_2O-N flux with water-filled pore space (left) and relative soil gas diffusivity (right) at varying soil ρ_b (Mg m^{-3}).

Chamindu Deepagoda *et al*. (2020) found measured N_2O fluxes peaked around a diffusivity window of 0.005 to 0.01 for three intact pasture soils, where the corresponding WFPS ranged from 0.80 to 0.95. Promising correlations were also reported between D_p/D_o and measured N_2O fluxes from grazed pasture (Owens *et al.* 2017; Chamindu Deepagoda *et al.* 2019) with a similar range found.

Soil-water characteristics, D_p/D_o, and pore tortuosity/connectivity are strongly linked to the soil texture, thereby making N_2O emissions also largely soil type dependent (Ding *et al.* 2019). Consequently more research is needed to better understand the relationship between D_p/D_o and soil types. There is also a dearth of studies relating soil N_2O emissions to D_p/D_o data,

specifically: detailed studies examining relationships between D_p/D_o, WFPS and N_2O fluxes for intact soils are required.

II.3.4 Physical and mechanical soil characteristics affecting water content and O_2 diffusion in the soil

In an aggregated soil system, gas diffusion occurs predominantly inside the inter-aggregate pore space when intra aggregate pores are filled with water and when sufficient time has elapsed after rainfall or irrigation. Aggregate size distribution also affects inter aggregate drainage and thus gas diffusivity for example (Jayarathne *et al.* 2020a). Hence, soil gas diffusion is strongly dependent on soil physical properties such as soil texture, structure, total porosity, moisture content and organic matter content (Brady and Weil 2013).

Soil texture is defined, as the percentage, of sand, silt, and clay sized particles in a given soil volume. Texture affects surface area and the distribution of pore size, which subsequently controls water retention and availability. Soils with smaller particles (e.g. clay and silt) have a larger surface area than those with larger sand particles and hold more water by capillarity (McLaren and Cameron 1996). The literature provides evidence for higher N_2O emissions from fine-textured soils than from coarse-textured soils (e.g. Pelster *et al.*, 2012). This is due to the anaerobic microenvironments available in fine-textured soils that occur as a result of the large number of small pores present; these microenvironments favour denitrification-mediated N_2O production. Moreover, the portion of macropores is also strongly correlated to the soil ρ_b; higher soil ρ_b results in a lower percentage of macropores in the soil (Ruser *et al.* 2008). The portion of freely draining macropores is crucial for the aeration of a soil. Indeed, Horton *et al.* (1994) reported a sharp decrease of water infiltration with increasing soil ρ_b, resulting in water

logging after heavy rainfall events. Modification of the soil structure due to compaction, limits gas transport in the soil, since it decreases air-filled pore spaces where gas diffusion occurs. Movement of agricultural machinery is one example that increases the soil ρ_b, and causes O_2 diffusion rates to decrease (Horn *et al.* 2000; Czyż 2004).

Organic matter percentage also influences water-holding capacity: as the percentage increases, the water-holding capacity increases because of the affinity that organic matter has for water (Rawls *et al.* 2003). Rawls *et al*. (2003) are one of many, to prove this relationship with all soils showing an increase in water retention with increasing organic matter content. However the amplitude of variation was higher in sandy and silty soils and a decrease was observed for the fine-textured soils with low organic carbon content (Minasny and McBratney 2018).

II.4 Irrigation systems; an option to reduce agricultural N_2O emissions?

II.4.1 World's need for irrigation

Irrigation is the artificial application of water to the soil. Irrigation is usually used in areas where irregular seasonal rainfall or droughts are expected and where agriculture needs cannot be sustained by rainfall alone. Irrigation is a tool that has been used for centuries and increasingly sophisticated methods have been developed. Irrigation systems can lift yields and provide for reliable production. Currently, irrigation for primary production is the world's largest user of fresh water (UNESCO 2017). During the twentieth century, the amount of irrigated land in the world increased exponentially with a rapid expansion from 1950-1960 (Freydank and Siebert 2008). An estimated 21% of the World's cropland is now irrigated (FAO 2012) and in developing countries, irrigated agriculture accounts for 40% of all crop production and almost 60% of cereal production (FAO 2012). In New Zealand, some 77% of allocated water is for irrigation (Minister for Environment, 2006).

Irrigation in agriculture plays a vital role in meeting the global food demand of a growing population in the context of climate change. It is projected that the World's average temperature could rise by 0.2 ºC over each of the next two decades, and by 1.1 up to 6.4 ºC this century. New Zealand is not protected from the effects of global climate change and its climate patterns are also changing. It is likely that the country can expect more frequent droughts and floods, rising sea and snow levels, and changing rainfall patterns with higher or lower levels depending on the region (New Zealand and Statistics New Zealand 2010). The National Institute of Water and Atmospheric research (NIWA) investigated different climate change projections and predicted increasing drought in the eastern regions of New Zealand. For example, in

Canterbury, which already has a high annual average Potential Evapotranspiration Deficit (PED) of 322 mm, climate projections indicate the PED will increase by over 180 mm in 2080 (Mullan *et al.* 2005). Consequently, the demand for water, both the availability and quality of the resource, will increase in the agricultural sector.

Poor irrigation management can also lead to negative environmental impacts like waterlogging, river pollution, increase in GHG emissions, water wastage and the budgetary costs associated with irrigation (FAO 2012). Irrigation itself can affect GHG emissions by altering the capacity of the soil to act as a sink or source of N_2O and CO_2.

II.4.2 Impacts of irrigation systems on N_2O emissions

Irrigation, often represents a large and a sudden increase in the amount of water which would normally pass through a soil profile under natural conditions, and has the capacity to accelerate mineral weathering, to transport and leach soluble and colloidal material, to change soil structure and moisture content. When irrigation is applied to the soil, the soil pores fill with water. After gravitational drainage, the large soil pores are filled with air and water-films, while the smaller pores are still full of water. At this stage, the soil is said to be at field capacity (FC). At field capacity, the water and air contents of the soil are considered to be ideal for crop growth. In a conventional irrigation system, farmers apply uniform irrigation across every part of the farm without considering the variabilities of the field and the water need of the crop. Therefore, this method has a reduced water-saving capability and can cause over-irrigation in some parts of the farm.

Soil moisture has been identified as one of the most sensitive factors regulating N_2O emissions from farmed soils (Section II.3) since it directly regulates O_2 availability in soil pores, which determines the activity of nitrification and denitrification within the soil profile (Schindlbacher

et al. 2004). Irrigation and rainfall events displace air from soil pores, creating the anaerobic conditions required for the activity of denitrifying microorganisms. Studies focussing on the role of irrigation cycles on N_2O losses have measured high denitrification pulses following fertiliser application, which can account for up to 90% of annual N_2O losses (Scheer *et al.* 2008; Trost *et al.* 2013). Trost *et al.* (2013), by comparing N_2O emissions from irrigated and non-irrigated fields, showed that availability of reactive N compounds increased N_2O emissions under irrigation, in most cases (Figure 17).

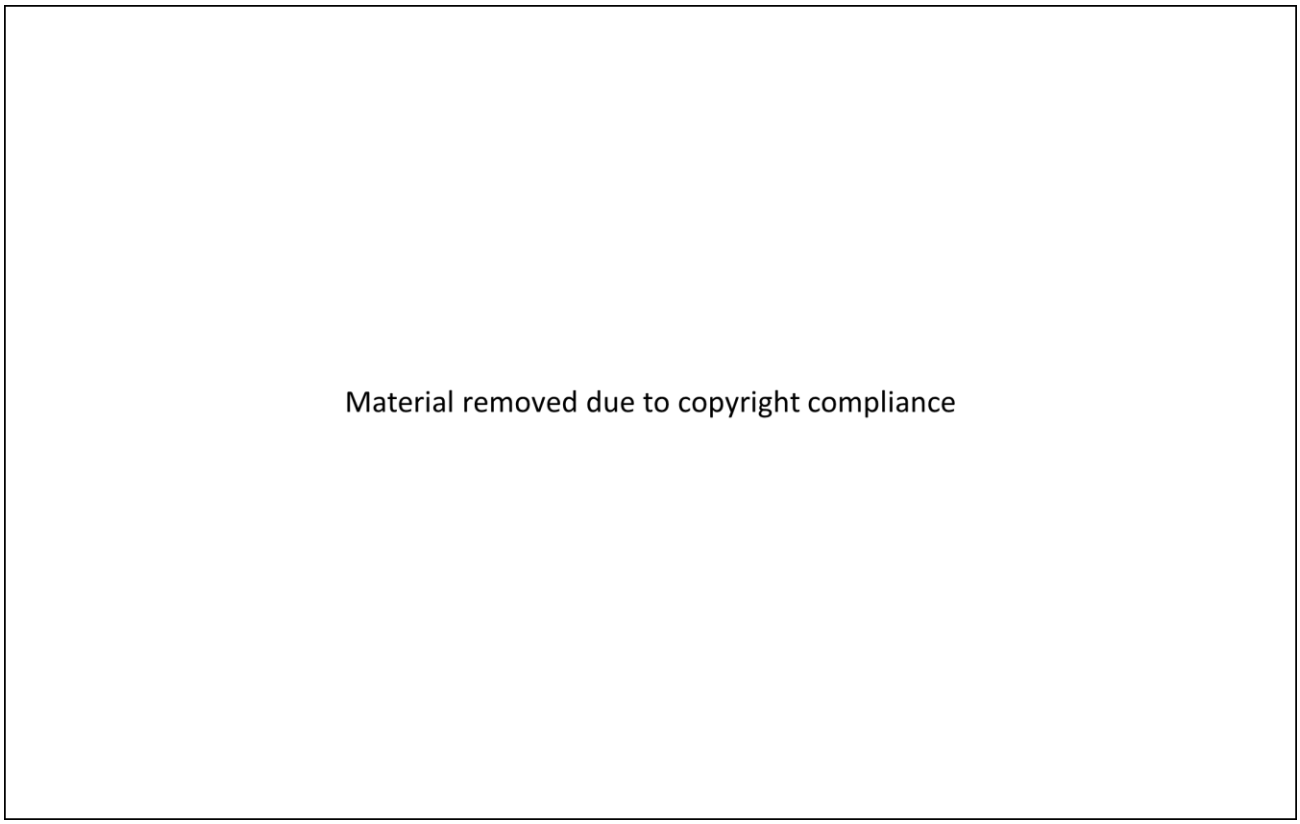

Figure 17: Changes (mean, minimum maximum) in N_2O emissions under irrigation compared with non-irrigated conditions, based on six investigations (Trost et al., 2013).

Irrigation will not only affect soil N_2O emissions via the amount of water applied in the system but also via the frequency of the application in the system.

The drying down of soil following rainfall or irrigation results in mineralisation of soil organic matter (Birch 1958). When the soil is rewetted there is a burst of CO_2, an effect previously

described as the "Birch effect" (Birch 1958; Bloem *et al.* 1992; Franzluebbers *et al.* 2000). During their study on the effect of irrigation scheduling on N_2O emissions, Mumford *et al.* (2019) suggested that higher N_2O emissions observed in a low irrigation frequency treatment (15 days interval) could be explained by the Birch effect.

Studies on arid and semiarid desert ecosystems demonstrate that wetting of previously dry soil, also has significant consequences for biological processes (such as respiration, photosynthesis and biological N fixation) which become active within seconds to hours after wetting (Austin *et al.* 2004; Abed *et al.* 2013). As a consequence of the high respiration activities, O_2 becomes limiting very rapidly, resulting in the formation of anoxic microsites (Garcia-Pichel and Belnap 1996) and thereby conditions become suitable for anaerobic processes such as denitrification and increasing N_2O emissions. Thus, application of water by irrigation and consequently higher soil moisture enhances soil microbial activity.

Wetting and drying cycles help also to break down clods of soil and produce finer aggregates (McLaren and Cameron 1996). Drying the soil assists in the aggregation of the soil into micro aggregates and wetting will cause the clay on the outside of a clod to swell quickly and crack by pressure differential. These mechanisms will cause rearrangement of particles promoting interparticle bonding that can have an impact in the gas diffusion. Soil strength is also known to decrease rapidly with increasing water content so that wet soil is generally more vulnerable to structural damage from mechanical stresses or animal disturbance. This loss of strength is due to the softening of cementing agents and the general weakening of cohesion between particles (Marshall *et al.* 1996). Irrigation places a number of stresses on soil structure and this can impact N_2O emissions.

When all these factors are considered, it is clear that irrigation has the capacity to change soil properties and influence N_2O production in soil.

II.4.3 Development opportunities to reduce N_2O production from agriculture with a focus on irrigation management

The changing times invite discussion of the sustainability of irrigated agriculture in a future where climate change is occurring, where global freshwater resources are becoming increasingly limited and where environmental pressures from legislation and the demand for food continue to increase. These pressures for improved quality and yield, for the profitable and efficient use of water and for the minimization of the environmental impacts, including N_2O emissions and N leaching, will lead to future changes in irrigated agriculture.

To mitigate N_2O emissions, research over the past recent decades has mainly focused on reducing the rate of nitrification with fewer studies examining controls on the denitrification level. Strategies to prevent N_2O emissions can be targeted at i) the input stage by minimising the N inputs to increase the NUE, improving fertiliser management, and using NI, or ii) at the output stage by decreasing the N_2O/N_2 ratio by ensuring the movement of N back to the atmosphere as N_2 or by reducing the sub-optimal conditions for nitrifiers and denitrifiers. Reduced N inputs means reduced N output and potentially decreased N_2O emissions. The 4R's of nutrient stewardship, or nutrient management demonstrates that farmers are willing to improve their nutrient applications. The 4R's stand for right source, right rate, right time, and right place and serve to guide farmers to the management practices that help keep nutrients on and in the field. However, minimising the N inputs is a delicate task considering that global agriculture and food supply is dependent on N inputs. Though the necessity of N inputs cannot be refuted, there are opportunities for the reduction of the total food chain production by reducing food waste and the meat consumption as plant products, even on protein basis, generally offer lower N footprints than meat (Pierer *et al.* 2014). The footprint indicators, trace

the losses of Nr which act as greenhouse gases and deplete stratospheric ozone (e.g. N_2O) or contribute to the formation of particulate matter, the acidification of soils and water bodies and the eutrophication of ecosystems (NH_x, NO_3^-). Thus, whereas N is crucial to sustain life on our planet, it is imperative to use it efficiently in the system (NUE) in order to prevent losses to the environment and the resulting negative impacts. Enhanced research has aimed to increase NUE of the plant and livestock while reducing Nr losses. With an average of only 30%–50% of N being taken up by the plant depending on the species and cultivar (McAllister *et al.* 2012) and an even lower average for dairy production which only convert 16 to 36% of feed (ratio of N in livestock products to the N input in feed) (Powell *et al.* 2010), there is room for improvement. The potential approaches to increase the NUE promoted in the past and for the future are the implementation of the 4R's of nutrient stewardship mentioned earlier (Noor 2017), development of advanced molecular breeding and transgenic plants to increase the use of N or biological fixation (Perchlik and Tegeder, 2017 for example) and livestock or the use of NI as mentioned in II.2.2.a section.

Suggestions can made on the potential of decreasing the soil N competition between plants and microorganisms to favour the plant NUE. Much of this competition contribution can be attributed to the anaerobic denitrifiers who favour the movement of fixed N in the soil back into the atmosphere (Thomson *et al.* 2012). Inherent to the denitrification process is also the enzymatic potential for further reduction of N_2O to N_2, so instead of decreasing N_2O production, an alternative solution to reduce emissions could be to encourage an equal amount of N_2O reduction to N_2. Complete denitrification which is known to be another important factor of N_2O productions has been under explored in prior researches. Nitrous oxide reductase activity is particularly sensitive to environmental conditions and amongst them the O_2 availability (Balaine *et al.* 2016). A general consensus is emerging that further research on

understanding the sub-optimal conditions for both nitrifiers and denitrifiers that promote N_2O production is needed.

The importance of N_2O emissions has led to the development of a variety of modelling frameworks trying to estimate the influence of soil management practices and the soil environment.

This thesis focuses on progressing a further understanding of the O_2 availability conditions based on soil gas diffusion in terms of the processes responsible for N_2O production and sinks in the soil with regards to irrigation management practices.

It is estimated that over 70% of global freshwater is consumed by irrigation. It is a context of rapid expansion of irrigation during the 20th century that motivates this research into the potential impacts that modern irrigation rates have on climate change. Farmers have slowly shifted from irrigation scheduling based on experience and assumptions to irrigation scheduling based on real-time soil-water monitoring to partially implement irrigation based on irrigation-decision support systems. However, such irrigation monitoring systems are often based on perceived plant growth requirements and soil water content and not on soil nutrient cycles or O_2 availability. As seen earlier, studies have shown an effect of varying irrigation frequency on N_2O emissions. However, D_p/D_o has not been routinely measured in irrigation studies either because WFPS or air content are considered easier to calculate or because D_p/D_o has simply not even been considered.

Moreover the potential for improved soil moisture management to reduce N_2O losses has been highlighted (Jamali *et al.* 2015, 2016; Mumford *et al.* 2019) but is still yet to be confirmed and ideally an improvement in crop NUE to be demonstrate. On top of this, optimal irrigation practices could lead to savings in N fertiliser and water use and have the potential to be adopted widely by farmers.

II.5 Scope of this thesis

Crop irrigation management practices are key for the sustainable use of water. By 2025, 1.8 billion people will be living in countries or regions with absolute water scarcity, and 2/3 of the world's population could be living under water-stressed conditions (UN-Water and FAO 2007). **Perhaps the optimisation of irrigation sits at the coalface to the ever-drying climate crisis and could be one of several solutions to decrease water waste while mitigating N_2O emissions?**

Relative gas diffusivity describes the diffusion of gas through soil relative to air. It enables the prediction of conditions aligned to N_2O generating processes that are affected by O_2 supply. Given that D_p/D_o has been shown to be a highly sensitive predictor of denitrifying conditions the aim of this research is to investigate how irrigation can be effectively managed to maximise soil D_p/D_o in order to minimise periods of anaerobic soil conditions that generate agricultural N_2O emissions mainly via denitrification. Experiments will focus on testing how robust the previous D_p/D_o thresholds found in the literature (cf. II.3.3) are as a predictor of N_2O emissions and how D_p/D_o might be used as a tool to trigger irrigation application. Field studies will also ascertain how D_p/D_o influences N_2O emissions following ruminant urine application and irrigation. Accompanying measurements will be taken on pasture dry matter (DM) yields and N content to assess N uptake and NUE, since soil gas diffusion not only influences soil microbial processes but also the root environment and thus plant growth. The potential loss of N from soil will also be determined within a pasture-soil system, in response to irrigation optimised with D_p/D_o through a lysimeter experiment.

The principal outcome of this project will be the possible demonstration of the use of a readily modelled variable D_p/D_o, that relies on simple attainable inputs (bulk density and soil

moisture), that will enable users to manage irrigation inputs so that NUE and DM production are optimised while N_2O emissions are mitigated and loss of water reduced.

- Objective 1: To enhance the understanding of D_p/D_o relative to N_2O emissions and observe its consistency across different soil types, and compare data sets against existing prediction model for D_p/D_o.
- Objective 2: To understand how wetting and draining events (D_p/D_o dynamics) influence N_2O fluxes, and through the use of ^{15}N also understand how soil N mineralization contributes to the N_2O fluxes.
- Objective 3: To better understand the effects of soil perturbations with ruminant urine and D_p/D_o manipulation, and their interaction on temporal N flows (N_2O flux dynamics, N leaching and plant N uptake).
- Objective 4: To provide information on the sensitivity of N_2O flux dynamics, within a pasture-soil system in response to optimisation of D_p/D_o through irrigation.
- Objective 5: To conclude on the outcomes of the four previous objectives for potential use of D_p/D_o as an integrated decision support for farmers' irrigation systems.

Chapter III Soil type, bulk density and drainage effects on relative gas diffusivity and N_2O emissions

This chapter has been published in 'Soil Research' the title and abstract follow below.

TITLE: Soil type, bulk density and drainage effects on relative gas diffusivity and N_2O emissions

Authors: Camille Rousset[A], Tim J Clough[A], Peter R. Grace[B], David W. Rowlings[B] and Clemens Scheer[B,C]

[A] Department of Soil and Physical Sciences, Lincoln University, PO Box 85084, Lincoln, 7647, New Zealand

[B] Queensland University of Technology, Institute for Future Environment, 2 George Street, Brisbane, Queensland, 4000, Australia

[C] Institut für Meteorologie und Klimaforschung, Department Atmosphärische Umweltforschung (IMK-IFU), KIT-Campus Alpin, Garmisch-Partenkirchen, Germany.

Received 8 June 2020, accepted 24 August 2020, published online 25 September 2020

DOI: 10.1071/SR20161

Keywords: agriculture, compaction, denitrification, relative gas diffusivity, greenhouse gas, matric potential, nitrous oxide, porosity.

III.1 Abstract

Nitrous oxide, a greenhouse gas, contributes to stratospheric ozone depletion. Agricultural fertiliser use and animal excreta dominate anthropogenic N_2O emissions. Soil relative gas diffusivity has been used to predict the likelihood of soil N_2O emissions, but limited information exists about how soil N_2O emissions vary with soil type in relation to D_p/D_o. It was hypothesised that regardless of soil type the N_2O emissions would peak at the previously reported D_p/D_o value of 0.006. Four pasture soils, sieved and repacked to three different bulk densities (ρ_b), were held at nine different soil matric potentials between near saturation and field capacity. Soil nitrate and dissolved organic matter concentrations were adequate for denitrification at all soil matric potentials. Increasing soil bulk density and soil matric potential caused D_p/D_o to decline. As D_p/D_o declined to a value of 0.006 N_2O fluxes increased, peaking at a D_p/D_o value of $\leq$ 0.006. This study shows that the elevation of N_2O fluxes as a D_p/D_o threshold of 0.006 is approached, holds across soil types. However, the variability in the magnitude of the N_2O flux as D_p/D_o declines is not explained by D_p/D_o and is likely to be dependent on factors affecting the N_2O:(N_2O+N_2) ratio.

III.2 Introduction

Nitrous oxide is a potent greenhouse gas and currently the dominant ozone depleting substance (Ravishankara *et al.* 2009). Atmospheric concentrations of N_2O have increased since preindustrial times by 23%, from 271 ppb to 333 ppb in 2020, due to land use and land use changes, especially in agriculture (Ciais *et al.* 2013; NOAA 2020). These agricultural emissions of N_2O have been predominately driven by the use of nitrogen (N) fertiliser and the deposition of animal excreta (Davidson 2009). Emissions of N_2O from agricultural soils arise from biotic and abiotic processes. Key biological pathways include nitrification, nitrifier-denitrification and denitrification (Zumft 1997; Wrage-Mönnig *et al.* 2018; Stein 2019). The relative dominance of a given biological pathway depends on substrate supply and the O_2 status of the soil. In well-oxygenated agricultural soils, fertiliser or excreta derived ammonia is oxidised, ultimately to nitrate (Figure 7). Under conditions of high ammonium supply, for example following urea fertiliser application, autotrophic ammonia oxidising bacteria (AOB) dominate nitrification (Hink *et al.* 2018) with N_2O emissions resulting from biotic and abiotic reactions of the intermediary metabolites (Stein 2019). Hypoxic conditions stimulate AOB to perform nitrifier-denitrification (Stein 2019). If the soil becomes anaerobic heterotrophic denitrification becomes the dominant process producing N_2O (Zhu *et al.* 2013; Butterbach-Bahl *et al.* 2013, II.2.2). Denitrification requires both a carbon (C) source and nitrate, or one of the obligate intermediary N compounds in the denitrification sequence, as substrates. Thus, production of N_2O from an agricultural soil is highly dependent on the soil's O_2 status, N substrate availability, and in the case of denitrification also the C supply.

Because the diffusion of a gas through water is ~$1x10^4$ times slower than in air, the effective diffusion coefficient for O_2 in soil is proportional to the volume fraction of soil that is water-filled (Farquharson and Baldock 2007). Consequently, measures of soil water content,

such as water-filled pore space (WFPS), have often been used as a predictor for determining the occurrence of denitrification. Farquharson and Baldock (2007) queried the use of WFPS as a predictor for N_2O emissions because WFPS is a normalised dimensionless value that fails to quantify the fraction of the entire soil volume that is filled with water, or air (Figure 14), and thus it is not directly proportional to the diffusion of gases. Hence, while adequate for comparing processes in a single soil with a constant soil ρ_b it becomes problematic when comparing soils with varying soil ρ_b. This was also demonstrated by Balaine *et al.* (2013) who showed that soil repacked to varying soil ρ_b, and maintained at different moisture contents, resulted in peak N_2O emissions occurring across a relatively wide range of WFPS (Figure 16). Above an upper limit of WFPS strongly anaerobic conditions also induce full denitrification, with N_2O reduced to dinitrogen (N_2). Farquharson and Baldock (2007) went on to suggest that measures of soil water content should be linked to structural parameter(s) to better describe gas diffusion in soils. Relative soil gas diffusivity accounts for pore connectivity and continuity of the functional gas pore phase: where D_p is the gas diffusion constant in the soil (m^3 soil air m^{-1} soil s^{-1}) and D_o is the gas diffusion coefficient of the same gas in free air (m^2 air s^{-1}). Accordingly, Balaine *et al.* (2013) were able to show that peak N_2O emissions were poorly explained by WFPS while a strong linear relationship ($P < 0.01$, $r^2 = 0.82$) with D_p/D_o was observed. Moreover, these N_2O peaks emissions from a soil repacked to varying soil ρ_b and held over a range of soil moisture contents aligned with a threshold value of D_p/D_o, equal to 0.006. Furthermore, Balaine *et al.* (2016) found that when examining cumulative N_2O emissions over 35 days there was an increase in N_2 emissions at D_p/D_o values < 0.006. Stepniewski (1981) reported that at a D_p/D_o value < 0.02 soils became anaerobic for plant roots. Friedl *et al.* (2018) confirmed a D_p/D_o threshold value (0.006) for denitrification-derived N_2O after applying ammonium-nitrate to subtropical pasture soils with maximum N_2O emissions at D_p/D_o = 0.006 on day 1 of the study. However, on day 2 the N_2O emissions reached their

maximum at D_p/D_o = 0.0068 with the shift thought to result from residual O_2 at day one and increasing anaerobic conditions on day 2, resulting in the enhanced reduction of N_2O to N_2 and/or the entrapment of denitrified N_2O in the soil. Thus the relationship between D_p/D_o and N_2O flux potentially alters with biological O_2 demand. After incorporating high C residues into a cropping system high N_2O fluxes were observed at calculated D_p/D_o values > 0.02, a value considered as a threshold for anaerobiosis (Stepniewski 1981), which was postulated to be due to the high C inputs increasing O_2 demand and denitrification activity (Petersen *et al.* 2013). In grazed pastures C inputs include root exudation and mineralisation of soil organic matter and these will vary with climate, soil fertility, management and soil type. Hence, the laboratory defined threshold for peak N_2O emissions, recorded by Balaine *et al.* (2013) for only one soil, may shift due to increased O_2 demand in different soil types. Interestingly, however, Owens *et al.* (2017) found that after applying ruminant urine to a pasture soil in situ, that the N_2O emissions only increased substantially when D_p/D_o values declined to ~ 0.006, consistent with the laboratory observations of Balaine *et al.* (2013; 2016) and Friedl *et al.* (2018). Further evaluation of N_2O emissions in relation to D_p/D_o, under controlled conditions for a range of soils, is still required to better understand the robustness of this threshold.

Thus, the objectives of this experiment were to further evaluate soil D_p/D_o in relation to the occurrence of N_2O emissions, under controlled conditions, across a wider range of soils, under a range of soil bulk densities and moistures in order to better validate the results obtained by Balaine *et al.* (2013; 2016). It was hypothesised that

i) the interactive effects of soil bulk density and water content on D_p/D_o, would result in elevated emissions of N_2O when the value of D_p/D_o declined to a threshold close to 0.006,

ii) the robustness of D_p/D_o as an indicator for N_2O emissions would be consistent across different soils and,

iii) D_p/D_o would indicate the onset of elevated N_2O emissions better than WFPS.

III.3 Materials and methods

III.3.1 Soil collection and experimental design

Four pasture soils were sampled (0-15 cm depth) in spring 2017: a Wakanui silt loam (Mottled Immature Pallic Soil) was collected from the dairy farm at Lincoln University (43°38'41.3"S; 172°26'34.6"E); a Waipara loam soil (Mottled-argillic Fragic Pallic Soil) was collected from a hill country farm at Limeworks Road, North Canterbury (42°58'2.28"S; 172°38'19.68"E); a Temuka silty loam (Typic Orthic Gley Soil) was collected from a dairy farm near Lincoln (43°39'11.88" S; 172° 29' 22.92" E); a well-drained Otorohanga loam, (Typic Orthic Allophanic Soil), was collected at Ruakura, AgResearch, Hamilton. (37°46'44.9"S 175°18'47.6"E). Soil classifications are as defined by Lilburne *et al.* (2012). Soils were air-dried and sieved to ≤ 2 mm and the gravimetric water content was determined (Blakemore *et al.* 1987). Soil particle densities (ρ_d) and particle sizes (Table 2) were analysed using recognised methods (Hao *et al.* 2008; Kroetsch and Wang 2008). The soil particle density for each soil was determined using pycnometers (Flint and Flint 2002). The pycnometers containing 10 g of air-dry soil sample were half filled with de-aired distilled water. Any soil adhering to the inside of the neck of the pycnometer was washed down. The entrapped air was removed by placing the pycnometer into a vacuum chamber (Figure 18) and by slowly applying a vacuum while being careful not to let the bubbles release soil from the bottle. Enough de-aired water was then added to fill the pycnometer. Then the stopper was carefully inserted to force the excess water out of the capillary.

The particle density (ρ_d) was calculated as follows:

$$\rho_d = \frac{[\rho_w(W_s - W_a)]}{[(W_s - W_a) - (W_{sw} - W_w)]} \quad (5)$$

where ρ_w is the density of water (g cm^{-3}) at the temperature observed, W_s is the weight of the pycnometer plus soil sample corrected to oven-dry water contents, W_a is the weight of the pycnometer filled with air (g), W_{sw} is the weight of the pycnometer filled with soil and water (g) (Figure 18), and W_w is the weight of the pycnometer filled with water (g) at the temperature of the observation.

Figure 18: Stoppered bottles used in the pycnometer method to determine particle density (left) and the vacuum chamber setup used to remove the air from the soil and the water (right).

Soil organic C contents (Table 2) were determined by loss on ignition (Blakemore *et al.* 1987). Repacked soil cores were constructed by compacting sieved soil to a depth of 5 cm into stainless steel (SS) rings (7.3 cm internal diameter, 7.4 cm deep) at ρ_b designated by treatment. The SS-rings had a fine nylon mesh placed over the bottom of the ring to prevent soil egress.

Table 2: Soil (0-10 cm) texture, particle density and carbon contents. Texture analyses were performed using a laser diffraction particle analyser (Mastersizer 3000, Malvern Panalytical)

	Wakanui		Waipara		Temuka		Otorohanga	
	IUSS[a]	USDA[b]	IUSS	USDA	IUSS	USDA	IUSS	USDA
Clay (%)	22.3	22.3	9.9	9.9	14.5	14.5	11.3	11.3
Silt (%)	53.4	72.1	22.2	46.8	34	55.7	39.7	66.6
Sand (%)	24.3	5.6	67.9	43.3	51.5	29.8	48.9	22.1
Particle density (g cm^{-3})[c]	2.59 ± 0.01		2.65 ± 0.02		2.61 ± 0.02		2.46 ± 0.02	
Carbon (%)[d]	1.57 ± 0.06		1.17 ± 0.15		1.85± 0.10		2.21 ± 0.12	

[a]International Union of Soil Science (Clay 0-2 µm, silt 2-20 µm, and sand 20-2000 µm),
[b]United States Department of Agriculture (Clay 0-2 µm, silt 2-63 µm, and sand 63-2000 µm) U.K.),
[c]Hao *et al*. (2008),
[d]Based on loss on ignition (Blakemore *et al*., 1987).

The experimental design consisted of 4 soils, 3 levels of soil ρ_b for each soil, and 9 levels of matric potential (-0.5, -1.0, -2.0, -3.0, -4.0, -5.0, -6.0, -8.0, and -10.0 kPa), replicated four times. Soil ρ_b treatments for the Wakanui, Waipara, and Temuka soils were set at either 1.0, 1.1 or 1.2 Mg m^{-3}. However, due to the allophanic nature of the Otorohanga soil and the relatively high organic matter content it could not be packed at 1.2 Mg m^{-3} and so the soil ρ_b treatments for the Otorohanga soil were set at either 0.9, 1.0, or 1.1 Mg m^{-3}.

So that the soil cores had excess NO_3^--N substrate available for denitrification the soil cores were pre-soaked in a KNO_3 solution (1800 µg mL^{-1} NO_3^-–N) for 2 days prior to being placed on the tension tables. The aim of this was to better enable observations of the effects of soil characteristics (bulk density, matric potential and organic matter content) on N_2O emissions. Soil tension tables (Figure 19) were prepared as described by Romano *et al.* (2002).

They allowed soil drainage - water retention characteristics to be determined over the range of 0 to -10 kPa. For this experiment, the tension table was made off one layer of sand and three layers of silica flour allowing a maximum suction of -10 kPa. Depending on the height of the water column between the water bottle reservoir and the porous barrier surface (Figure 19), different constant water suctions could be obtained up to approximately 1 m of 'hanging' water (-10 kPa).

Figure 19: Tension table setup

Soil cores were placed on the tension tables to equilibrate for 4 days. Before placing soils cores on the tension tables, 10 mL of the KNO_3 solution were poured evenly across the tension tables to provide a good connection between soil cores and the tension table. Soil cores were weighed daily to determine when the equilibrium at the desired matric potential was achieved. It was physically impossible to run all soil cores simultaneously. Thus, a total of 108 soil cores (3 levels of soil ρ_b x 9 levels of soil ψ x 4 types of soil) were on the tension tables at any given time (one replicate), with subsequent replicates run in batches (Balaine *et al.* 2013). Using a new set of cores, with air-dried repacked soil for each replicate, ensured that the initial soil

NO_3^- concentration and soil conditions were the same for each replicate. The tension tables were sited in a room where the temperature fluctuations were negligible (20 ± 1°C).

III.3.2 Nitrous oxide and relative gas diffusivity measurements

Nitrous oxide fluxes were measured after soil cores had attained equilibrium on the tension table (4 days). Each soil core was placed in a 1 L mason jar, which was then sealed with an air-tight lid equipped with a septum. Gas samples (10 mL) were taken at 0, 15, and 30 min after sealing using a 25G hypodermic needle attached to a 3-way stopcock that was in-turn connected to a 20 mL glass syringe (Figure 20).

Figure 20: Gas sampling setup showing soil cores inside gas-tight 1 L jars.

Collected gas samples were injected into pre-evacuated 6 mL Exetainer® vials. Immediately prior to analysis the gas samples were brought to ambient pressure and then analysed for N_2O on a gas chromatograph (Clough *et al.* 2009a). Reference gases, N_2O in N_2 (0.2 ± 0.004, 1.0 ± 0.01, 2.0 ± 0.04, 5.0 ± 0.1, supplied by BOC Gas New Zealand) were used for constructing

standard curves. The change in N_2O concentration over time was used to calculate N_2O fluxes (Hutchinson and Mosier 1981) using the following equation:

$$F_{N2O} = \frac{V_c(C_1 - C_0)^2}{(2C_1 - C_2 - C_0)} ln\left[\frac{C_1 - C_0}{C_2 - C_1}\right] \frac{P \times M \times C}{[G_c(T_k - T_c)A_c t_1]} \qquad (6)$$

Where:

F_{N2O} = nitrous oxide flux (µg N_2O-N m^{-2} h^{-1}),

C_0 = N_2O concentration at time t_o (µL L^{-1} = ppm),

C_1 = N_2O concentration at time t_1 (15 or 20 min) (µL L^{-1} = ppm),

C_2 = N_2O concentration at time t_2 (30 or 40 min) (µL L^{-1} = ppm),

P = atmospheric pressure = 101325 (Pa),

V_c = chamber volume (m^3),

A_c = chamber area (m^2),

G_c = Gas constant = 8.314 (J mol^{-1} K^{-1})

T_k = absolute temperature at 0°C = 273.15 (K)

T_c = air temperature (°C)

M = molecular weight of N_2O-N = 28.0134 (g mol^{-1})

C = minutes/hour = 60

t_o = start of cover period (min),

t_1 = t_2 / 2 (min),

t_2 = total cover period =30 min.

Measurements of D_p/D_o were performed after N_2O emission measurement using the method described by Rolston and Moldrup (2002). In brief repacked soil cores were positioned, isolated, inside a chamber that was flushed with an O_2-free gas mixture (90% Ar and 10% N_2) until the chamber was O_2 free (Figure 21). Then, the soil core base was connected to the chamber, allowing ambient air to diffuse through the soil core into the chamber. A pre-calibrated sensor (KE-12, Figaro Inc.) recorded the increase in the O_2 concentration in the chamber. In the sensor, O_2 molecules diffuse through a non-porous fluorine resin membrane into an electrochemical cell. The electrical current that flows between the electrodes (lead anode and gold cathode) is proportional to the O_2 concentration. The signal was read as terminal voltages across the electrodes, with the change in output voltages representing the change in O_2 concentration. Sensors were calibrated using an N_2/Ar gas misture with 0% O_2 and ambient air (0 and 21% O_2, respectively).

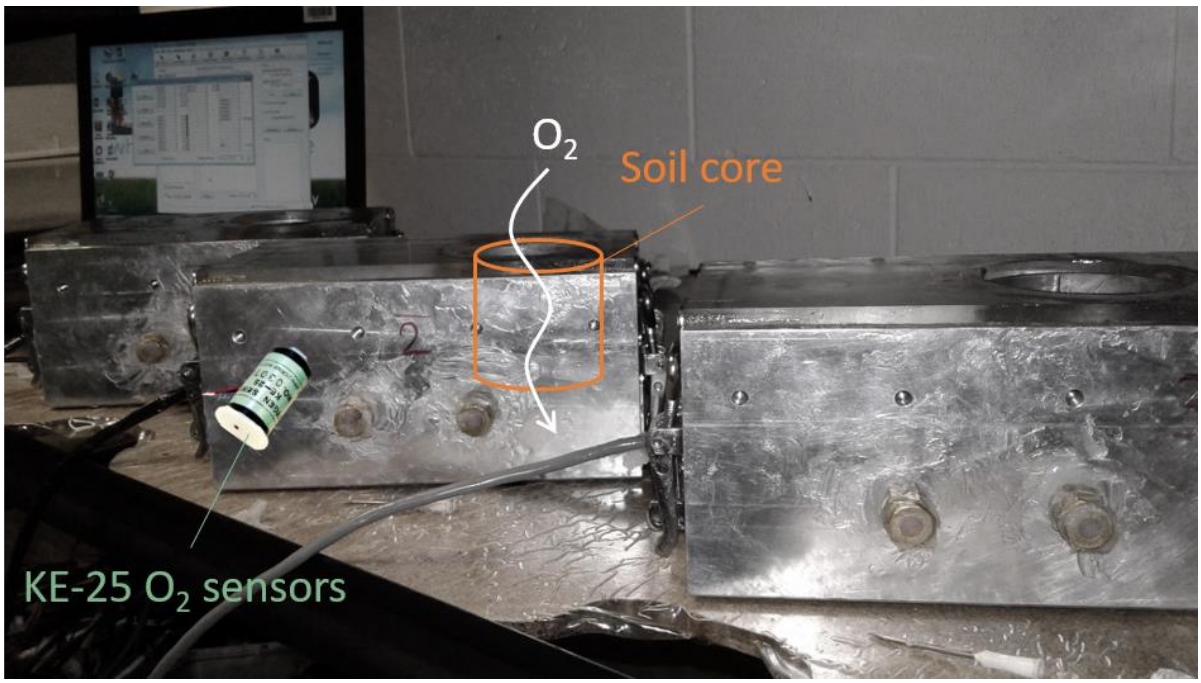

Figure 21: Diffusion chambers apparatus made O_2 free containing a soil core and a KE-25 O_2 sensors connected to a datalogger (not present in the picture).

Subsequently, the method of Rolston and Moldrup (2002) was used to calculate D_p/D_o. The natural logarithm of the relative concentration of O_2 in the chamber (ln Cr) was calculated where Cr was calculated as follows:

$$C_r = \frac{(C_g - C_s)}{(C_0 - C_s)} \quad (7)$$

Where C_g is the concentration of O_2 in the chamber at a time t, C_0 is the concentration of O_2 in the chamber at the beginning of the experiment (= 0) and C_s is the O_2 concentration (=20.9%) above the soil core. The linear slope of the plot of ln C_r vs. *t* was determined (Figure 22) and is equal to:

$$\frac{-D_p \alpha_1^2}{\varepsilon} \quad (8)$$

Then D_p was determined using the calculated value of ε and the value of α_1 taken from Table 46-1 in Rolston and Moldrup (2002). The soil gas diffusion coefficient in air (D_0) was calculated according to the Currie (1960).

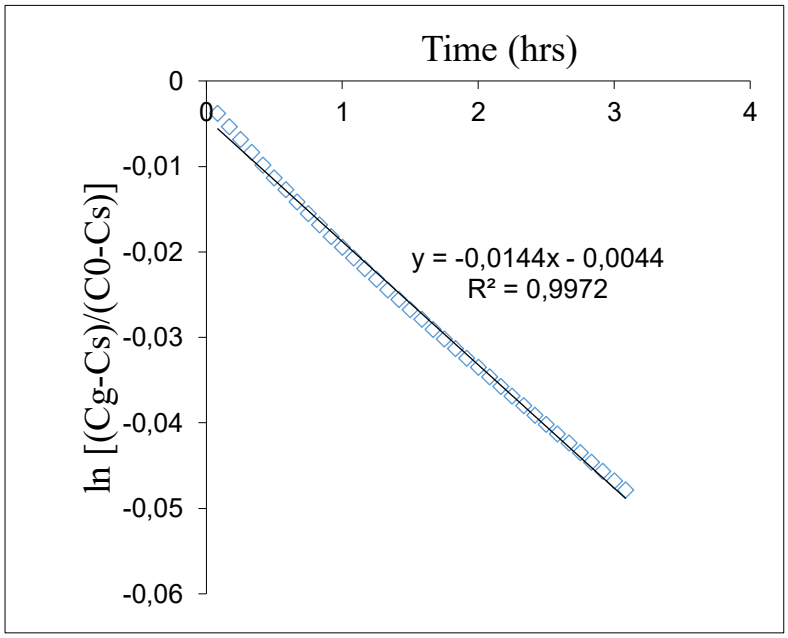

Figure 22: Example of ln (Cr) vs time graph plotted to measure the diffusion coefficient (D_p) in the soil cores. The black line was obtained by fitting linear regressions to the data. The linear slope of the line (= – 0.0144) corresponded to $-D_p \alpha_1^2/\varepsilon$.

III.3.3 Soil analyses

After taking N_2O samples and measuring D_p/D_o the soil cores were extruded into a Ziploc® plastic bag. The soil was well mixed before taking a 10 g subsample to determine gravimetric water content, at 105ºC for 24 h. A calibrated flat surface pH electrode was used to measure the pH of the extruded-mixed soil (Broadley James Corp., Irvine, CA.). The equivalent of 4 g of dry soil were extracted with 40 mL of 2M KCl for 1 h to determine inorganic-N concentrations. After filtering (Whatman 42) the extracts were analysed for NO_3^--N and NH_4^+-N on a flow injection analyser (Blakemore *et al.* 1987). Soil inorganic N concentrations were determined using the equation as follows:

$$N = \frac{N_i \times V}{m} \quad (9)$$

Where:

N = inorganic N content (µg g^{-1} dry soil),

N_i = inorganic N concentration in KCl extract (µg mL^{-1}),

V = volume of KCl extract (mL) and

m = weight of dry soil (g)

Similarly, dissolved organic carbon (DOC) was extracted using 5 g equivalent of dry soil and 30 mL of deionised water shaken for 30 minutes prior to centrifugation (3,500 rpm for 20 minutes) and filtration (Whatman 42), with analyses performed on a Shimadzu TOC analyser (Shimadzu, Oceania Ltd., Sydney, Australia). Soil DOC concentrations were determined using the equation as follows:

$$C = \frac{C_i \times V}{m} \quad (10)$$

Where:

C = dissolved organic C content (µg C g^{-1} dry soil),

C_i = total C concentration in H_2O extract (µg C mL^{-1}),

V = volume of H_2O extract (mL) and

m = weight of dry soil (g)

III.3.4 Statistical analyses

Statistical analyses were performed using R studio (Version 1.1.447, RStudio Team 2016), also used to create the graphics presented in this thesis using "ggplot2" package. Before any statistical analysis were made, data were visually tested for normality, residual repartition and the homoscedasticity. The function "shapiro.test" was used to double test the normality of the residues. If the value of the Shapiro-Wilk Test was greater than 0.05, the data was normal. If it is below 0.05, the data significantly deviate from a normal distribution and then the best fit transformation was applied using the "bestNormalize" as a decision tool. The package is built to estimate the best normalizing transformation for a vector consistently and accurately. The log transformation was the transformation adopted for this thesis if transformation need it. The outliers in a linear regression model were detected by plotting the residuals vs leverage and using cook's distance line as an indicator of the effect of deleting a point on the combined parameter vector.

A repeated measures analysis, using two-way ANOVA, with matric potential and soil ρ_b as factors, was used to test for overall treatment differences between measured variables, with Tukey's post-hoc test used to determine specific differences between means with the least significant set to 5% level. Comparisons were made between soil ρ_b treatments within soils and

across matric potential, and where common soil ρ_b occurred comparisons were made across soils. The variables used for the statistical tests are summarised in the Appendix 4 table.

Most of the graphics present the averages of the replicates (minimum 3) and in the absence of any notification, the error bars are the standard error of the mean (s.e.m) and calculated as follows:

$$S.E.M = \frac{\sigma}{\sqrt{n}} \quad (11)$$

With σ the standard deviation of the mean and n the sample size.

III.4 Results

III.4.1 Soil chemical and physical properties

Soil pH varied with soil type ($P < 0.05$): averaged across soil matric potential the Waipara, Otorohonga, Temuka and Wakanui soils had soil pH values of 5.15, 5.28, 5.73 and 6.00, respectively. As drainage increased (more negative soil matric potential) the soil pH within each soil also decreased ($P < 0.05$; Figure 23). The most significant decrease in soil pH was observed in the Wakanui soil: at -0.5 kPa, soil pH ranged from 6.34 to 6.41 and then declined to range from 5.67 to 5.70 at -10 kPa. For each soil type, increasing soil ρ_b generally resulted in an increase in soil pH at all levels of soil matric potential ($P < 0.05$; Figure 23).

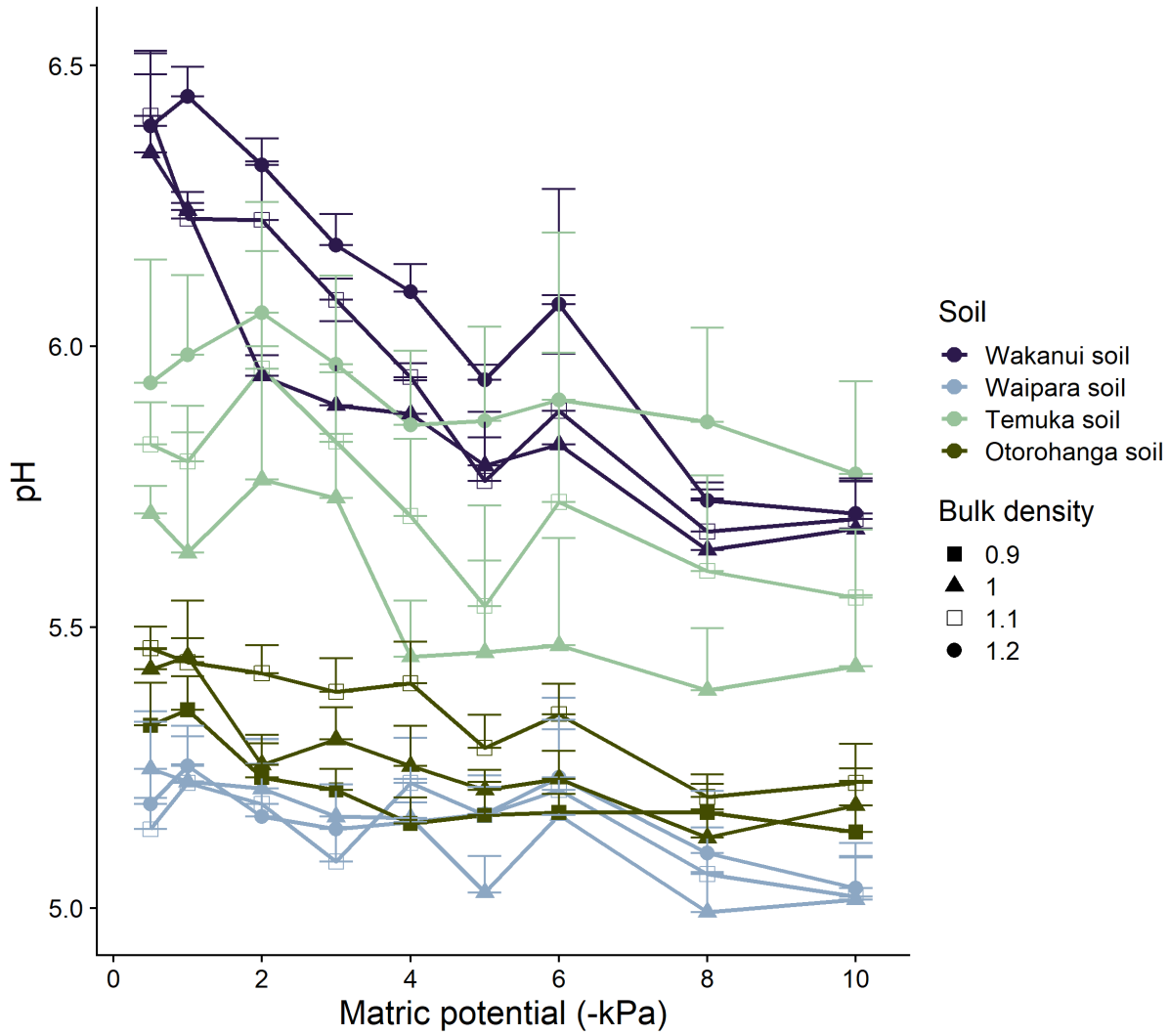

Figure 23: Mean soil pH versus soil matric potential. Numerals in the legend indicate soil bulk density treatments applied (Mg m^{-3}). Error bars = s.e.m, n=4.

Soil DOC concentrations varied with soil type ($P < 0.05$): averaged across soil matric potential the Waipara, Otorohonga, Temuka and Wakanui soils had DOC concentrations of 75, 114, 162, and 208 µg g^{-1} soil, respectively. These soil DOC concentrations either remained relatively stable (Temuka and Waipara soils) or tended to decline (Wakanui and Otorohanga soils) as soil matric potential became more negative (Figure 24), however, there was no significant interaction between soil ρ_b and soil matric potential on DOC concentrations within a given soil ($P > 0.05$). Neither soil ρ_b, or soil matric potential, caused significant changes to DOC concentration for the Waipara or Temuka soils ($P > 0.1$). However, in the Wakanui and

Otorohonga soil, DOC concentrations varied with soil ρ_b ($P < 0.05$): DOC concentrations were higher for the highest soil ρ_b (1.2 and 1.1 Mg m^{-3}) than for the lowest soil ρ_b (1 and 0.9 Mg m^{-3}). In these same soils the soil DOC concentrations were significantly lower at -8 and -10 kPa than at -0.5 and -1 kPa ($P < 0.05$, Figure 24).

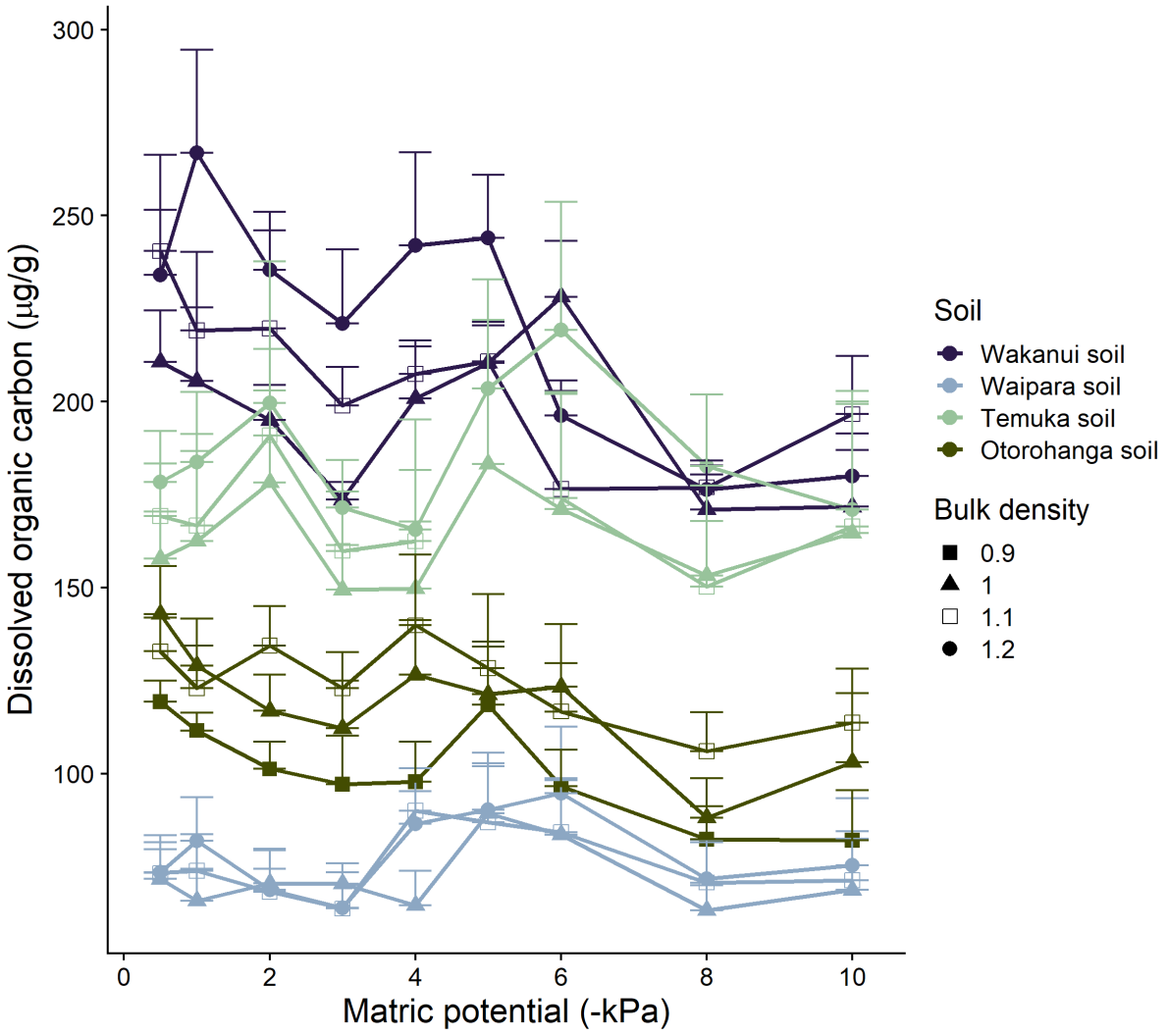

Figure 24: Mean dissolved organic carbon concentration (mg g–1) versus soil matric potential. Numerals in the legend indicate soil bulk density treatments applied (Mg m^{-3}). Error bars = s.e.m, n = 4.

There was no consistent effect of soil matric potential on soil NO_3^--N concentrations (Figure 25). However, soil ρ_b did affect soil NO_3^--N concentrations in the Wakanui soil when averaged across soil matric potential: at 1.0 Mg m^{-3} these were higher ($P < 0.05$) than at 1.1 Mg m^{-3} and 1.2 Mg m^{-3}. In the Temuka soil the NO_3^--N concentrations also declined ($P <$

0.05) as soil ρ_b increased, when averaged across soil matric potential, equalling 741, 644 and 555 mg NO_3^--N kg^{-1} of soil, at soil ρ_b of 1.0, 1.1 and 1.2 Mg m^{-3}, respectively. Similarly, in the Otorohanga soil at a soil ρ_b of 0.9, 1.0 and 1.1 Mg m^{-3} average NO_3^--N concentrations equalled 751, 688 and 604 NO_3^--N kg^{-1}, respectively ($P < 0.05$). The Waipara soil was the only soil where NO_3^--N concentrations did not vary with soil ρ_b.

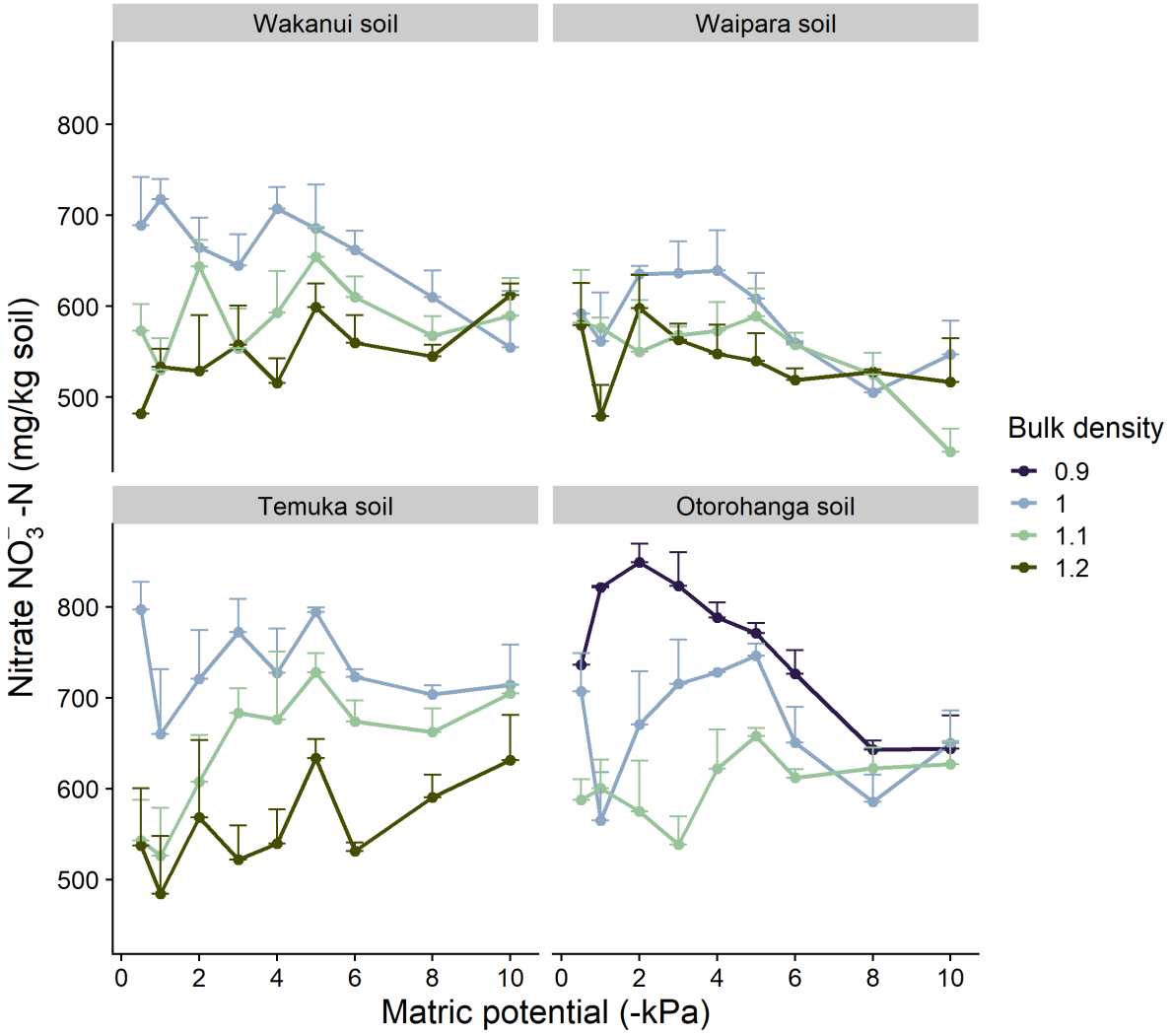

Figure 25: Soil nitrate concentrations versus soil matric potential for the four soils. Numerals in the legend indicate soil bulk density treatments applied (Mg m^{-3}). Error bars = s.e.m, n=4.

As expected, the soil WFPS decreased with progressively more negative soil matric potentials ($P < 0.05$) but the rate of decrease varied with soil type: averaged across soil matric potential and soil ρ_b, the Wakanui, Otorohonga, Waipara and Temuka soils had WFPS values of 85.4%, 85.7%, 86.3% and 90.6%, respectively and ranged from 60.0% to 97%, 55.1% to 100%, 61.4% to 100% and 68.7% to 100%, respectively. Soil WFPS also varied with soil ρ_b ($P < 0.05$) with the lowest WFPS observed at the lowest soil ρ_b; 1 Mg m^{-3} for the Wakanui, Waipara and Temuka soils and 0.9 Mg m^{-3} for the Otorohanga soil. An interaction between soil ρ_b and matric potential resulted in WFPS declining at a faster rate at lower soil ρ_b values for all soils, except the Waipara soil (Figure 26).

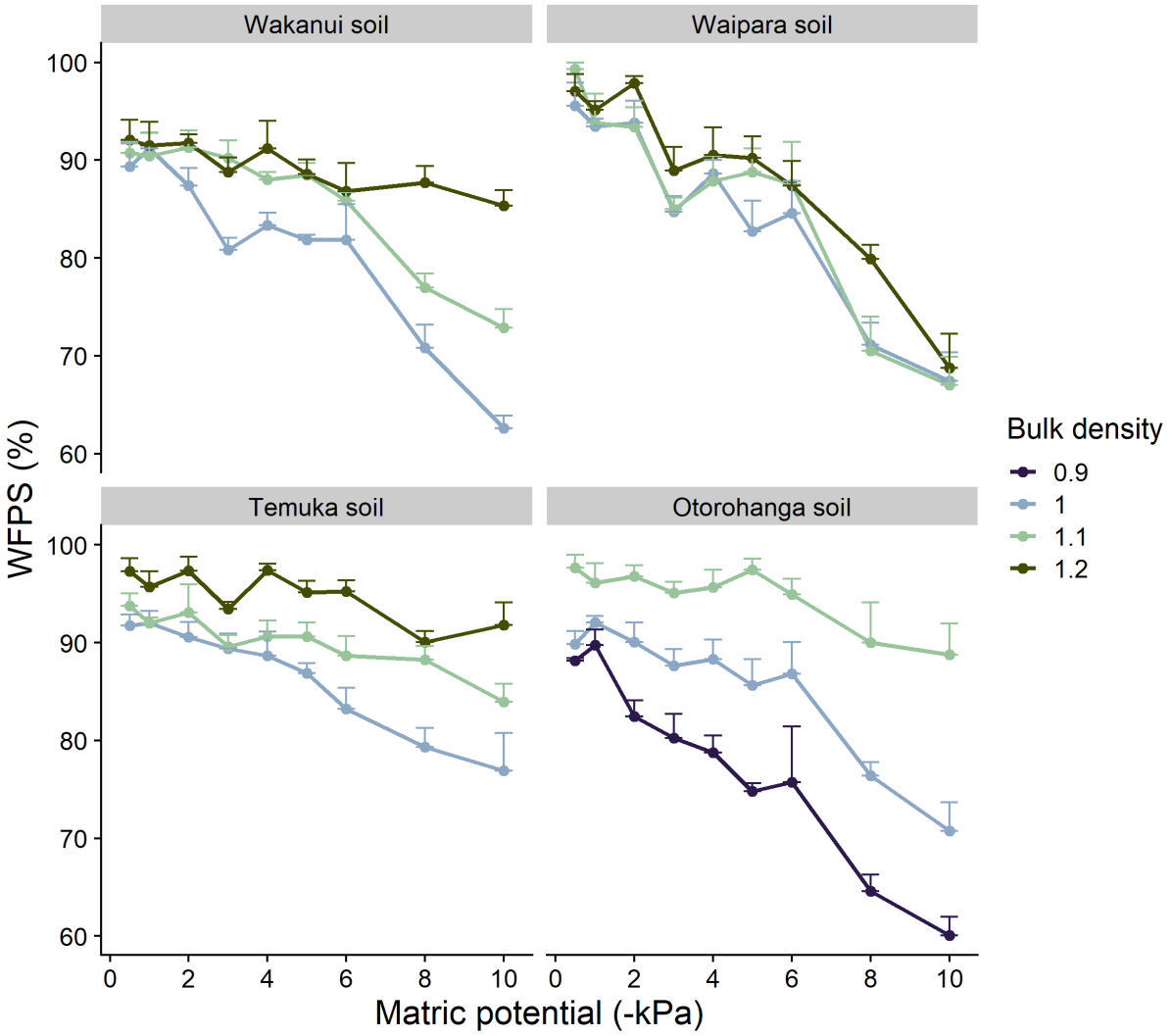

Figure 26: Water-filled pore space (WFPS, %) versus soil matric potential for the four soils. Numerals in the legend indicate soil bulk density treatments applied (Mg m^{-3}). Error bars = s.e.m, n= 4.

The range in measured mean D_p/D_o across the soil matric potential treatments, when averaged across all soil ρ_b treatments, was 0.003 to 0.014 for the Wakanui soil, 0.003 to 0.015 for the Waipara soil, 0.004 to 0.007 for the Temuka soil and from 0.005 to 0.017 for the Otorohanga soil. An interaction between soil ρ_b and soil matric potential affected D_p/D_o in the Wakanui soil where D_p/D_o at 1.2 Mg m^{-3} was lower ($P < 0.05$) than D_p/D_o at 1.0 Mg m^{-3} for soil matric potentials lower than -2 kPa (Figure 27). The same was observed in the Temuka soil except that D_p/D_o values were significantly lower at 1.2 Mg m^{-3} compared to values at 1.0 Mg m^{-3}, for soil matric potentials lower than -3 kPa (Figure 27). Similarly, the D_p/D_o values

for the 1.0 and 1.1 Mg m^{-3} were lower for the 0.9 Mg m^{-3} treatment in the Otorohanga soil below -2kPa (Figure 27). However, in the Waipara soil there was no effect of soil ρ_b on D_p/D_o (Figure 27). A plot of D_p/D_o versus soil air-filled porosity showed the D_p/D_o values occurred over a range of air-filled porosity from zero to 0.3 cm^3 cm^{-3} (Figure 28).

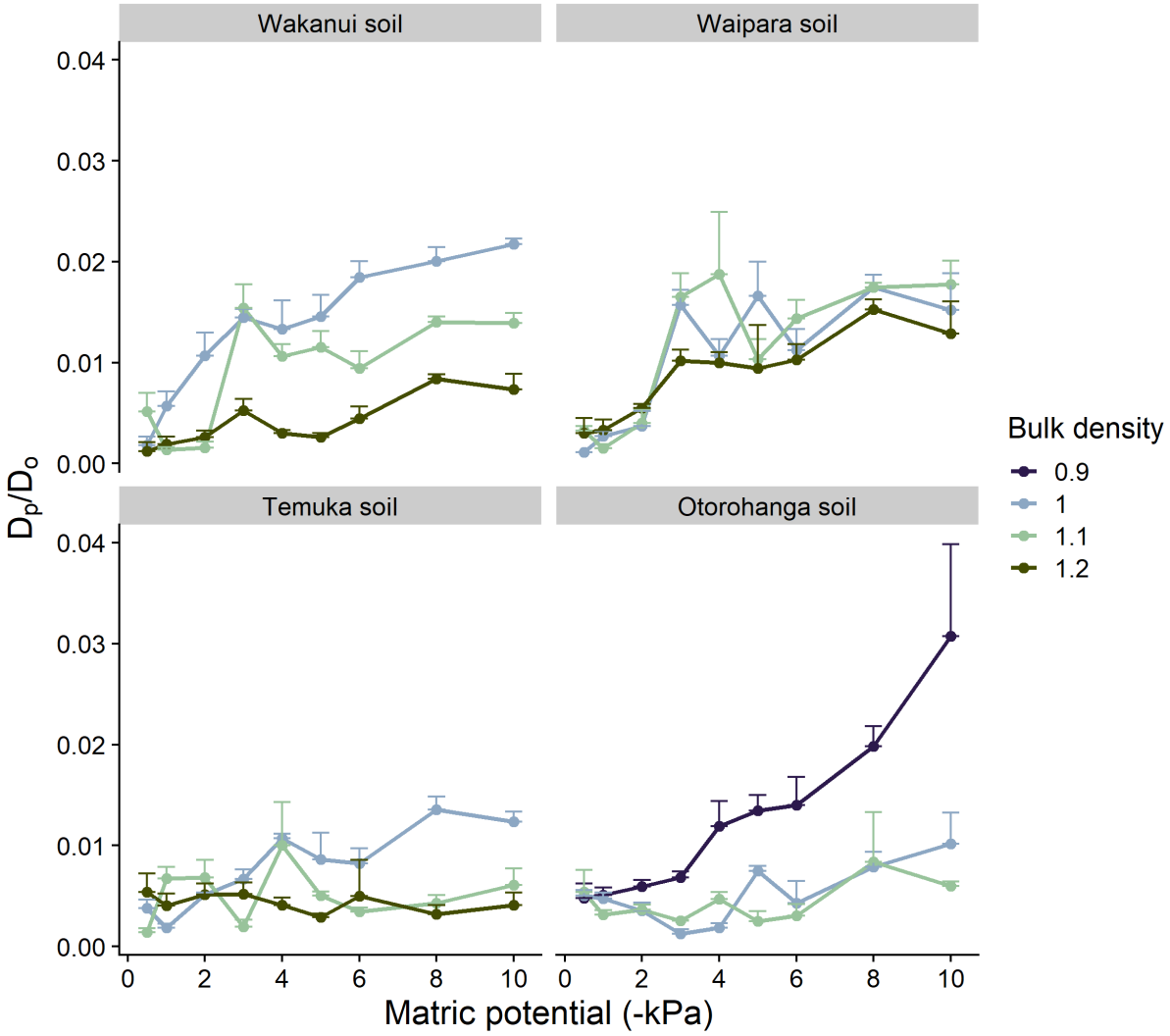

Figure 27: Relative gas diffusivity (D_p/D_o) at varying soil bulk density and soil matric potential. Numerals in the legend indicate soil bulk density treatments applied (Mg m^{-3}). Error bars = s.e.m., n= 4.

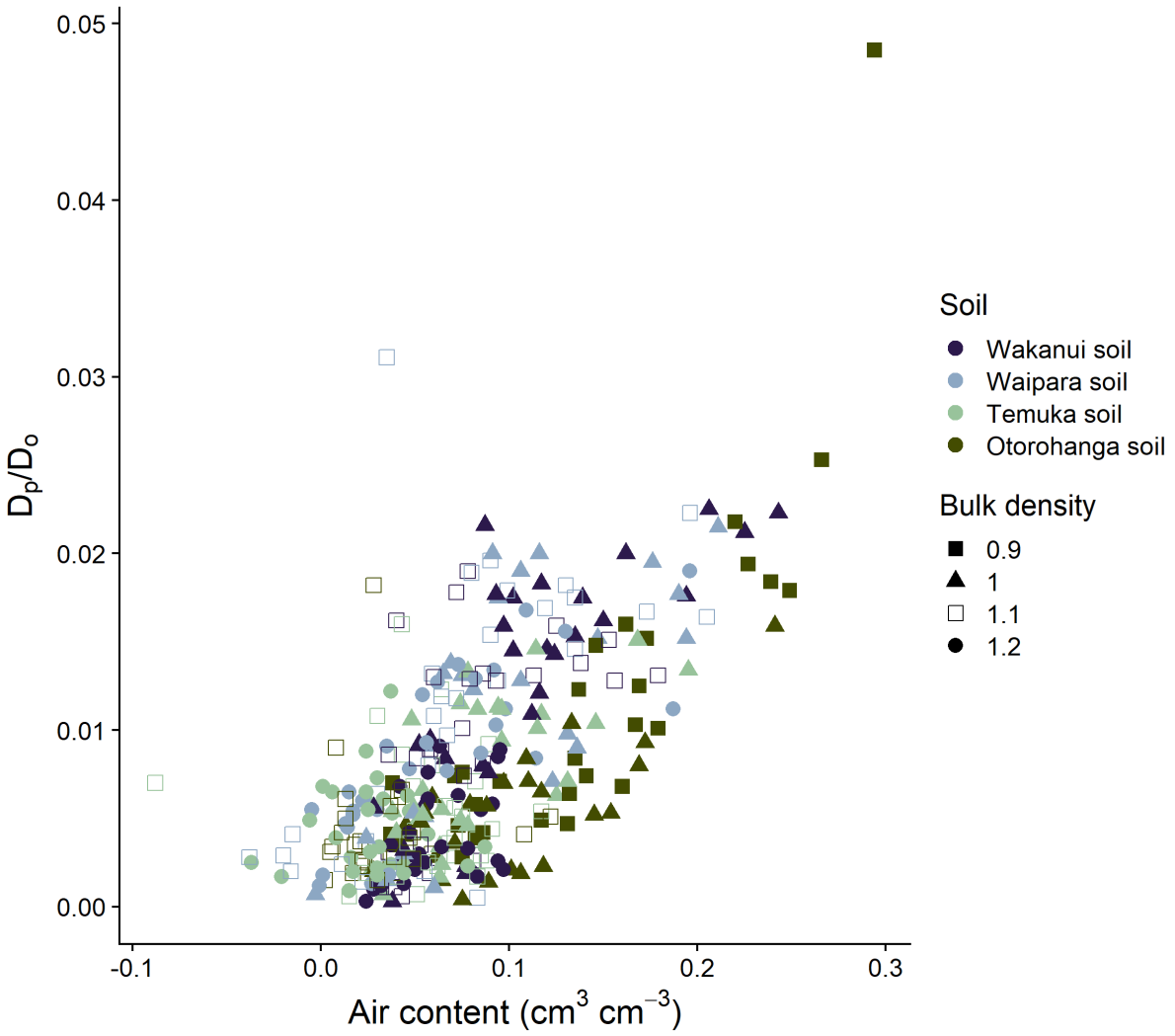

Figure 28: Soil relative gas diffusivity (D_p/D_o) versus soil air-filled porosity (cm^3 cm^{-3}).

III.4.2 Soil N_2O fluxes and relationships with soil physical parameters

For each soil, the N_2O-N fluxes were highest at the lowest soil matric potential (-0.5 kPa), with N_2O-N fluxes decreasing as the soil matric potential decreased (Figure 29). The range in the N_2O-N fluxes varied with soil type ($P < 0.05$). The highest fluxes occurred in the Otorohanga soil (from 0.12 to 691 mg m^{-2} h^{-1}), closely followed by the Wakanui soil (from 0.08 to 660 mg m^{-2} h^{-1}). The Temuka soil N_2O-N fluxes ranged from 0.22 to 408 mg m^{-2} h^{-1}

while the lowest N_2O-N fluxes occurred in the Waipara soil ranging from 0.07 to 124 mg m^{-2} h^{-1}. The soil total N_2O-N fluxes were higher with increasing soil ρ_b ($P < 0.05$) and in the Temuka and Otorohanga soils where soil ρ_b and soil matric potential interacted ($P < 0.05$): soil N_2O-N fluxes decreased more slowly at the highest soil ρ_b as soil matric potential became more negative.

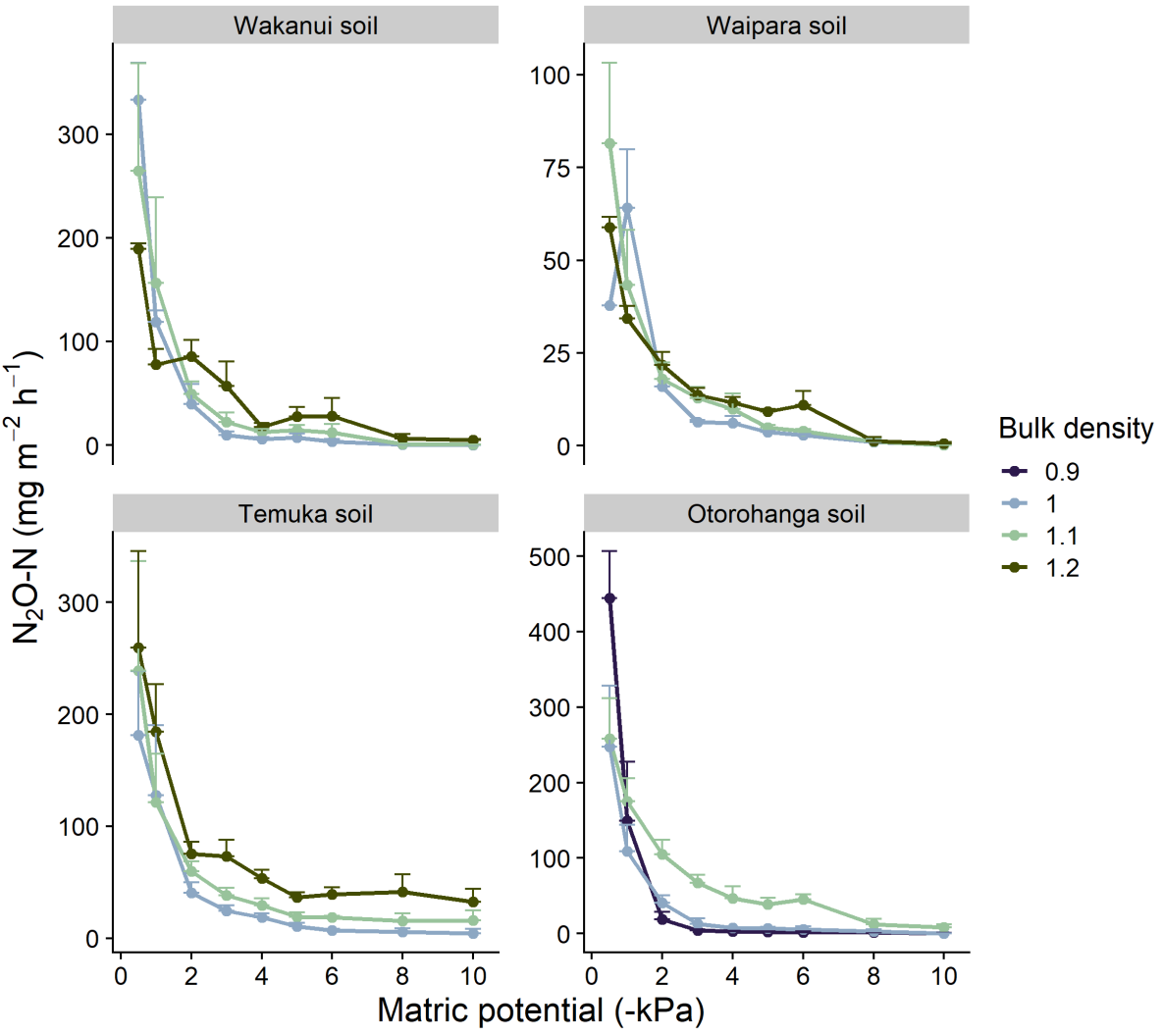

Figure 29: Relationship between measured N_2O-N fluxes and measured matric potential (-kPa) for each soil separately and at varying soil ρ_b (Mg m^{-3}). Numerals in the legend indicate soil ρ_b treatments applied (Mg m^{-3}). Error bars = s.e.m, n = 4.

When plotted against D_p/D_o the N_2O-N flux increased as D_p/D_o declined with peak N_2O fluxes at a D_p/D_o value close to or less than a value of 0.006 (Figure 30). Plotting N_2O-N fluxes versus WFPS (Figure 31) or volumetric soil water content (Figure 32) showed no clear

relationship across soils or soil ρ_b: while N_2O-N fluxes increased with increasing soil moisture, peak N_2O-N fluxes occurred at varying WFPS or volumetric soil water content values depending on soil type and soil ρ_b (Figure 31, Figure 32).

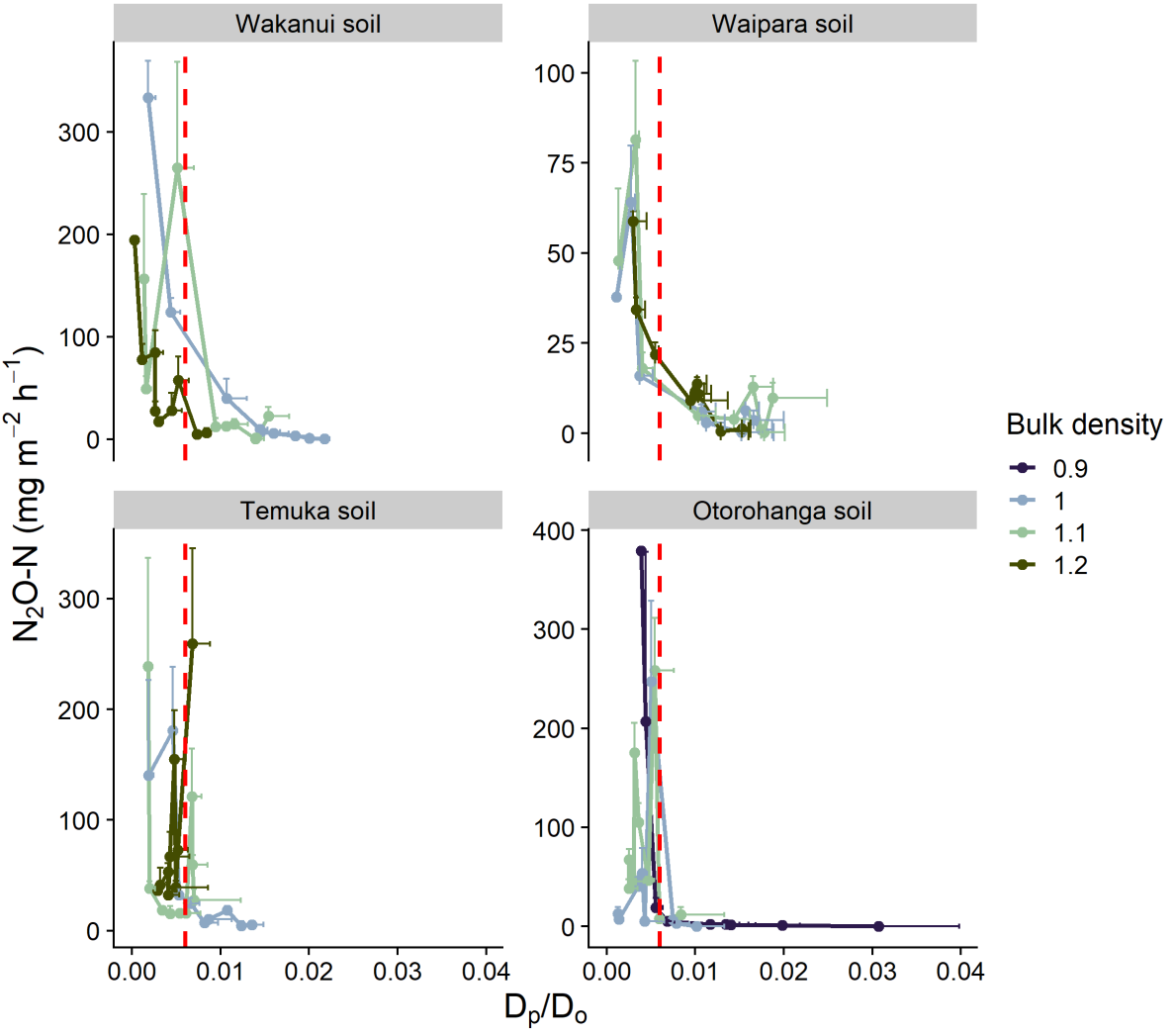

Figure 30: Relationship between measured N_2O-N fluxes and measured D_p/D_o for each soil separately and at varying soil bulk density. Numerals in the legend indicate soil bulk density treatments applied (Mg m^{-3}). Error bars = s.e.m., n=4. The vertical red lines show the 0.006 threshold from Balaine et al. (2013)

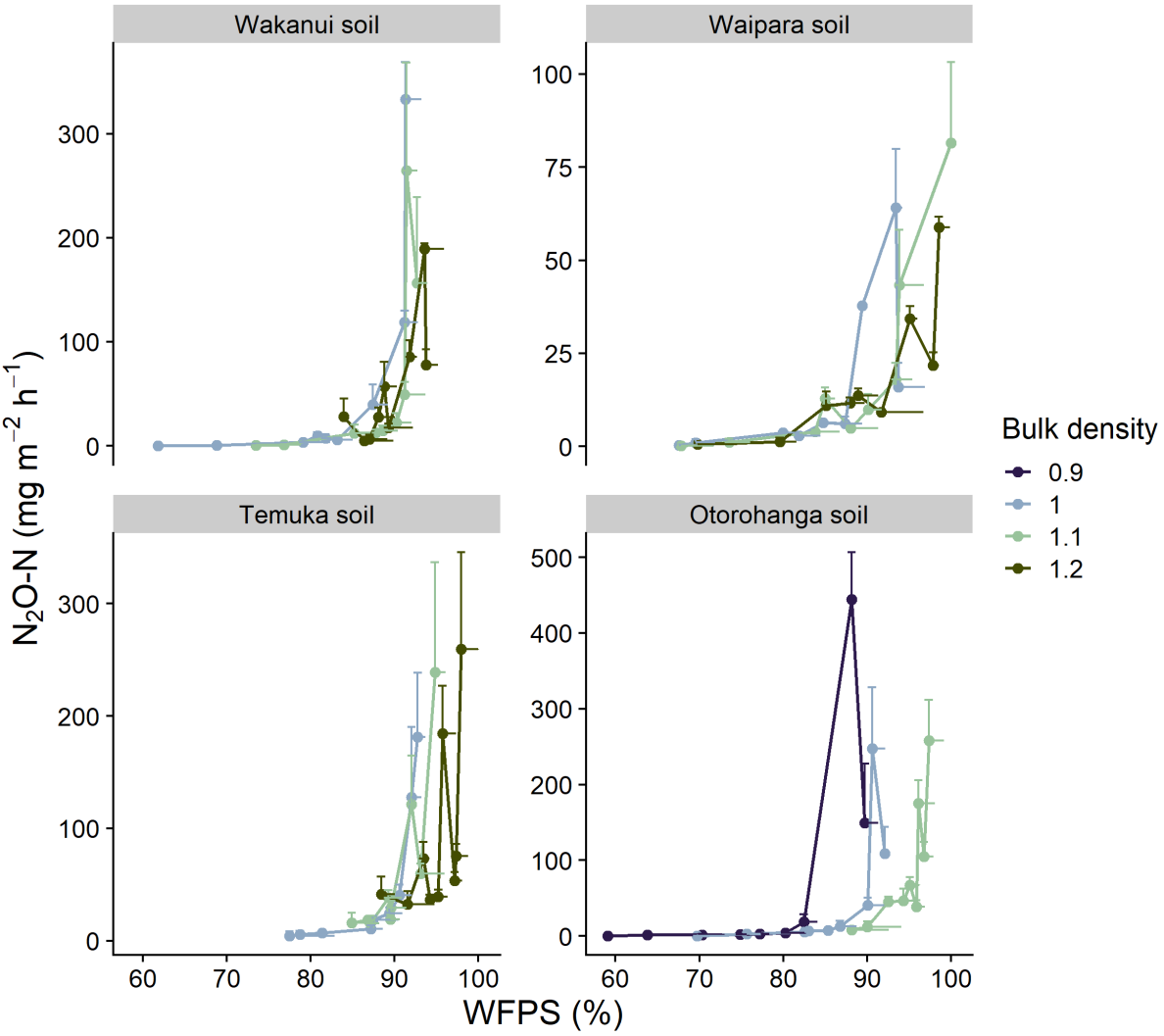

Figure 31: Relationship between measured N_2O-N fluxes and WFPS (%) for each soil at varying soil bulk density. Numerals in the legend indicate soil bulk density treatments applied (Mg m^{-3}). Error bars = s.e.m, n = 4.

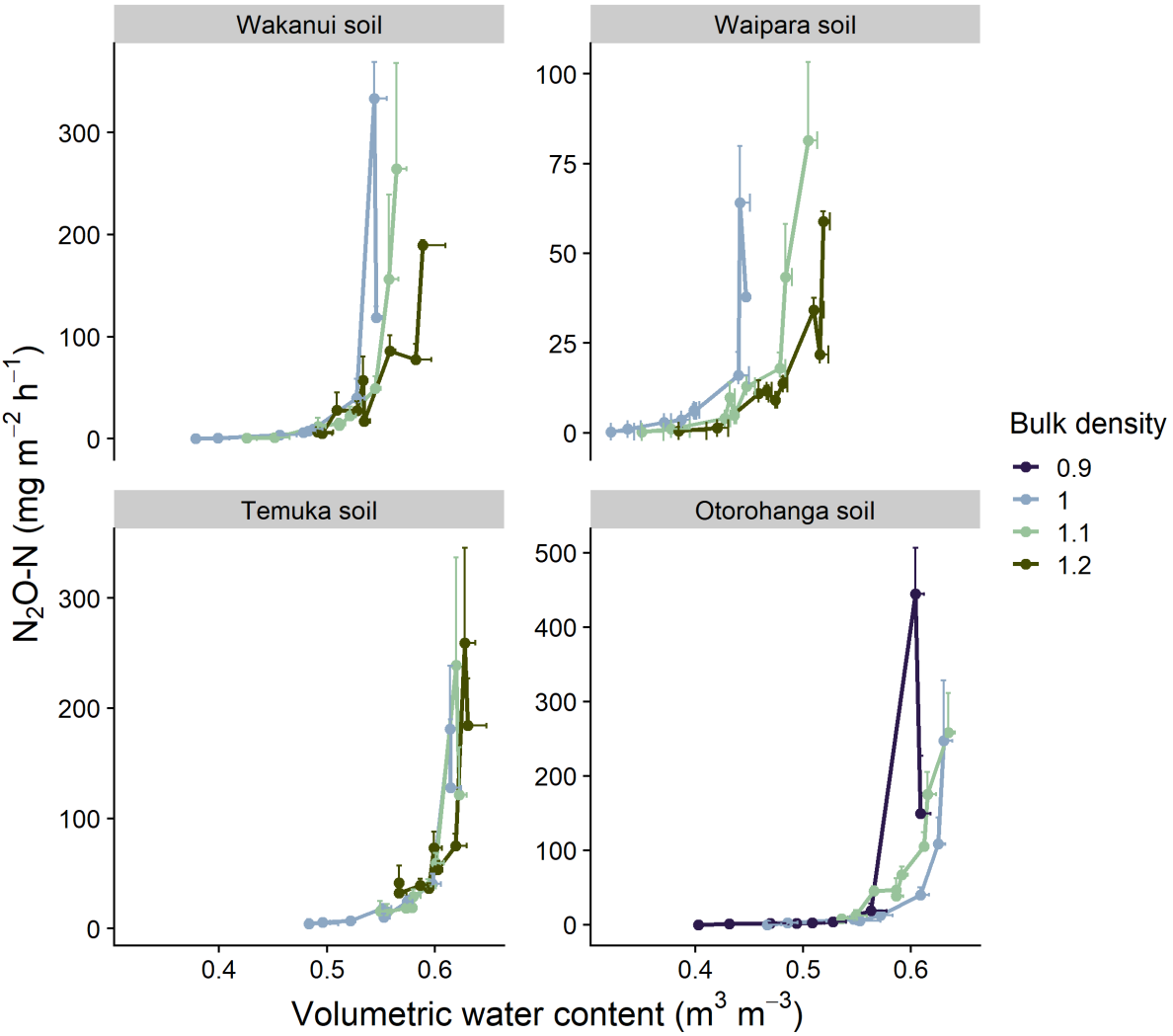

Figure 32: Relationship between measured N_2O-N fluxes and volumetric water content (m^3 m^{-3}) for each soil at varying soil ρ_b (Mg m^{-3}). Numerals in the legend indicate soil ρ_b treatments applied (Mg m^{-3}). Error bars = s.e.m, n= 4.

III.5 Discussion

III.5.1 Soil chemical and physical characteristics

Minimum soil concentrations of NO_3^- and DOC, required to support denitrification in soil, have previously been reported to be ≥ 5 mg N kg^{-1} soil and 40 mg C kg^{-1} soil, respectively (Ryden 1983; Beauchamp *et al.* 1989). High concentrations of NO_3^- increase the denitrification rate in the presence of a C substrate (Weier *et al*. 1993) since the DOC assumes the role of the electron donor during NO_3^- reduction under denitrifying conditions. Thus, based on the results of this experiment, it can be assumed that the soil NO_3^--N and DOC concentrations, which were comparable in magnitude to those previously observed by Balaine *et al.* (2013), were not limiting for denitrification regardless of soil type or treatment.

Elevated soil pH values, observed in the higher soil ρ_b treatments, are consistent with such conditions creating more anaerobic conditions, (lower D_p/D_o and higher WFPS), suitable for denitrification which results in a net release of OH^- ions (Wrage *et al*. 2001). Declines in soil pH with increasing soil drainage were likely the result of reduced denitrification rates and/or increased rates of mineralisation with ensuing nitrification and subsequent soil acidification as soils were drained.

Soil WFPS decreased as soil matric potential became more negative with the rate of decrease lower at higher soil ρ_b because increasing soil ρ_b (compaction) not only decreases total porosity but also creates a shift in pore size distribution, observed as a reduction in macroporosity and an increase in microporosity (Chamindu Deepagoda *et al.* 2019). This results in an increase in the air-entry pressure and a decrease in air-permeability making the soils relatively more anaerobic as soil ρ_b increases at a given soil matric potential. Soil texture also affects pore size distribution and the reason the Waipara soil WFPS was less affected by

increasing bulk density was most likely due to the higher sand content of the Waipara soil, facilitating the retention of a higher fraction of pore space with macroporosity.

Values of D_p/D_o decreased when both soil ρ_b and soil matric potential increased, resulting in a concurrent decline in air-filled porosity and increasing soil moisture, which in turn enhanced tortuosity of the soil pore network (Chamindu Deepagoda *et al*. 2020). Soil D_p/D_o values were within the range previously observed for repacked soil cores held over a similar range of soil ρ_b and moisture (Balaine *et al*. 2013).

III.5.2 Soil N_2O Fluxes and relationships with soil physical parameters

Based on the prior studies of Balaine *et al*. (2013; 2016) it was hypothesised that soil N_2O emissions would become elevated as the value of D_p/D_o decreased towards 0.006. Using only one soil type, Balaine *et al.* (2013) found that the soil N_2O fluxes peaked at a D_p/D_o value of 0.006, regardless of soil ρ_b, and declined as D_p/D_o values decreased further. The increase in N_2O fluxes occurred as the increasingly anaerobic conditions, as defined by a decline in D_p/D_o, created an environment suitable for N_2O production. The decline in N_2O fluxes, as D_p/D_o decreases further, has been shown to be due to N_2O being denitrified to N_2 (Klefoth *et al.* 2014; Balaine *et al.* 2016). In the current study the interactive effects of soil ρ_b and soil matric potential generally resulted in enhanced N_2O fluxes at a D_p/D_o value close to 0.006, or less, but not necessarily peaking at a value of 0.006. Thus under the conditions of this study the variation in the soil C content, postulated to potentially alter the level of oxygen consumption, did not cause a significant shift in the D_p/D_o value where N_2O emissions readily increased. Following a freeze-thaw event, the presence of labile C inducing an increased O_2 demand was postulated

by Petersen *et al.* (2013) to be a reason for denitrification activity at D_p/D_o values > 0.02, a threshold normally considered to indicate the onset of anaerobiosis (Stepniewski 1981). However, Owens *et al.* (2017) found that in ruminant urine-affected soil, in situ, N_2O fluxes also increased when the soil D_p/D_o value was ~ 0.006, despite labile C being supplied via plant root exudation. Chamindu Deepagoda *et al.* (2019) found that N_2O emissions peaked in intact soil cores taken from pastures over a D_p/D_o range of 0.005 to 0.01. Friedl *et al.* (2018) also found N_2O and N_2 fluxes from subtropical dairy pasture soils increased exponentially as D_p/D_o declined, with maximum N_2O fluxes at a D_p/D_o value of 0.0068. Hence, these current results examining a wider number of soils sit well with previous work and support the use of D_p/D_o as an interpretive tool for understanding the occurrence of N_2O emissions or for predicting the potential for N_2O emissions given soil ρ_b and soil moisture data are available for calculating (e.g. Moldrup *et al*. 2013). The potential onset of soil N_2O emissions has often been considered by determining the degree of WFPS, but as Farquharson and Baldock (2007) explain: for a given WFPS the volume fraction of air varies depending on the soil ρ_b. The variable D_p/D_o is an integrated measure of the interactive effects of soil ρ_b and WFPS on air-filled porosity and thus gas diffusion. Hence, the onset of N_2O emissions occurs over a relatively wide range of WFPS. This was most noticeable in the Otorohonga soil.

However, the magnitude of the N_2O fluxes, and the anticipated decline in the N_2O fluxes occurring below D_p/D_o < 0.006, was not consistent across soils. In the Otorohanga soil, where the highest N_2O fluxes occurred, N_2O emissions peaked at a D_p/D_o of 0.006 regardless of soil ρ_b and then declined; in the Waipara soil where the lowest N_2O fluxes occurred, N_2O emissions peaked at a similar D_p/D_o, but < 0.006, regardless of soil ρ_b before declining. This variation in the magnitude and the decline in the N_2O fluxes below a D_p/D_o of 0.006 may possibly be due to other factors affecting the denitrification rate and the N_2O:(N_2O+N_2) ratio. Soil O_2 supply acts as the primary determinant of denitrification commencing. Friedl *et al.*

(2018) found a shift in the N_2O response to D_p/D_o between days 1 and 2 after rewetting of subtropical pasture soils and proposed the presence of residual O_2 on day 1 and increasing anaerobic conditions on day 2 to explain the proposed effect of D_p/D_o on a relative shift in N_2:N_2O partitioning. However, other soil variables, soil pH and anoxic C mineralization, have also been shown to influence both the denitrification rate and the N_2O:(N_2O+N_2) ratio in pasture soils with liming and enhanced C supply promoting N_2O reduction to N_2 and denitrification rates (Samad *et al*. 2016; Senbayram *et al*. 2019). Conversely, elevated soil NO_3^- concentrations may prevent N_2O reduction, thus enhancing the N_2O:(N_2O+N_2) ratio. Recently, this effect of soil NO_3^- concentration was shown to override the effect of liming with respect to the N_2O:(N_2O+N_2) ratio in a sandy cropping soil: high concentrations of NO_3^- (45 mg N kg^{-1} soil) almost completely inhibited N_2O reduction (Senbayram *et al*. 2019). Hence, the variation in the four soils used in the current study, in terms of the delayed or lack of N_2O reduction may have been a partial consequence of the relatively high soil NO_3^- concentrations enhancing the N_2O:(N_2O+N_2) ratio. Future research is needed to examine the role of these factors in altering the N_2O:(N_2O+N_2) ratio with respect to the soil D_p/D_o value. In conclusion this study shows that across a range of soils, varying in texture and C content, the soil D_p/D_o value is a valuable, and theoretically robust, tool for determining the onset of N_2O emissions when denitrification substrates are present.

III.6 Conclusion

The results of this chapter showed that soil D_p/D_o is a robust tool for determining the onset of N_2O emissions when denitrification substrates are present across a range of soils, varying in texture and C content. It was observed that, again, N_2O maximum emissions occurred in a range of D_p/D_o values close to or less than 0.006. Those low D_p/D_o values denote anaerobic

conditions with decreasing O_2 content and gas diffusivity. These conditions, consequently, favour the process of denitrification. However, denitrification is not only a source it is also the only sink for N_2O, via reduction to N_2 in the soil (Figure 6). Complete denitrification was one of the hypothesis behind the decrease of N_2O emissions observed for $D_p/D_o < 0.006$ along with N_2O emission trapping (Balaine *et al.* 2016). In this experiment the magnitude of the N_2O fluxes, and the anticipated decline in the N_2O fluxes occurring below $D_p/D_o < 0.006$, was, however, not consistent across soils. Further research is thus needed to examine the N_2O:(N_2O+N_2) ratio with respect to the soil D_p/D_o value. Thus, in the next chapter, ^{15}N isotope and continuous flow isotope ratio mass spectrometer were used in an attempt to quantify the N_2 emissions from soil while varying D_p/D_o through two wetting and drainage cycles.

Chapter IV : Soil wetting and drainage cycles: effects on relative gas diffusivity, N_2O emissions and denitrification rate

Highlights:

- Denitrification emissions are highest when D_p/D_o is <~0.006
- D_p/D_o integrates moisture and bulk density effects on O_2 supply and subsequent denitrification emissions
- High organic matter may alter O_2 demand and D_p/D_o - denitrification relationships
- High NO_3^- concentration and acidic pH were potentially unfavourable for N_2 production

Keywords: ^{15}N, bulk density, dinitrogen, matric potential, mineralization, nitrification

IV.1 Abstract

Nitrous oxide (N_2O) is a potent greenhouse gas generated in agricultural soils by microbial processes that vary according to soil redox. Soil oxygen (O_2) supply and demand strongly influence soil redox. Migration of O_2 into the soil primarily occurs via gas diffusion, expressed

as relative gas diffusivity (D_p/D_o), and is influenced by soil structure (air-filled porosity and tortuosity of pores) and soil water content. Soil N_2O emissions have been shown to increase at low values of D_p/D_o but detailed studies examining the relationship between D_p/D_o and soil N_2O emissions remain limited, with relatively few soil types examined, and no studies of repeated wetting-drainage cycles. Thus, the objectives of this study were to examine how successive wetting-drainage cycles affected both D_p/D_o dynamics and associated N_2O emissions in two soils; a pallic silt loam and an allophanic sandy-silt, with the later also having a higher organic matter content. Soil cores, repacked to varying density, were wetted up with ^{15}N enriched NO_3^- solution and placed on tension tables where they underwent two consecutive 12-day wetting-drainage cycles from saturation to field capacity (0 to -10 kPa). Over time measurements were made of N_2O, N_2, inorganic-N and soluble carbon, while D_p/D_o was modelled using soil physical characteristics. For both soils each wetting-drainage cycle induced N_2O fluxes but with 5-fold lower fluxes in the allophanic soil. Greater aggregation and sand content in the allophanic soil generated higher porosity and D_p/D_o values that were almost always greater than recognised anaerobic limits. Thus, wetting-induced N_2O fluxes in the allophanic soil were concluded to result from denitrification of ^{15}N labelled NO_3^- due to a higher demand for O_2. While wetting-drainage events induce N_2O emissions by altering D_p/D_o and the soil aeration status, the drying of soils, especially soils high in organic matter, may enhance O_2 demand generating anaerobic zones conducive to denitrification. Further detailed studies examining the interaction between soil structure and soil organic matter content and their effect on N_2O emissions under wetting-drainage events, with measures of soil O_2, are needed.

IV.2 Introduction

Nitrous oxide formation constitutes a direct link between reactive N and climate change (Erisman *et al.* 2011) since N_2O is a potent greenhouse gas. Currently N_2O is the single most important stratospheric ozone depleting substance (Ravishankara *et al.* 2009). Atmospheric concentrations of N_2O have increased at a rate of 0.73 ± 0.03 ppb yr^{-1}, with the current N_2O concentration in the atmosphere 20% higher than pre-industrial levels (MacFarling Meure *et al.* 2006). Annually, it is estimated that agriculture dominates anthropogenic N_2O sources, accounting for 4.1 (1.7-4.8) TgN (N_2O) yr^{-1} out of an estimated 6.9 TgN (N_2O) yr^{-1} of non-natural global emissions of N_2O (Ciais *et al.* 2013). Reportedly, 80% of the observed increase in atmospheric N_2O results from food production (Ciais *et al.* 2013), as a consequence of fertiliser N and animal excreta deposition (Davidson 2009).

Fertiliser and manure N, applied to soils, contribute to N_2O emissions as the result of N transformations, predominately via microbial pathways, that include nitrification and denitrification (Wrage *et al*. 2001; Wrage-Mönnig *et al.* 2018). The soil O_2 concentration influences the relative dominance of N_2O producing pathways: nitrification and denitrification are aerobic and anaerobic processes, respectively. Several other microbial pathways, such as the DNRA and nitrifier-denitrification can also generate N_2O (Friedl *et al*. 2018; Wrage-Mönnig *et al*. 2018) and these are also influenced by soil O_2 concentration or redox status.

Thus, critical to understanding the role microbes perform in controlling N_2O emissions is a better grasp of how the availability of O_2 within a soil may change. Subsurface movement of gas within a soil occurs primarily via diffusion. Assuming no change in atmospheric pressure or wind-induced disturbance the movement of gas across the soil atmosphere interface is also diffusion controlled. The migration of a gas can be described by a soil gas diffusion coefficient (D_p, cm^3 soil air cm^{-1} s^{-1}) which is a parameter that varies with the characteristics of a gas, soil

atmosphere temperature and pressure, soil structure (e.g. air-filled porosity and tortuosity of pores) and soil water content (Rolston and Moldrup 2012). The diffusion coefficient of the same gas in free air (D_o, cm^2 air s^{-1}) is used to normalise D_p, so that soil-gas diffusivity (D_p/D_o) can be expressed under a given set of conditions (Rolston and Moldrup 2012).

Since the conceptual work of Linn and Doran (1984), changes in a soil's water-filled pore space (WFPS) have routinely been used to explain variation in N_2O fluxes. However, WFPS, which defines the proportion of total pore space filled with water, is a normalised dimensionless value and Farquharson and Baldock (2007) stated that "…WFPS does not quantify the fraction of the entire soil volume that is filled with water or air and hence is not directly proportional to the diffusion of gases and solutes that regulate process rates across soils with different total porosities". This was demonstrated by Balaine *et al*. (2013) who found that peak N_2O emissions, from soil cores treated with nitrate and spanning bulk densities from 1.1 to 1.5 Mg m^{-3}, occurred across a WFPS range of 67-80%. Farquharson and Baldock (2007) went on to suggest that simple measures of soil water content combined with soil structural parameters should be considered, in conjunction with volume fractions of air or water. Thus, Balaine *et al*. (2013) further assessed N_2O emissions relative to D_p/D_o and found strong relationships between N_2O emissions and D_p/D_o with N_2O emissions peaking at a D_p/D_o value of 0.006 regardless of the soil bulk density. Further assessment of this relationship was undertaken by Balaine *et al*. (2016) who found, using the same soil, that cumulative N_2O and N_2 emissions, after 35 days, also depended on D_p/D_o. A laboratory study by Petersen *et al.* (2008) also found D_p/D_o explained N_2O emissions better than WFPS when examining soil across seven matric potentials. Petersen *et al*. (2013) observed that carbon (C) inputs, resulting from crop system management or freeze-thaw effects could potentially affect the relationship between peak emissions of N_2O and calculated D_p/D_o. Values of $D_p/D_o < 0.006$ in laboratory and field studies have also been observed to coincide with maximum N_2O fluxes and increasing production of

N_2 fluxes (Friedl *et al.* 2018; Friedl *et al.* 2017; Owens *et al.* 2017). A key determinant of a soil's D_p/D_o status are wetting-drainage cycles brought about by rainfall or irrigation events. Given that the frequency of irrigation and/or volume can potentially be manipulated to mitigate N_2O emissions (Mumford *et al.* 2019) and the fact that climate change may also lead to altered rainfall frequency and volumes it is important to better understand how soil D_p/D_o and associated N_2O emissions are affected by wetting-drainage cycles. To date the number of detailed studies that have examined the relationship between D_p/D_o and N_2O emissions remains limited, with few soil types examined, and no repeated wetting-drainage cycles. Thus the objectives of this study were (i) to examine how successive wetting and drainage cycles affected both D_p/D_o dynamics and associated N_2O emissions across soil bulk densities and (ii) to observe if these dynamics were influenced by soil texture and density.

IV.3 Materials and Methods

IV.3.1 Soil collection, Experimental Design, and Setup

Wakanui and Otorohanga soils from Chapter II were chosen for this experiment and their characteristics can be found in Table 2. The Waipara soil was not considered for this experiment given the low N_2O fluxes, low pH and low DOC concentration previously measured in the first experiment (Figure 29, Figure 23 and Figure 24, respectively). The Otorohanga and Wakanui soils had the most diverse physical characteristics (Table 2). Wetting and drying cycles are also known to affect positively the mineralisation rate (Mumford *et al.* 2019), thus this experiment used two soils differing ($P < 0.05$) in DOC concentrations (Figure 24).

After determining the gravimetric water content of the air dried soils, 24 soil cores were constructed by uniaxially compacting the air-dried soils inside stainless steel rings (7.3 cm

internal diameter, 7.4 cm deep), to a depth of 4 cm. These soil cores were assigned to treatments according to the experimental design.

The experimental design consisted of two soil types and three levels of bulk density for each soil type, replicated four times. Soil bulk density treatments for the Wakanui soil were 1.0, 1.1 and 1.2 Mg m^{-3}, while those for the Otorohanga soil were 0.9, 1.0, and 1.1 Mg m^{-3}. A lower soil bulk density was used for the Otorohanga soil because it could not be manually packed to a bulk density of 1.2 Mg m^{-3}. In addition, another 36 soil cores were made (3 replicates for each soil type by bulk density) in order to perform destructive soil analyses on days 0 and 12. The original 24 soil cores were destructively sampled on day 25.

In order to evaluate both D_p/D_o dynamics and N_2O emissions, across successive wetting-drainage cycles, six levels of soil matric potential (0, -2.0, -4.0, -6.0, -8.0 and -10.0 kPa) were used based on the earlier study (Chapter III). To enable this tension tables were prepared as described by Romano *et al.* (2002) and in III.3.1. Before placing soils cores on the tension tables, deionised water was poured evenly across the tension tables to provide a good connection between soil cores and the tension table. The tension tables were housed in a laboratory where temperature fluctuations were negligible (20 ± 1ºC).

Prior to placing soil cores on the tension table, cores were saturated with a ^{15}N labelled KNO_3 solution (300 µg N g^{-1} soil) with an enrichment of 50 atom% excess (Figure 33). This soil NO_3^- concentration emulated the maximum typically found under bovine urine patches in grazed pasture (e.g. Clough *et al*., 2009). The soil cores used for destructive sampling, on days 0 and 12, were treated similarly but with a KNO_3 solution at natural abundance.

Figure 33: Soil cores saturated with 50 atom% ^{15}N solution just before putting them on the tension tables.

Once saturated the soil cores were placed on the tension tables set at 0 kPa. Then every 48 h soil drainage was increased by adjusting the tension tables to the next drainage step, so that by day 12 the soil cores had spent 48 h at -10 kPa. Upon the completion of one drainage cycle, soil drainage ceased and the soil cores were returned to 0 kPa. To avoid cross contamination of NO_3^--^{15}N enrichments, soil cores were placed into individual jars and wetted from the bottom up with deionised water, prior to being placed back on the tension tables set at 0 kPa. The drainage cycle was then repeated with drainage once again progressively increased every second day so that by day 24 the soil cores had again been at -10 kPa for 48 h. Soil cores were weighed daily, prior to any required adjustments to drainage settings.

Soil total porosity (ϕ) was calculated using the following equation:

$$\phi\ (cm^3 pores/cm^3 soil) = 1 - \left(\frac{\rho_b}{\rho_d}\right) \qquad (11)$$

with ρ_d, the measured soil particle density (g cm^{-3}) and ρ_b, the soil bulk density (g cm^{-3}).

Daily core weights and Φ were used to calculate WFPS (%) and soil air content Ɛ (cm^3 air cm^{-3} soil), cf. Equation 3 (II.3.1) and Equation 1 (II.3.2).

IV.3.2 Determination of D_p/D_o, N_2O and N_2 fluxes.

Nitrous oxide fluxes were measured each day of the experiment using the ^{15}N enriched soil cores. This was performed by removing the soil core from the tension table and placing it in a 1 L mason jar which was then sealed with an air-tight lid equipped with a septa. Gas samples (10 mL) were taken at 0, 20, and 40 min, after sealing the jar, using a 20 mL glass syringe equipped with a 3-way stopcock and a 25G hypodermic needle. Gas samples were injected into pre-evacuated 6 mL Exetainer® vials. Prior to analysis the gas samples were brought to ambient pressure and analysed using a gas chromatograph (8610; SRI instruments, Torrance, CA) connected to a Gilson autosampler (Gilson 222XL; Gilson, Middleton, WI) as previously described (Clough *et al*., 2009). The change in the jar headspace N_2O concentration, over time, was used to calculate the N_2O flux according to Hutchinson and Mosier (1981) and as described in III.3.2 section. Cumulative N_2O emissions were calculated by manually integrating the daily fluxes over times.

On days 3, 4, 6, 8, 10, 12, 14, 16, 18, 22, and 24 a further 15 mL gas sample was taken after 3h, to enable N_2 flux determinations, and placed in a 12 mL Exetainer® vial. The ^{15}N enrichments of the N_2O and N_2 samples were determined on a continuous flow isotope ratio mass spectrometer (Sercon 20/20; Sercon, Chesire, UK) according to the methodology of Mulvaney and Boast (1986) and Stevens and Laughlin (2001). Replicated N_2O standards with ^{15}N enrichments of 0.366, 10.0 and 40.0 atom% were included in every batch of samples analysed. The N_2 flux detection limit (74 $\mu g\ m^{-2}\ h^{-1}$) was determined using the between batch

standard deviation (n = 100) of ambient air samples and the associated 95% confidence intervals for △29 and △30, 9.1 x 10^{-6} and 4.1 x 10^{-5}, respectively (Stevens and Laughlin 2001).

Using daily soil core mass, and prior knowledge of soil dry mass, particle density, and bulk density, the soil air content (ε) values were determined as described in section II.3.1 (equation 1).

Soil air content was then used to calculate D_p/D_o according to Moldrup *et al*. (2013) as follows:

$$\frac{D_p}{D_o} = \varepsilon^{[1+C_m\Phi]}\left(\frac{\varepsilon}{\Phi}\right) \qquad (12)$$

Where D_p and D_o are as defined above, Ɛ is soil-air content (cm^3 soil air cm^{-3} soil), Φ is soil total porosity (cm^3 soil pore space cm^{-3} soil), and C_m is the media complexity factor. As the experiment was performed using repacked soil, C_m = 1 (Moldrup *et al*., 2013).

The SWLR model (equation 12) was used based on the findings of Moldrup *et al*. (2013) to predict D_p/D_o. They showed that the SWLR model outperformed similar, simple D_p/D_o models also based on Φ and Ɛ for repacked (or intact) soils containing between 0 and 54% clay. The Wakanui and Otorohanga soils clay percentages were 22.3 and 11.3%, respectively (Table 2). Based on the models comparison against D_p/D_o observed in 11 sieved, repacked soils made by Moldrup *et al*. (2013), SWLR (C_m = 1) and WLR-Marshall (Marshall 1959) models are excellent predictors for D_p/D_o data from repacked soils and sands (RMSE = 0.017 for both). The measured D_p/D_o values in the first experiment (Chapter III) were compared with those two models (Figure 34) in order to make a final decision. Models are compared and tested for general accuracy and tendency for overprediction (positive bias) or underpredition (negative bias) by the root square error (RMSE) and bias respectively using the following equations:

$$\mathrm{RMSE} = \sqrt{\frac{1}{\mathrm{n}}\sum_{\mathrm{i}=1}^{\mathrm{n}}(\mathrm{d_i})^2} \quad (13)$$

$$bias = \frac{1}{n}\sum_{i=1}^{n}(d_i) \quad (14)$$

with d_i the difference between predicted and observed gas diffusivities for the n number of measurements involved. The RMSE and bias values obtained for Otorohanga and Wakanui soils are presented on Table 3 and Figure 34. Both model; WLR-Marshall and SWLR fitted the measured data well, however, the SWLR provided the best fit giving the lowest RMSE values (0.006 and 0.0072 for Otorohanga and Wakanui soils, respectively) which concurs with the results of Moldrup *et al*. (2013) results.

Table 3: Results of the general accuracy and tendency test comparing WLR-Marshall model and Moldrup et al. (2013) SWLR model for Wakanui and Otorohanga soils.

	Wakanui soil		Otorohanga soil	
	WLR-Marshall model	SWLR-Moldrup model	WLR-Marshall model	SWLR-Moldrup model
RMSE	0.0073	0.0072	0.0079	0.006
bias	0.003	0.002	-0.001	0.0005

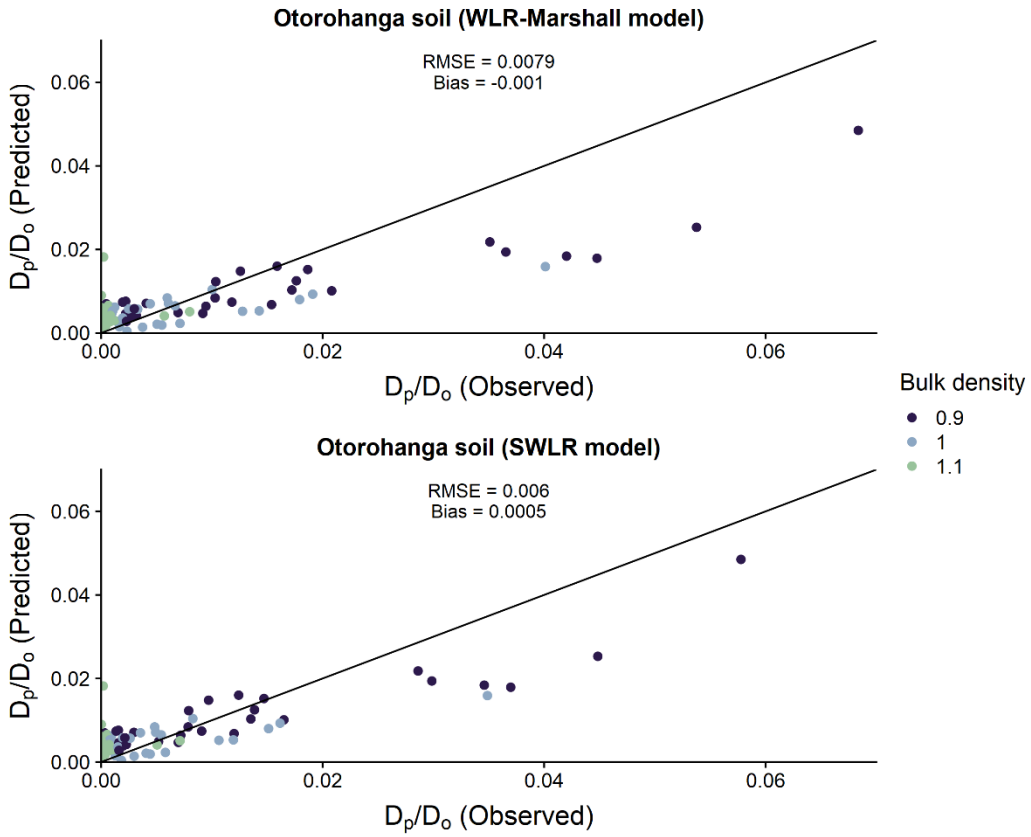

Figure 34: Test of two D_p/D_o models against D_p/D_o observed data for Otorohanga soil. SWLR, structure-dependent water induced; WLR, water induced linear reduction; Cm, media complexity factor. The observed D_p/D_o data have been collected in the diffusion chambers and are presented in Chapter II. The black line represents the identity line (y=x).

IV.3.3 Destructive soil analyses

For destructive soil analyses the soil core was first extruded into a Ziploc® plastic bag where it was mixed prior to a 10 g subsample being taken for gravimetric water content. This was oven-dried at 105 ºC for 24 h. Soil pH was measured using a calibrated flat surface pH electrode (Broadley James Corp., Irvine, CA.). Soil inorganic-N concentrations were determined by extracting the equivalent of 10 g of dry soil with 100 mL of 2M KCl and shaking for 1 h. Then the extracts were filtered (Whatman 42) with the filtrate analysed for NO_3^- and NH_4^+ on a flow injection analyser (Blakemore *et al*., 1987). To determine dissolved organic carbon (DOC) a further sample (equivalent of 5 g dry soil) was extracted in 30 mL of deionised water by shaking

for 30 minutes prior to centrifugation (3,500 rpm for 20 minutes) and filtration (Whatman 42), with analyses performed on a Shimadzu TOC analyser (Shimadzu, Oceania Ltd., Sydney, Australia) (Figure 35).

Figure 35: Picture of the Shimadzu TOC analyser used to measure the DOC concentrations from soil extraction samples. Chain loop of the samples on the left picture.

IV.3.4 Statistical analyses

Statistical analyses were also performed using R studio and followed the same procedure as described in section III.3.4. Time (days of the experiment), soil types (2 levels: Otorohanga and Wakanui) and soil ρ_b (3 levels per soil) were the explanatory variables (Appendix 4).

IV.4 Results

IV.4.1 Soil physical conditions

The Wakanui soil had a greater percentage of clay and silt (Table 2) and fewer fine soil aggregates than the Otorohanga soil: on a gravimetric basis the Wakanui soil had 6.5 and 18.2% more aggregates passing through 0.6 and 0.25 mm sieves, respectively (Figure 36). The uniformity coefficient (C_u) expressing the variety in particle sizes of soil (Hazen 1892) and defined as the ratio of D_{60} to D_{10} was calculated (Figure 36). The value D_{60} is the grain diameter at which 60% of soil particles are finer and 40% of soil particles are coarser, while D_{10} is the grain diameter at which 10% of particles are finer and 90% of the particles are coarser. The coefficient D_{10} was extrapolated using the inverse of the polynomial regressions for each soil. The uniformity coefficient for the Wakanui soil was < 4 so the soil is classified as poorly graded/uniformly graded while the C_u for the Otorohanga soil was > 4 so the soil is classified as well graded (Hazen 1892). Soil pH remained stable throughout the experiment but was higher in the Wakanui soil (5.6 ± 0.1) compared to the Otorohanga soil (5.1 ± 0.1) as observed during the first experiment (Figure 23). The soil organic matter content was higher ($P < 0.05$) in the Otorohanga soil than in the Wakanui soil (Table 2).

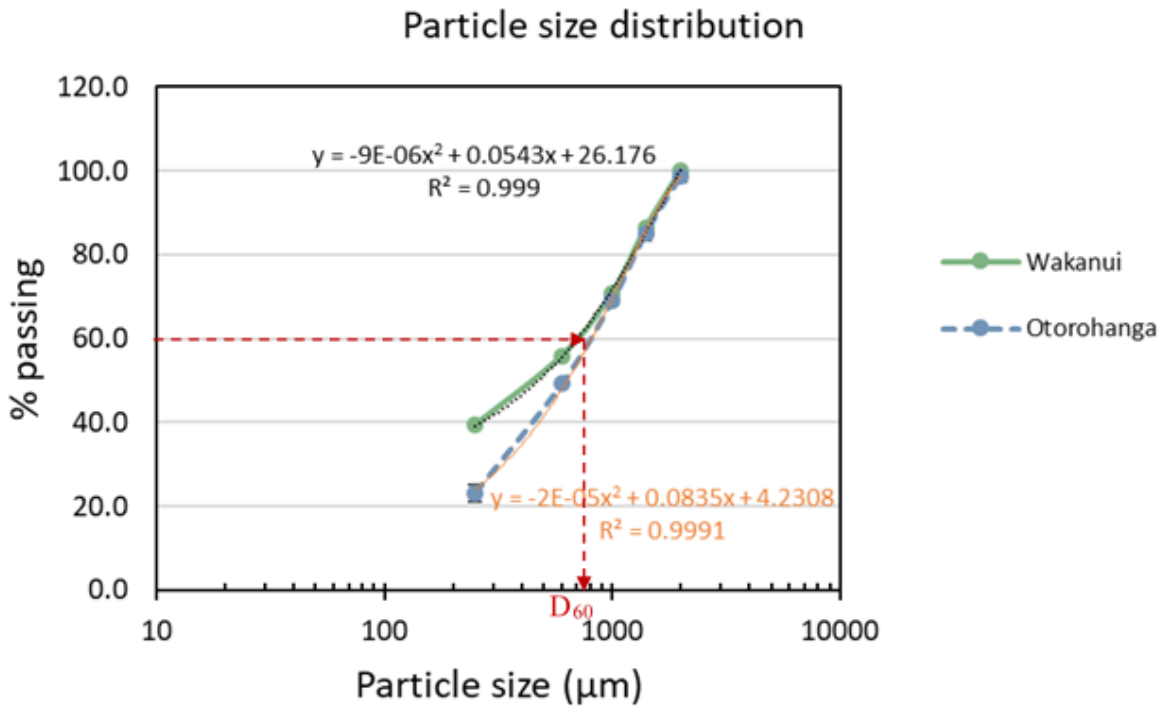

Figure 36: Percentage of soil mass passing through sieves at a given particle size for the Wakanui and Otorohanga soils. The black and orange lines were obtained by fitting a polynomial regression to the data.

Table 4: Soil pH, dissolved organic carbon (DOC), ammonium-N (NH_4^+-N) and nitrate-N (NO_3^--N) concentrations at destructive sampling times. Days 12 and 25 are at the end of the first and second drainage cycles, respectively.

		Day 0			Day 12			Day 25		
Wakanui	Bulk density (g cm^{-3})	1.0	1.1	1.2	1.0	1.1	1.2	1.0	1.1	1.2
	pH	ND	ND	ND	5.6 ± 0.1	5.6 ± 0.1	5.6 ± 0.2	5.6 ± 0.1	5.7 ± 0.1	5.3 ± 0.1
	DOC (μg C g^{-1} soil)	388 ± 14	460 ±26	402 ± 64	271 ± 5	227 ± 15	250 ± 14	169 ± 6	166 ± 2	147 ± 9
	NO_3^--N (μg NO_3^--N g^{-1} soil)	169 ± 92	170 ± 56	177 ± 95	282 ± 43	262 ± 11	214 ± 53	205 ± 28	216 ± 35	182 ± 18
	NH_4^+-N (μg NH_4-N g^{-1} soil)	48 ± 4	26 ± 8	37 ± 7	70 ± 3	63 ± 5	43 ± 13	1.2 ± 0.2	1.3 ± 0.2	1.6 ± 0.7
Otorohanga	Bulk density (g cm^{-3})	0.9	1.0	1.1	0.9	1.0	1.1	0.9	1.0	1.1
	pH	ND	ND	ND	5.2 ± 0.1	5.2 ± 0.1	5.2 ± 0.1	5.2 ± 0.1	5.2 ± 0.1	5.2 ± 0.1
	DOC (μg C g^{-1} soil)	181 ± 40	141 ±13	152 ± 6	147 ± 12	105 ± 21	149 ± 39	74 ± 5	81 ± 6	79 ± 2
	NO_3^--N (μg NO_3^--N g^{-1} soil)	78 ± 15	175 ± 82	32 ± 24	228 ± 97	178 ± 20	236 ± 43	130 ± 25	166 ± 31	144 ± 15
	NH_4^+-N (μg NH_4-N g^{-1} soil)	3.2 ± 0.4	3.9 ± 0.4	3.6 ± 0.2	9.1 ± 3	11 ± 3	11 ± 3	1.1 ± 0.4	0.7 ± 0.1	2.5 ± 1.6

Conversely, soil DOC concentrations were higher ($P < 0.05$) in the Wakanui soil than in the Otorohanga soil when comparing individual sampling days (Figure 37; Table 4). In the Wakanui soil DOC did not vary with bulk density ($P = 0.373$) but did decline over time averaging 415, 249, and 161 µg C g^{-1} soil on days 0, 12, and 25, respectively, when averaged across bulk density treatment (Figure 37; Table 4). Similarly, bulk density did not affect DOC concentrations in the Otorohanga soil ($P = 0.140$), with no difference in DOC concentrations between days 0 and 12, but lower DOC concentrations occurred at day 25 (Figure 37; Table 4).

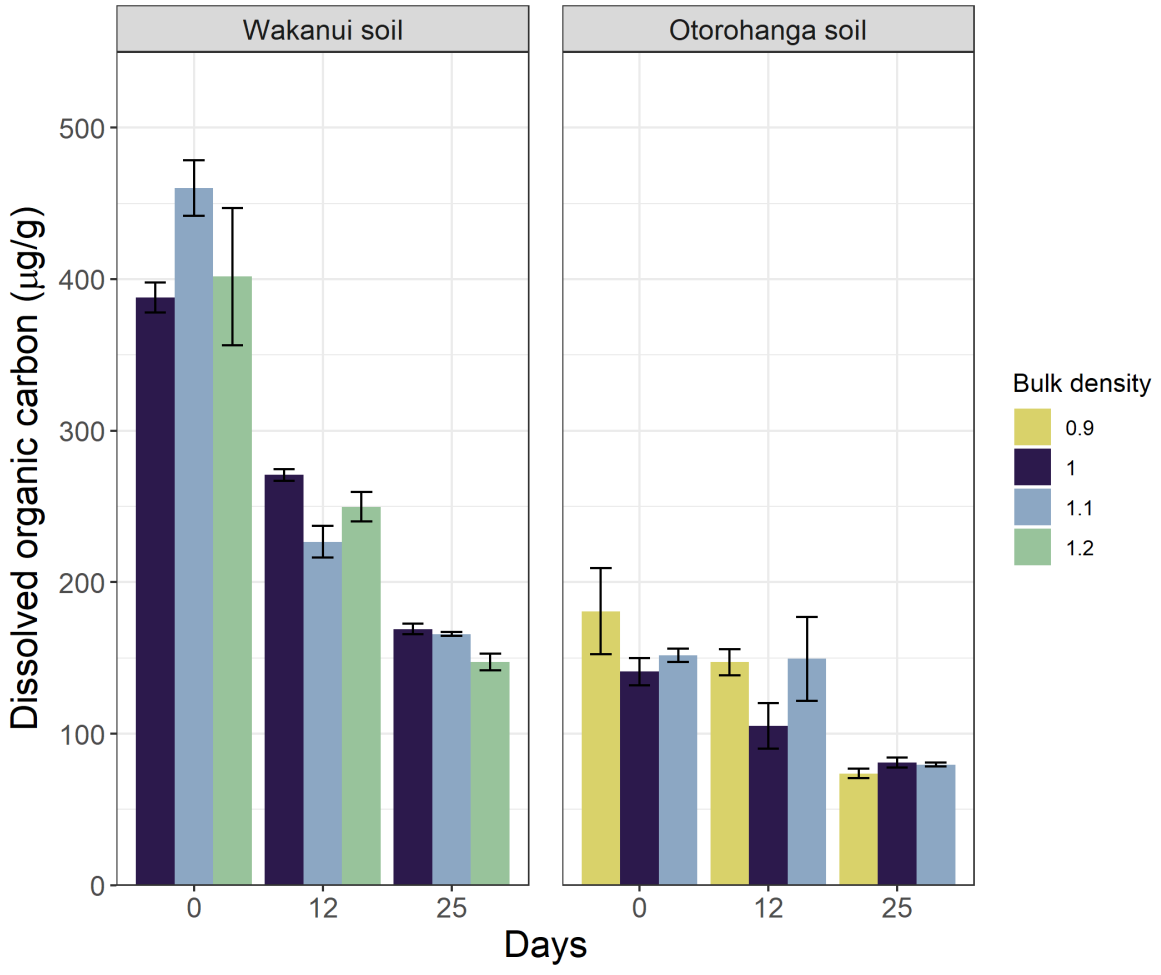

Figure 37: Mean dissolved organic carbon content (DOC) for the Wakanui and Otorohanga soils at the beginning of the experiment (Day 0), after the end of the first wetting-drainage cycle (Day 12) and at the end of the second wetting-drainage cycle (Day 25). Numerals in the legend indicate the soil bulk density treatments applied (Mg m^{-3}). Error bar = s.e.m; n=4.

Soil NO_3^--N concentrations were not affected by soil bulk density in the Wakanui soil, where they were highly variable at day 0, and declined from day 12 to day 25 (Figure 38; Table 4). A similar trend occurred in the Otorohanga soil (Figure 38). The NH_4^+-N concentrations were 1 or 2 orders of magnitude less than the soil NO_3^- concentrations with few consistent differences over time. However, NH_4^+-N concentrations had decreased in the Wakanui soil by day 25 (Table 4).

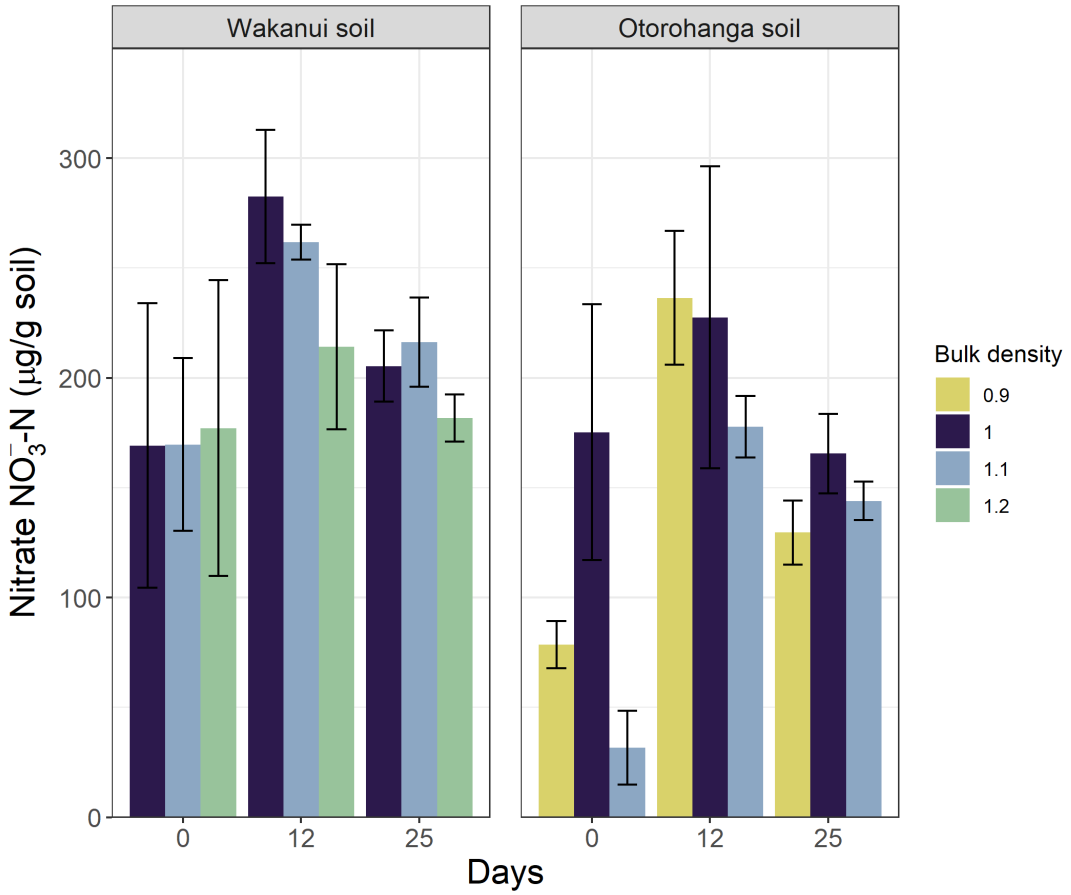

Figure 38: Mean nitrate (NO_3^-) concentrations for the Wakanui and Otorohanga soils at the beginning of the experiment (Day 0), after the end of the first wetting-drainage cycle (Day 12) and at the end of the second wetting-drainage cycle (Day 25). Numerals in the legend indicate the soil bulk density treatments applied (Mg m-3). Error bar = s.e.m; n=4.

Air-filled porosity (ε) increased as drainage increased (more negative matric potential) with higher ε values in the Otorohanga soil at any given level of drainage (Figure 39), with no statistical effect of soil bulk density on ε in the Wakanui soil, but with higher ε values in the Otorohanga soil at 0.9 Mg m^{-3} than at 1.0 or 1.1 Mg m^{-3} ($P < 0.05$; Figure 39). Modelled values

of D_p/D_o reflected these trends and differences in the ε values with higher D_p/D_o in the Otorohanga soil (Figure 40).

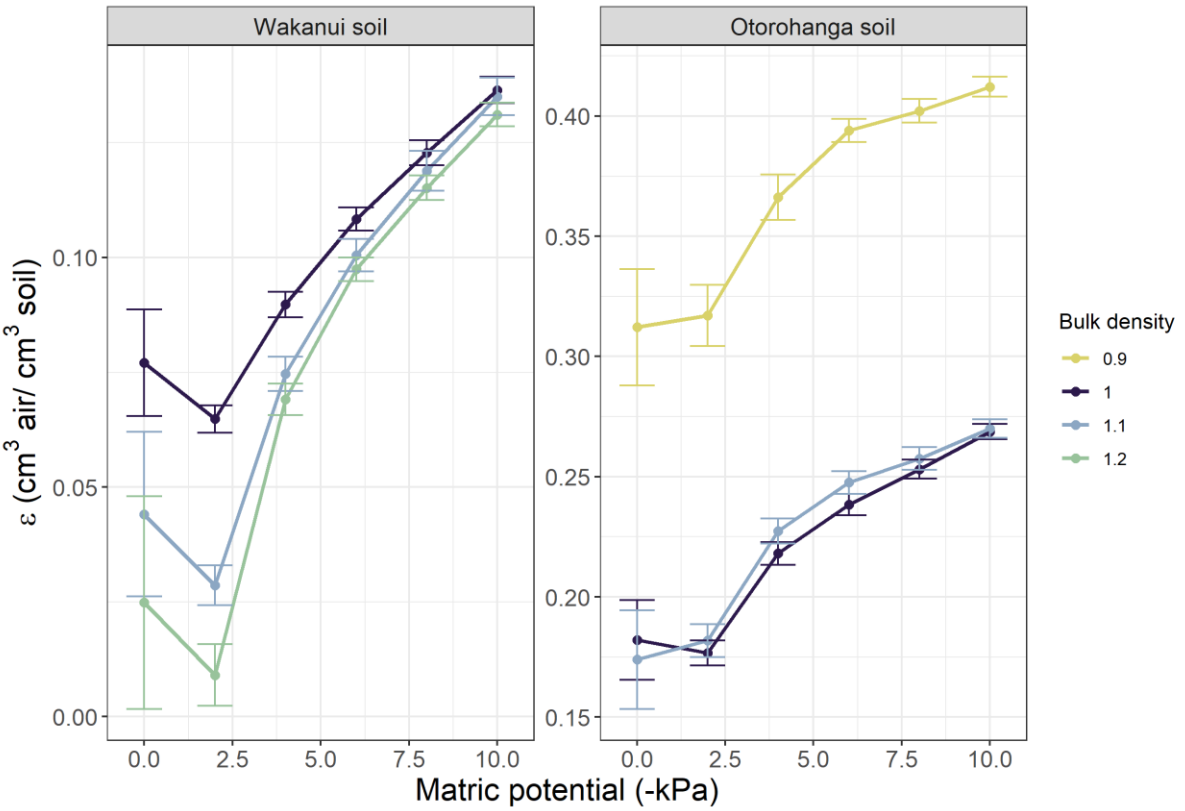

Figure 39: Soil air content (Ɛ), as a function of relative matric potentials (-kPa) for the Wakanui soil and the Otorohanga soil. Numerals in the legend indicate the soil bulk density treatments applied (Mg m^{-3}). Error bar = s.e.m; n=4. Note the different scales for the y-axis.

The density induced effects on D_p/D_o, are presented with air-filled porosity normalised as a function of total porosity (Ɛ/Φ) in Figure 40, along with the previously reported limits of Balaine *et al*. (2013) and Stepniewski (1981) for reference. The Otorohanga soil generally had D_p/D_o values greater than these limits while in the Wakanui soil almost all D_p/D_o data values were < 0.02.

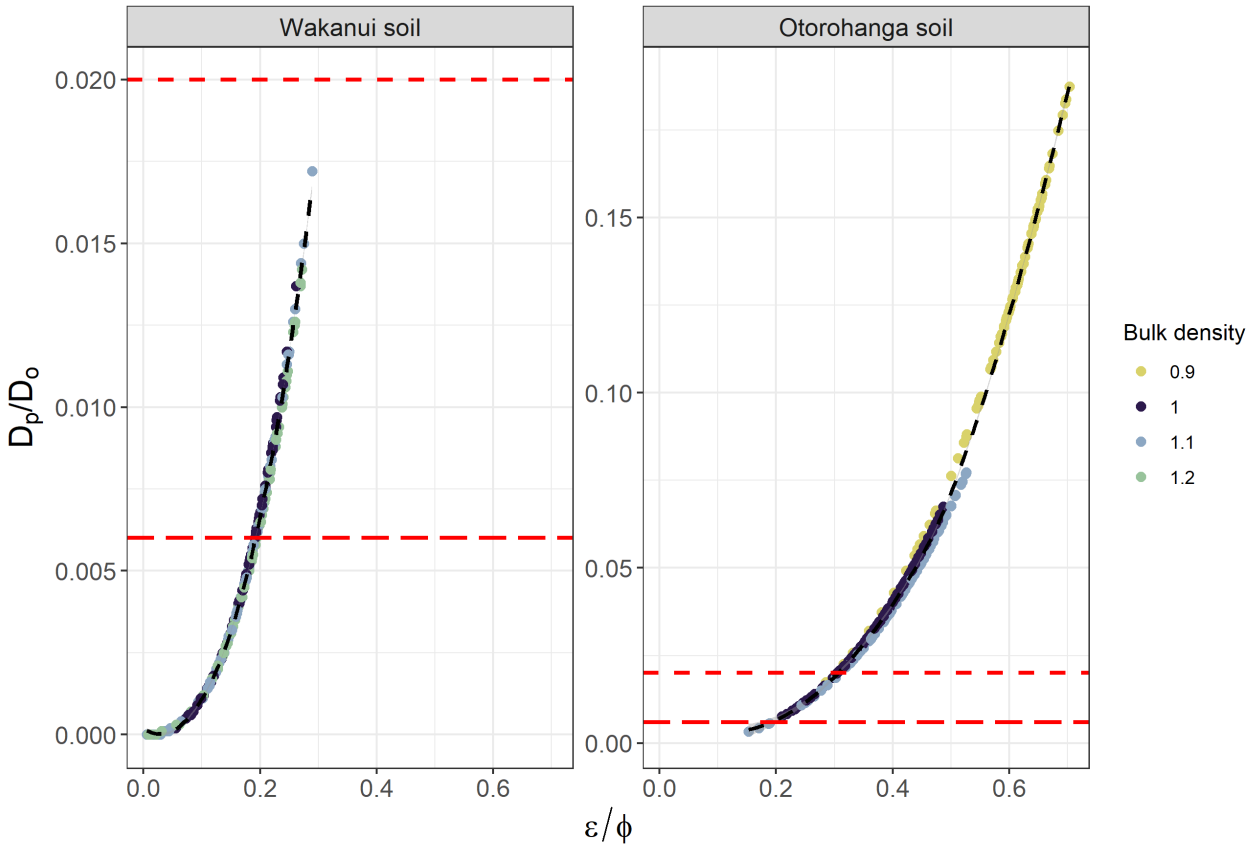

Figure 40: Soil-gas diffusivity (D_p/D_o), as a function of relative air-filled porosity (ε/Φ) for the Wakanui soil and the Otorohanga soil. Also shown are the previously reported gas diffusivity values for peak N_2O fluxes at D_p/D_o = 0.006 (– – – –; Balaine et al. 2013) and anaerobic conditions D_p/D_o = 0.02 (------; Stepniewski 1981). Numerals in the legend indicate the soil bulk density treatments applied (Mg m^{-3}).Note the different scales for the y-axis.

IV.4.2 N_2O and N_2 emission trends during the two cycles

Following the initial saturation of the soils the N_2O fluxes peaked on day 2 in the Otorohanga soil and day 3 in the Wakanui soil (Figure 41, Figure 42) at 28.1 and 145.4 mg m^{-2} h respectively, overall soil ρ_b. However, fluxes were 5-fold higher in the Wakanui soil than the Otorohanga soil. The N_2O fluxes then declined over time until day 12 whereupon the soil cores were again saturated, which caused the N_2O fluxes to increase once more, regardless of soil type, before they again declined. However, in the Wakanui soil the N_2O fluxes did not increase to the same level as seen on day 2 with mean N_2O-N fluxes < 15.0 mg m^{-2} h on days 13-15

(Figure 41), while in the Otorohanga soil the N_2O emissions after re-saturation of the soil closely mimicked the lower N_2O flux trend observed over days 1 to 12 (Figure 41).

A plot of N_2O fluxes versus D_p/D_o shows that N_2O fluxes in the Wakanui soil peaked at D_p/D_o values < 0.006 during the first drainage cycle, regardless of soil bulk density, and the same occurred during the second drainage cycle (Figure 41). This was not the case in the Otorohanga soil, where lower fluxes occurred, and where N_2O fluxes peaked at a D_p/D_o value close to 0.02 at soil bulk densities of 1.0 and 1.1. However, at the Otorohanga soil bulk density of 0.9 the highest N_2O fluxes generally occurred over a D_p/D_o range of 0.05 to 0.13 (Figure 42). In the Wakanui soil N_2O fluxes plotted against WFPS showed fluxes increasing from 80% WFPS, with peak fluxes between 85-93% and 90-100% WFPS for the first and second wetting-drainage cycles, respectively (Figure 43). In the Otorohanga soil N_2O fluxes peaked at 45% WFPS at 0.9 Mg m^{-3} while at 1.0 and 1.1 Mg m^{-3} peak N_2O fluxes occurred over a broader WFPS range of 60-75% (Figure 44).

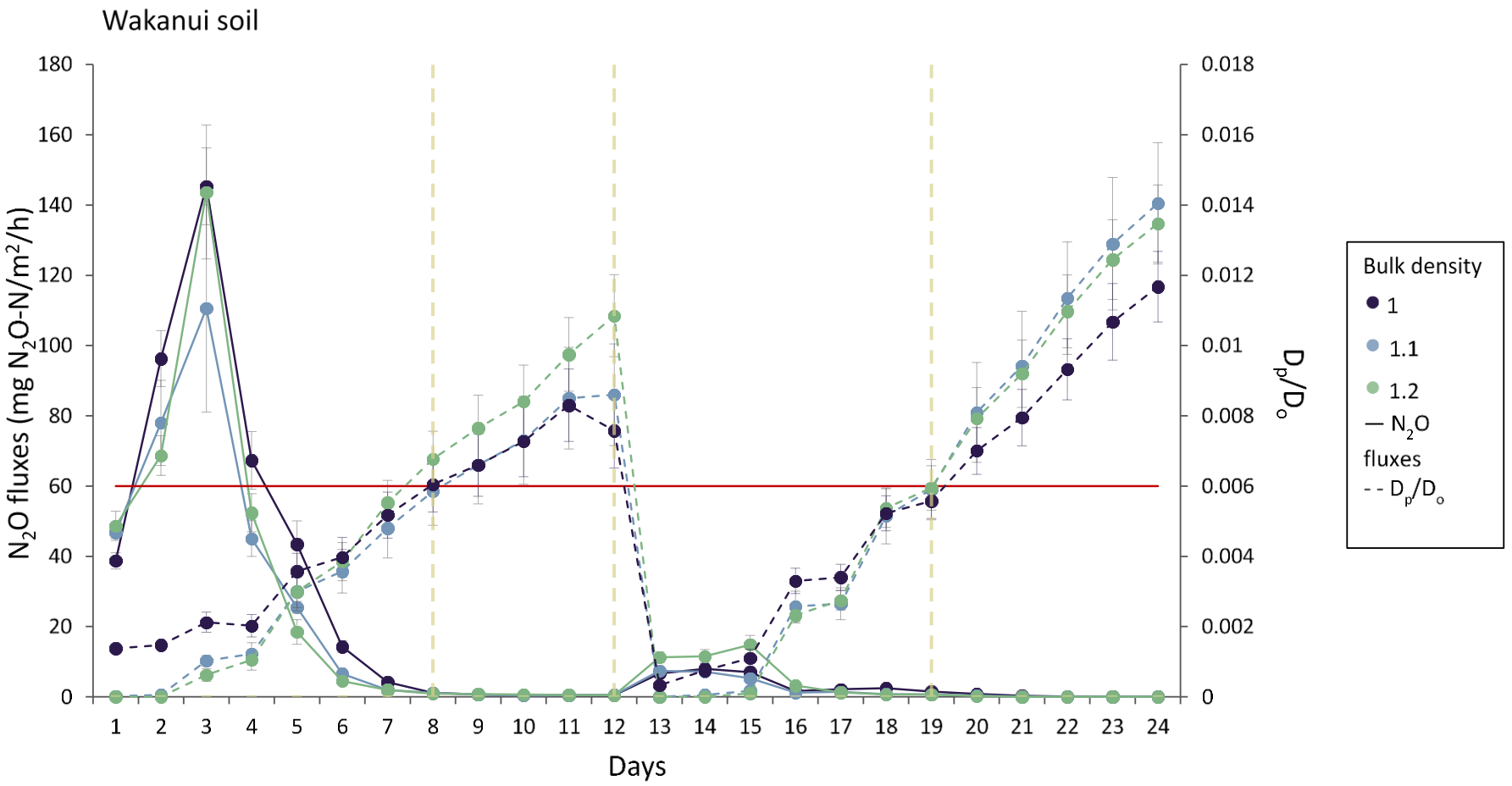

Figure 41: Mean daily N_2O fluxes from soil cores and gas diffusivity (D_p/D_o) over time for the Wakanui soil. The 2 wetting-draining cycles are represented with the first cycle from day 0 to 12 and the second from day 13 to 25. The solid red line represent D_p/D_o = 0.006. Numerals in the legend indicate the soil bulk density treatments applied (Mg m^{-3}). Error bars = s.e.m, n=4. The vertical yellow lines are here to show the days where D_p/D_o = 0.006.

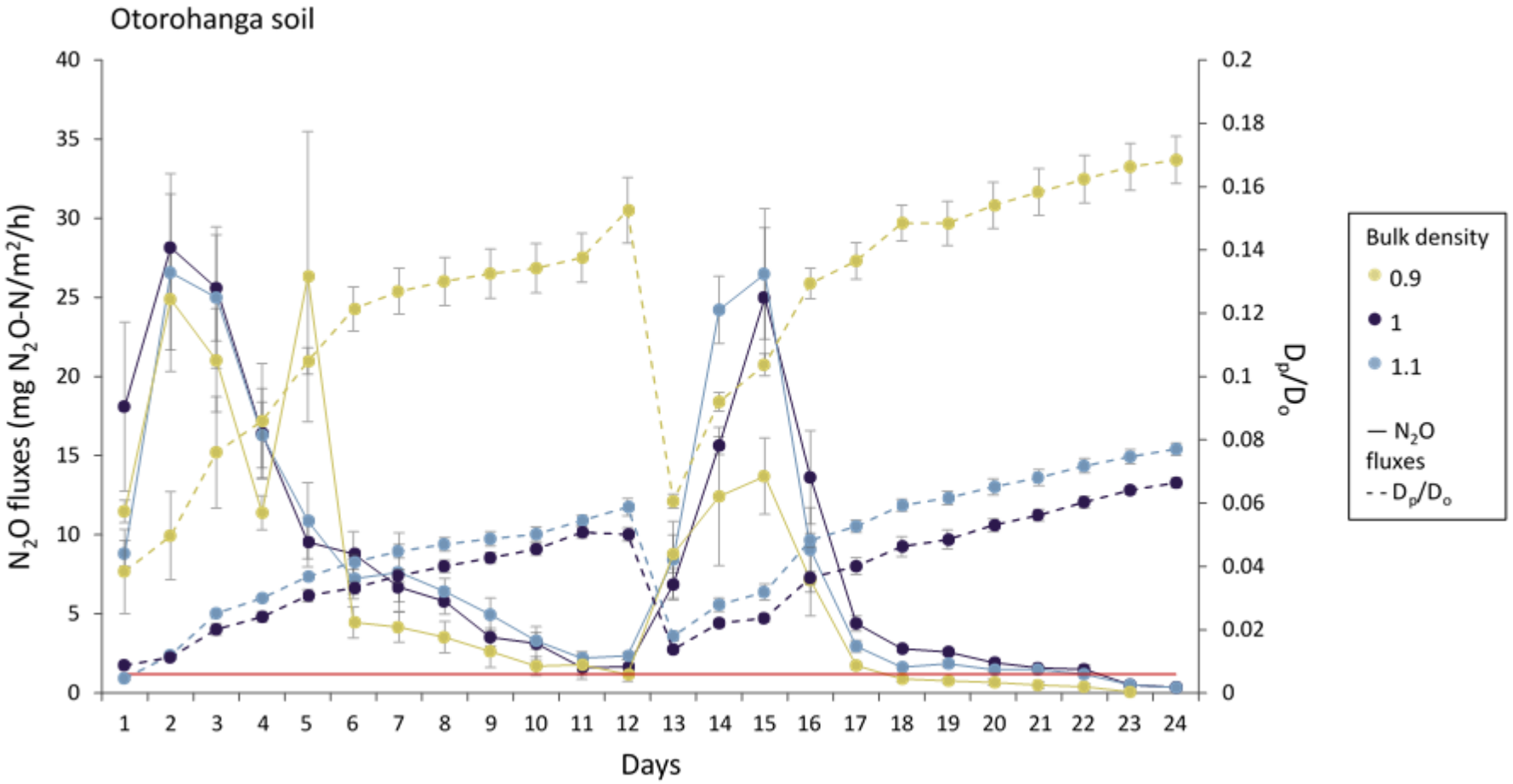

Figure 42: Mean daily N_2O fluxes from soil cores and gas diffusivity (D_p/D_o) over time for the Otorohanga soil. The 2 wetting-drainage cycles are represented with the first cycle from day 0 to 12 and the second from day 13 to 25. The solid red line represent D_p/D_o = 0.006. Numerals in the legend indicate the soil bulk density treatments applied (Mg m-3). Error bars = s.e.m, n=4. Note D_p/D_o scale is greater than in Figure 8.

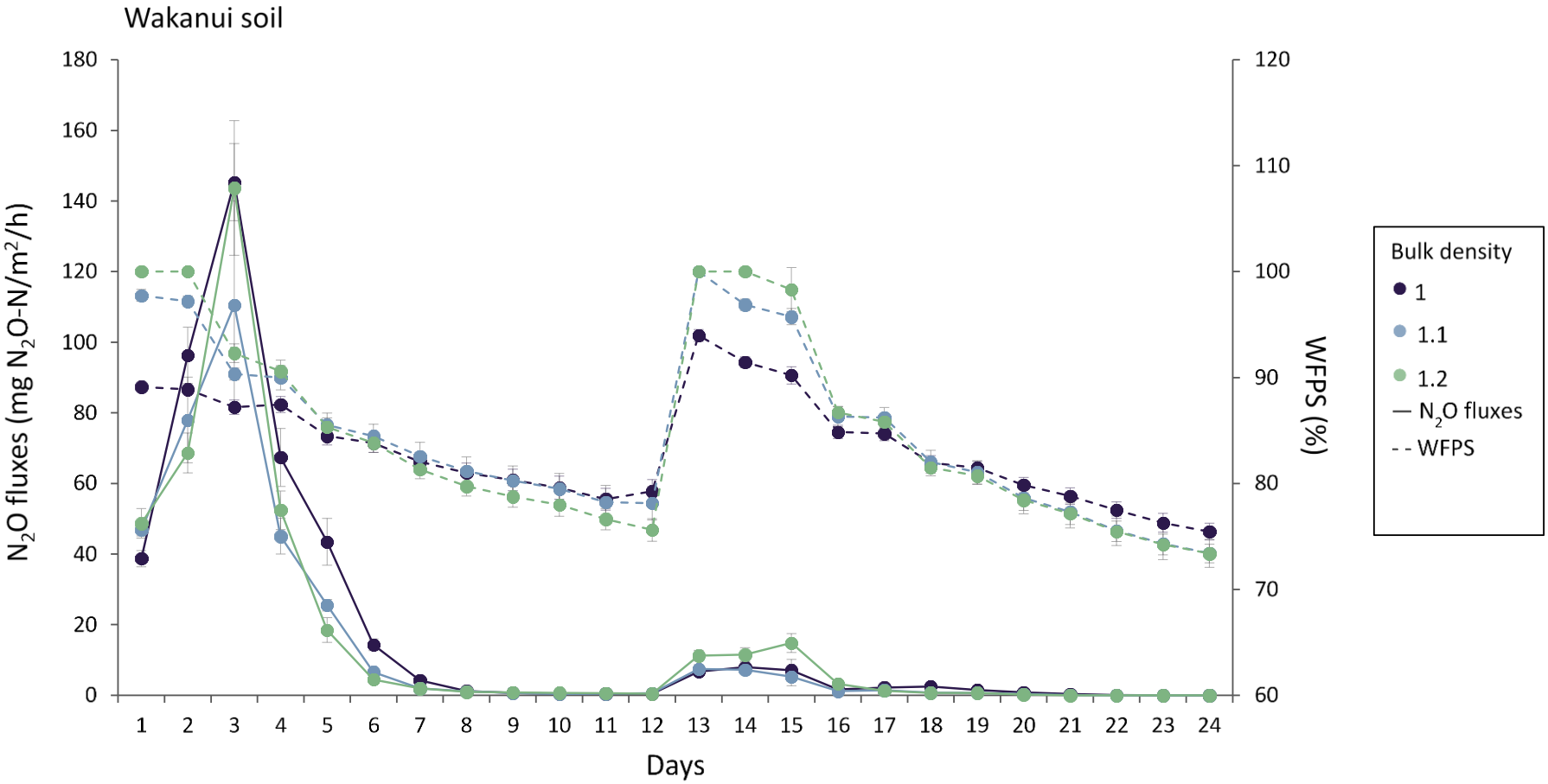

Figure 43: Mean daily N_2O fluxes from soil cores and WFPS over time for the Wakanui soil. The 2 wetting-draining cycles are represented with the first cycle from day 0 to 12 and the second from day 13 to 25. Numerals in the legend indicate the soil bulk density treatments applied (Mg m^{-3}). Error bars = s.e.m, n=4.

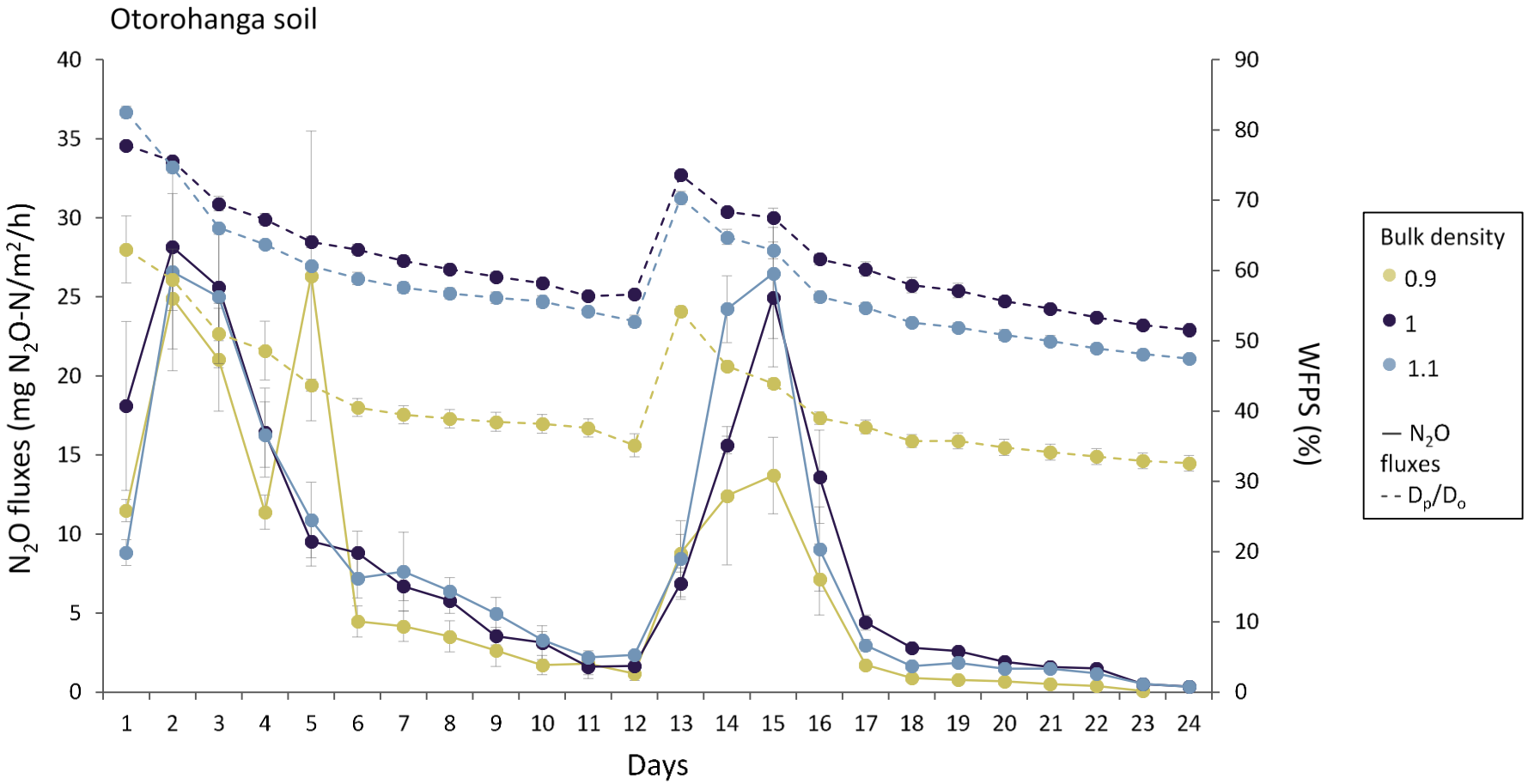

Figure 44: Mean daily N_2O fluxes from soil cores and WFPS over time for the Otorohanga soil. The 2 wetting-draining cycles are represented with the first cycle from day 0 to 12 and the second from day 13 to 25. Numerals in the legend indicate the soil bulk density treatments applied (Mg m^{-3}). Error bars = s.e.m, n=4.

From day 1 to 24 mean daily N_2O-N fluxes were higher for the Wakanui soil compared to the Otorohanga soil ($P < 0.05$), as were the cumulative N_2O-N fluxes from day 1 to 24 (Figure 46). Over this time, there was no significant effect of soil ρ_b, for either soil, on the cumulative N_2O fluxes ($P = 0.132$ and 0.237 for Wakanui and Otorohanga soil, respectively). For the Otorohanga soil, there was a difference ($P < 0.001$) in the cumulative N_2O fluxes between the first (day 12) and second (day 24) saturation events with averages across soil ρ_b equal to 2.92 g N_2O-N m^{-2} and 4.55 g N_2O-N m^{-2}, respectively. This significant difference was not observed for the Wakanui soil; the N_2O fluxes did not increase significantly in the second cycle. Recovery of N_2O as % of applied N (Figure 45) in the Wakanui soil was 64.1% when averaged across soil ρ_b with a non-significant increase in cumulative flux between day 12 and 24 ($P = 0.27$). While in the Otorohanga recovery of N_2O as % of applied N was 32.1% of applied N when averaged across ρ_b at the end of the experiment with a significant ($P < 0.001$) increase between day 12 and 24 (Figure 45). For Otorohanga soil, the soil ρ_b had also a significant effect ($P = 0.02$) on cumulative N_2O fluxes at the end of the experiment with lower cumulative emission for ρ_b equals to 0.9 Mg m^{-3} compared to 1 and 1.1 Mg m^{-3} (Figure 46).

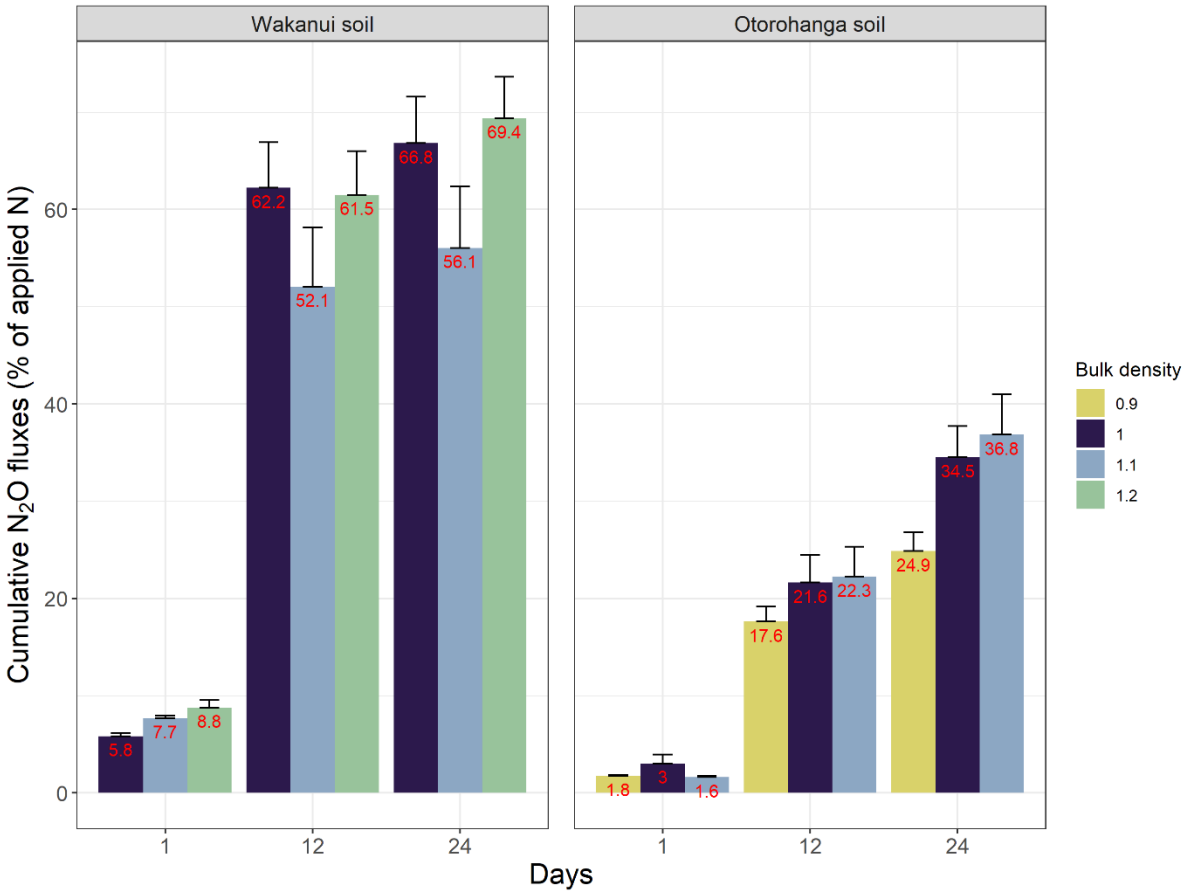

Figure 45: Cumulative N_2O fluxes (% of applied N) for days 1, 12 and 24 for the Wakanui soil and the Otorohanga soil. Day 12 was the last day of the 1st cycle and 24 the last day of the 2nd cycle. Numerals in the legend indicate the soil bulk density treatments applied (Mg m-3). Error bars = s.e.m, n=4.

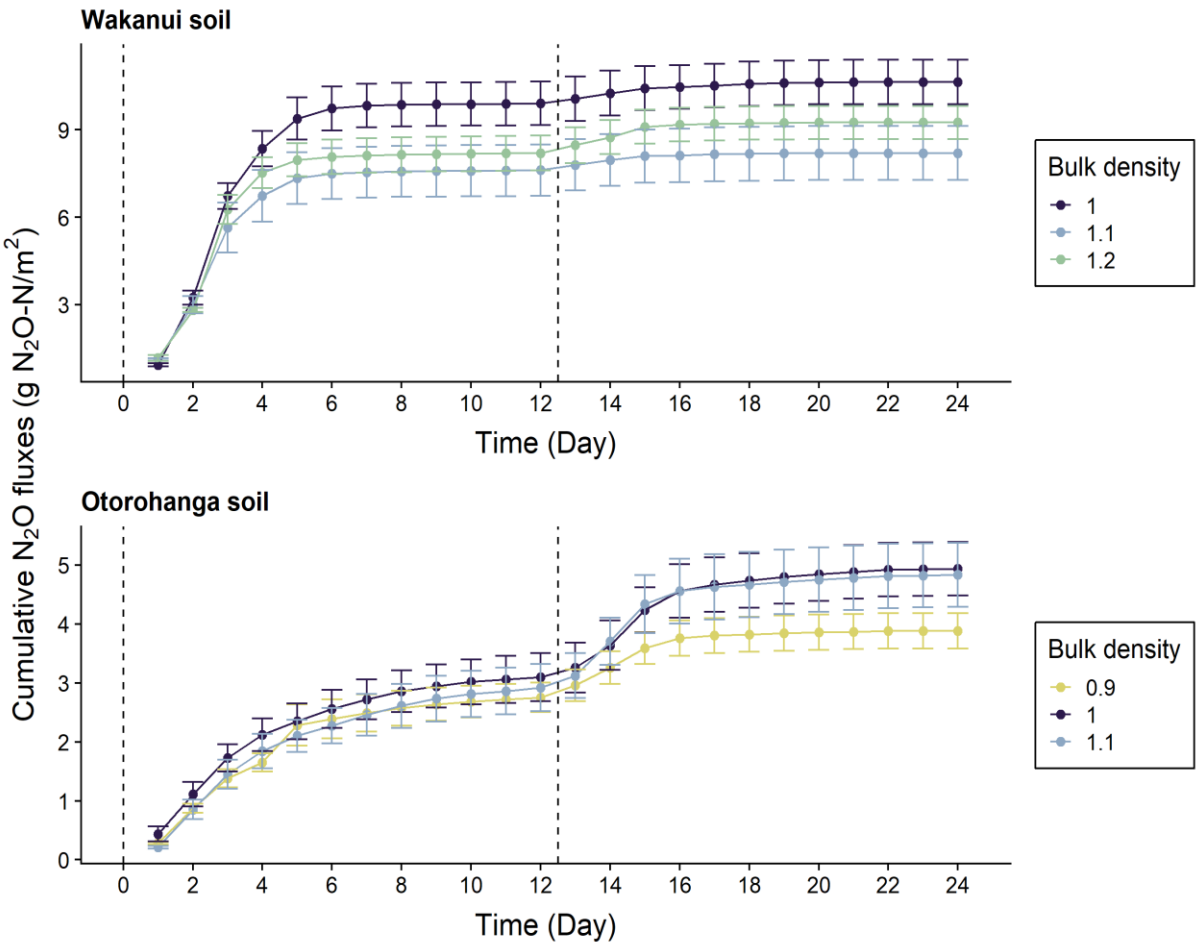

Figure 46: Cumulative N_2O fluxes over time for the Wakanui soil and the Otorohanga soil. Also are shown the 2 saturation events (vertical dashed lines). Numerals in the legend indicate the soil bulk density treatments applied (Mg m^{-3}). Error bars = s.e.m, n=4.

The ^{15}N enrichment of the N_2O-N was highest in the Wakanui soil during the first drainage cycle decreasing from a mean value of 26.0 atom% on day 3, averaged across soil bulk densities, to a mean of 13.6 atom% prior to re-saturation of the soil on day 12. After re-saturation the ^{15}N enrichment of the N_2O flux increased slightly on day 14 again to a mean value of 16.0 atom% before declining again to be 3.7 atom% on day 24 (Figure 47). There were few differences in N_2O-^{15}N enrichment due to soil bulk density in the Wakanui soil (Figure 47). In the first drainage cycle the Otorohanga soil N_2O-^{15}N enrichment was initially 4.0 atom% on day 1 before increasing to 7.4 atom% on day 6 (Figure 47), where after values declined over time to average 5.6 atom% on day 24 at bulk densities of 1.0 or 1.1 Mg m^{-3}, and 4.1 atom% at a bulk density of 0.9 Mg m^{-3}. The N_2O-^{15}N enrichments in the 0.9 Mg m^{-3} treatment were generally lower ($P < 0.01$) than in the other bulk densities for the Otorohanga soil (Figure 47).

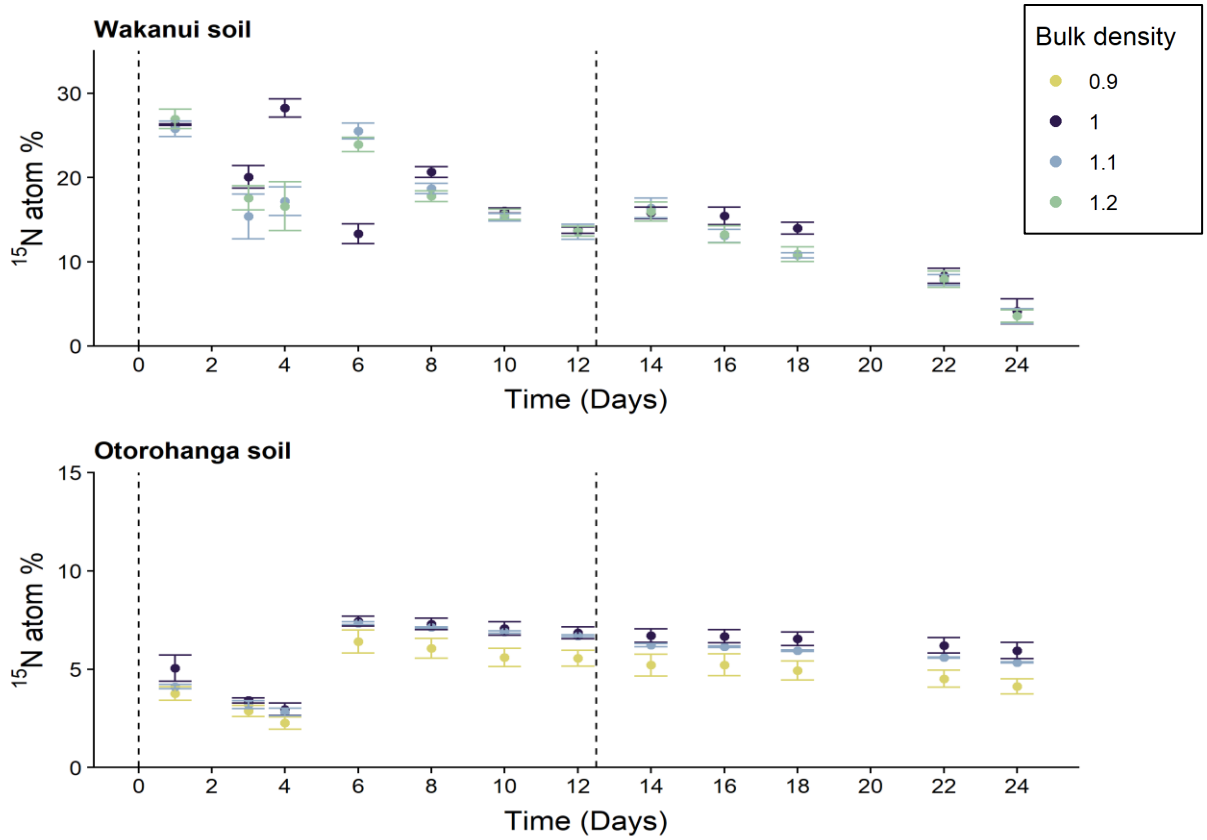

Figure 47: Mean daily N_2O ^{15}N enrichment (atom %) over time for the Wakanui soil and the Otorohanga soil. Also are shown the 2 saturation events (vertical dashed lines). Numerals in the legend indicate the soil bulk density treatments applied (Mg m^{-3}). Error bars = s.e.m, n=4.

Soil N_2 fluxes (Figure 48) in the Wakanui soil peaked on day 6 (1.8 mg N m^{-2} h^{-1}) and days 16 (4.5 mg N m^{-2} h^{-1}) during the first and second drainage cycles, respectively, with the N_2 peak fluxes one or two orders of magnitude lower than the peak N_2O-N fluxes (Figure 41) with few differences due to bulk density. Fluxes of N_2 from the Otorohanga soil were an order of magnitude lower than those observed in the Wakanui soil (Figure 48). Flux of N_2 varied sporadically with soil bulk density treatment in the Otorohanga soil until day 14 when N_2 flux increased regardless of soil bulk density (). At 0.9 Mg m^{-3}, the soil N_2 flux then declined relatively slowly, while at soil bulk densities of 1.0 and 1.1 Mg m^{-3} N_2 fluxes declined by day 16 before they again increased (Figure 48).

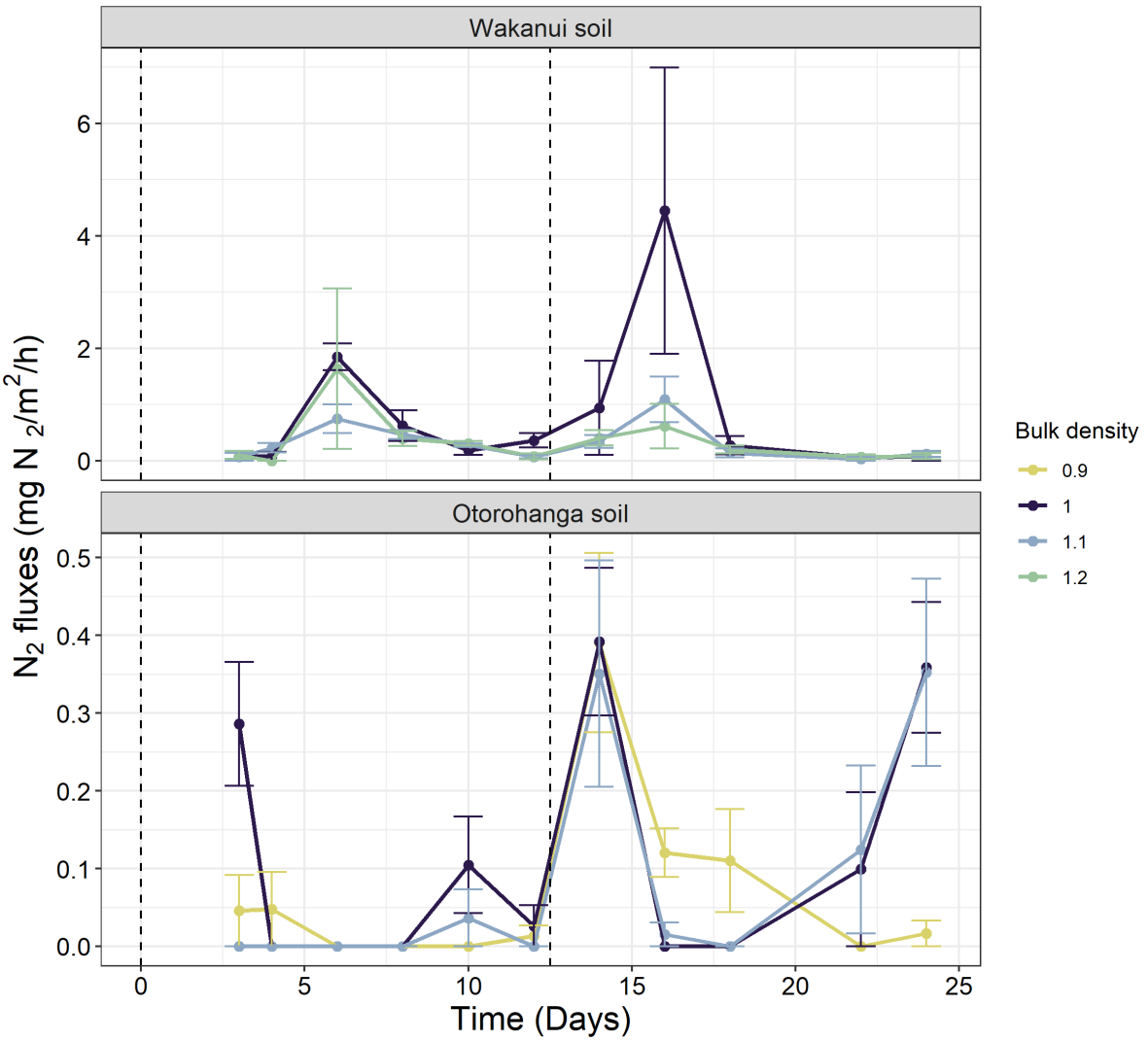

Figure 48: Mean daily N_2 fluxes over time for the Wakanui soil and Otorohanga soil. Also shown are the 2 saturation events (dashed vertical lines). Numerals in the legend indicate the soil bulk density treatments applied (Mg m^{-3}). Error bars = s.e.m, n=4.

IV.5 Discussion

Although the Otorohanga soil had a lower particle density the total porosity was only 2-3% higher than the Wakanui soil at comparable bulk densities (1.0 and 1.1 Mg m^{-3}). However, the fact that the Otorohanga soil's air-filled porosity values were consistently higher, at any given matric potential demonstrates that the Otorohanga soil contained a higher percentage of macropores (pores with a diameter > 30 µm) since macropores drain at matric potentials over

the range of 0 to -10 kPa (Schjønning *et al.* 2003). Greater macroporosity in the Otorohanga soil resulted from there being a coarser texture and fewer soil aggregates < 0.6 mm in size (Figure 36). At the lower bulk density of 0.9 Mg m^{-3} in the Otorohanga soil the macroporosity was higher still due to reduced aggregate damage, as a consequence of reduced compaction, resulting in the observed enhanced air-filled porosity. The higher occurrence of air-filled macropores in the Otorohanga soil consequently caused a greater proportion of the total porosity to be air-filled and explains the higher values of D_p/D_o determined in the Otorohanga soil (Figure 40).

The higher air-filled porosity in the Otorohanga soil equated with higher normalised air-filled porosities which explains the majority of the D_p/D_o values being above Stepniewski's (1981) anaerobic limit of 0.02, where plants roots are considered to begin experiencing anaerobiosis, and the previously described threshold for peak N_2O emissions of 0.006 (Balaine *et al*. 2013). Conversely, in the Wakanui soil, the finer texture and the higher percentage of finer aggregates, explains the reduced macroporosity, which resulted in almost all D_p/D_o values being < 0.02, and with most D_p/D_o values < 0.006. Thomas *et al*. (2019), in their study on the effect of soil compaction, showed that N_2O emissions were aligned with a loss of macroporosity. This loss of macropores corresponds with an increase in microporosity and thus longer periods of saturation due to reduced drainage rates. The varying D_p/D_o regimes affected N_2O fluxes accordingly.

In the Wakanui soil, during the first wetting-drainage cycle, the highest N_2O fluxes following saturation coincided with the soil being anaerobic (D_p/D_o < 0.006), with the observed decline in the N_2O fluxes corresponding with increased drainage and the ensuing increase in soil O_2, as manifested in the higher D_p/D_o values (> 0.006). The elevated ^{15}N enrichment of the N_2O demonstrates that the ^{15}N labelled NO_3^- contributed strongly to the N_2O flux in the Wakanui

soil but this enrichment declined over the drainage cycle demonstrating that the NO_3^- pool was being diluted as a consequence of mineralization and nitrification of antecedent-N.

Potentially, DNRA (dissimilatory nitrate reduction to ammonium) or denitrification are the likely anaerobic pathways generating the N_2O fluxes observed. The addition of N has been shown to reduce DNRA in N-limited rice paddy soils (Pandey *et al.* 2019) with DNRA dominating over denitrification as the soil organic carbon (SOC): NO_3^- ratio increases. Similarly, bacterial culture studies have demonstrated the co-existence of DNRA and denitrification processes, with DNRA dominating when NO_3^- is limited, and denitrification dominating when organic C becomes limiting denitrification dominated (Van den Berg *et al.* 2016). However, in a study by Friedl *et al*. (2018) the drying, sieving and subsequent rewetting of subtropical pasture soils, as performed in the current study, resulted in not only denitrification increasing but also DNRA, with the increase in DNRA thought to be the result of the increasing supply of labile C (soil organic C contents ranged from 4.1 – 4.9%,). In the current experiment, given the relatively low SOC content of the Wakanui soil, the observed DOC concentrations, and the relatively high soil NO_3^- concentrations, it can be assumed that denitrification was predominately responsible for the high N_2O fluxes when soil was anaerobic ($D_p/D_o < 0.006$). This is further evidenced by the flux of N_2 which peaked on day 6, following the decline in the N_2O flux. This delay in the N_2 peak flux relative to the peak N_2O flux results from the need for N_2O reductase to be formed, and also the fact that N_2 cannot be released from the soil until the air-entry potential of the soil, which facilitates gas diffusion, has been meet (Balaine *et al.* 2013): O_2 entry into the soil causes denitrification to decline while any entrapped denitrification products are able to diffuse out of the soil.

While there was lag in peak N_2 fluxes in the Wakanui soil, for reasons noted above, the size of the N_2 flux was lower relative to the N_2O flux. Those low N_2 fluxes relative to the N_2O fluxes, low $N_2O/(N_2O+N_2)$ flux ratios, may have been the result of the abundant NO_3^- supply.

Laboratory studies have shown that for some denitrifiers, under anaerobic conditions, the addition of NO_3^- can reduce the flow of electrons through nitrite reductase, resulting in a decrease in the $N_2O/(N_2O+N_2)$ ratio (Liu *et al*., 2013; Scheer *et al*., 2016; Senbayram *et al*., 2012). A two-year field study by Qin *et al.* (2017) showed that elevated NO_3^- concentrations averaging only 30 mg kg^{-1} (range 17-58 mg kg^{-1}) were sufficient to consistently lower the $N_2O/(N_2+N_2O)$ ratio. Previously, N_2O concentrations have been observed to peak at D_p/D_o values of 0.006 with N_2 fluxes increasing at values < 0.006, unless the N_2 is entrapped (Balaine *et al.* 2013, 2016). High NO_3^- concentrations that result in competition between the NO_3^- and N_2O enzymatic reducing pathways may also explain why peak N_2O concentrations occurred at D_p/D_o values < 0 .006. Furthermore, the relative low soil pH values may have hindered the function of N_2O reductase.

While the highest N_2O fluxes again aligned with D_p/D_o values < 0.006 during the Wakanui soil's second wetting-drainage cycle these fluxes were an order of magnitude lower than in the first wetting-drainage cycle. The D_p/D_o values indicate anaerobic pathways were again responsible for the N_2O fluxes. The fact that the N_2O fluxes were an order of magnitude lower in the second drainage cycle possibly indicates a lower rate of N_2O production, which is unlikely given the anaerobic conditions and NO_3^- substrate supply, however, the quality of the DOC available is unknown and it may have been less readily available to soil microbes. Alternatively, a greater rate of N_2O reduction to N_2 may have occurred, but again the high NO_3^- concentration would not necessarily favour this. Production of N_2 was not readily detectable after day 16 due to the continuing decline in the denitrifying pool ^{15}N enrichment. The low N_2 fluxes for the Otorohanga soil might also be a result of the acidic pH of the soil (5.2). Čuhel *et al.* (2010) in their field study showed that for acidic pH (average 5.52), the $N_2O/(N_2O + N_2)$ ratio increased due to changes in the total denitrification activity, while no changes in N_2O production were observed confirming that the acidic soils are unfavourable to N_2O reduction

into N_2. They also demonstrated that the NH_4^+ concentration was higher in the acidic soil than in the natural pH and alkaline soils, while the NO_3^- concentration was higher in the soils with alkaline pH and decreased significantly with decreasing pH. Friedl et al (2018) observed that changes in redox potential, the result of pasture soils containing high amount of labile C and wetting events inducing reductions in soil redox, altered patterns of NO_3^- consumption between denitrification and DNRA. This competition may explain the relatively low N_2O fluxes observed in the Wakanui soil's second drainage cycle.

Temporal declines in the ^{15}N enrichment of soil inorganic-N pools have been reported previously, for both temperate and subtropical pasture or grassland soils (Rutting *et al.* 2010; Muller *et al.* 2014; Moser *et al.* 2018; Friedl *et al.* 2018). Both heterotrophic and autotrophic nitrification processes may be responsible for NO_3^- production and the dominance of either process depends on a soil's aeration status and texture. For example, upon incubating soils (25ºC over 2 days) of varying texture, Friedl *et al*. (2018) found heterotropic nitrification dominated the production of NO_3^- when WFPS was 95% in both a clay and a sandy soil, while in a loam it dominated at all WFPS values (40-95%), autotropic nitrification peaked at 60% WFPS in clay and sandy soils. The dilution of a given NO_3^- pool by ongoing nitrification processes can be rapid following soil rewetting with gross nitrification rates > 20 μg g^{-1} soil day^{-1} reported for subtropical pasture soil (Friedl *et al.* 2018). At cooler temperatures the dilution rate declines, for example, Thomas *et al.* (2019) applied weekly wetting-drainage cycles to intact silt loam soil cores receiving 250 kg N ha^{-1} as KNO_3, maintained at 14ºC over 74 days, and observed a gradual decline in the ^{15}N atom% of N_2O from ~48 to ~20 atom%. Hence, the temporal decline in the ^{15}N enrichment of the Wakanui soil's denitrifying pool can be attributed to nitrification of antecedent soil N. This further demonstrates the difficulty of attempting to measure N_2 fluxes when the ^{15}N enrichment of the denitrifying pool declines

rapidly and it is likely to be a greater problem where soils have been air-dried and repacked as opposed to intact soil studies.

The relatively lower fraction of air soil content in the Wakanui soil (Figure 39) was due to the higher clay content, the lower sand content, and the greater mass of smaller aggregates (Figure 36). This decreased air water content resulted in lower values of D_p/D_o driving down the O_2 diffusion so that both the volume of anaerobic soil and the period of anaerobicity were theoretically higher than in the Otorohanga soil. However, the Otorohanga soil generated N_2O fluxes in response to the wetting-drainage cycles, even though they were 5-fold lower, suggesting that aerobic mechanisms were responsible for inducing these N_2O fluxes. Indeed, these N_2O fluxes began increasing at soil D_p/D_o values generally considered aerobic (> 0.02): at bulk densities of 1.0 and 1.1 Mg m^{-3} the N_2O fluxes began to increase at a D_p/D_o value ~0.05 while at a bulk density of 0.9 Mg m^{-3} peak N_2O fluxes generally occurred between D_p/D_o 0.05 and 0.10. Thus, while soil physical conditions were indicative of the soil being generally aerobic for much of the wetting-drainage cycles other factors must have contributed to the formation of anaerobic conditions in response to the wetting-drainage cycles. The lower N_2O-^{15}N enrichment in the Otorohanga soil N_2O fluxes also shows the applied NO_3^- made a much lower contribution to the N_2O flux than in the Wakanui soil indicating that antecedent soil N comprised a significant portion of the N_2O evolved. Given these results and the higher C content of the Otorohanga soil, along with the decline in DOC, it is likely that higher rates of respiration in the Otorohanga soil resulted in greater O_2 consumption. Petersen *et al*. (2013) recorded N_2O emissions from cropping system soils at D_p/D_o > 0.02 following a simulated freeze-thaw cycle, and attributed this to an increased O_2 demand due to inputs of C from crop residues. Friedl *et al.* (2018) also observed N_2 fluxes at D_p/D_o values > 0.02 due to the wetting up of dry pasture soil releasing C and N. In their ^{15}N tracing study Friedl *et al.* (2018) were able to show that the wetting of dry pasture soil increased DNRA, with both DNRA and

denitrification responding positively to NO_3^- supply, with increasing heterotrophic respiration generating a reduction in the redox potential which in turn shifted NO_3^- consumption from denitrification to DNRA. The current study does not permit such a delineation of microbial pathways for N_2O generation but it is likely that redox effects similar to those observed by Friedl *et al.* (2018) also occurred.

The initial dilution of the NO_3^--^{15}N enrichment occurred as a consequence of NO_3^- formation during air-drying. Subsequent declines in the ^{15}N dilution rate of the NO_3^- pool, assumed to match that of the N_2O-^{15}N enrichment, were much slower in the Otorohanga soil than observed in the Wakanui soil, indicating a slower net rate of nitrification. Friedl *et al.* (2018) observed higher rates of NO_3^- production, dominated by heterotrophic nitrification in clay and loam soils while lower net nitrification rates occurred in a sandy clay loam dominated by autotrophic nitrification. Thus, the Otorohanga soil, with greater porosity and sand content, may have had a lower denitrification rate due to the dominance of autotrophic nitrification. Accordingly, nitrification will also have contributed to the observed N_2O emissions.

Clearly there is an effect of soil texture and structure on drainage rate and residual soil moisture which in turn directly effects D_p/D_o. While the results confirm the relationship between D_p/D_o and N_2O emissions they also demonstrate that the soil O_2 demand may further reduce soil redox in soils with high organic matter contents following wetting-drainage events. The *in situ* effects of this in perennial pasture systems should be further assessed, ideally with accompanying measures of soil O_2, respiration and soil structure. Also highlighted by these results is another obstacle in the determination of N_2 fluxes: the dilution of ^{15}N enriched nitrate pools over longer experimental periods due to the relatively rapid dilution of the ^{15}N pool by antecedent soil N. This calls for adjustments in the experimental designs and/or the use of more sensitive methods of N_2 flux determination (e.g. Scheer *et al.*, 2016) when assessing the effects of wetting-draining cycles over realistic time frames.

IV.6 Synthesis of the data from the previous two chapters

In Chapter III and Chapter IV it was shown that D_p/D_o was arobust measure for predicting the onset N_2O emissions from denitrification from varying soil types and ρ_b treatments. This is consistent with the theory of Farquharson and Baldock (2008) who explained that for a given WFPS the volume of fraction of air varies depending on the soil ρ_b, making D_p/D_o a better predictor for N_2O emissions. Plotting D_p/D_o and WFPS density distribution curves also showed that values of D_p/D_o had lower scatter distribution curves and produced a better relationship than WFPS over treatments (Figure 49, Figure 50). The increase in N_2O fluxes occurred as condition became increasingly anaerobic, as defined by a decline in D_p/D_o. Maximum N_2O-N fluxes occurred at a mean D_p/D_o value ≤ 0.006 (Figure 49) which supports the earlier results found by Balaine *et al*. (2013), and studies published since the commencement of these experiments (Friedl *et al*. 2018; Chamindu Deepagoda *et al*. 2020). Some lower fluxes were observed for D_p/D_o values < 0.004 suggesting N_2O entrapment in soil which can increase the potential to have a complete denitrification process and a reduction of N_2O into N_2 (Clough *et al*. 2005). No N_2O emissions were observed for D_p/D_o values > 0.02 in the Chapter II (Figure 49, Figure 50), the limit for the onset of anaerobic condition in soils (Stepniewski, 1981). Similar trends were observed in Chapter IV except for the Otorohanga soil (

Appendix 1) where the O_2 demand may have been increased due to a higher soil C content enhancing N_2O emissions for D_p/D_o values > 0.02 but these N_2O fluxes were also 5-fold lower. The N_2O peak intensity also varied according to the soil type which may suggest the involvement of other factors in the denitrification rate. The pH was acidic in all soils, especially after a cycle of drainage, and which is not favourable for N_2O reduction (Hénault *et al.* 2019).

Soil texture and structure were also proved to have an effect on drainage rate as observe in Chapter IV which in turn directly affects D_p/D_o. The high organic matter contents in the original soil or caused by the wetting-drainage events, may be favourable for the soil O_2 demand to reduce the soil redox even further.

Plants compete with soil microorganisms for N. Thus, increased uptake of N by plants can lead to decreased N_2O emissions (Niklaus *et al*., 2006; Baral *et al*., 2014). On the other hand, root exudation of easily metabolised organic compounds may increase microbial activity and then N_2O production (Henry *et al.* 2008).

The results so far were obtained from bare soil experiences. Thus, it is necessary to examine the relationships highlighted above in the context of a system that includes the plant factor(s). Moreover, in the next chapters the ability of the D_p/D_o threshold (keeping the soil D_p/D_o over 0.02) as a tool to schedule irrigation will be developed in order to explore the effect on N_2O emissions.

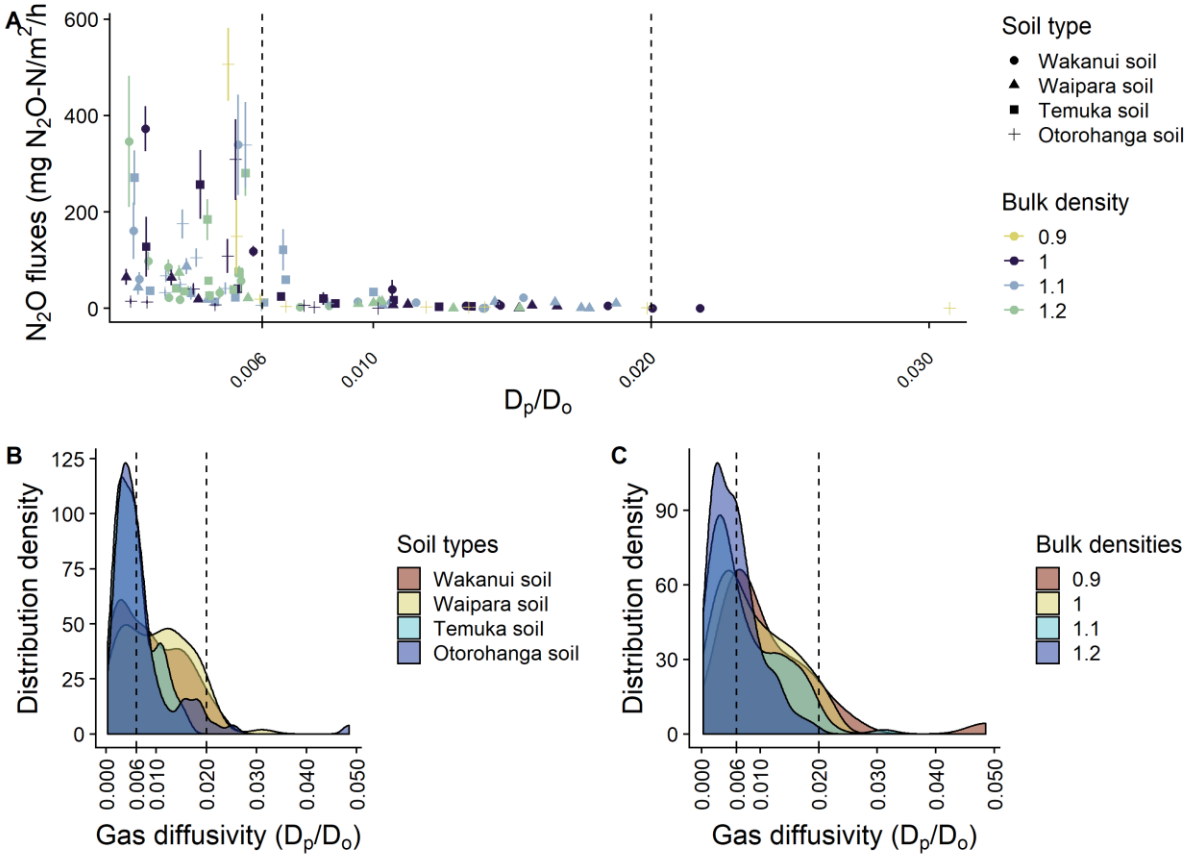

Figure 49: Data distribution graphs showing the general distribution of N_2O fluxes over gas diffusivity (A) and the density estimates of D_p/D_o for the 4 different soil types (B) and bulk densities (C) in the first lab experiment (Chapter II). The dashed lines represent the 0.006 threshold (Balaine et al. 2013) and 0.02 threshold (Stepniewski 1981).

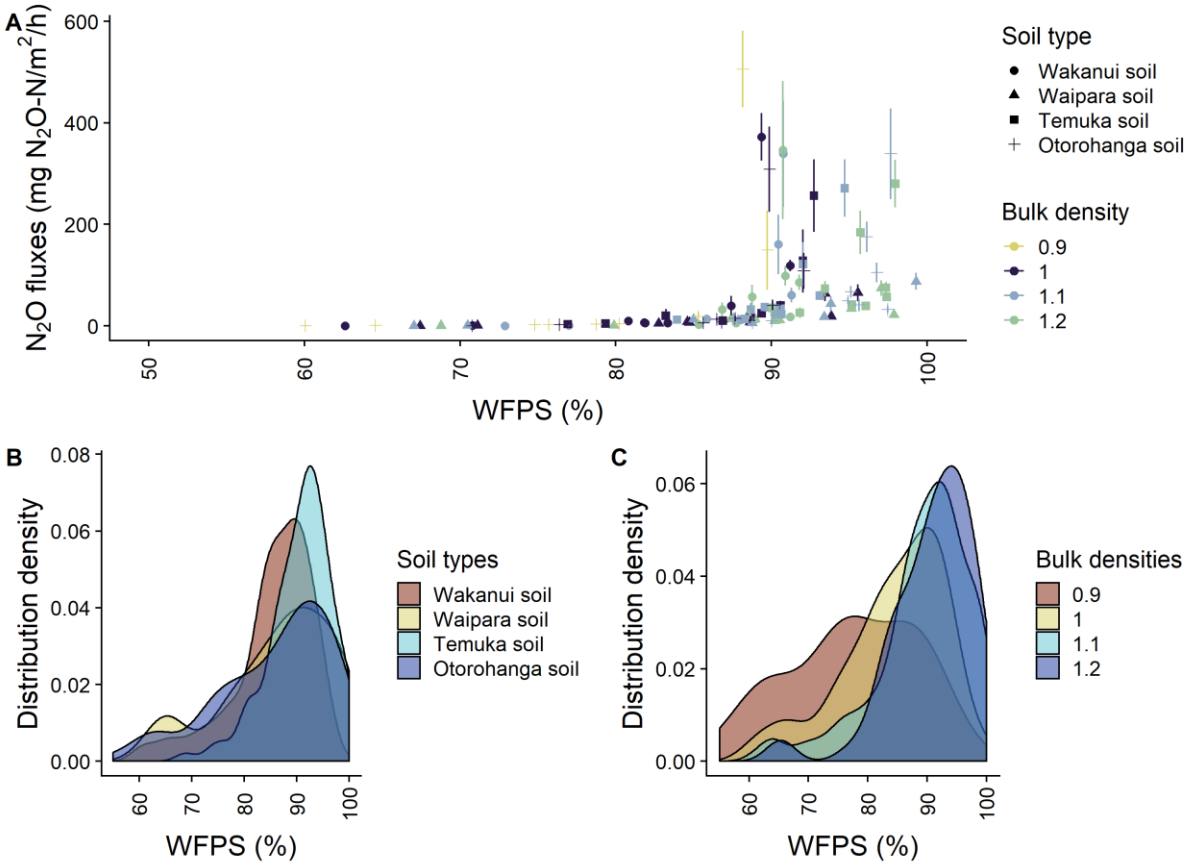

Figure 50: Data distribution graphs showing the general distribution of N_2O fluxes over WFPS (A) and the density estimates of the WFPS for the 4 different soil types (B) and bulk densities (C) in the first lab experiment (Chapter II).

Chapter V Can pasture irrigation be scheduled using soil gas diffusivity: implications for urinary-N derived N_2O fluxes, leaching and plant N uptake.

Highlights:

- Standard irrigation increased the frequency of anaerobic periods in the soil compared to optimised irrigation.
- Anaerobic conditions did not favour N uptake by the plants and a significant decrease in the dry matter biomass was observed.
- High irrigation frequency (standard treatment) did not increase the N_2O emissions.
- Long drying periods followed by a re-wetting event in the optimised irrigation may transform the aggregates and favour the Birch effect leading to release of labile substrates for denitrifiers.

Keywords: Lysimeter, ^{15}N, plant N uptake, N-inorganic leaching, irrigation frequency, modelled D_p/D_o

V.1 Abstract

Ruminant urine deposited onto temperate pasture generates hot spots for N_2O emission. Such emissions are undesirable since N_2O is a greenhouse gas and emissions from grazed pastures make a significant contribution to national greenhouse gas inventories. Processes generating N_2O emissions from pasture soils are controlled by soil O_2 levels. A measure of the ability for O_2 to enter the soil is relative soil gas diffusivity (D_p/D_o). The aim of this experiment was to examine the potential for managing soil N_2O emissions by altering irrigation timing based upon modelled D_p/D_o. This was investigated using repacked lysimeters, sown with perennial ryegrass (*Lolium perenne*), that received either a standard irrigation treatment (15 mm every three days), or an optimised irrigation treatment where irrigation was applied when soil D_p/D_o was 0.085 (equivalent to 50% of plant available water). Fresh cow urine enriched with ^{15}N labelled urea was used to simulate a ruminant urine deposition event (700 kg N ha^{-1}). In addition to N_2O fluxes, soil moisture content, gas diffusivity, pasture dry matter production, and inorganic-N leaching data were collected. Standard irrigation resulted in lower cumulative N_2O emissions than the optimised irrigation, potentially due to a greater periods of anaerobic conditions. Emission factors over the first 39 days of the experiment for optimised and standard irrigation treatments with urine were 1.26 and 0.12%, respectively. Cumulative pasture dry matter production and N uptake were higher in the optimised irrigation treatment. Macropores flow of urine derived N was lower under optimised irrigation.

V.2 Introduction

Anthropogenic emissions of N_2O are dominated by agricultural sources (Ciais *et al*. 2013), with increases in emissions predominately the result of fertiliser-nitrogen (N) and animal manure use (Davidson 2009). Atmospheric concentrations of N_2O have continued to increase at a rate of 0.73 ± 0.03 ppb yr^{-1} over the last three decades, due to the creation of reactive N and the ensuing anthropogenic N_2O emissions from agriculture (Ciais *et al*. 2013). This is of environmental concern because N_2O is both a potent greenhouse gas and, currently, the dominant ozone depleting emission (Ravishankara *et al.* 2009; Ciais *et al.* 2013). Grazed grasslands generate > 10% of global N_2O emissions (Oenema *et al.* 1997) as a result of fertiliser-N inputs and ruminant urine patch formation. The ruminant urine patch forms after ruminant urine deposition and results in a N loading far in excess of the pasture's immediate N demands (Clough *et al.* 2020).

Production of N_2O within the urine patch results from a cascade of N transformations. Initially ammonia (NH_3) is transformed in an aerobic process termed 'nitrification'. In the urine patch this is predominately performed by NH_3 oxidising bacteria (AOB) (Di *et al.* 2009), rather than the NH_3 oxidising archaea (AOA), to produce hydroxylamine, nitric oxide, nitrite and nitrate (Caranto and Lancaster 2017; Stein 2019). If soil conditions become hypoxic AOB generate N_2O through an enzyme driven process termed 'nitrifier-denitrification', and N_2O may also be generated via abiotic and biotic transformations of the metabolic intermediaries as AOA and/or AOB oxidise NH_3 (Stein 2019). If conditions become anaerobic AOB may also generate N_2O via the anaerobic oxidation of hydroxylamine (Stein 2019). Under anaerobic conditions denitrification also produces N_2O as an obligate intermediary following the reduction of nitrate, nitrite, and/or nitric oxide (Zumft 1997), with the ultimate step the reduction of N_2O to the dinitrogen molecule, N_2 (Zumft 1997). This last step is highly sensitive

to oxygen (O_2). Even though N_2 is environmentally benign, emissions of N_2 can result in a significant economic loss of N from pasture soils and reduced N use efficiency. Thus, the level of O_2 within the soil dictates the process generating N_2O and its fate within the soil.

Although N_2O production can occur in pasture soils across a variety of soil O_2 concentrations, the bulk of the N_2O emissions from urine patches in pasture soils tend to occur under soil conditions that are at least hypoxic, if not anaerobic; during seasons when the soil is wetter, such as autumn and winter (de Klein *et al.* 2006), or following irrigation events (Vogeler *et al.* 2019). Soil water-filled pore space (WFPS) has traditionally been used to describe the susceptibility of soils to N_2O production (Linn and Doran 1984) . However, Farquharson and Baldock (2007) show this becomes problematic when comparing soils of varying bulk densities. Trampling by grazing animals can alter the gas diffusion in the soil by compacting the topsoil, which is indicated by increased bulk density and decreased macroporosity (Sitaula *et al.* 2000) (Singleton *et al*. 2000). Soil compaction by tractor traffic is also a widespread problem in modern agriculture (Hansen *et al.* 1993; Breland and Hansen 1996).

The O_2 concentration within the soil is a function of supply, the ability for O_2 to diffuse into the soil, and the demand for O_2, the consumption of O_2 via respiration. The diffusion of O_2 through the soil primarily occurs due to soil-gas diffusion as described by the dimensionless soil gas diffusivity term D_p/D_o, where: D_o is the gas diffusion coefficient of O_2 in free air (m^2 air s^{-1}) and D_p is the gas diffusion coefficient of O_2 in the soil (m^3 soil air m^{-1} s^{-1}). Stepniewski (1981) reported anaerobic conditions commenced when D_p/D_o was < 0.02. However, anaerobic conditions may be attained prior to diffusivity dropping to such a value in C rich soils as a consequence of higher consumption of O_2 (Petersen *et al.* 2013; Friedl *et al.* 2016). Balaine *et al.* (2013) found that for a sieved soil, repacked to varying bulk densities and held at varying water contents, measures of D_p/D_o were better than WFPS for predicting N_2O emissions, with peak N_2O emissions for all bulk density treatments aligning at a D_p/D_o value of 0.006. Rousset

et al. (2020) found this result to be consistent when comparing several repacked pasture soils. Stimulation of N_2O emissions has also been observed in situ when D_p/D_o declined to 0.006 in a pasture soil (Owens *et al.* 2017) and in intact soils cores within a D_p/D_o range of 0.005-0.01 (Chamindu Deepagoda *et al.* 2019). Further studies, with both repacked soil cores and in situ, have shown increases in N_2 emissions as soil D_p/D_o declines below 0.006 (Balaine *et al.* 2016; Friedl *et al.* 2017). Consistent with this is the observed consumption of ^{15}N-labelled N_2O at D_p/D_o values of 0.003 (Klefoth *et al.* 2014).

Manipulation of D_p/D_o could be an approach to mitigating N_2O emissions and reducing N_2 emissions. A management practice that alters soil D_p/D_o is irrigation. The manipulation of irrigation has been shown to mitigate N_2O emissions for cotton and sorghum crops (Scheer *et al.* 2008; Jamali *et al.* 2015). The effects of irrigation frequency and intensity were modelled by Vogeler *et al.* (2019) who found high frequency/low intensity irrigation that resulted in zero moisture deficits after irrigation generated the highest N_2O emissions. Conversely, Mumford *et al.* (2019) found that higher N_2O emissions occurred under low frequency (15 day interval) irrigation events applied to pasture receiving fertiliser (26 kg N ha^{-1} after simulated grazing events; 381 kg N ha-1 yr^{-1}), potentially due to the soil environment being less conducive to N_2O consumption and an enhanced availability of carbon (C). The potential for irrigation management to mitigate N_2O emissions from pasture ruminant urine patches, where urine-N rate deposition may average 613 kg N ha^{-1} (Selbie *et al.* 2015), has not been investigated.

Using a lysimeter set-up this experiment measured N_2O fluxes, plant N uptake and nitrate leaching following ruminant urine application under a standard and optimised irrigation with the later based on maintaining a value of D_p/D_o where O_2 diffusion could occur. It was hypothesised that maintaining the soil D_p/D_o above a value of 0.02 would mitigate urine-N induced N_2O emissions.

V.3 Materials and methods

V.3.1 Lysimeter design

Soil, classified as a Wakanui silt loam soil (Mottled Immature Pallic Soil; Lilburne *et al*. 2012), was obtained in June 2019 from a dairy farm pasture at Lincoln University (43°38'27.0456"S, 172°27'45.7308"E). The soil was air dried and sieved to ≤ 2 mm, and then a subsample was taken to determine the gravimetric water content by drying at 105ºC for 24 h. Sixteen repacked soil lysimeters were constructed using polyvinyl chloride (PVC) cylinder pipe (200 mm long x 150 mm diameter, Figure 51). Air-dried sieved soil was packed into the PVC cylinders to a depth of 180 mm to achieve a soil ρ_b of 1.2 g cm^{-3}. This soil ρ_b was chosen because in Chapter III, the soil total N_2O-N fluxes were higher with increasing soil ρ_b ($P < 0.05$). A nylon mesh (0.25 mm) was fastened to the base of the lysimeter to prevent soil egress and the lysimeter base was supported by an aluminium wire mesh (Figure 51). This, in turn, sat within a funnel that was connected to a 1 L leachate collection bottle. Perennial ryegrass (*Lolium perenne* cultivar -Excess AR37) pasture was then sown (20 kg ha^{-1}). The lysimeters were placed on benches in the glasshouse to allow pasture to establish (3 weeks in total). Glasshouse temperatures ranged between 16 and 24ºC (Figure 54) and the plants received 16 hours of light (Lumatek HPS 600W lamps) every 24 hours to mimic summer growth conditions. Before starting the experiment, a subsample of the sieved soil was taken and analysed for pH, DOC and soil inorganic-N concentrations (Table 5).

Table 5: Soil (0-10 cm) characteristics before urine application. Texture analyses were performed using a laser diffraction particle analyser (mastersizer 3000, Malvern Panalytical). IUSS stand for International Union of Soil Science (clay 0-2 µm, silt 2-63 µm, and sand 63-2000 µm).

Coordinates	43° 38' 27.0456" S; 172° 27' 45.7308" E
Soil type	Wakanui Mottled Immature Pallic Silty Loam
Texture class	Silty Loam
Clay (%) IUSS	22.3
Silt (%) IUSS	53.4
Sand (%) IUSS	24.3
DOC (µg g^{-1})	225.9 ± 2.2 (s.e.m)
NO_3^--*N (µg g^{-1})*	8.96 ± 0.35 (s.e.m)
NH_4-*N (µg g^{-1})*	6.42 ± 0.41 (s.e.m)
pH	5.34
Bulk density (g cm^{-3})	1.2

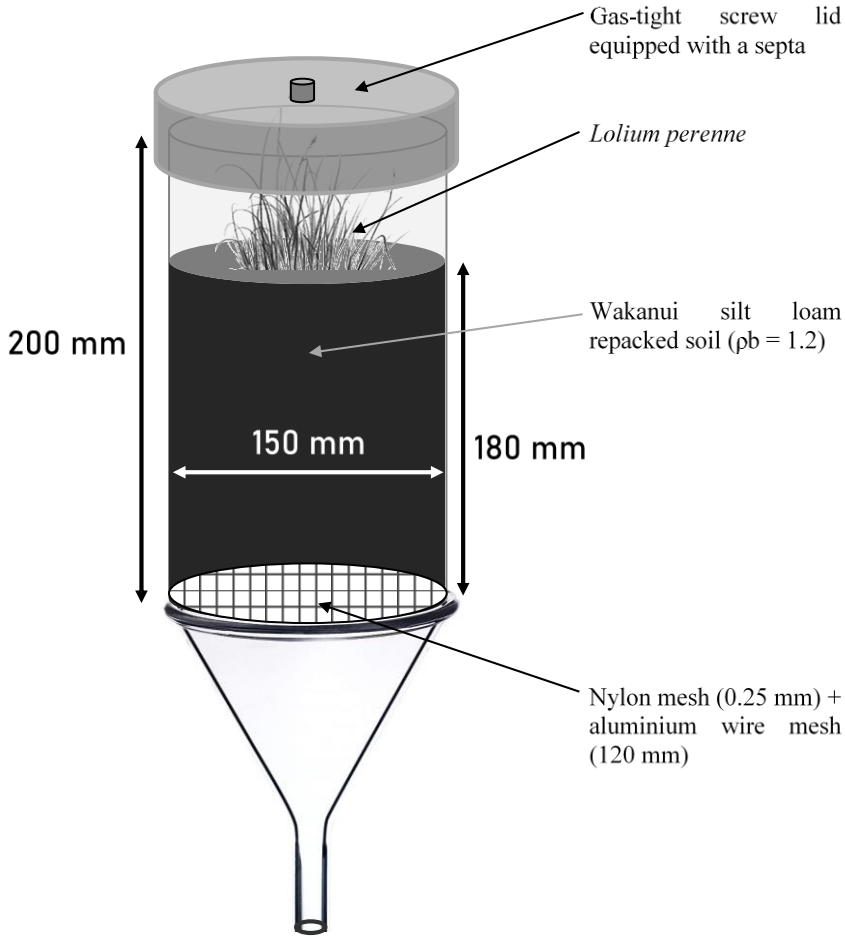

Figure 51: A schematic of the lysimeter setup

V.3.2 Experimental design

The experiment had a factorial design consisting of four treatments replicated four times: treatments were cow urine (plus or minus) and irrigation (standard or optimised). Fresh dairy cow urine, containing 5.23 g N L^{-1}, was collected from the Lincoln University Dairy Farm (Figure 52). The urine-N rate to be applied was 700 kg N ha^{-1}, typical of a cow urination event (Selbie *et al.* 2015). The collected urine was adjusted with ^{15}N-labelled urea so that the urine applied had an N concentration of 13.6 g N L^{-1} (calculation based on the average size and concentration of a urine patch, Moir *et al.* 2011) and an enrichment of 14.5 atm% excess. On the 18th of July 2019, day 1 of the experiment (Figure 54), 0.091 L of urine was applied to the aligned treatments while non-urine treatments received the same volume of water. In general, the total N content in cow urine ranges from 6.8-21.1 g N L^{-1} of which about 69% is present as urea (Bristow *et al.* 1992). In the soil, urea is hydrolysed to form NH_4^+ which forms an equilibrium with NH_3 based on soil pH (Sigurdarson *et al.* 2018). Ammonia was present at the lysimeters surface, as evidenced by the NH_3 odour, at the beginning of the experiment. To limit the possible loss of NH_3-N, 15 mm of water was applied in both irrigation treatments 5 days after the urine application (Figure 54).

Figure 52: Tim helping out at the farm to collect cow's urine during the milking.

Based on typical evapotranspiration rates and irrigation return times farmers in Canterbury, New Zealand, typically apply 12-15 mm every 3 days to pastures during the summer months (Owens *et al.* 2016). With a lysimeter surface area of 176.7 cm^2 and a 15 mm irrigation event this equated to 265 cm^3 of water. The standard irrigation treatments consisted of 265 mL of water applied on each lysimeter every 3 days (Figure 54, blue triangles). A survey of farmers in Canterbury, to document irrigation strategy, found 57% of farmers started irrigation in the shoulder seasons when soil contained the equivalent of 50% of plant available water (PAW) with the majority stopping irrigation at 80% of PAW (Birendra *et al.* 2018), this approach follows the good practice irrigation guidelines. Thus optimised irrigation occurred at an irrigation trigger point (TP) equal to 50% of PAW, a soil moisture content that avoids plant stress and yield loss, and which aimed to restore soil moisture to 80% PAW (Figure 53). The amount of PAW is the difference between the soil moisture at field capacity (FC) and permanent wilting point (PWP).

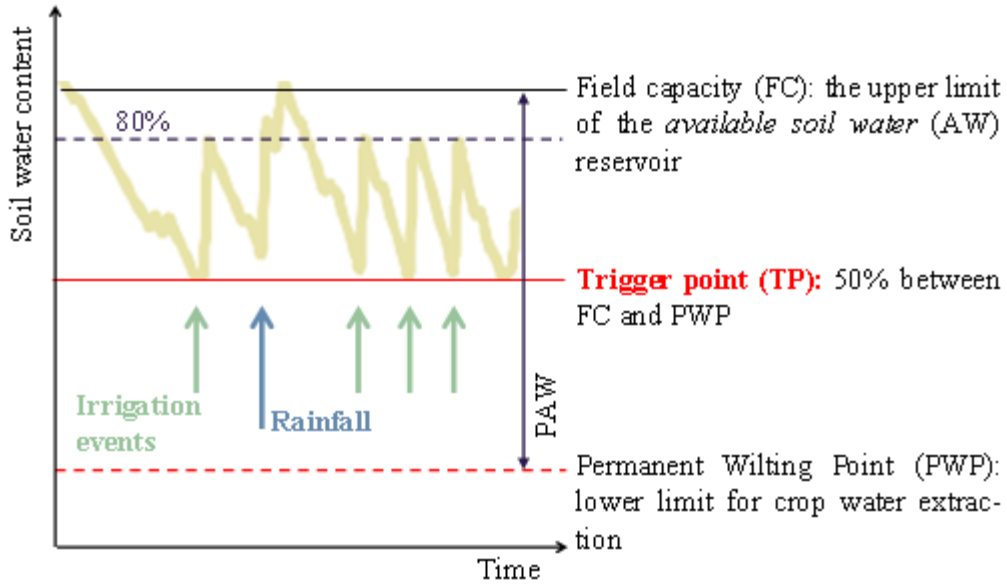

Figure 53: Diagrammatic soil water response to irrigation events and rainfall with field capacity (solid black line), trigger point (solid red line), permanent wilting point (dashed red line) and 80% of PAW-plant available water (dashed black line).

The value of PAW was determined by first determining the soil's FC: the lysimeters were saturated and allowed to drain for 24 h and then the volumetric soil moisture content (θ_v) was calculated. Then the soil PWP, the value of θ_v at -1500 kPa, was determined using a soil subsample and a WP4C dew point potentiometer (Decagon Devices Inc.). Values of θ_v at FC, 80% of FC, TP, and PWP were 0.413, 0.346, 0.236 and 0.140 cm^{-3} cm^{-3}, respectively.

Up until day 39 of the experiment the observed N_2O fluxes were relatively low in the standard irrigation treatment. Thus, to determine the potential for higher N_2O fluxes to occur from this treatment both irrigation treatments were withheld for two periods; from days 39 to 46 and from days 58 to 68. At the end of these irrigation withholding periods lysimeters were rewetted past the trigger point of the optimised irrigation treatment, up to 80% of PAW. These drying events resulted in a volume change potential of the soil generating the formation of a gap between the soil and the cylinder which could have compromised the leaching measurement. As a result, this gap was filled with liquefied petrolatum (Vaseline) as described

in Cameron *et al.* (1992) and the lysimeter weight was adjusted to account for the added weight of the Vaseline.

Lysimeters were weighed daily, prior to gas sampling, to determine their mass. This mass was used to calculate soil water-filled pore space (WFPS), which was in turn used to calculate θ_v and volumetric soil-air content (ε, m^3 of air m^{-3} of soil) of the soil in each lysimeter. Then, these measurements were converted to D_p/D_o values according to Moldrup *et al.* (2013) using the same equation (12) for a repacked soil used in section IV.3.2 with *Cm*, the media complexity factor, set to equal a value of *Cm* = 1 for repacked soil (Moldrup *et al.* 2013).

Values of D_p/D_o for FC, 80% of FC, TP, and PWP were 0.008, 0.026, 0.085, and 0.174, respectively. Note, the D_p/D_o value at 80% of FC value (0.026) was over the threshold observed in the 2 previous chapters where N_2O emissions decline, > 0.02, and also above onset of anaerobic condition in soils (Stepniewski 1981).

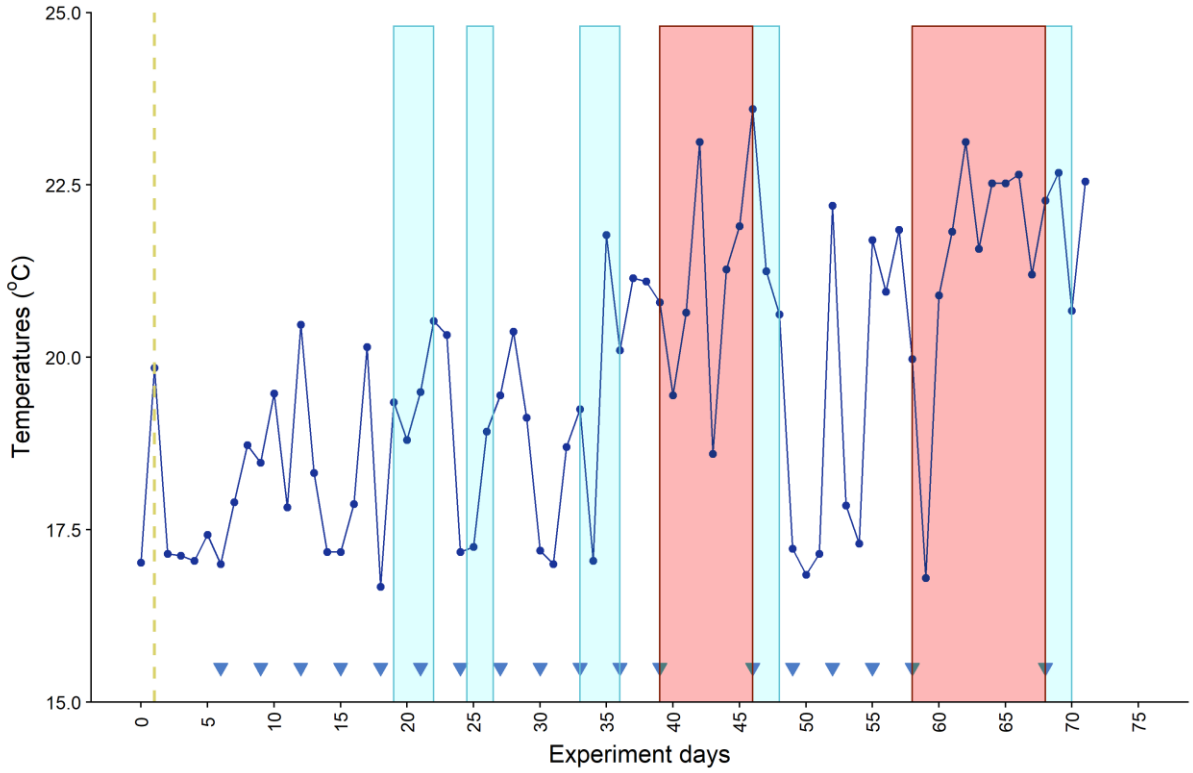

Figure 54: Daily temperatures being measured for the gas sampling period. Urine was applied on day 1 (yellow dashed line), the standard irrigation applications are shown by the blue triangles and the optimised irrigation by the blue highlighted areas. The red highlighted areas show the two periods where both irrigation treatments were withheld.

V.3.3 Nitrous oxide fluxes

Nitrous oxide fluxes were measured daily, from the 17th of July to the 26th of September 2019, by screwing a gas-tight cover equipped with a septa onto the top of each lysimeter. Gas samples (10 mL) were taken at 0, 20, and 40 min, after placing the cover, using a 20 mL glass syringe equipped with a 3-way stopcock and a 25G hypodermic needle. Gas samples were injected into pre-evacuated 6 mL Exetainer® vials. Prior to analysis, the gas samples were brought to ambient pressure and analysed using a gas chromatograph (8610; SRI instruments, Torrance, CA) connected to a Gilson autosampler (Gilson 222XL; Gilson, Middleton, WI) as previously described (Clough *et al.* 2009). The change in the lysimeter headspace N_2O

concentration over time was used to determine the N_2O flux according to Hutchinson and Mosier (1981). See equation (6) in section III.3.2.

Emission factors (EF) were calculated by subtracting the cumulative N_2O emissions occurring in a control treatment where no N was added (N_2O_0) from the cumulative N_2O emissions in a given experimental treatment where N was added (N_2O_x), then dividing this by the amount of N applied (N_{APPx}) as follows:

$$EF = \left(\frac{N_2O_x - N_2O_0}{N_{APPx}}\right) \times 100 \qquad (15)$$

where the units of N_2O and N inputs are the same (e.g., cumulative N_2O in mg N_2O-N m^2 and N_{APPx} in mg N m^2).

V.3.4 Soil, pasture biomass, root biomass, leachate sampling and ^{15}N recovery

Leachates were collected before each optimised irrigation event with the volume recorded and a subsample taken for NH_4^+ and NO_3^- determination (Figure 55). The leachates were filtered (0.45 μm) and the filtrate was analysed for NO_3^- and NH_4^+ on a flow injection analyser (Blackmore *et al.* 1987).

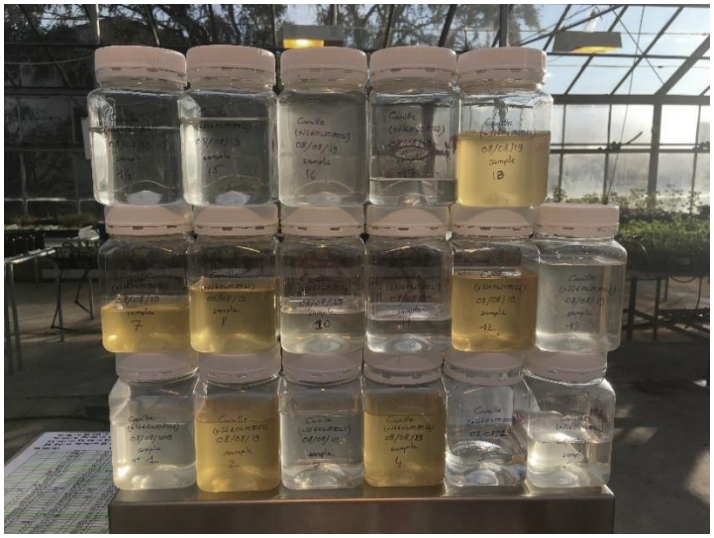

Figure 55: Leachates collected on the 31st of July 2019 (day 14). The darker leachates came from the lysimeters under the standard irrigation treatment.

Pasture biomass was hand-harvested by cutting to a 2 cm height above the soil, corresponding to the top of the lysimeters (Figure 56). Harvested pasture was dried for 2 days at 70ºC and the dry matter production recorded. Pasture total N content and atom% ^{15}N enrichment were determined by combustion on an isotope ratio mass spectrometer (IRMS, Sercon 20/20; Sercon, Chesire, UK).

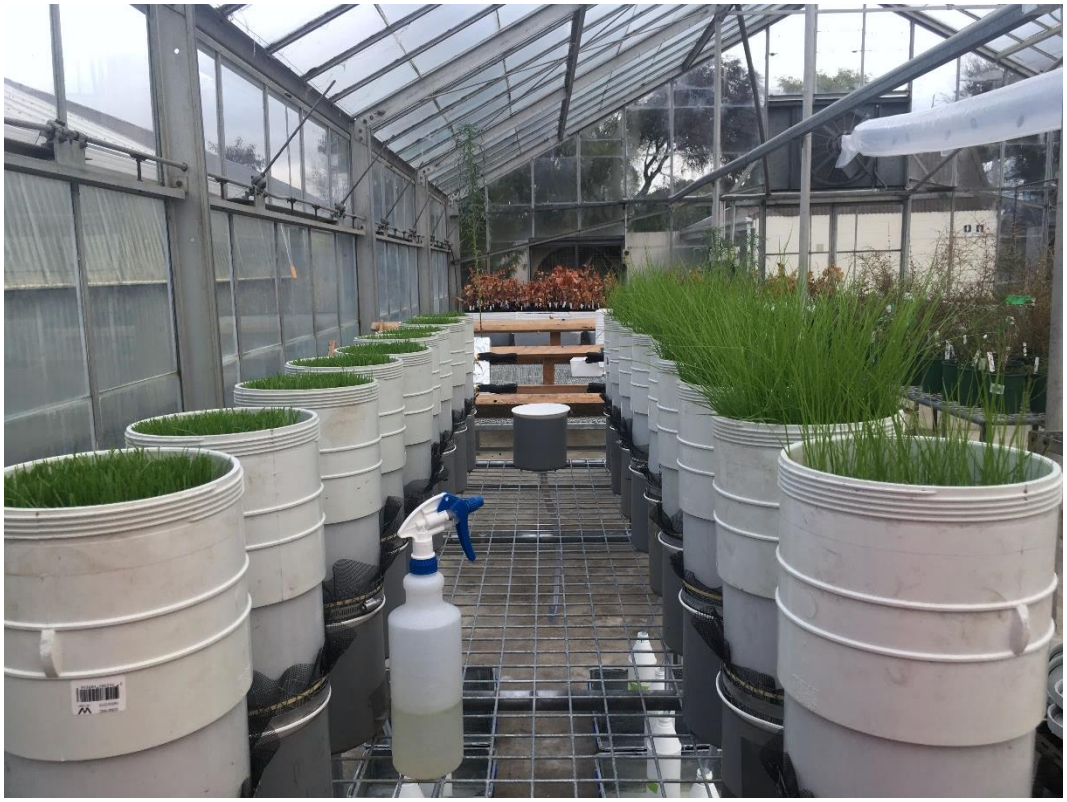

Figure 56: Picture taken during harvesting of ryegrass.

After the final N_2O sampling event (70 days after the urine application) the lysimeters were destructively sampled. Pasture was harvested and the soil inside the lysimeters was extruded into a Ziploc® plastic bag. The roots were separated from the soil and then the soil was mixed before taking a 10 g subsample for gravimetric water content determination, after drying at 105ºC for 24 h. The roots in the subsurface soil were washed and dried for 2 days at 70ºC and the dry matter weight recorded. Pictures were also taken of the bottom of each lysimeters to observe the root density (Figure 57). Then soil pH was measured using a calibrated flat surface pH electrode (Broadley James Corporation, Irvine, CA.) for the surface, middle (9 cm) and bottom (18 cm) depths of the lysimeters. A further subsample of soil, equivalent to 4 g of oven dry soil, was shaken for 1 h with 40 mL of 2M KCl. After this time the extracts were filtered (Whatman 42) and analysed for NO_3^--N and NH_4^+-N on a flow injection analyser (Blackmore *et al.* 1987). The atom% ^{15}N enrichments of the NH_4^+ and NO_3^- were determined by using the diffusion technique for KCl extracts and leachates samples as

described by Brooks *et al*. (1989), followed by IRMS analyses. The ^{15}N recoveries from the ^{15}N–labeled urine in the plant, leachate and soil were calculated using the method of Cabrera and Kissel (1989):

$$N\ recovered = 100\ \times \big(p\ \times (c-b)\big)/\big(f \times (a-b)\big) \qquad (16)$$

Where, p = moles of N in the labelled sample, f = mole of N in the urine applied, c = atom% ^{15}N abundance in the labelled sample, a = atom% ^{15}N abundance in the urine and b = atom% ^{15}N abundance in the control (unlabelled sample). To determine dissolved organic carbon (DOC) a soil subsample (equivalent to 5 g of oven dry soil) was extracted with 30 mL of deionised water by shaking for 30 minutes prior to centrifugation (3,500 rpm for 20 minutes) and filtration (Whatman 42), with subsequent analyses performed on a Shimadzu TOC analyser (Shimadzu, Oceania Ltd., Sydney, Australia). Total soil carbon was also measured by combustion on an elemental analyser.

Figure 57: Lysimeter soil destructive sampling day (26/09/2019-day 71). Left: whole lysimeters out of PVC cylinder. Top right: incision in the middle to take pH measurements and soil samples. Bottom right: two views from the bottom of lysimeters number 8 (urine on) with few roots and number 9 (urine off) with greater root density.

V.3.5 Statistical analyses

Statistical analyses were also performed using R studio and followed the same procedure as explained in section III.3.4. Urine (2 levels: on and off), irrigation conditions (2 levels: Opt and Std), combined treatments (4 levels: off_Std, on_Std, off_Opt and on_Opt) and days were the explanatory variables (Appendix 4).

V.4 Results

V.4.1 Soil water content and gas diffusivity

Over the first 40 days of the experiment standard irrigation returned the soil water content, regardless of urine treatment, close to field capacity (ca. 75% WFPS). During the periods that irrigation was withheld the soil moisture in the standard irrigation treatment was reduced to as low as ~20% WFPS with the urine treatment losing more water during these periods than the non-urine treatment (Figure 58). Under optimised irrigation WFPS ranged from 43 to 66% before the withholding periods, it gradually declined until the irrigation trigger point was reached on day 19 with irrigation then increasing WFPS. When withholding irrigation the optimised irrigation treatments attained a lower WFPS than the standard irrigation treatments, with the urine treatment drying at a faster rate (Figure 58).

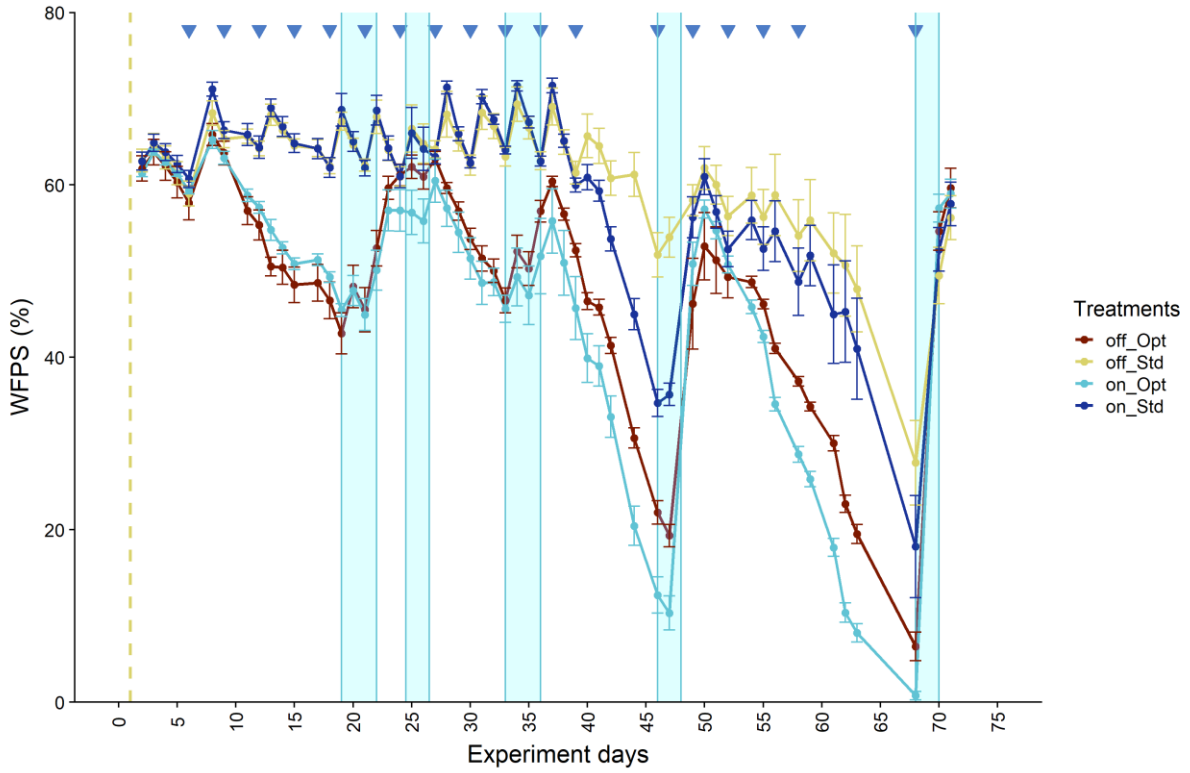

Figure 58: Water-filled pore space (WFPS) dynamics over time for optimised (Opt) and standard (Std) irrigation treatments with urine applied (on) or no urine applied (off). Data points are means of four replicates ± s.e.m. Urine has been applied on day 1 (yellow dashed line), the standard irrigation applications are shown by the blue triangles and the optimised irrigation by the blue highlighted areas.

Trends in the modelled D_p/D_o values mirrored those observed for soil WFPS with standard irrigation causing diffusivity to decrease, with values oscillating around those aligned with FC. During optimised irrigation D_p/D_o values were maximised at the designated trigger point for irrigation (0.085) and declined, following irrigation, to values that were slightly higher than those calculated for soil at 80% FC (Figure 59). When irrigation was withheld modelled D_p/D_o values increased faster in the optimised irrigation treatments, to such an extent that the D_p/D_o values were higher than the theoretical value for PWP (0.174). In the standard irrigation treatment the peak modelled D_p/D_o values were not as high (Figure 59).

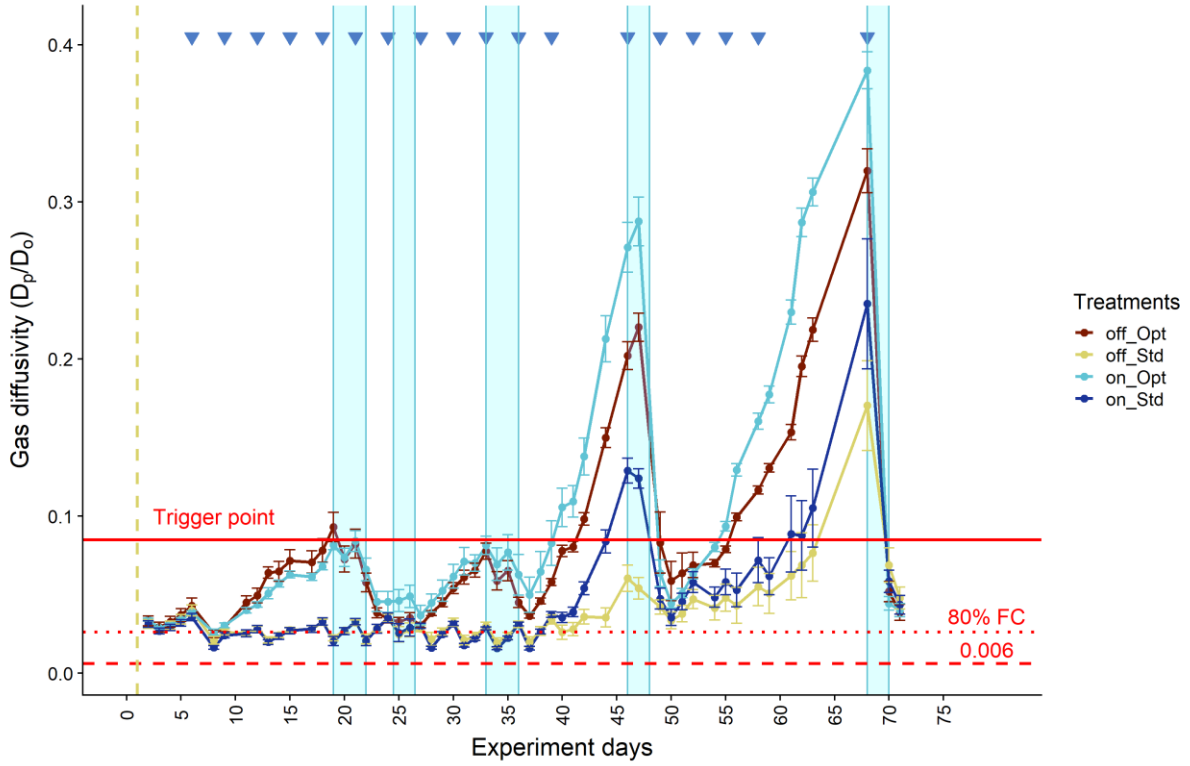

Figure 59: Modelled soil gas diffusivity dynamics over time for optimised (Opt) and standard (Std) irrigation treatments with urine applied (on) or no urine applied (off). Data points are means of four replicates ± s.e.m. Urine has been applied on day 1 (yellow dashed line), the standard irrigation applications are shown by the blue triangles and the optimised irrigation by the blue highlighted areas. The 0.006 red dashed line is based on the study from Balaine et al. (2013).

V.4.2 N_2O fluxes

From day 1 to 71 mean daily N_2O-N fluxes were higher as a result of urine application ($P < 0.05$; Figure 60), as were the cumulative N_2O-N fluxes from day 1 to 71. From day 1 to 39, optimised irrigation also resulted in higher ($P < 0.05$) mean daily fluxes and cumulative fluxes, under urine, when compared with standard irrigation (Figure 60, Figure 61). Daily increases in N_2O fluxes occurred from day 8 in the optimised irrigation treatment following the slow decline of D_p/D_o toward the TP and these increased significantly after the first irrigation event (Figure 60). Nitrous oxide emissions in the optimised irrigation treatment with urine applied reached a maximum of 4.91 ± 2.23 mg m^{-2} h^{-1} on day 24 (Figure 60). In the standard

irrigation treatment smaller but regular fluxes did occur post irrigation, between days 18 to 25 (Figure 60). Cumulative N_2O fluxes under the urine treatments from days 1 to 39 were almost 10-fold higher in the optimised irrigation treatment than under standard irrigation ($P < 0.05$) and were 884 ± 268 and 88 ± 50 mg m^{-2}, respectively (Figure 61). Without urine, cumulative N_2O fluxes were lower than in the urine treatments and did not differ due to irrigation treatment, averaging 3.6 ± 0.1 mg m^{-2} over the first 39 days. Emission factors for optimised and standard irrigation treatments with urine were 1.26 and 0.12%, respectively, after 39 days. To ascertain the potential for increases in N_2O fluxes within the standard irrigation treatment after day 39 the irrigation treatments (both optimised and standard for uniformity) were withheld for two periods; from days 39 to 46 and from days 58 to 68. Following soil rewetting at the end of these non-irrigation periods significant increases in daily N_2O fluxes occurred for both irrigation treatments where urine had been applied (Figure 60). Cumulative N_2O fluxes under the urine treatments for days 39 to 71 for the standard and optimised irrigation treatments were 197 and 280 mg m^{-2}, respectively, and did not differ significantly.

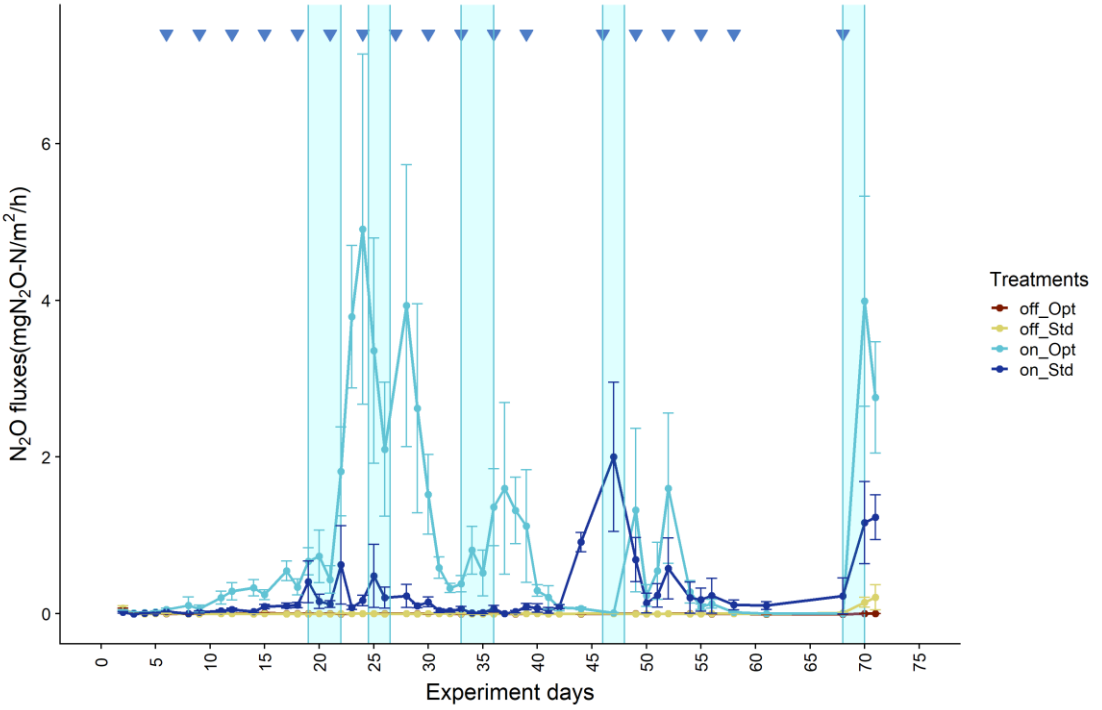

Figure 60: Daily average N_2O-N fluxes over time for optimised (Opt) and standard (Std) irrigation treatments with urine applied (on) or no urine applied (off). Data points are means of four replicates ± s.e.m. The standard irrigation applications are shown by the blue triangles and the optimised irrigation by the blue highlighted areas.

Over the entire experimental period cumulative N_2O fluxes in the standard and optimised irrigation treatments, without urine, were 12 ± 0.4 and 4 ± 0.1 mg m^{-2}, respectively. The cumulative N_2O flux under optimised irrigation was higher ($P < 0.05$) than under the standard irrigation when considering the entire experimental period (Figure 61) with fluxes of 1.15 ± 0.3 g m^{-2} and 285 ± 7 mg m^{-2}, respectively, equivalent to emission factors of 1.66 and 0.39%, respectively.

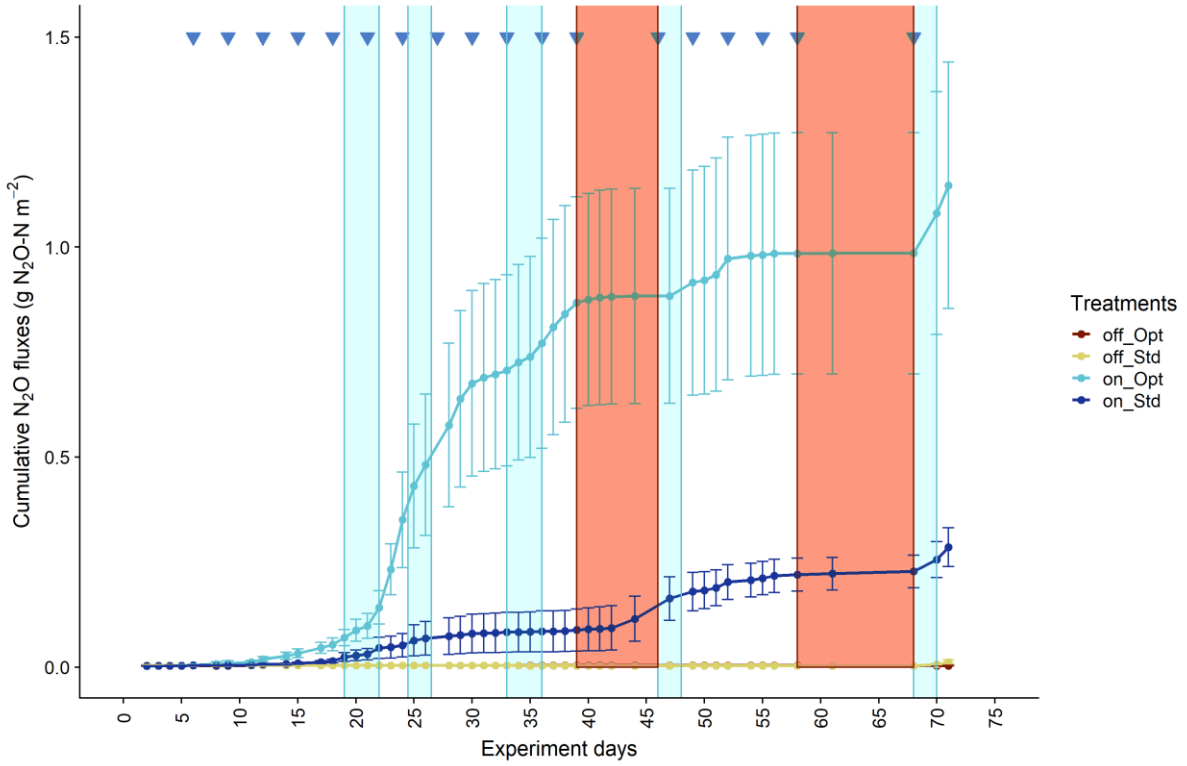

Figure 61: Cumulative average N_2O-N fluxes over time for optimised (Opt) and standard (Std) irrigation treatments with urine applied (on) or no urine applied (off). Data points are means of four replicates ± s.e.m. The standard irrigation applications are shown by the blue triangles and the optimised irrigation by the blue highlighted areas. The red highlighted areas show the two periods where both irrigation treatments were withheld.

V.4.3 Root characteristic, dry matter production and N uptake

Cumulative dry matter production at the end of the experiment was affected by an interaction between irrigation and urine treatments: cumulative dry matter production increased with urine application ($P < 0.01$) but the increase was lower under the standard irrigation treatment ($P < 0.05$). With urine, the cumulative dry matter yields per lysimeter, at the end of the experiment were 7.43 ± 0.27 and 6.39 ± 0.49 g DM in the optimised and standard irrigation treatments, respectively (Figure 62). While without urine, the optimised and standard irrigation treatments, per lysimeter, were 3.54 ± 0.18 and 2.93 ± 0.05 g DM, respectively (Figure 62).

Similar dry matter production trends were observed during the first withholding irrigation: on day 44, with urine, the cumulative dry matter yields, per lysimeter, were 5.02 ± 0.17 and 3.50 ± 0.18 g DM in the optimised and standard irrigation treatments, respectively, equal to daily growth rates of 65 and 45 kg DM ha^{-1} d^{-1}, respectively. While without urine, the optimised and standard irrigation treatments yielded 2.95 ± 0.01 and 2.11 ± 0.07 g DM per lysimeter, respectively, over the 44 day period (38 and 27 kg DM ha^{-1} d^{-1}, respectively).

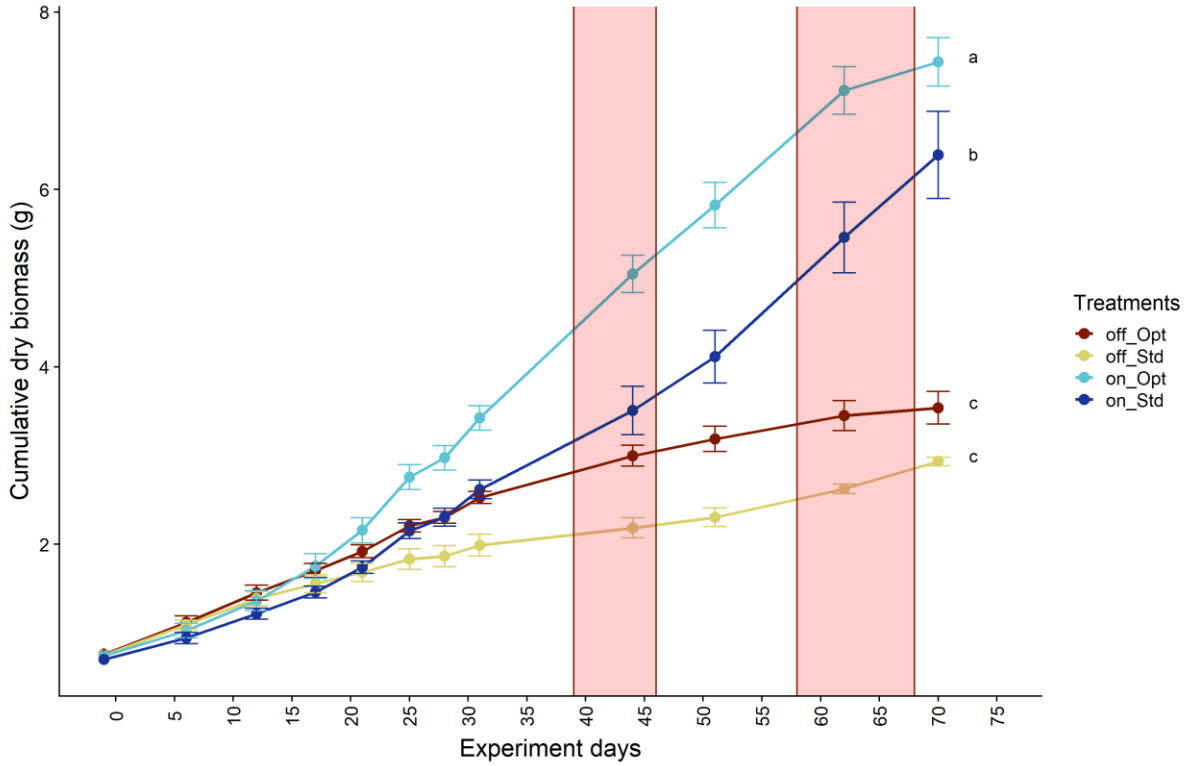

Figure 62: Cumulative dry biomass collected 12 times over the total period of the experiment for optimised (Opt) and standard (Std) irrigation treatments with urine applied (on) or no urine applied (off). Data points are means of four replicates ± s.e.m. The red highlighted areas show the two periods where both irrigation treatments were withheld.

Differences in dry matter yields were reflected in N uptake, a function of dry matter yield and N content. Non-urine treatments had pasture N concentrations ranging from 2.39-3.64% with a mean of 2.98 ±0.07% which resulted in a mean N uptake of 0.0045 ±0.0002 moles N per lysimeter. With urine applied the average N content of pasture was higher ($P < 0.05$) ranging from 3.86 - 5.39%, with a mean of 4.40 ± 0.13%, for standard irrigation, and from 3.79-5.66%,

with a mean of 4.56 ± 0.16%, for optimised irrigation. Under standard and optimised irrigation, with urine, the respective N uptake equalled 0.0183 ± 0.0018 and 0.0242 ± 0.0011 moles N per lysimeter. After allowing for the N taken up by the non-urine treatments this resulted in higher ($P < 0.05$) N uptake of urine-N by the optimised than the standard irrigation treatment, with mean values of 22.6 ± 1.2% and 15.9 ± 2.0% of urine-N applied, respectively. This trend was reflected in the update of ^{15}N by dry matter (Table 6) with higher ($P = 0.019$) ^{15}N recovery in the optimised irrigation (20.2 ± 0.9 %) compared to the standard irrigation treatment (14.8 ± 1.2 %).

Root biomass at the end of the experiment for the 0-5 cm depth of the lysimeters was significantly higher in the standard irrigation treatment without urine compared to the others (Figure 63). A visual analysis of the bottom part of the lysimeters showed that the root density was higher in the non-urine treatment compared to the urine treatment (Figure 57).

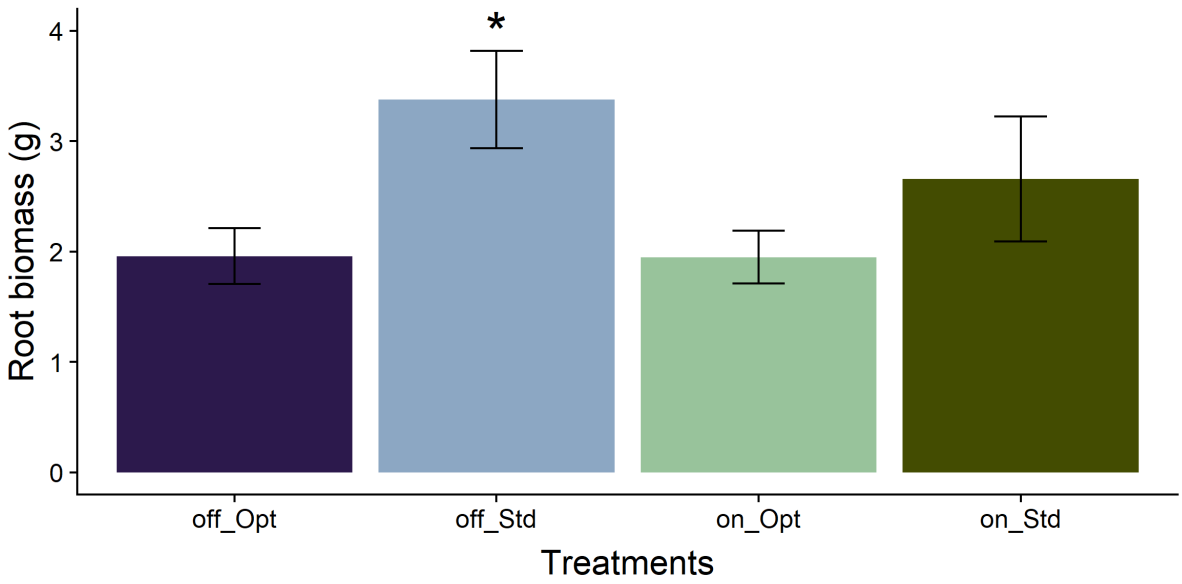

Figure 63: Root biomass (0-5 cm) per treatments at the end of the experiment.

Table 6: ^{15}N recovery (%) among the herbage, leachate and soil. Values are means (n = 4) at the end of the experiment and errors are standard error of the mean (s.e.m).

	Plant	Leachate NO_3^-	Leachate NH_4^+	Leachate Total	Soil Total
Irrigation treatments	Means of ^{15}N recovery (%)				
Standard	14.8 (1.2)	0.9 (0.2)	4.6 (0.9)	5.5 (0.9)	4.2 (1.7)
Optimised	20.2 (0.9)	1.0 (0.3)	1.1 (0.4)	2.1 (0.5)	2.0 (1.0)
P value	**0.0188 ***	0.725	**0.0189 ***	**0.0413 ***	0.365

V.4.4 Drainage and inorganic-N leaching

Leachate was collected on days 14, 22, 35, 49 and 68. At day 35, the last leachate collection prior to the withholding of irrigation, cumulative drainage differed due to irrigation treatment ($P < 0.001$) but not urine treatments ($P = 0.3$) averaging 347 ± 39 and 271 ±51 mm for the optimised irrigation, with and without urine, respectively, while in the standard irrigation treatment values were 648 ± 34 and 698 ± 60 mm for plus and minus urine treatments, respectively. This equated, on average, to 0.18 and 0.39 pore volumes of drainage for the optimised and standard irrigation treatments at this time. After the final leachate collection cumulative drainage under optimised irrigation, with or without urine, totalled 539 ± 96 and 617 ± 179 mm, respectively. Higher cumulative drainage occurred under standard irrigation at this time, equal to 1321 ± 92 and 1359 ± 179 mm with or without urine, respectively. On average, cumulative drainage equated to 0.34 and 0.78 pore volumes for the optimised and standard irrigation treatments after final leachate collection.

The amount of NH_4^+-N leached varied due to the effects of irrigation treatment, urine and time which interacted ($P < 0.01$) to cause higher NH_4^+-N leaching under urine, and in particular the standard irrigation treatment (Table 7). Under both irrigation treatments the amount of urine N leached as NH_4^+-N was highest on day 14 where, despite similar leachate NH_4^+-N concentrations, more NH_4^+-N was leached under standard irrigation (Table 7). Under optimised irrigation NH_4^+-N leaching effectively ceased after day 14, but under standard irrigation NH_4^+-N concentrations remained higher, with significant leaching until day 35 (Table 7). Ignoring the relatively minor contribution of soil to NH_4^+-N leaching as observed in the non-urine treatments, the NH_4^+-N leached under the urine treatments equated to 1.38 and 5.76% of the urine-N applied in the optimised and standard irrigation treatments, respectively. The cumulative recovery of ^{15}N labelled urine as NH_4^+-N in the leachate at the end of the

experiment was 4.6 ± 0.9% and 1.1 ± 0.4% for standard and optimised irrigation treatments (only samples with urine), respectively (Table 6). This recovery was higher (P = 0.02) in the standard irrigation treatment.

Leachate NO_3^--N concentrations were affected by urine, irrigation and time interaction (P < 0.01). This resulted in higher NO_3^--N concentrations in leachate collected from under urine treated lysimeters, with higher concentrations in the optimised irrigation treatment from day 35 onwards (Table 7). While the total amount of NO_3^--N leached, a function of drainage NO_3^--N concentration and volume, tended to be higher under the optimised irrigation it was not statistically significant (Table 7) with NO_3^--N from urine treatments representing 2.22 and 1.46% of urine-N applied after allowing for contributions from soil N as observed in the non-urine treatments. For NO_3^-, the ^{15}N recovery in the cumulative leachate did not differ with irrigation treatments (P = 0.72) with an average of 0.9 ± 0.15% and 1.0 ± 0.3% for standard and optimised irrigation treatments, respectively (Table 6).

Table 7: Mass of inorganic-N collected in the leachates and concentration of inorganic-N at collection time for both NO_3^--N and NH_4^+-N. Values are means (n = 4) and errors are standard error of the mean (s.e.m).

Inorganic-N	Day	Irrigation and Urine Treatment			
		Optimised plus urine	Standard plus urine	Optimised nil urine	Standard nil urine
NO_3^--N (mg)	14	0.37 (0.28)	0.37 (0.13)	0.43 (0.17)	0.59 (0.05)
	22	1.64 (0.47)	1.46 (0.78)	0.22 (0.06)	0.18
	35	11.98 (4.83)	4.69 (2.00)	0.78 (0.38)	0.19 (0.04)
	49	8.04 (3.85)	5.00 (0.94)	0.41 (0.08)	0.41 (0.02)
	68	6.58 (3.22)	7.92 (4.39)	< 0.20	< 0.20
	Total	28.61 (6.99)	19.44 (4.98)	1.84 (0.43)	1.37 (0.08)
NO_3^--N (mg l^{-1})	14	2.45 (1.92)	0.77 (0.31)	3.76 (1.77)	0.78 (0.48)
	22	9.82 (3.36)	6.88 (4.00)	1.80 (0.12)	0.10 (0.28)
	35	61.56 (32.55)	10.97 (4.94)	3.20 (1.71)	0.33 (0.10)
	49	74.34 (56.32)	7.25 (1.42)	0.84 (0.06)	0.11 (0.11)
	68	98.11 (40.41)	13.22 (4.90)	< 0.03	0.06 (0.23)
NH_4^+-N (mg)	14	15.82 (5.09)	55.00 (9.99)	0.13 (0.26)	0.31 (0.05)
	22	0.39 (0.11)	8.20 (2.72)	0.01 (0.10)	0.05 (0.01)
	35	0.46 (0.15)	6.36 (2.15)	0.08 (0.06)	0.14 (0.03)
	49	0.17 (0.11)	0.49 (0.20)	0.06 (0.07)	0.12 (0.04)
	68	0.03 (0.01)	0.10 (0.02)	0.01 (0.12)	0.10 (0.04)
	Total	16.87 (5.09)	70.15 (10.58)	0.29 (0.32)	0.72 (0.08)
NH_4^+-N (mg l^{-1})	14	93.45 (26.74)	102.9 (12.7)	0.78 (0.21)	0.60 (0.08)
	22	2.27 (0.64)	39.3 (12.6)	0.10 (0.004)	0.25 (0.10)
	35	2.29 (1.00)	15.57 (5.44)	0.33 (0.19)	0.28 (0.09)
	49	1.77 (1.60)	0.70 (0.29)	0.12 (0.04)	0.23 (0.11)
	68	0.45 (0.03)	0.20 (0.04)	0.06 (0.003)	0.17 (0.04)

V.4.5 Soil pH, DOC and inorganic-N concentrations

Soil pH at day 71 was higher ($P < 0.05$) than at the start of the experiment (5.34) but did not differ without urine applied, averaging 6.08 between irrigation treatments and sampling locations. Regardless of the sampling depth, optimised irrigation with urine resulted in no significant change to soil pH (5.94) but under standard irrigation it was lower (5.86; $P < 0.05$). For every treatments, the pH at the top (surface) of the cylinder was significantly higher than the pH taken at the bottom (18 cm) and middle part (9 cm) of the cylinder (Figure 64).

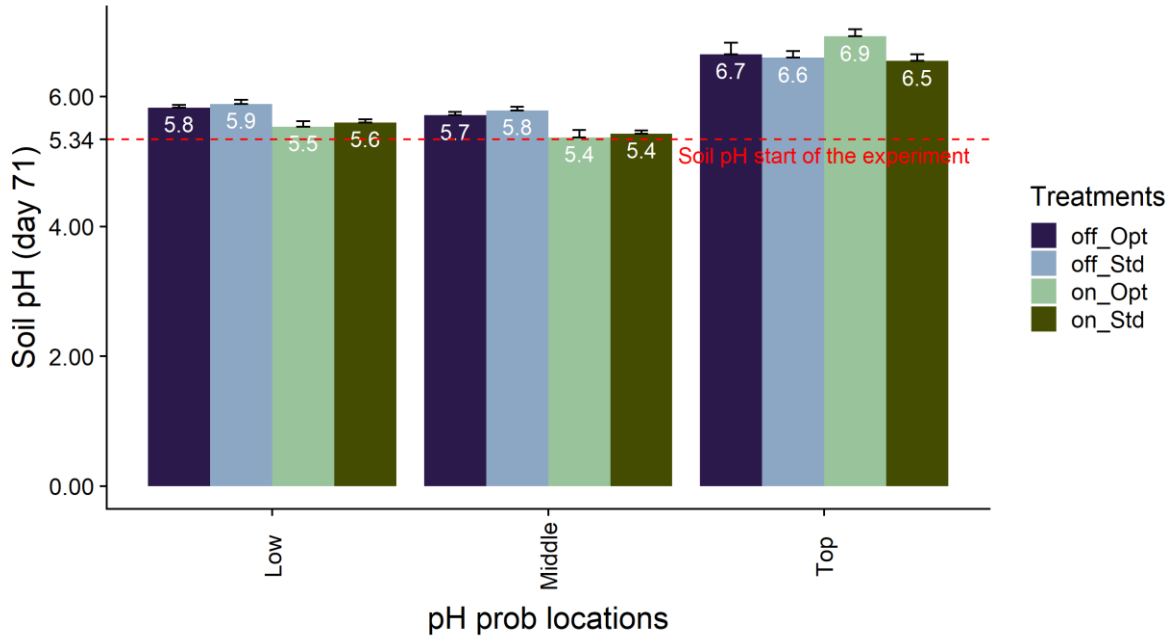

Figure 64: pH averages at different depths in the lysimeters (low = 18 cm, middle = 9 cm and top = soil surface) during the destructive sampling (day 71) for optimised (Opt) and standard (Std) irrigation treatments with urine applied (on) or no urine applied (off). The red dashed line represents the pH at the beginning of the experiment before applying urine. Values are means (n = 4) ± s.e.m

Mean concentrations of DOC in the soil, extruded from the lysimeters, did not vary with treatment: without urine in the optimised and standard irrigation treatments DOC concentrations were 133 ± 4 and 118 ± 8 μg g^{-1} soil, respectively, while with urine the optimised and standard irrigation treatments had DOC concentrations of 121 ± 19 and 127 ± 3 μg g^{-1} soil, respectively.

Prior to urine addition sieved soil mean (n = 3) NO_3^--N and NH_4^+-N concentrations were 9.0 ± 0.4 and 6.4 ± 0.4 mg kg^{-1}, respectively (Table 5). In the extruded soil at the end of the experiment more ($P < 0.01$) NO_3^--N remained in the urine-treated soil than in soil where urine was not applied: when averaged across irrigation treatments mean NO_3^--N concentrations were 22.7 ± 6.1 and 3.8 ± 1.3 mg kg^{-1}, respectively. Soil NO_3^--N concentrations were unaffected by irrigation treatment with optimised and standard irrigation having mean NO_3^--N concentrations of 8.6 ± 4.0 and 18.0 ± 6.5 mg kg^{-1}, respectively. No treatment interaction occurred to affect soil NO_3^--N concentrations.

While there was a tendency for higher NH_4^+-N concentrations under urine treatments the soil NH_4-N concentrations at the end of the experiment were statistically similar under urine ($P = 0.30$) or irrigation ($P = 0.38$) treatments. Averaged across irrigation treatments mean soil NH_4-N concentrations were 19.6 ± 16.0 and 2.1 ± 0.3 mg kg^{-1} in the urine and non-urine treatments, respectively. When averaged across urine treatments, mean NH_4^+-N concentrations were 3.5 ± 1.2 and 18.5 ± 23.3 mg kg^{-1} in the standard and optimised irrigation treatments, respectively.

The ^{15}N recovery as NH_4^+-N in the soil at the end of the experiment was low (< 0.7%). Consequently, the ^{15}N recovery as soil inorganic-N was predominately due to NO_3^--N ^{15}N recovery. Table 6 shows that the ^{15}N recovery in the soil at the end of the experiment was 4.2 ± 1.7% and 2.0 ± 1.0% in the standard and optimised irrigation treatment, respectively, with no significant treatment effects observed.

V.5 Discussion

Daily dry matter production under the optimised irrigation treatment, with urine, was typical of summer growth rates for a fertilised irrigated pasture within the South Island of New Zealand (Dairy NZ 2020). The N content of this dry matter was also typical of pasture under a urine patch (e.g. Buckthought *et al.* 2015, 2016). The lower dry matter production under standard irrigation indicates conditions were not as conducive for pasture growth. Under standard irrigation, prior to day 36, values of modelled D_p/D_o were generally < 0.02 indicative of the onset of anaerobic conditions (Stepniewski 1981): hypoxic conditions have previously been shown to result in lower dry matter yields and macronutrient uptake in winter rye (Stępniewski and Przywara 1992). A study by Eysholdt-Derzsó and Sauter (2017) showed that hypoxic conditions cause the primary root to grow sidewise in a low O_2 environment, possibly to escape soil patches with reduced O_2 availability. This is consistent with the higher root biomass observed in the standard treatment without urine and the visual analysis at the bottom of the lysimeters. While the N content of the dry matter produced under urine in the standard irrigation did not differ from optimised irrigation the resulting N uptake, a function of dry matter yield and N content, was lower due to the reduction in dry matter yield and this was also supported by the low ^{15}N uptake in the standard irrigation treatment. Leaching of inorganic-N as NO_3^--N, a function of NO_3^--N concentration and drainage volume, was expected to be higher under standard irrigation due to the expected higher drainage losses. This did not occur. Instead leaching of inorganic-N initially commenced with macropore flow of urine derived N as evidenced by the relatively high NH_4^+-N concentrations under urine treatments, collected in drainage up until day 14. Leaching of NH_4^+-N had effectively ceased by day 22 in the optimised irrigation treatment under urine, but under standard irrigation it persisted until day 35. This was potentially the result of further macropore flow of NH_4^+-N in soil solution resulting from a reduction in the NH_4^+-N oxidation rate, a consequence of the hypoxia indicated by the low

D_p/D_o at this time. This greater loss of NH_4^+-N potentially contributed to the lower concentrations of NO_3^--N in the drainage from the standard irrigation treatment from day 35 onwards. Regardless of irrigation treatment, under urine the presence of NO_3^--N in the leachate indicated there was sufficient NO_3^--N substrate available for denitrification.

Similarly, the soil DOC concentrations at the end of the experiment indicated there was sufficient DOC for denitrification to occur (Beauchamp *et al.* 1989). During the periods where irrigation was withheld (after day 44) the drier soil conditions under optimised irrigation enhanced the formation of NO_3^--N but the lower drainage volumes were insufficient to generate a statistically greater NO_3^--N leaching loss. However, further irrigation and drainage events might have resulted in more NO_3^--N eventually being leached as only 0.34 pore volumes had been collected at the end of the experiment under optimised conditions. Although countering this is the fact that NO_3^--N concentrations within the soil at the end of the experiment, under urine treatments, did not differ with respect to irrigation treatment.

The higher N_2O fluxes under the urine treatment resulted from the hydrolysis of urea, contained in the urine, and the ensuing generation of inorganic-N pools (Clough *et al.* 2020). The N_2O fluxes commenced at ca. day 7, typical of urine patch emissions (e.g. Clough *et al*. 2009), once nitrite and the ensuing NO_3^--N pool were generated. The resulting EFs over the first 44 days of the experiment are of a typical magnitude for pasture systems (Van der Weerden *et al.* 2020). However, contrary to the hypothesis, N_2O fluxes were higher under the optimised irrigation. Measured N_2O fluxes are of course net fluxes, the difference between the production of N_2O and its consumption to N_2 (Jayarathne *et al.* 2020b). While soil WFPS values indicate that the soil conditions in the urine treated soil with standard irrigation were potentially suitable for denitrification to occur (Linn and Doran 1984), the values of D_p/D_o in this treatment over the first 37 days (the period prior to withholding irrigation) confirm soil conditions were in fact predominately anaerobic and, following irrigation events, close to the threshold identified by

Balaine *et al*. (2016) where N_2O was further reduced to N_2. In the current study anaerobic conditions suitable for N_2 production may also have occurred at a higher threshold than that observed by Balaine *et al*. (2016) if the O_2 demand was exacerbated as a result of using repacked sieved soils, which may have enhanced microbial availability of C. The wetter soil conditions under the standard irrigation treatment would have also enhanced entrapment of N_2O generated, increasing the opportunity for conversion to N_2 (Letey *et al.* 1980; Clough *et al.* 2001, 2005) . Hence, lower N_2O fluxes in the standard irrigation treatment under urine most likely resulted from conversion of N_2O to N_2 by denitrifiers. While standard irrigation resulted in wetter soil conditions the lower N_2O fluxes under urine with standard irrigation were still responsive to irrigation events with lower fluxes on irrigation days (during days 15-30) and higher fluxes the day after an irrigation event, when D_p/D_o increased, permitting the diffusion of N_2O out of the soil.

Nitrous oxide fluxes from the optimised irrigation treatment under urine were again likely the result of its formation from the nitrite and NO_3^--N pools after day 7. These N_2O fluxes were higher in the optimised treatment at this time due to lower WFPS and higher D_p/D_o, which facilitated gas exchange with the atmosphere, and which demonstrate the presence of relatively higher aerobic conditions than in the standard irrigation. These conditions were not conducive to N_2 production, since N_2O reductase is highly sensitive to O_2 (Zumft 1997), as demonstrated by Friedl *et al.* (2017) who recorded N_2 fluxes from intensively managed subtropical pastures when D_p/D_o declined below 0.02. Higher diffusivity would have allowed entry of O_2 and the release of N_2O via diffusion. Clearly, conditions were suitable for generation of N_2O and this may have occurred via nitrifier-denitrification or incomplete denitrification. These more aerobic conditions under the optimised irrigation treatment were hypothesised to result in lower N_2O fluxes following urine application but instead resulted in significant fluxes after optimised irrigation events. The first significant event came when

irrigation was applied 19 days after urine application, and which was still occurring on day 26 when top-up irrigation was applied and after the last optimised irrigation event which was 7 days after the top-up irrigation or 11 days after the first irrigation event. Mumford *et al.* (2019) examined the effects of irrigation frequency on N_2O emissions from fertilised and intensively managed pastures, and found that reducing the irrigation frequency from 15 days to either 4 or 10 days, with corresponding adjustments to irrigation rate, reduced N_2O losses by 35-44%. They assumed that the higher N_2O losses from under the lower irrigation frequency could have occurred as a consequence of the 'Birch' effect or changes in the N_2O:(N_2O+N_2) ratio. The Birch effect (Birch 1958) results in the generation of available microbial C and N substrates as a result of wetting and drying events enhancing mineralisation and potentially disrupting aggregates which makes available further substrate (Bottner 1985). The consequences are two-fold: first the provision of substrate and second enhanced aerobic respiration upon soil rewetting that in turn reduces O_2 levels thereby promoting anaerobic conditions. A 7.4-fold higher N_2O:(N_2O+N_2) ratio was demonstrated when rewetting repacked soil cores, previously dried to 10% WFPS, back up to 90% WFPS, versus drying to 45% WFPS and rewetting to 75% WFPS: this was the result of more extensive drying stimulating mineralisation of N (Guo *et al.* 2014). Compounding this issue under urine patches may be the fact that solubilisation of soil organic matter occurs, a result of elevated soil pH within the urine patch.

The periods of withholding irrigation further demonstrated this effect with elevated fluxes in urine treatments after subsequent irrigation on days 46 and 68. However, it is likely the substrate for these N_2O fluxes was still dominated by the urine derived NO_3^--N due to the significant urinary-N loading The elevated N_2O fluxes under the standard irrigation treatment following these irrigation events also confirms that the application of standard irrigation up until day 35 was enhancing N_2O reduction.

This lysimeter study confirms irrigation plays a role in altering N dynamics under urine affected pasture. The standard irrigation treatment, under the environmental conditions of the experiment, effectively overwatered the pasture as evidenced from the reduced growth rate of pasture. This was likely due to lower evapotranspiration than might be expected *in situ* due to factors such as a lack of wind. However, this irrigation regime also points to how maintaining soil moisture can reduce the N_2O emission by promoting N_2O consumption to N_2. While the N_2O emissions from the optimised irrigation treatment were higher the irrigation trigger point is typical of that used by many farmers in Canterbury (Birendra *et al.* 2018).

Clearly, there exists a 'sweet-spot' within the soil where N_2O reductase activity is maximised as a result of soil moisture and structure reducing D_p/D_o and hence O_2 supply, with the potential for increasing O_2 demand to further influence this. Nitrous oxide reductase activity generates N_2, reducing N use efficiency. Ideally irrigation activity should generate a 'sweet-spot' for plant growth, optimising N uptake, and result in conditions that are sub optimal for the generation of N_2O: upon completion of irrigation and water redistribution within the soil profile the soil profile should not develop hypoxia. The results of the treatments imposed in the current study indicate there was N_2 production and impeded plant growth (standard irrigation) or the generation of hypoxia following irrigation (optimised irrigation). Conditions that fall outside the desired post irrigation sweet-spot. Glasshouse conditions may have contributed to standard irrigation developing N_2O reducing conditions, with the lack of wind reducing evapotranspiration, and the use of sieved repacked soils may have also increased O_2 demand in both irrigation treatments.

While over irrigation can be readily prevented there remains a need to identify what level of PAW should be used to trigger irrigation. Currently, this level of PAW is based on plant requirements (Birendra *et al.* 2018). But the current data, and other recent irrigation studies show that, potentially, shorter more frequent irrigation events can result in reduced N_2O

emissions and improved water use efficiency (Scheer *et al.* 2008; Mumford *et al.* 2019) possibly due to reduced mineralisation. Soil D_p/D_o may be a tool that could be used to determine this frequency as it can be used to 'finger print' the interaggregate (fast draining) and intra-aggregate (slow draining) pore structure (Jayarathne *et al.* 2020a). Modelling of soil D_p/D_o is based upon readily available data (soil moisture and soil bulk density). Knowledge of the ability for O_2 to diffuse into soil aggregate structures may help predictions, or understanding, of the potential for mineralisation as soils dry.

V.6 Conclusion

For this experiment, standard and optimised irrigation treatment were compared in terms of N dynamics and soil D_p/D_o. Soil gas diffusivity values used to trigger irrigation (50% of PAW) were established according to good practice irrigation guides. And the top up value (80% FC) for D_p/D_o was supported by the results from Chapter III and Chapter IV, in other words, keeping the soil $D_p/D_o > 0.02$. Drying of the soil between irrigation events, triggered when soil moisture was equivalent to 50% of PAW, generated more N_2O than when irrigation was routinely applied every three days. Applying irrigation every three days increased anaerobic conditions as identified through lower soil D_p/D_o which, in turn, reduced plant growth, N uptake and N_2O emissions. Reductions in N_2O emissions are attributed to complete reduction to N_2. Higher N_2O emissions following set irrigation events were attributed to enhanced mineralisation of C, during drying, resulting in increased substrate for microbial respiration that in turn promoted hypoxia and N_2O generating processes. Future studies should examine respiration fluxes (O_2 demand and CO_2 production) over differing levels of drying (varying D_p/D_o) and subsequent rewetting and their relationship with N_2O production to improve our understanding of how to minimise N_2O emissions through irrigation management.

Chapter VI Effect of irrigation scheduling, using soil gas diffusivity as a decision tool to mitigate N_2O emissions from a urine-affected pasture (2 field trials)

This chapter for the 2nd field trial has been accepted in 'Agriculture' special issue 'Strategies for Nitrous Oxide Emission Mitigation in Agrosystems', the title is as follows:

TITLE: Irrigation scheduling with soil gas diffusivity as a decision tool to mitigate N_2O emissions from a urine-affected pasture.

Authors: Camille Rousset[A], Timothy J. Clough[A], Peter R. Grace[B], David W. Rowlings[B], Clemens Scheer[B,C].

[A] Department of Soil and Physical Sciences, Lincoln University, PO Box 85084, Lincoln, 7647, New Zealand

[B] Queensland University of Technology, Institute for Future Environment, 2 George Street, Brisbane, Queensland, 4000, Australia

[C] Institut für Meteorologie und Klimaforschung, Department Atmosphärische Umweltforschung (IMK-IFU), KIT-Campus Alpin, Garmisch-Partenkirchen, Germany.

Received 8 Avril 2021, accepted 11 Mai 2021

Highlights:

- Higher cumulative N_2O fluxes for the standard compared to the optimised irrigations
- Dry matter production unaffected by irrigation treatment
- Need for adjusting irrigation cycles to prevent the D_p/D_o declining to ≤ 0.006, in the event of subsequent rain.

Keywords: Automatic chambers, optimised irrigation, modelled D_p/D_o, field application.

VI.1 Abstract

Often posited as the main limiting factor for plant growth, water is also indirectly responsible for soil N_2O emissions. Soil moisture is the most important factor regulating the denitrification rate. Pastures require year-round access to water and in some location rely on irrigation during dry periods. Currently, there is a dearth of knowledge about the potential for using irrigation to mitigate N_2O emissions. This study aimed to mitigate N_2O losses from intensely managed pastures by adjusting irrigation frequency using soil gas diffusivity thresholds. This was investigated, over two field trials (field trial 1 and field trial 2), using automatic chambers in a field where perennial ryegrass (*Lolium perenne*) pasture was predominant. Two irrigation regimes were compared; a standard irrigation treatment based on routine farmer practice (15 mm applied every 3 days) versus an optimised irrigation treatment where irrigation was applied when soil relative gas diffusivity (D_p/D_o) was ≈ 0.033 (equivalent to 50% of plant available water). Cow urine was applied at a rate of 700 kg N ha^{-1} to simulate a ruminant urine deposition event. In addition to N_2O fluxes, soil moisture content and modelled D_p/D_o were monitored automatically every hour and pasture dry matter production was measured. During the irrigation period for field trial 1, standard irrigation practices resulted in higher ($P = 0.09$) cumulative N_2O emissions than the optimised irrigation treatment. The optimised irrigation treatment was also favoured in field trial 2 as there was a significant decrease in cumulative N_2O emissions compared to the standard irrigation. Despite growth rates lower than the summer average for fertilised irrigated pastures, both irrigation treatments with urine were not significantly different. Denitrification during re-wetting events (irrigation and rain) contributed to soil N_2O emissions. Future models for irrigation management based on D_p/D_o thresholds and considering the rain and evapotranspiration predictions should be developed in order to reduce N_2O and N_2 emissions from intensively managed pasture soils.

VI.2 Introduction

Nitrous oxide (N_2O) is a potent greenhouse gas and is also the dominant ozone depleting substance (Ravishankara *et al*. 2009; IPCC 2014). Tropospheric concentrations of N_2O have increased by 23% from 271 ppm to 333 ppb from about 1750 to 2020 (Ciais *et al*. 2013, NOAA 2020). Since 1960 a key driver of this increase globally has been the increased use of synthetic nitrogen (N) fertiliser, while before 1960 the expansion of agricultural is thought to have increased atmospheric N_2O as a result of soil N mineralisation (Davidson 2009). New Zealand has not been immune to the drive to intensify agricultural systems with a 627% increase in the annual application of N fertiliser between 1990 and 2017. Moreover, within some regions of New Zealand (Southland, Canterbury, Otago, West Coast) the amount of N fertiliser applied, predominately urea, doubled between 2002 and 2017 (Statistics New Zealand 2019).

A major reason for this increased use of N fertiliser has been the intensification of land use resulting from the expansion of irrigation: the area of irrigated land doubled between 2002 and 2017 (Statistics New Zealand 2019). In New Zealand 747,000 ha of land is irrigated with the bulk of this concentrated in Canterbury (478,000 ha; 64% of irrigated land) and Otago (94,000; 13%): intensification of irrigated land has substantially increased dairy cattle numbers in these regions (Statistics New Zealand 2019).

In these irrigated systems the ingestion of relatively N rich ryegrass-based pastures exceeds the metabolic N requirements of ruminants (Selbie *et al.* 2015). This leads to excess N being excreted predominately as urine-N (Jarvis *et al.* 1995), at rates that exceed the pasture's immediate requirements (Selbie *et al.* 2015). As a consequence of these elevated soil inorganic-N concentrations (nitrate and ammonium) nitrate leaching and N_2O emissions are enhanced. Consequently, research has focused on feeding alternative forages, utilisation of catch crops, and nitrification inhibitors to reduce nitrate leaching and N_2O emissions (Selbie *et al.* 2015; Gardiner *et al.* 2016; Van der Weerden *et al.* 2017; Cheng *et al.* 2017; Dalley *et al.* 2017;

Carlton *et al.* 2019; Bryant *et al.* 2020; Malcolm *et al.* 2020). While some studies have examined the effect of irrigation management on nitrate leaching (Waddell *et al.* 2000; Carlton *et al.* 2018) few studies have examined the role of irrigation management on N_2O emissions.

High ammonium concentrations in pasture urine-patches stimulate ammonia oxidising bacteria (AOB) who produce N_2O as a result of both abiotic and biotic transformations of their metabolic intermediates, and through nitrifier-denitrification (Stein 2019). The process of nitrifer-denitrification is stimulated when the soil becomes hypoxic (Zhu *et al.* 2013b; Wrage-Mönnig *et al.* 2018; Stein 2019). The denitrification of nitrate is an anaerobic process where N_2O is an obligate intermediary (Butterbach-Bahl *et al.* 2013) . Hence, soil O_2 status, a function of supply and consumption, is a key determinant of the N_2O production pathway in pasture soils.

Soil moisture content, often measured as water-filled pore space (WFPS), influences the ability of O_2 to diffuse into the soil and it is well recognised that increasing moisture leads to hypoxia and ultimately anaerobic conditions and increases in N_2O emissions (Farquharson and Baldock 2007; Van der Weerden *et al.* 2014). However, at a constant WFPS the volume fractions of air and water vary with different soil bulk densities making comparisons of soils problematic (Farquharson and Baldock 2007). Balaine *et al.* (2013) showed that relative gas diffusivity (D_p/D_o; where D_p is the soil gas diffusion coefficient (m^3 soil air m^{-1} soil s^{-1}) and D_o is the gas diffusion coefficient in free air (m^2 air s^{-1})) was better than WFPS for identifying the threshold of N_2O production when comparing soils across a range of bulk densities and soil moistures. This was further confirmed using repacked soil cores, intact soil cores and *in situ* (Owens *et al.* 2017; Chamindu Deepagoda *et al.* 2019, 2020; Rousset *et al.* 2020). A D_p/D_o value ≤ 0.02 indicates the onset of anaerobic soil conditions (Stepniewski 1981) while a value of 0.006 has been shown to result in peak N_2O emissions (Balaine *et al.* 2013).

Irrigation impacts the soil O_2 status displacing air from soil pores and creating hypoxic or even anoxic conditions in the soil required for the bacteria to create N_2O emissions. While the manipulation of irrigation has been shown to mitigate N_2O emissions in cropping systems (Scheer *et al.* 2014; Jamali *et al.* 2015) few studies have examined this concept with respect to pasture urine-patch N_2O emissions. Vogeler *et al.* (2019) modelled the effects of irrigation frequency and intensity (with application based on soil water deficit) on N losses from pasture, across soil types, and found higher denitrification and N_2O emissions under high-frequency/low intensity irrigation regimes that resulted in a zero moisture deficit after irrigation. Mumford *et al.* (2019) determined the effects of irrigation frequency (4, 10 or 15 day intervals, with the number of application events based on rainfall and evapotranspiration rates) on N_2O emissions from intensively managed sub-tropical pastures receiving urea fertiliser (381 kg N ha^{-1} yr^{-1}) and simulated grazing: this study demonstrated the potential for strategic irrigation practices to reduce N_2O emissions. The highest cumulative losses of N_2O were from the low frequency treatment (15 day interval) and were attributed to the potential for reduced N_2 production being limited (lower N_2O reductase activity in the low frequency treatment compared to high frequency treatment) and enhanced C and N supply for denitrification due to the well-recognised 'Birch effect' (Birch 1958). This study demonstrated the need to adjust irrigation cycles to reduce GHG emissions. The objective of this experiment was to investigate the potential to manipulate N_2O emissions from ruminant urine-affected soil using irrigation and D_p/D_o as a decision tool for the irrigation treatment, while maintaining pasture growth.

VI.3 Materials & methods

This experimental work was conducted over two periods: summer 2019 and summer 2020. These two experimental periods shared the same experimental site and the same instrumentation. In the interest of clarity, the results will be distinguished by periods, named "field trial 1" for summer 2019 and "field trial 2" for summer 2020.

VI.3.1 Experimental site

The field trials were conducted on a regularly mown pasture at Lincoln University, New Zealand (43° 38' 54.02" S, 172° 28' 6.556" E), where perennial rye grass (*Lolium perenne*) was the predominant pasture species. The soil was a Wakanui Mottled Immature Pallic Silty Loam (Lilburne *et al.* 2012). The site is under sprinkler irrigation during the summer period (November to March) and receives irregular N fertiliser inputs. A total of 8 soils cores were used to determine the soil ρ_b that averaged 1.1 ± 0.03 (s.e.m) g cm^{-3}. The soil N-inorganic and DOC concentration characteristics of the paddock are given in Table 8 (values for the 15th of November 2018) for field trial 1 and Table 9 (values for the 13th of February 2020) for field trial 2.

An automatic weather station on site logged hourly rainfall, air temperature, humidity, solar radiation, wind speed and soil temperature (10 cm depth) data. The data were recorded on Vista Data Vision software. Potential evapotranspiration for short grass was calculated according to (Allen 2006): with the Sz parameter used to select which crop reference to use for the ETsz calculation (Allen 2006) a value of zero was entered, similar to clipped grass.

VI.3.2 Experimental design

VI.3.2.a *Field trial 1*

A factorial randomised experiment was conducted comprising two urine treatments (nil urine or plus urine) and two irrigation frequencies (standard or optimised), replicated three times. Treatments were applied to 0.25 m^2 plots defined by 12 pneumatically operated automated sampling chambers that were separated by 1 m buffer areas (Figure 65). Treatments were as follows:

- standard irrigation – non urine (control);
- standard irrigation – plus urine;
- optimised irrigation – non urine;
- optimised irrigation – plus urine.

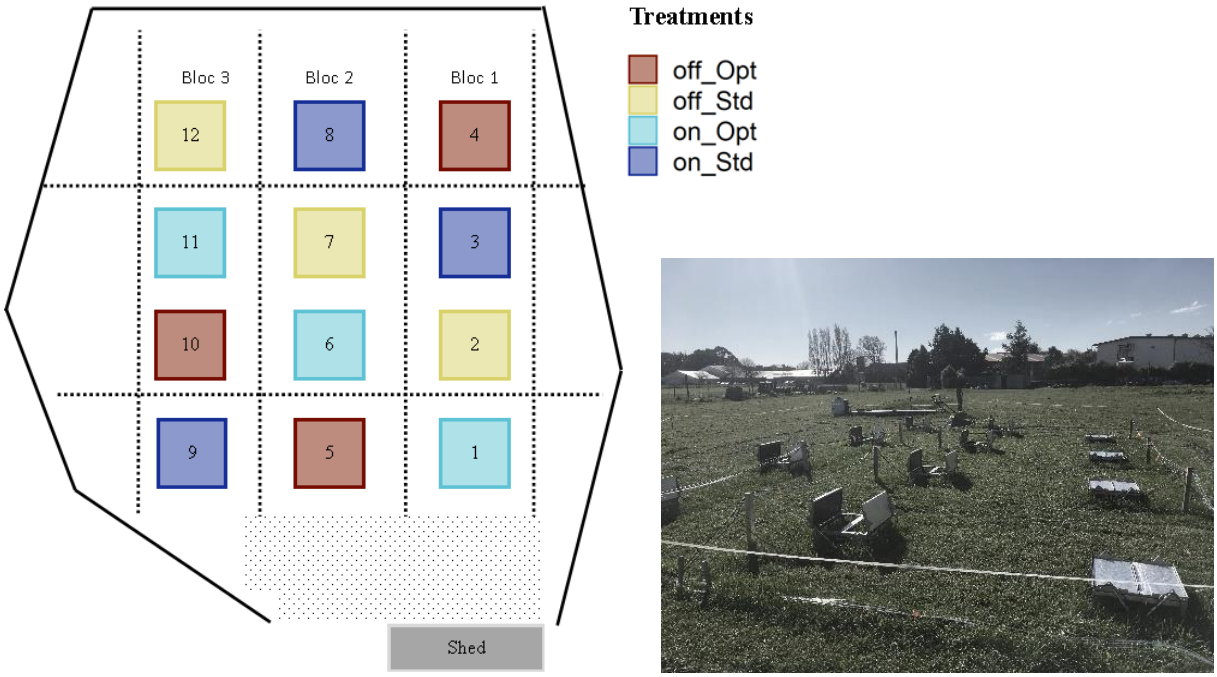

Figure 65: A schematic of the field trial 1 with the 12 chambers locations randomised per treatments with optimised (Opt) and standard (Std) irrigation treatments with urine applied (on) or no urine applied (off). Photo of the final result on the field taken from the shed is shown on the right corner.

Standard irrigation comprised of a 3 day irrigation interval with 3.75 L (equivalent to 15 mm) of water applied at each irrigation event. This was chosen to simulate routine application rate and frequency used by local farmers (Owens *et al.* 2017) as explained in section V.3.2. The optimised irrigation treatment was determined based on using relative soil gas diffusivity (D_p/D_o). First the soil's field capacity (FC), defined as soil volumetric water content (θ_v) following saturation and 24 hours drainage, and permanent wilting point (PWP), defined as soil volumetric moisture content at -1500 kPa, were determined. Field capacity was measured by taking 8 undisturbed soil cores from the field site (Figure 66) which were then saturated and covered for 24h until the rapid drainage had effectively ceased.

Figure 66: Soil cores taken in the field to determine field capacity by saturation method.

The difference between FC less the PWP equated to the plant available water (PAW). Optimised irrigation aimed to replenish soil water reserves to a value equal to 80% of PAW, a moisture content less than FC. The trigger level for optimised irrigation to be applied was when 50% of PAW was reached. The values of θ_v for FC, PWP, the optimised irrigation trigger point and 80% of FC were 0.43, 0.14, 0.29 and 0.40 cm^{-3} cm^{-3}, respectively.

Soil moisture in situ was logged at 1 minute intervals and then averaged hourly using a series of frequency domain reflectometry (FDR) probes (Siemens and TM5) with sensors placed within the first 10 cm of the soil (Figure 67).

Figure 67: Application of urine in the chamber. The FDR probes is placed in the middle of the chamber to measure the volumetric water content for the subsurface soil (first 10cm)

Probes were calibrated using soil water characteristics identified by analysing intact soil cores from the site with output provided as θv. These measurements and predetermined measures of soil ρ_b and soil Φ over the 0-10 cm soil depth were used to determine volumetric air content (ε, m^3 air m^{-3} soil) as described in equation 1 (II.3.1). Hourly D_p/D_o, and daily average values were then calculated (SWLR model, Moldrup *et al.* 2013) as described earlier (Equation 12). However, the measurements were taken on intact soil so the Cm, the media complexity factor, was set to equal a value of Cm = 2.1 for intact soil (Moldrup *et al.* 2013). Values of D_p/D_o corresponding to FC, PWP, the optimised irrigation trigger point and 80% of FC were 0.004, 0.122, 0.033 and 0.01, respectively. The 80% of FC D_p/D_o value calculated (0.01) was > at 0.006. In the optimised irrigation treatment the volume of water required to bring the soil back to 80% of FC, i.e. from a D_p/D_o value of 0.033 to 0.01, was 2.75 L (11 mm). Note that 0.033 value is closed to the boundary that demarcates the inter and intra-aggregate pore regions found by Jayarathne *et al*. (2020b) for pasture soil with a value of Ɛ equals to 0.3 cm^3 cm^{-3} i.e. the equivalent of = 0.036 in the SWLR model used for this study.

Vista Data Vision software was used to visualise the daily soil data results and make decision for the optimised irrigation. For field trial 2, the weather forecast for the optimised treatment (MetService) was part of the decision tool i.e. if the D_p/D_o was close to TP (0.033) but rainfall

was expected, then irrigation was postponed. The non-urine treatment was used to determine the trigger irrigation point for field trial 1, given that most of a pasture area is unaffected by urine.

Fresh bovine urine was collected from cows grazing perennial ryegrass-white clover (*Trifolium repens*) pasture and a 2 L volume of urine was applied per plot, to urine-receiving plots, at a rate equivalent to 700 kg N ha^{-1} on the 16th of November 2018 (Figure 67).

VI.3.2.b *Field trial 2*

For field trial 2, conducted over a year after field trial 1, the 12 chambers were shifted one meter from their original places. Three spare plots on the right side of the field were also added to allow soil samples to be taken during the experiment without disturbing the chamber' soil (Figure 68). Another major change compared to the field trial 1, concerned the number of treatments. After analysing the data for field trial 1, suggestions were made to improve the number of replicates (only 3 for the first trial). Since the nil urine treatments being really similar in term of N_2O emissions (Figure 79) regardless of the irrigation condition (standard or optimised), the decision was taken to have three treatments with four replicates for the second field trial as follows:

- standard irrigation – non urine (control);
- standard irrigation – plus urine;
- optimised irrigation – plus urine;

The same FDR probes were used and identical thresholds for D_p/D_o were identified. Fresh bovine urine was collected and applied in the chambers, to urine-receiving chambers, at a rate equivalent to 700 kg N ha^{-1} on the 13th of February 2020.

Figure 68: A schematic of the field trial 2 with the 12 chambers locations randomised per treatments with optimised (Opt) and standard (Std) irrigation treatments with urine applied (on) or no urine applied (off). Photo of the final result on the field taken from the side is shown on the right.

VI.3.3 Sample collection and analysis

VI.3.3.a *Automatic chambers for N_2O fluxes*

Daily N_2O fluxes were measured with pneumatically operated, automated sampling chambers (Mumford *et al.* 2019; Grace *et al.* 2020). The chambers (headspace height of 150 mm) were made from stainless steel frames with Perspex® walls and lids (insulated) to enable plant growth. Chamber bases (0.25 m^2) were embedded 10 cm into the soil. During a sampling event, 4 chambers (one replicate) closed for 60 minutes as observed in Figure 65 (chambers from bloc 1 are closed while chambers from bloc 2 and 3 are open). Over this time automated sampling of the chamber headspaces occurred with a sample taken every 3 minutes in a sequential order, followed by a reference N_2O gas sample (1 µL L^{-1} N_2O, BOC, New Zealand), taking a total of 15 minutes. The sampling sequence was repeated a further three times giving a total of four

samples per chamber headspace over the 60 minute period (Figure 69). Two independent software programs were run simultaneous to operate the autosampling system:

- The GHG system software, which was developed by Queensland University of Technology, was used to control the entire sampling process. It connected to the program logic controller (inside the sample unit, Figure 70) to be able to start or stop the sample loop. This software also have a manual mode to be able to test each chamber line.
- Peaksimple, a free software package provided by SRI Instruments, recorded data from the GC. It analysed the chromatography from the ECD providing the N_2O data. Starting the sample loop sequence on the GHG system caused the measurement process on the Peaksimple software to start simultaneously.

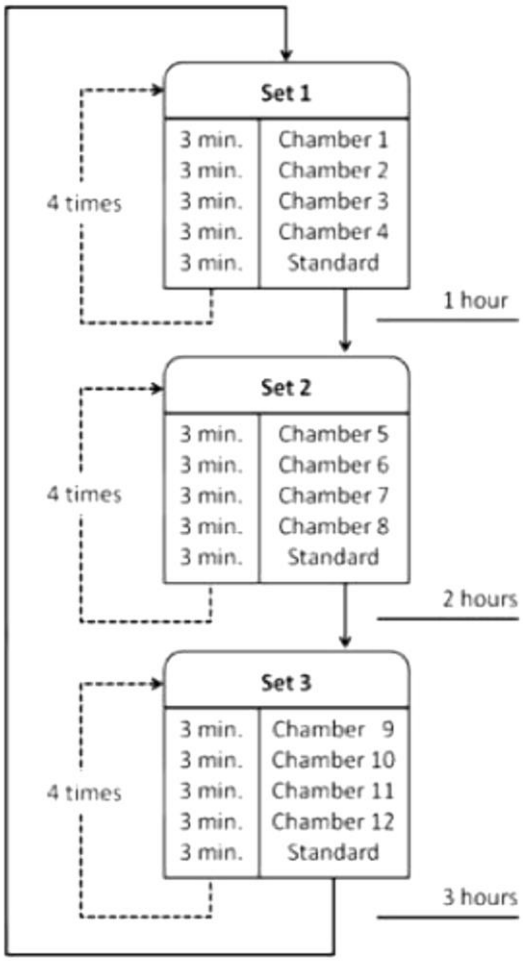

Figure 69: A twelve chamber sampling sequence.

The automated chambers were sealed airtight during the sampling procedure by two lids that closed and opened via pneumatic actuators and using an air compressor (Figure 70).

Gas samples were automatically transferred and injected into an *in situ* gas chromatograph (SRI 8610C, USA) via a sampling box (Figure 70). The 4 chambers sampled were then automatically opened where upon the next set of 4 chambers closed, and the sampling sequence (Figure 69) was repeated. All 12 chambers were sampled once every 3 hours and eight times every 24 hours. PeakSimple™ software was used to integrate the GC output in order to determine sample N_2O concentrations. Any CO_2 and H_2O from the gas samples were removed before N_2O was analysed via a scrubber containing sodium hydroxide and magnesium perchlorate to avoid any contamination during the GC determination of N_2O concentration. The system was calibrated using reference N_2O standards (BOC, NZ). The slope of the change in chamber headspace N_2O concentration versus time was used to calculate the magnitude of the N_2O flux as follows:

$$F_{N_2O} = \frac{\partial C}{\partial t} \frac{V_c M_{mol}}{A V_{mol}} \quad (16)$$

Where, $\partial C/\partial t$ is the rate of change of N_2O concentration inside the chamber, A is the surface area (m^2) of the chamber, Vc is the total volume (L) of the chamber corrected for temperature and relative humidity, Mmol is molar mass of N_2O (g mol-1) and Vmol is the volume of a mole of N_2O (L mol-1) inside the chamber corrected for air temperature using the ideal gas law. The automated system and flux calculation details are further described in detail by (Barton *et al.* 2008). The N_2O flux rates were calculated and corrected for air temperature, atmospheric pressure and the ratio of chamber volume to surface area and expressed on an elemental weight basis as g N_2O–N ha^{-1} day^{-1}.

An automated tipping bucket to measure rainfall was also connected to the automated chamber sampling system: rainfall events exceeding 5 mm triggered the opening of all chambers until rainfall ceased.

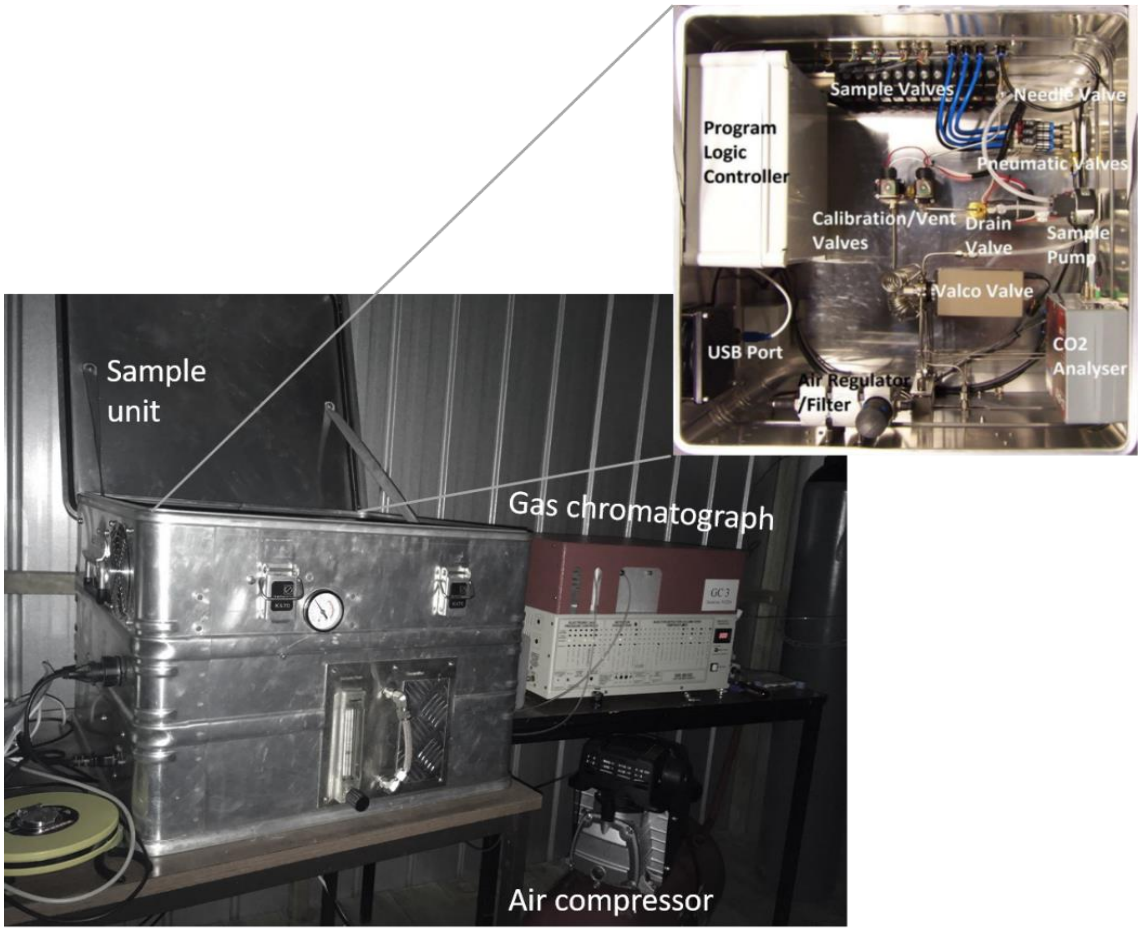

Figure 70: The complete Sampling Unit setup in the shed including the top view of the sample unit. The computer is not present on the picture but was connected to the left of the sample unit. The calibration gas and carrier gas were on the right.

VI.3.3.b *Pasture biomass and soil samples*

Field trial 1:

Pasture was cut to a uniform height of 5 cm prior to treatment application and harvested once at the end of the experiment (Figure 71). Harvested grass samples were dried at 60°C for 2 days and then weighed to determine dry matter (DM) production (Figure 71). Soil inorganic-N concentrations were determined pre-urine application, 6 days after urine application and at the end of the experiment (27 days after urine application). Soil cores (2 cm diameter, 7.5 cm long, Figure 72) were taken adjacent to the plots pre-urine and inside the plots post-urine application. Holes left following soil coring, 6 days after urine application, were plugged with Falcon™

tubes to prevent water and air ingress. Soil gravimetric water contents were determined prior to extracting the soil cores with 2 M KCl for one hour, filtering (Whatman 42) (Figure 72), with flow injection analysis (Alpkem FS3000) used to determine NO_3^--N and NH_4-N concentrations (Blakemore *et al.* 1987).

Finally, further soil subsamples were extracted for dissolved organic carbon (DOC) using 5 g equivalent of dry soil and 30 mL of deionised water which was shaken for 30 min before centrifugation (2280 x g for 20 min, T=25 ºC, model Kubota 8420), and filtration (Whatman 42), with analyses performed on a Shimadzu TOC analyser (Shimadzu Oceania Ltd, Sydney, Australia). Water samples from the irrigation water were analysed for nitrate-N content and the average NO_3^--N value was equal to 7.11 ± 0.03 (s.e.m) mg/L.

Figure 71: Pasture harvest in one chamber (left) and dry biomass weigh taken (right).

Field trial 2:

Pasture was cut to a uniform height of 5 cm prior to treatment application and harvested twice until the end of the experiment (Figure 71). Harvested grass samples were dried at 60ºC for 2 days and then weighed to determine dry matter (DM) production.

Soil inorganic-N concentrations and DOC concentrations were determined as described above pre-urine application, and then before every irrigation treatments on the spare chambers (Figure 68) and at the end of the experiment inside the 12 chambers (Figure 72).

Figure 72: Soil samples taken on the last day of the experiment for the field trial 2 (left) and the filtering step during the KCL extraction in the lab (right).

VI.3.4 Statistical analyses

Statistical analyses were also performed using R studio and followed the same procedure as explained in section III.3.4. Urine (2 levels: on and off), irrigation conditions (2 levels: Opt and Std), combined treatments (4 levels: off_Std, on_Std, off_Opt and on_Opt) and days were the explanatory variables (Appendix 4).

VI.4 Results

VI.4.1 Rainfall, soil temperature and irrigation cycles

VI.4.1.a *Field trial 1*

Potential evapotranspiration ranged from 0.6 to 5.7 mm day^{-1} (Figure 73). Daily soil temperature was generally between 15 and 20^{o}C (Figure 73). The field site received above average rainfall totalling 97 mm during the experimental period from 15 November 2018 to 13 December 2018. On average, < 60 mm rainfall is normally recorded November-December at the site. Significant rainfall occurred soon after urine application from 18 – 21st November (Figure 73). Consequently, this delayed the commencement of irrigation treatments. Standard irrigation was applied from the 1st of December while the trigger for optimised irrigation occurred only on the 10th of December (Figure 73).

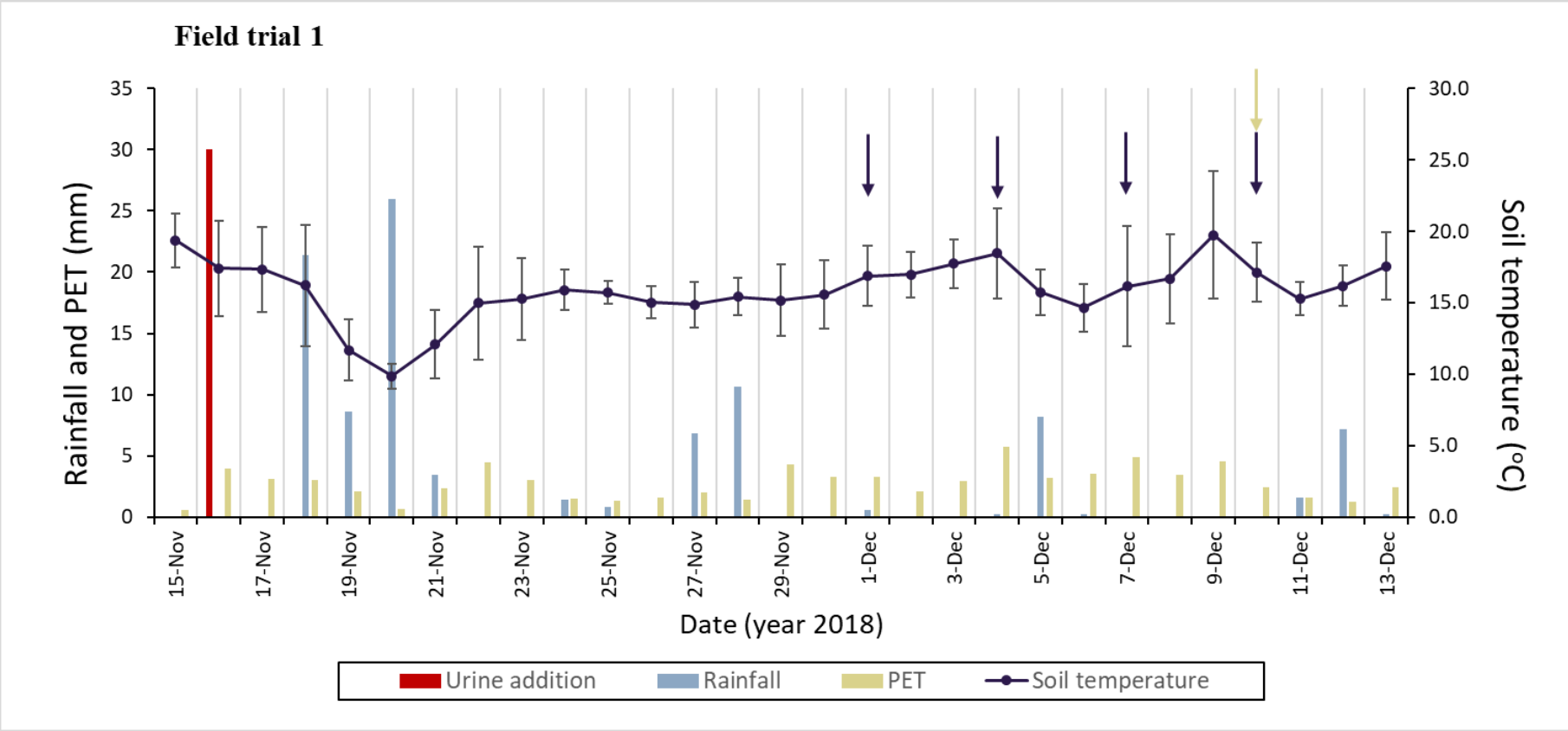

Figure 73: Daily rainfall (blue bar), potential evapotranspiration (PET; yellow bar) and soil average temperature (black line) of a ryegrass pasture in Lincoln from the 15 November 2018 to 13 December 2018 following ruminant urine application (red bar). Blue and yellow arrows denote standard and optimised irrigation events, respectively. The error bars represent the night and day variations (s.d)

VI.4.1.b *Field trial 2*

Potential evapotranspiration ranged from 0.9 to 4.9 mm day^{-1} (Figure 74). Daily soil temperature was generally between 10 and 15ºC (Figure 74), slightly cooler than for the field trial 1. The field site received low rainfall, totalling 21 mm during the experimental period from 13 February 2020 to 24 March 2020. It was a particularly dry period as on average, around 50 mm rainfall is normally recorded in February-March at the site. Significant rainfall occurred on the 22nd of February with 12.8 mm of rain (Figure 74). The first irrigation treatment was applied 3 days and 5 days after urine application for standard and optimised, respectively (Figure 74).

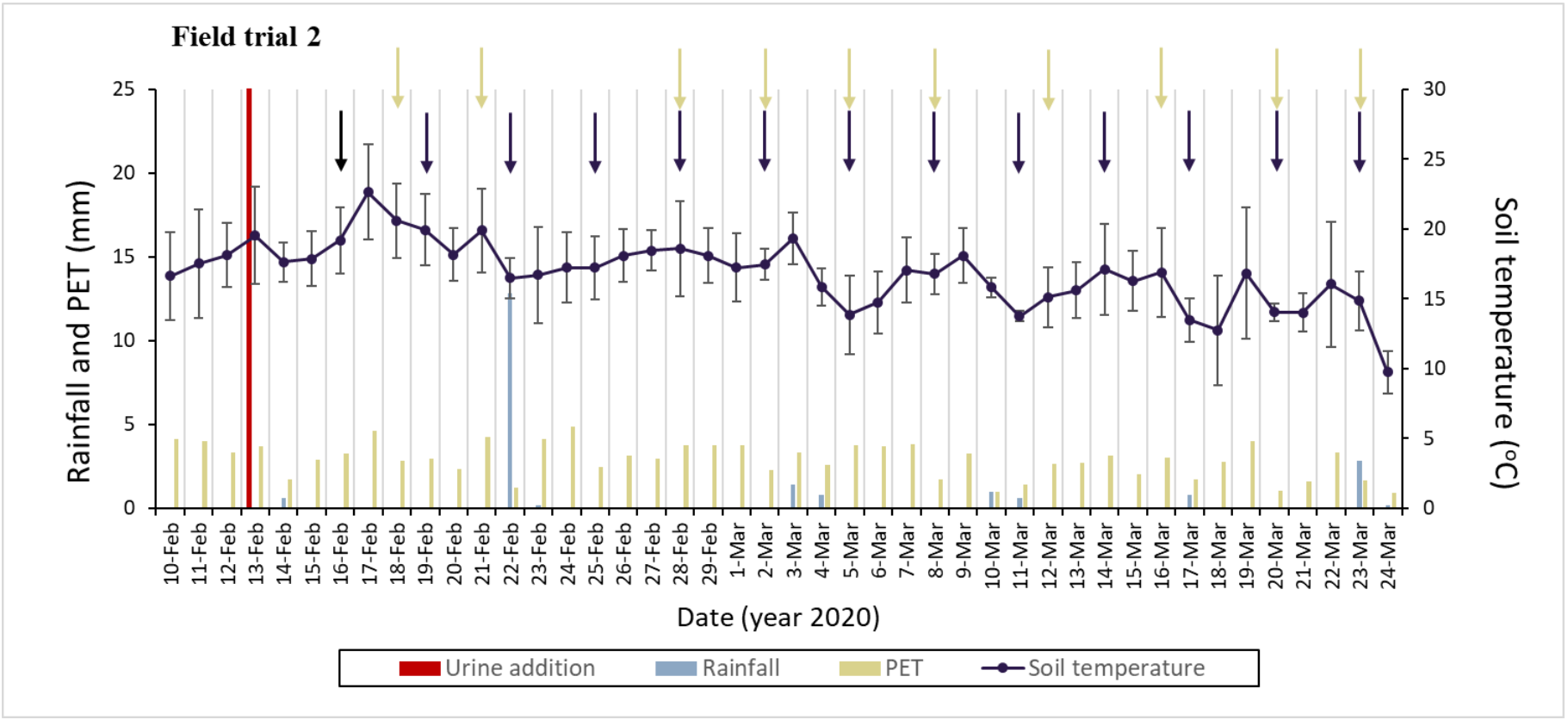

Figure 74: Daily rainfall (blue bar), potential evapotranspiration (PET; yellow bar) and soil average temperature (black line) of a ryegrass pasture in Lincoln from the 10 February 2020 to 24 March 2020 following ruminant urine application (red bar). Blue and yellow arrows denote standard and optimised irrigation events, respectively and the dashed blue line the rain simulation (6.7mm) on the 24th March 2020. The error bars represent the night and day variations (s.d)

VI.4.2 Soil water content and gas diffusivity evolution

VI.4.2.a *Field trial 1*

Figure 75 shows the changes in WFPS, measured for each chamber using the FDR probes. Without urine no water was applied to compensate for urine application in the urine treatment and soil moisture declined until rainfall occurred. Without urine replicate measures of WFPS were reasonably consistent for each chamber over time showing that rainfall and standard irrigation events returned the soil moisture to 80% WFPS, close to the calculated FC of 83%, and that after 30th November soil WFPS was predominately close to 60% WFPS under standard irrigation (replicates 1 and 2). The exception was replicate 3 where WFPS followed the same trend but charted higher over this period. For optimised irrigation, without urine, WFPS after 30th November was generally 50-60% with clear increases due to rainfall (5th and 12th December) or irrigation (10th December) and good agreement between replicates. Under urine with standard irrigation similar maximum WFPS values were observed without the initial drying over the first two days seen in the non-urine treatment. However, following heavy rain on 18-20th November the WFPS under the urine treatments inexplicably decreased. This phenomena might be explained by the probes settling and losing soil contact/opening up air gaps after the rain event. Further inexplicable increases in WFPS occurred in the optimised irrigation treatment (29th November) despite no rainfall or irrigation at this time (replicates 1 and 3). Subsequently, data from these two FDR probes were not used further to calculate D_p/D_o for these replicates.

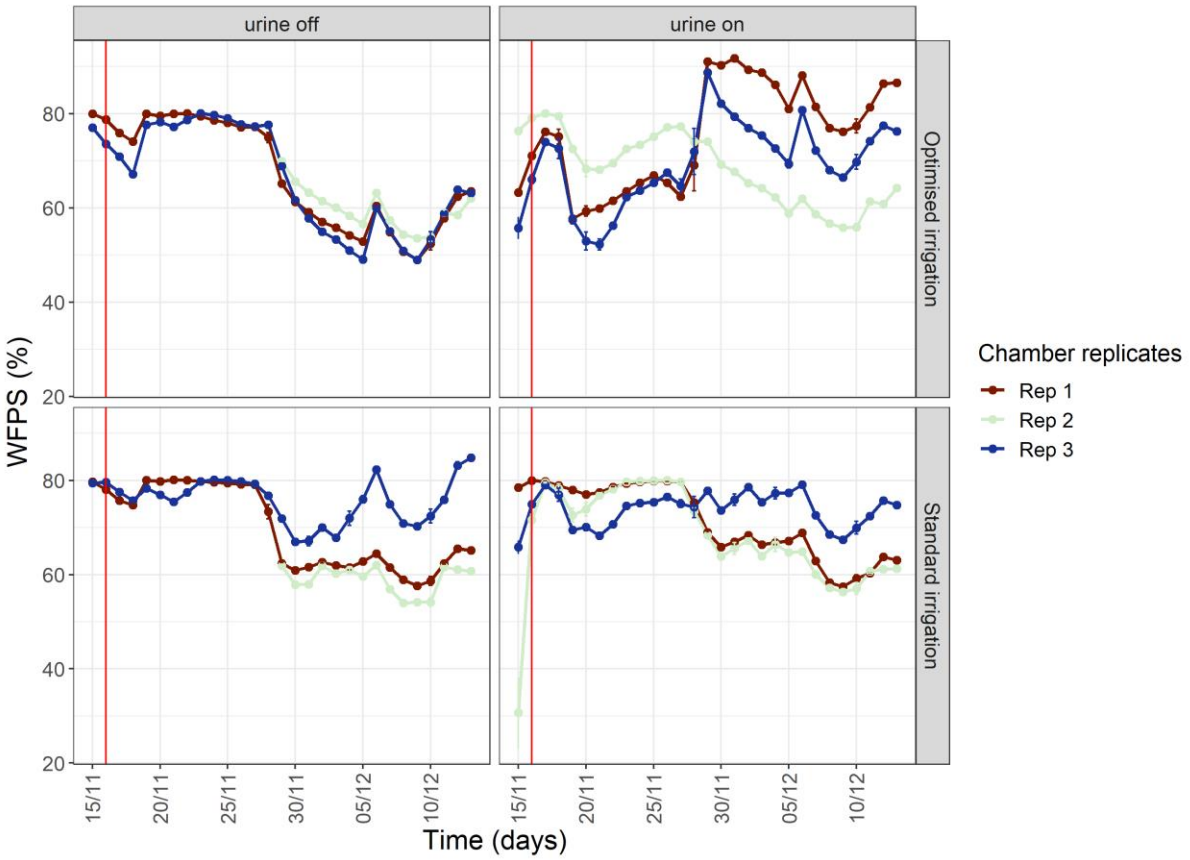

Figure 75: Field trial 1 daily average in situ WFPS (%) from the 15 November 2018 to 13 December 2018 with or without urine and under standard (STD) or optimised (OPT) irrigation. The data are represented per replicates. The red bar shows the date of the urine application event. Error bars = s.e.m. with n = the number of sample per day per chamber (24).

The rainfall events early in the experiment (Figure 73) resulted in soil D_p/D_o values being below a value of 0.006 until the 28th November (Figure 76). After this time standard irrigated treatments had D_p/D_o values between 0.006 and 0.02 while optimised irrigation treatments had D_p/D_o values that were in excess of 0.02 as the soil became drier. Under the optimised irrigation treatment D_p/D_o values increased, with a decline due to rainfall on 5 December, until the trigger point was reached where upon irrigation applied in conjunction with rainfall increased the D_p/D_o in the irrigated treatment to above 0.01 at the end of the experiment (Figure 76).

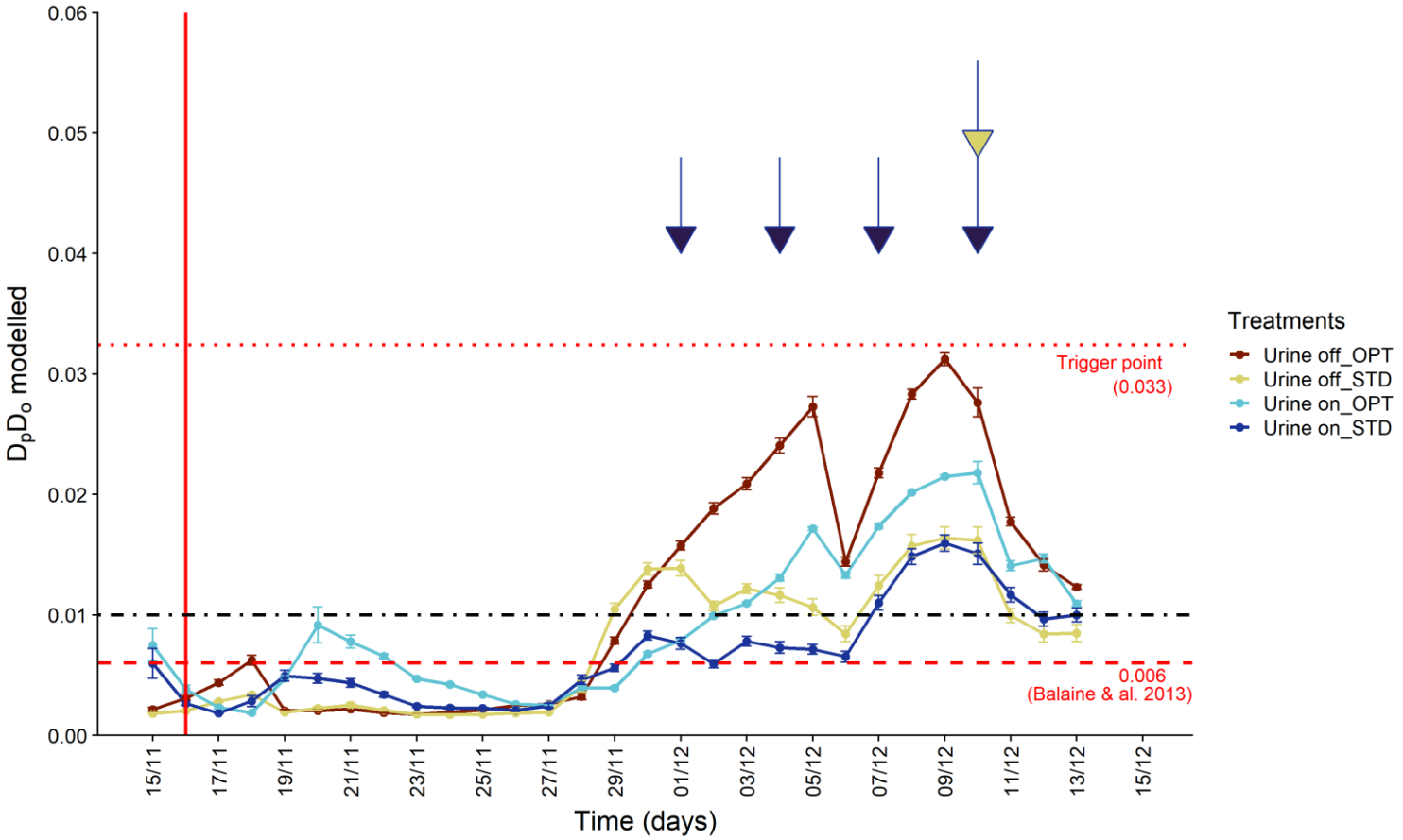

Figure 76: Field trial 1 modelled, daily average soil relative gas diffusivity (D_p/D_o) from the 15 November 2018 to 13 December 2018. The vertical red bar shows the date of the urine application event. Blue and yellow arrows denote the standard (STD) and optimised (OPT) irrigation applications, respectively. Error bars = s.e.m, n=3.The black dashed horizontal line represents 80% FC while diffusivity values are shown by red dotted/dashed lines.

VI.4.2.b *Field trial 2*

Figure 77 shows the changes in WFPS, measured for each treatment using the FDR probes for field trial 2. The urine application (and water for the non-urine treatment) on the 13th of February was followed by a significant increase in the WFPS content in the soil. Every irrigation day was followed by an increase in WFPS. Despite a greater volume of water being added during an irrigation event in the standard treatments (3.75 L vs 2.75 L for optimised), the increase of WFPS after every irrigation was not higher. Under standard irrigation, measures of WFPS were reasonably consistent over time (Figure 77), with or without urine, showing that standard irrigation events returned the soil moisture to ~ 65% WFPS every 3 days, lower than FC (83%). However, on the 16th of March, the WFPS in the standard irrigation with urine treatment dropped and only returned to 66% after the rain simulation on the 24th of March (Figure 77). For this last date, and with the same volume of water added in each chambers, WFPS were 58 and 80% for optimised irrigation with urine and standard irrigation without urine, respectively. The WFPS in the standard irrigation with urine reached its maximum (71%) after the rain event on the 23rd of February (vertical blue line, Figure 77).

Soil D_p/D_o values decreased after every irrigation events (Figure 78). Optimised irrigation was triggered when the D_p/D_o value was ~ 0.033 and D_p/D_o values stayed ≥ 0.01 (80% FC) over the experiment for this treatment. The lowest values for D_p/D_o were observed on the 13th, 14th, 18th and 23rd of February for the optimised treatment. After urine application, the standard irrigation D_p/D_o values were ≤ 0.02 (Figure 78). The rainfall event early on the 23rd of February (Figure 78) resulted in standard irrigation soil D_p/D_o values being equal to a value of 0.006. This threshold was also crossed by the standard without urine treatment (D_p/D_o = 0.0025) at the end of the experiment after the rain simulation event.

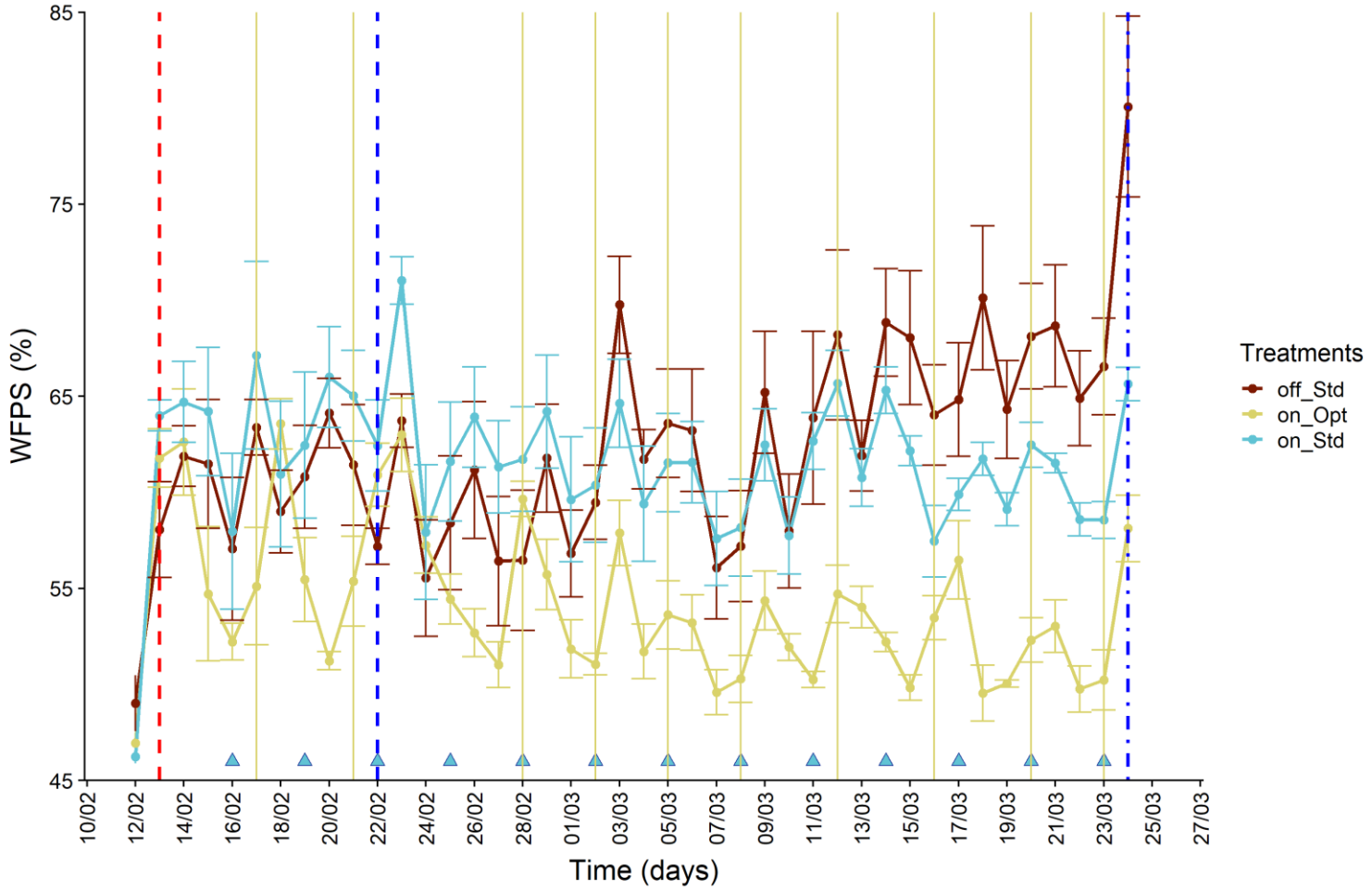

Figure 77: Field trial 2 daily average WFPS (%) from the 12/02/2020 to the 24/03/2020. The red bar represents the urine application, blue triangles and yellow horizontal lines denote the standard (Std) and optimised (Opt) irrigation applications, respectively. Error bars = s.e.m, n=4. Treatment with urine applied (on) or no urine applied (off).The blue vertical dashed line on the 22/02/2020 represent the rain event (12.8mm) and the one at the end the rain simulation.

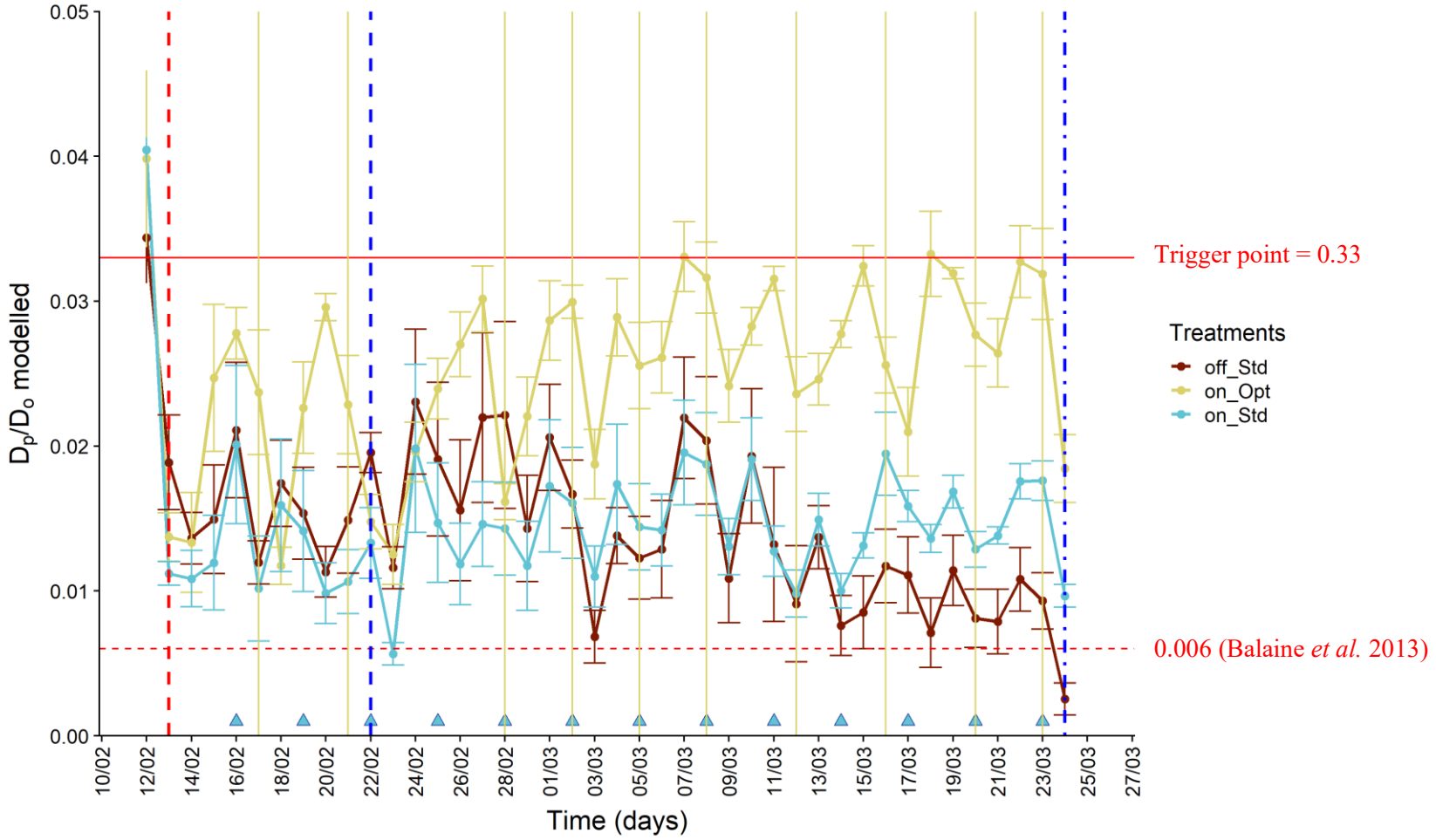

Figure 78: Field trial 2 modelled daily average relative gas diffusivity (D_p/D_o) from the 12/02/2020 to the 24/03/2020. The red vertical bar represents the urine application, blue triangles and yellow horizontal lines denote the standard (Std) and optimised (Opt) irrigation applications, respectively. The blue vertical dashed line on the 22/02/2020 represents a major rain event (12.8mm) and the one at the end the rain simulation. Error bars = s.e.m, n=4. Treatment with urine applied (on) or no urine applied (off).

VI.4.3 Dry matter production, inorganic-N, DOC and N_2O fluxes

VI.4.3.a *Field trial 1*

Dry matter production increased due to urine application but was unaffected by irrigation treatment. With urine the dry matter yields were 18.2 ± 1.2 (s.e.m) and 16.6 ±1.6 kg DM ha^{-1} day^{-1} in the optimised and standard irrigation treatments, respectively. While without urine the optimised and standard irrigation treatments had growth rates of 11.1 ±2.8 and 8.2 ±1.5 kg DM ha^{-1} day^{-1}, respectively.

Soil NH_4-N and NO_3^--N concentrations pre-urine application were 16.2 ± 0.2 (± s.e.m) and 2.9 ± 0.1 µg N g^{-1}, respectively. Six days after urine application soil NH_4^+-N and NO_3^--N concentrations were 322 ± 33.0 and 10 ± 1.4 µg N g^{-1}, respectively, in the chambers receiving urine on (Table 8). Under urine application soil NH_4^+-N concentrations had declined by the end of the experiment but no significant irrigation effect was observed ($P = 0.176$) with averages equal to 27.8 ± 8.8 and 13.4 ± 1.7 µg N g^{-1} for optimised and standard irrigation, respectively. Soil NO_3^--N concentrations increased during the experiment ($P < 0.05$) but no irrigation effect was observed ($P = 0.324$) with an average of 157 ± 13 µg N g^{-1} and 134 ± 10 µg N g^{-1} in the soil for optimised and standard irrigation, respectively. Inorganic-N concentrations in the non-urine control remained low with NH_4^+-N and NO_3^--N concentrations ≤ 12.6 ± 3.7 and 6.0 ± 1.7 µg N g^{-1}, respectively (Table 8). NO_3^--N concentrations were significantly lower ($P < 0.05$) in the non-urine treatments.

Soil DOC concentration pre-urine application was 149.3 ± 14.1 µg g^{-1} (Table 8). At the end of the experiment, the urine treatment receiving standard irrigation had a lower DOC concentration (124.9 ± 14.9 µg g^{-1}) compared to the start. The remaining treatments resulted in increases ($P < 0.05$) in soil DOC with concentration ≥ 217.9 µg g^{-1} (Table 8).

Table 8: Field trial 1 concentration of inorganic-N for both NO_3^--N and NH_4^+-N and dissolved organic carbon measured in the soil (0–7.5 cm) per treatments. Values are means (n=3) and errors are standard error of the mean (s.e.m)

		Total N-inorganic (µg N g^{-1} dry soil)		Dissolved organic carbon
Treatments	Date	NH_4^+-N (± s.e.m)	NO_3^--N (± s.e.m)	µg g^{-1} dry soil
urine on_OPT	15-Nov	16.1 (0.1)	2.9 (0.01)	149.3 (14.1)
	22-Nov	380.0 (29.2)	7.6 (2.6)	–
	12-Dec	27.8 (8.8)	157.3 (12.7)	217.6 (13.5)
urine off_OPT	15-Nov	16.1 (0.6)	2.9 (0.1)	149.3 (14.1)
	22-Nov	2.8 (0.1)	2.0 (0.3)	–
	12-Dec	7.2 (1.7)	3.1 (0.9)	227.4 (35.8)
urine on _STD	15-Nov	16.1 (0.1)	2.9 (0.02)	149.3 (14.1)
	22-Nov	264.6 (25.5)	12.5 (2.4)	–
	12-Dec	13.4 (1.7)	133.6 (9.7)	124.9 (14.9)
urine off_STD	15-Nov	16.1 (0.1)	2.9 (0.02)	149.3 (14.1)
	22-Nov	7.5 (4.7)	1.9 (0.05)	–
	12-Dec	12.6 (3.7)	6.0 (1.7)	226.8 (18.2)

Figure 79 shows that the average daily N_2O-N fluxes increased markedly three days after urine application, peaking 5-6 days after urine application before gradually declining. Further rainfall on 27th November increased N_2O-N fluxes again. When irrigation commenced the earlier and more regular irrigation events in the standard irrigation treatment resulted in higher N_2O-N fluxes from the 1st to the 8th of December (Figure 79). These daily N_2O-N fluxes determined the trends observed in the cumulative N_2O-N fluxes (Figure 80). Total cumulative losses in the optimised and standard urine treatments did not differ ($P < 0.44$) when considering the entire experimental period and were 2040 ± 464 (s.e.m) g N ha^{-1} and 2676 ± 587 g N ha^{-1}, for optimised and standard irrigation with urine, respectively. Over the total period the non-urine optimised treatment emitted a lower ($P = 0.03$) total cumulative N_2O-N flux than the standard non-urine treatment: 62 ± 17 g N ha^{-1} and 131 ± 9 g N ha^{-1}, respectively. Total cumulative mean N_2O-N fluxes under urine resulted in emission factors (Equation 15, V.3.3) of 0.28 and 0.36% for the optimised and standard urine irrigation treatments, respectively.

Considering only the irrigation period, 1st of December onwards (Figure 80), resulted in lower cumulative N_2O-N fluxes in the optimised treatment (at P = 0.09) compared with the standard irrigation treatment 306 ± 147 g ha^{-1} and 1087 ± 319 g ha^{-1}, respectively.

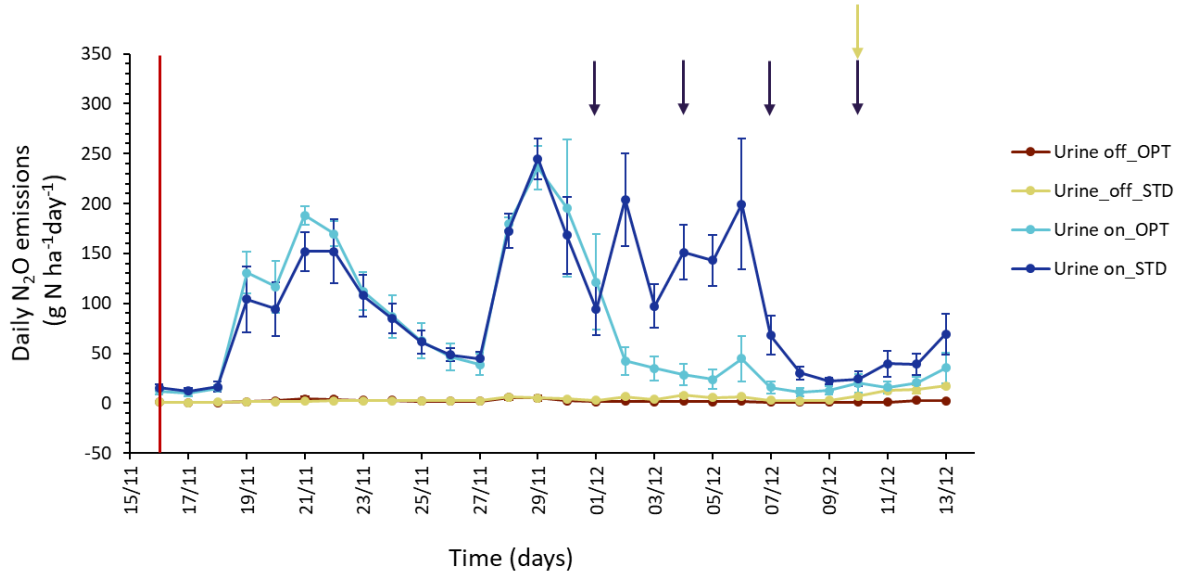

Figure 79: Field trial 1 daily N_2O emissions (g N $ha^{-1}day^{-1}$) from the 15/11/2018 to the 13/12/2018 for the four treatments. The red bar represents the urine application, blue arrows and yellow arrow denote the standard (STD) and optimised (OPT) irrigation applications, respectively. Error bars = s.e.m, n=3.

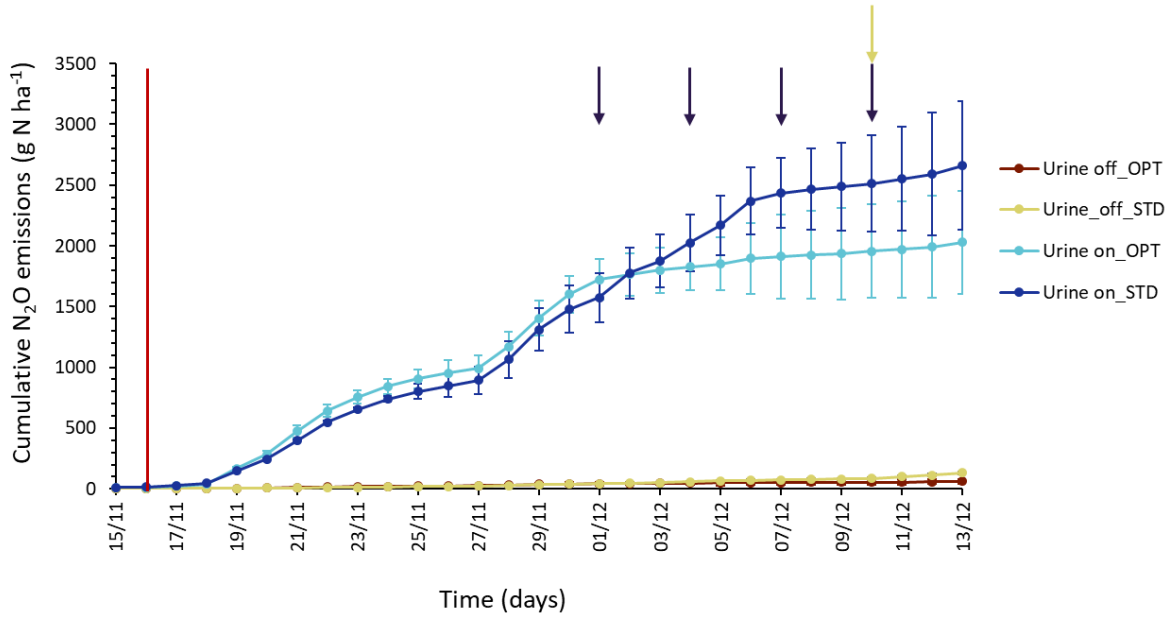

Figure 80: Field trial 1 cumulative N_2O emissions (g N ha^{-1}) from the 15/11/2018 to the 13/12/2018 for the four treatments. The red bar represents the date of urine application. Blue and yellow arrows denote standard (STD) and optimised (OPT) irrigation events, respectively. Error bars = s.e.m, n=3.

VI.4.3.b *Field trial 2*

Dry biomass was unaffected by irrigation or urine treatments (Figure 81). At the end of the experiment, an average of 57.3 g of cumulative dry biomass was harvested from the control chambers, similar to chambers with urine under standard and optimised irrigation with 55.9 g and 53.5 g of cumulative dry biomass respectively (Figure 81). With urine the growth rates were 26.8 ± 2.0 (s.e.m) and 30.8 ± 1.3 kg DM ha^{-1} day^{-1} in the optimised and standard irrigation treatments, respectively. While in the control (without urine and with standard irrigation), the growth rates was 30.9 ±1.5 kg DM ha^{-1} day^{-1}.

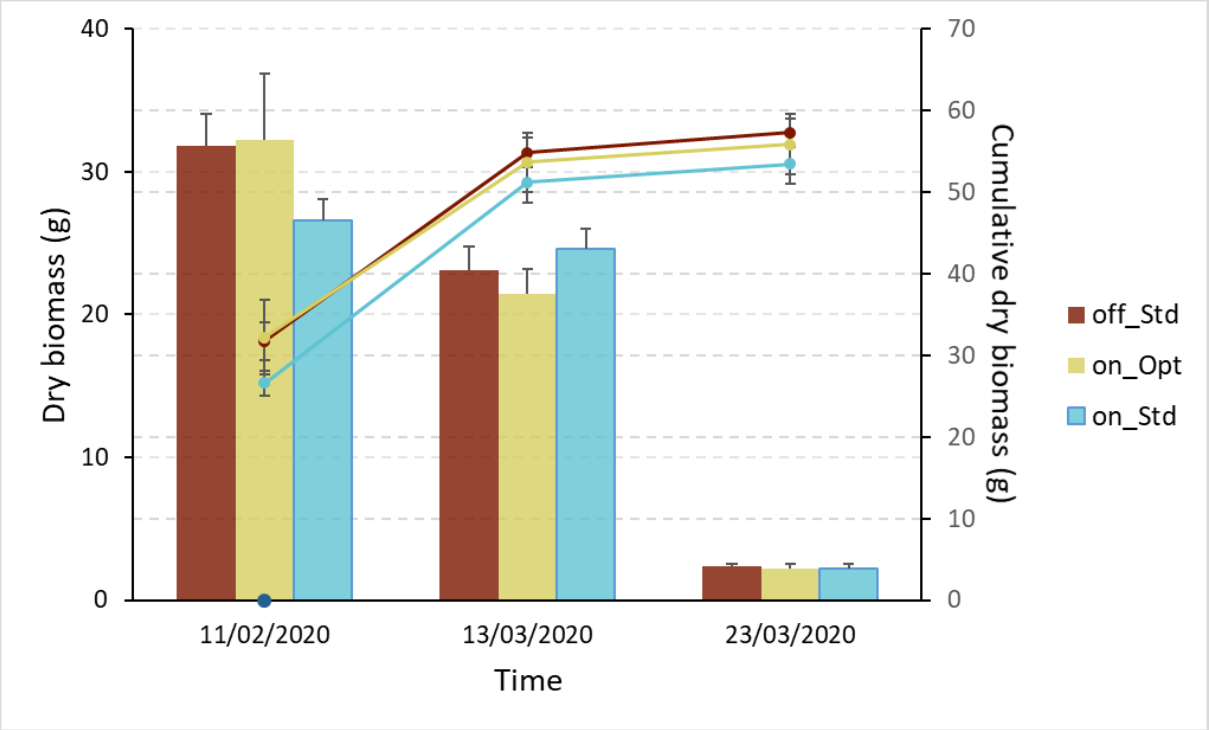

Figure 81: Field trial 2 dry biomass and cumulative dry biomass collected 3 times over the total period of the experiment for optimised (Opt) and Standard (Std) irrigation treatment with urine applied (on) or no urine applied (off). Data points are means of four replicates ± S.E.M.

Figure 82 shows that the average daily N_2O-N fluxes increased markedly the day of the urine application, to then gradually decline until the first irrigation event. Until the 5th of March, N_2O-N flux peaks were observed after every irrigation event (Figure 82). After the 5th of March, the N_2O fluxes were $\leq 9.8 \pm 1.5$ g N ha^{-1} day^{-1} regardless of treatment until the rain simulation (6.7 mm) on the 24th March. The more regular irrigation events in the standard irrigation treatment resulted in higher N_2O-N fluxes from the urine applied until the 5th of March (Figure 82) and especially on the day following the rain event (22nd of February). The peak emissions observed on the 23rd differed significantly ($P < 0.05$) in all treatments and were, on average, equal to 235.4 ± 31.8, 60.3 ± 11.4 and 24.3 ± 19.5 g N ha^{-1} day^{-1} for standard and optimised irrigation with urine, and standard irrigation without urine, respectively. A significantly higher peak of 69.2 ± 32 g N ha^{-1} day^{-1} in the standard irrigation without urine was observed at the end of the experiment after the rain simulation when compared to the urine-on treatments.

These daily N_2O-N fluxes determined the trends observed in the cumulative N_2O-N fluxes (Figure 83). Total cumulative losses in the standard and optimised urine treatments differed (P = 0.09) when considering the entire experimental period and were 941 ± 136 g N ha^{-1} and 609 ± 27 g N ha^{-1}, respectively. Over the total period the non-urine treatment emitted a significantly lower (P = 0.002) total cumulative N_2O-N flux than the urine treatments: 252 ± 100 g N ha^{-1}.

Total cumulative mean N_2O-N fluxes under urine resulted in emission factors of 0.05 and 0.1% for the optimised and standard urine irrigation treatments, respectively.

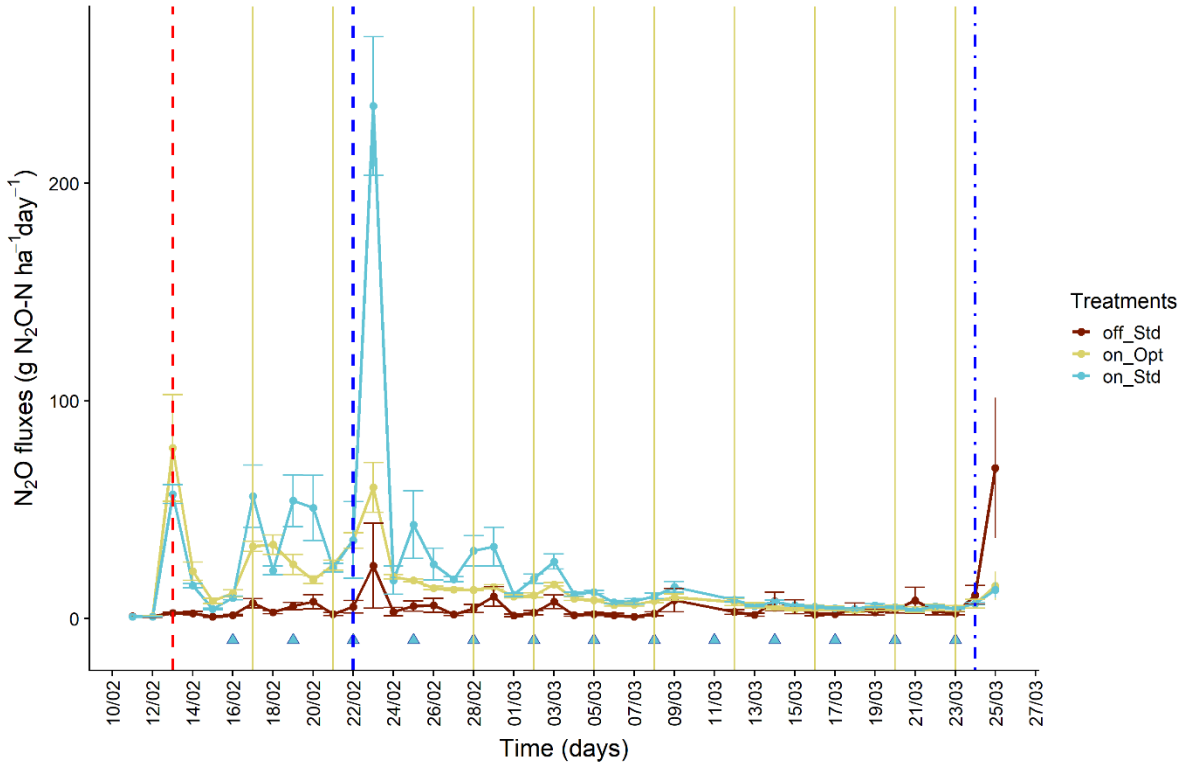

Figure 82: Field trial 2 daily N2O emissions (g N ha-1day-1) from the 11/02/2020 to the 25/03/2020. The red bar represents the urine application, blue triangles and yellow horizontal lines denote the standard (STD) and optimised (OPT) irrigation applications, respectively. Error bars = s.e.m, n=4. Treatment with urine applied (on) or no urine applied (off). The blue vertical dashed line on the 22/02/2020 represents a major rain event (12.8mm) and the one at the end the rain simulation.

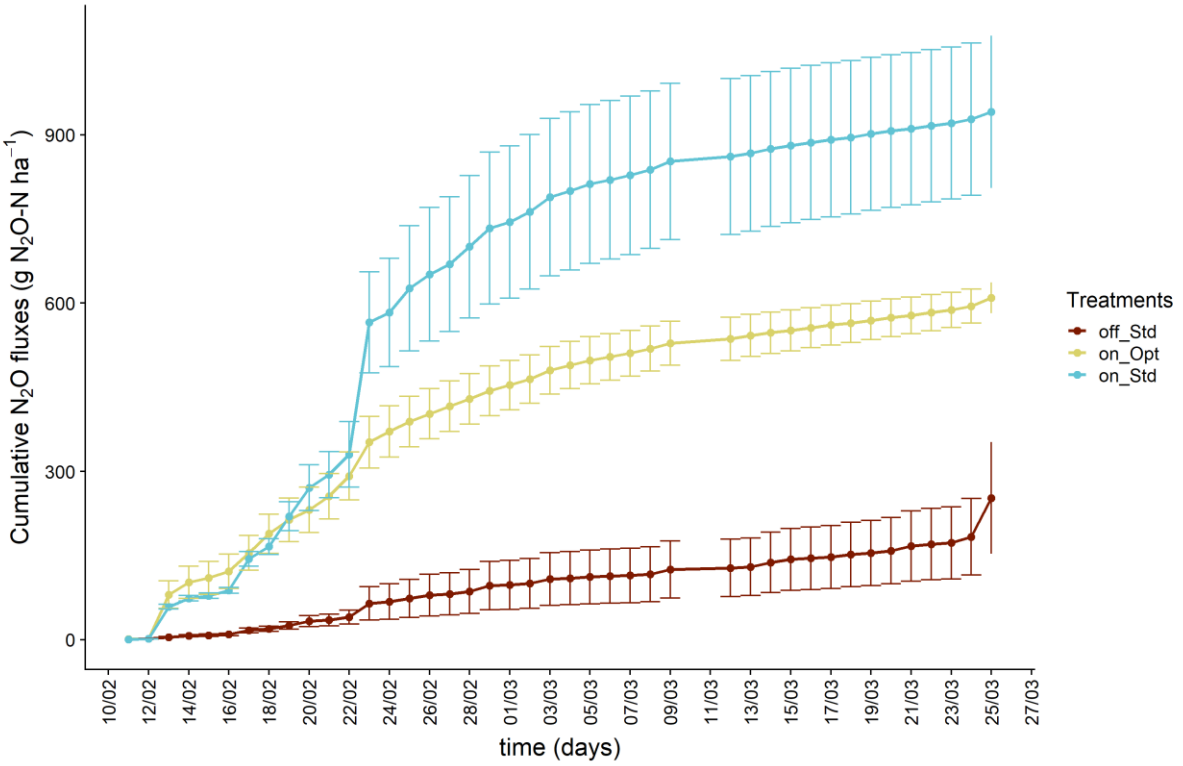

Figure 83: Field trial 2 cumulative N_2O emissions (g N ha^{-1}) from the 11/02/2020 to the 25/03/2020 for the optimised (Opt) and standard (Std) irrigation treatments with urine applied (on) or no urine applied (off). Data points are means of four replicates ± s.e.m.

Soil NH_4^+-N and NO_3^--N concentrations pre-urine application were 18.9 ± 1.8 (± s.e.m) and 2.7 ± 0.9 µg N g^{-1}, respectively (Table 9). Until the 2nd of March, the NO_3^--N concentrations increased up to 218.7 and 133.8 µg N g^{-1} for optimised and standard irrigation with urine, respectively. However, the NO_3^--N concentrations had decreased significantly by the end of the experiment ($P < 0.05$, Table 9). The values measured in the spare chambers with urine were not significantly different than the values measured in the chambers at the end of the experiment for NH_4^+-N and NO_3^--N concentrations (Table 9), except for the urine off standard treatment where the value for NO_3^--N concentrations in the spare chamber (1.3 ± 0.1 µg N g^{-1}) was lower than the chambers' value (7.6 ± 3 µg N g^{-1}). An irrigation effect with urine was observed in the NO_3^--N concentrations with higher values for the optimised compared to the standard irrigation: 98.2 ± 8.3 and 55 ± 10.7 µg N g^{-1}, respectively, at the end of the experiment.

Under urine application, soil NH_4^+-N concentrations had increased up to the 21st of February and then declined by the end of the experiment but no significant irrigation effect was observed in the spare chambers (P = 0.25) with averages equal to 11.6 ± 5.9 and 4.9 ± 1.4 µg N g^{-1} for optimised and standard irrigation, respectively.

Inorganic-N concentrations in the non-urine control remained low with NH_4^+-N and NO_3^--N concentrations ≤ 14.8 and 7.6 ± 3 µg N g^{-1}, respectively (Table 9). NO_3^--N concentrations were significantly lower (P < 0.05) in the non-urine treatments at the end of the experiment.

Soil DOC concentration pre-urine application average across all treatments was 239.7 ± 26.9 µg g^{-1} (Table 9). At the end of the experiment, all the treatments had lower DOC concentrations (≤ 142.9 ± 5.9 µg g^{-1}) when compared to the start. A treatment effect was also observed (P = 0.048) with the lowest value for the optimised irrigation with urine treatment (109.1 ± 5.4 µg/g).

Table 9: Field trial 2 concentration of inorganic-N for both NO_3^--N and NH_4^+-N and dissolved organic carbon (DOC) measured in the soil (0–7.5 cm) per treatments. The values with a pink background were sampled in the spare chambers (2 cores mixed in a zip bag for each / date / chamber). The last line of the table (no pink background) represents the data from the autosampling chamber samples. For the last date, values are means (n=4) and errors are standard error of the mean (s.e.m).

		Urine on Optimised	Urine on Standard	Urine off Standard	Urine on Optimised	Urine on Standard	Urine off Standard	Urine on Optimised	Urine on Standard	Urine off Standard
date	details	NO_3^- – N (µg/g)			NH_4^+ – N (µg/g)			DOC (µg/g)		
13/02/2020	start (before urine)	4.6	0.9	2.8	19.8	22.2	14.8	301.3	188.8	229.1
16/02/2020	Before std irrigation	—	4.9	1.9	—	128.8	13.4	—	196.2	194.6
17/02/2020	Before opt irrigation	13.2	—	—	61.9	—	—	330.7	—	—
19/02/2020	Before std irrigation	—	39.5	0.7	—	311.2	3.5	—	383.5	269.9
21/02/2020	Before opt irrigation	103.8	—	—	472.1	—	—	381.3	—	—
2/03/2020	Before opt & std irrigation	218.7	133.8	3.0	74.6	34.0	3.8	275.8	190.0	214.7
24/03/2020	end	116.6 (±23)	39.2 (±13)	1.3 (±0.1)	11.6 (±5.9)	4.9 (±1.4)	2.2 (±0.3)	136.0	172.5	214.5
24/03/2020	end	98.2 (± 8.3)	55 (± 10.7)	7.6 (± 3.0)	10.2 (± 2.1)	2.2 (± 0.5)	3.6 (± 0.5)	109.1 (± 5.4)	120 (± 6.9)	142.9 (± 5.9)

VI.5 Discussion

VI.5.1 Field trial 1

The atypical rainfall over the initial experiment period, with rainfall events in excess of 20 mm, maintained the soil at field capacity for about 10 days following urine application. While this level of soil moisture negated the immediate need for irrigation it provided the opportunity to observe rainfall effects on D_p/D_o. Rainfall events reduced the ability of O_2 to diffuse into the soil as indicated by the values of D_p/D_o which were generally < 0.006 over this time. Stepniewski (1981) reported soils commenced becoming anaerobic for plant roots at D_p/D_o values < 0.02. Balaine *et al.* (2013, 2016) found a D_p/D_o equal to 0.006 induced denitrification-derived maximum N_2O fluxes, and that lower D_p/D_o values caused complete reduction of N_2O to dinitrogen (N_2). While Chamindu Deepagoda *et al.* (2020) showed, using intact soil cores, that D_p/D_o above 0.005-0.01 could improve soil aeration and minimise N_2O emissions. Similar results were reported by in Rousset *et al.* (2020), Chapter III, where an increase in N_2O fluxes occurred as D_p/D_o declined, creating an environment suitable for N_2O production. In the current study despite D_p/D_o values < 0.006, where decrease of N_2O fluxes might have been expected due to N_2O consumption producing N_2, the N_2O fluxes increased rapidly and then steadily declined, 2 days and 6-10 days after urine application, respectively (Figure 79). The two day lag for the onset of N_2O fluxes may have resulted from soil microbiology adapting to urine deposition and the subsequent development of substrate for N_2O producing mechanisms and the fact a heavy rainfall event would have impeded N_2O fluxes on the second day after urine application. Petersen *et al*. (2004) and Harrison-Kirk *et al*. (2015) also found an inhibitory effect from urea and urine applied, respectively, on both nitrification and denitrification in the first 3 days following the application. Given that soil inorganic-N is dominated by NH_4^+-N in

the first week following urine deposition (Clough *et al.* 2009), as was the case in this study, and the fact that N_2O fluxes did not increase in the control soils, the rapid increase in the N_2O flux under urine must be related to N_2O production via nitrification and/or nitrifier-denitrification mechanisms, the latter occurring under hypoxic conditions. The ruminant urine patch is not a niche favoured by ammonia oxidising archaea (AOA) and they cannot perform nitrifier denitrification but ammonia oxidising bacteria (AOB) are promoted in urine patches and can perform nitrifier denitrification (Di *et al.* 2009; Stein 2019). Hence, the N_2O fluxes were most likely the result of AOB initiating nitrification. The AOB require O_2 for the first step of nitrification, the oxidation of ammonia to hydroxylamine. This indicates, given the anaerobic conditions of the bulk soil, and the fact soil diffusivity was so low, that N_2O production and its release was likely occurring at or near the soil surface, where O_2 supply could still exceed O_2 demand, and where N_2O diffusion from the soil could occur prior to being reduced to N_2. Supporting the occurrence of nitrification was the relatively small increase in soil NO_3^--N by day 6 (Table 8).

Nitrite (NO_2-N), a key precursor of nitrifier denitrification induced N_2O fluxes, has been shown to elevate N_2O emissions (Venterea *et al.* 2015). High ammonia concentrations following urine deposition can inhibit NO_2-N oxidation elevating NO_2-N. The low D_p/D_o values indicate that diffusion of ammonia out of the soil would have been relatively slow, potentially prolonging the inhibition of NO_2-N oxidation. Hence nitrification induced NO_2-N dynamics may have also been responsible for the increase in N_2O fluxes. A decline in the net N_2O production rate occurs when N_2O consumption exceeds production. Consumption of N_2O occurs when soil microbes containing the nosZ gene reduce N_2O to N_2. These microbes may be complete denitrifiers, containing nosZ clade I, or they may be organisms containing nosZ clade II where over half of these are non-denitrifying organisms (Hallin *et al.* 2018). Thus the decline in the N_2O flux after day six was due to either a decrease in the N_2O production rate, a

change in N_2O production mechanisms, enhanced consumption of N_2O, or a combination of these. While the D_p/D_o values indicate that the bulk soil was anaerobic until 11 days after urine application, and by day 6 soil NO_3^--N was higher under urine than under pre-urine conditions, favouring denitrification, the consumption of N_2O by denitrifiers at the surface of the soil could not have happened with oxygen present. This further implies it was a decline in NO_2-N concentrations, and associated N_2O production via nitrifier denitrification, that caused the decreased N_2O flux at this time.

After 13 days the maximum N_2O flux occurred (29th Nov). This occurred after smaller rainfall events (~ 5-10 mm, 27-28th Nov.) that caused relatively little change in WFPS. Instead the maximum N_2O flux aligned with D_p/D_o values close to 0.006. Balaine *et al.* (2013) showed peak N_2O fluxes occurred following soil drainage when a soil's air-entry point was reached. Effectively, when the air-entry point is reached a sufficient number of soil pores have drained to facilitate both oxygen entry into the soil, inhibiting N_2O reductase, and the diffusion of entrapped N_2O from the soil.

After commencing standard irrigation, every three days, relatively small shifts in WFPS occurred. But when WFPS data were used to calculate D_p/D_o there were relatively greater shifts in D_p/D_o due to the value of D_p/D_o being an exponential function of air-filled porosity. The standard irrigation regime maintained a lower D_p/D_o value than in the optimised irrigation treatment, with conditions more favourable for N_2O generation via denitrification (close to 0.006) at a time when NO_3^--N substrate was prevalent in the urine patch inorganic-N cycle. As a consequence elevated N_2O fluxes occurred under standard irrigation (1st – 8th December) when compared with the optimised irrigation. At this time the optimised irrigation had not been triggered, resulting in higher D_p/D_o and lower N_2O fluxes as a result. Consequently, the rainfall event on the 5th of December resulted in a near 5-fold lower N_2O flux on the 6th December in the optimised irrigation treatment as a result. When optimised irrigation was triggered the

application of 12 mm of water did not promote the same N_2O flux as seen under earlier standard irrigation events. However, even the standard irrigation treatment had a relatively low N_2O flux at this time because of the prior evapotranspiration loss of soil moisture and so D_p/D_o did not drop to a value required for significant denitrification to occur.

Emission factors under the urine treatments were relatively small but within the order of magnitude expected for pasture urine patch emissions (IPCC 2007, Saggar *et al.* 2015). Further extension of the experimental period with additional irrigation events would have resulted in further N_2O fluxes and an increase in the EF provided NO_3^--N did not leach with further irrigation. Cumulative fluxes under urine after the commencement of irrigation differed due to irrigation treatment at P = 0.09 but it's likely that this difference would have become more significant if the experiment had been able to proceed longer. The nitrate in the irrigation water (7.11 mg NO_3^--N L^{-1}), may explain higher N_2O emissions from the non-urine treatment under standard irrigation. The N_2O emission changes between standard and optimised irrigation without urine occurred during the irrigation phase (Figure 79). While 62 g N ha^{-1} is not huge – over an irrigation season, this could potentially be significant.

In both irrigation treatments with urine, the water content in the soil remained above the TP leading to a similar yield at the end of the experiment. Supporting the similarity in the dry biomass yield was the soil NH_4^+-N and NO_3^--N concentrations at the end of the experiment, not significantly different for optimised and standard irrigation with urine. N availability is a strong determinant of plant growth and crop productivity. Consequently, logic suggests that significant lower yields would be observed in the non-urine treatment due to a lower NO_3^--N concentration and has been confirmed by our results.

Mumford *et al.* (2019) demonstrated that irrigation management, based on predictions of evapotranspiration, could effectively be used to reduce N_2O emissions from fertilised subtropical pastures. However, Mumford *et al.* (2019) also highlighted the need to prevent

excessive drying of the soil profile between irrigation events after observing that repeated 15 day intervals between irrigation events increased N_2O emissions. This was attributed to excessive drying creating a Birch effect (Birch 1958). Such an effect enhances N_2O production following rewetting due to previously protected intra-aggregate organic matter being released, following aggregate degradation, and microbial senescence (Bottner 1985; Denef *et al.* 2001). Hence, the extent of the Birch effect has been hypothesised to be regulated by the soil's structure and the history of a soil's physical disturbance (Schimel 2018). Soil D_p/D_o can be used to gauge the extent of soil gas diffusion both within (intra-aggregate) and between (inter-aggregate) aggregates (Resurreccion *et al.* 2008; Jayarathne *et al.* 2020a). Potentially, prolonged periods of intra-aggregate diffusion could indicate greater availability of organic matter upon rewetting and D_p/D_o could be explored as a predictor of the Birch effect magnitude. The values of D_p/D_o used as the trigger point for optimal irrigation in the current study were not as high as those previously ascribed to intra-aggregate gas diffusion (Resurreccion *et al.* 2008; Jayarathne *et al.* 2020b) and no enhanced N_2O flux was observed following optimised irrigation. But further investigation is needed to examine this in relation to using D_p/D_o as a tool to trigger irrigation.

VI.5.2 Field trial 2

Daily dry matter production in all treatments was under the typical summer growth rates for a fertilised irrigated pasture at Lincoln University (67 kg DM ha^{-1} day^{-1}, Dairy NZ 2020). This indicates that the conditions were not as conducive for pasture growth. The whole experimental period was particularly dry with only 20 mm of rain, however WFPS values remained above PWP but 20% under FC, on average, for all treatments which may explain the growth rate restriction. Most surprisingly, there was no difference between the control chambers (without urine) and the chambers receiving urine despite significantly lower values of inorganic-N in

the non urine treatment soil. This is in direct contrast with many studies suggesting that in urine patches, pasture yield and annual N uptake are dramatically increased (e.g. Moir *et al*., 2016). This suggests that the inorganic-N concentration in the non urine treatment was not a limiting factor. Further evidence that supports this hypothesis is the significant peak of N_2O in the non urine treatment at the end of the experiment (69.2 ± 32 g N ha^{-1} day^{-1}). At this time, the D_p/D_o value for the control was lower than 0.006 suggesting maximum N_2O emission by denitrification (Balaine *et al.* 2013; Rousset *et al.* 2020). The DOC concentration was also suitable for denitrification with concentration > 40 mg C kg^{-1} soil (Ryden 1983; Beauchamp *et al.* 1989).

As observed for field trial 1, the standard irrigation regime maintained D_p/D_o at lower values than in the optimised irrigation treatment. However, most of those D_p/D_o values are ≥ 0.01. Previously, Chamindu Deepagoda *et al.* (2020) showed, using intact soil cores, that D_p/D_o above 0.005-0.01 could improve soil aeration and minimise N_2O emissions. This explains the low EF observed during the field trial 2 for the standard irrigation with urine. Similar conditions are observed in the optimised treatment with $D_p/D_o \geq 0.01$ and ≥ 0.02 after the 3rd of March (Figure 78) and well correlated with low N_2O emissions. Given that soil inorganic-N is dominated by NH_4^+-N in the first week (Table 9) following urine deposition (Clough *et al*. 2009), as for field trail 1 (Table 8), and the fact that N_2O fluxes did not increase in the control soils, the rapid increase in the N_2O flux during the day of urine application must be related to N_2O production via nitrification and/or nitrifier-denitrification mechanisms, the latter occurring under hypoxic conditions. Denitrification utilising existing NO_3^--N and organic C (Table 9) could have also taken place in the soil. Bateman and Baggs (2005) also reported that N_2O emission from nitrification occurs when the soil is between 35 and 60% WFPS as observed after every optimised irrigation event at the beginning of the experiment.

The cumulative N_2O flux in the standard irrigation with urine was higher (P = 0.09) than the cumulative N_2O flux in the optimised irrigation. However, this intensity variation was also caused by the major rain event on the 22nd of February 2020, which brought the D_p/D_o to 0.006 in the standard irrigation with urine. The maximum N_2O fluxes aligned once more with D_p/D_o values close to 0.006, but despite differences in cumulative losses, much of it was not directly related to individual irrigation events but rather to a treatment legacy amplified during rainfall period as observed by Mumford *et al*. (2019).

VI.5.3 Conclusion

This was the first study to examine soil gas diffusivity in conjunction with varying irrigation treatments and N_2O fluxes from management urine patches. Despite the short irrigation period of these two field experiment the significant changes in D_p/D_o resulting from rainfall or irrigation events demonstrate that D_p/D_o is a sensitive gauge of soil aeration that has the potential to be used in a decision framework that optimises irrigation to reduce N_2O while maintaining a good pasture production. This study demonstrates the need to adjust irrigation cycles to prevent the soil gas diffusion declining to ≤ 0.006, in the event of subsequent rain. Furthermore, measures of D_p/D_o in this experiment have highlighted the need to examine the N_2O formation pathway(s) with respect to soil depth, over time, in order to better understand the implications for N_2O mitigation via irrigation management. Further consideration should also be given to understand how irrigation interval influence the Birch effect and the interaction with N_2O production.

Chapter VII Conclusion

The purpose of this last chapter is to provide a summary of the findings relating to irrigation systems and pasture soils that links to N_2O emissions, with an emphasis on soil relative gas diffusivity being used as a management tool and on how soil physical conditions impact upon this and N_2O emissions.

VII.1 The current problematic

One of the major challenges of sustainable ecosystem management is to mitigate the negative effects of global climate change caused by steadily increasing atmospheric GHG emissions. While concerns about human-induced effects on the Earth's climate have mainly concentrated on CO_2 and CH_4, reducing anthropogenic N_2O flux, mainly of agricultural origin, also represents an opportunity for substantial mitigation. In New Zealand, agricultural N_2O emissions contributed almost 94% of the total N_2O emissions in 2017 (Ministry of the Environment New Zealand 2019) and these were coming mainly from adding N to the soil, e.g., through manure, urine or fertiliser. Pasture soils are inherently complex in relation to N_2O emissions due to the interaction of a multitude of soil physical, chemical, and microbiological functions and processes (Clough *et al*. 2020).

Oxygen supply has been identified as a key determinant of the biological denitrification and nitrification pathways that produce and/or also consume N_2O in soils (Wrage-Mönnig *et al.* 2018). Both pathways respond differently to soil water status, largely due to the effect of soil water content on O_2 diffusion, this is why most studies have used water-filled pore space (WFPS) as a gauge to determine and predict N_2O fluxes from soils. However, even though Farquharson and Baldock (2008) have clearly justified why WFPS should not be used to predict

N_2O from soils that vary in soil ρ_b, studies using other measures such as relative gas diffusivity (D_p/D_o) as an alternative predictor for N_2O emissions are still limited. Notably, D_p/D_o is a function of porous media characteristics facilitating diffusive gas migration, namely the air-filled content, and the tortuosity of the functional gaseous pore network. Because the volumetric water content and the volumetric air content share the soil total pore space they complement each other while D_p/D_o varies markedly in response to soil water dynamics and has the advantage of accounting for soil characteristic such as soil compaction (Balaine *et al*. 2013) and aggregation (Jayarathne *et al*. 2020a).

Irrigation, which is to be found in 20% of the total agricultural land area and which contributes to 40% of the total food production (FAO 2014), often represents a large and sudden increase in the amount of water which impacts the soil structure and moisture content and consequently D_p/D_o. Mumford *et al.* (2019) in their study comparing different irrigation frequency (low-15 day interval, medium-10 day and high-4 day) reported significant differences in N_2O emissions from fertilised agroecosystems. However, they suggested that much of the variance between treatments was more specifically attributed to the treatment legacy during rainfall events and linked to the Birch effect, suggesting a focus on the wetting and drying cycles.

To develop a solution that neither induces the transfer of N pollution through leachate, nor decreases agricultural production, I specifically:

- targeted an improved understanding of how soil physics (bulk density, soil type and drainage) affects the N_2O emissions under controlled lab conditions and particularly in relation to D_p/D_o (Chapter III and IV);
- investigated the significance of soil wetting and draining cycles on N_2O emissions (Chapter IV and V) and;

- tested an optimal irrigation practice based on D_p/D_o thresholds to minimise N_2O losses from intensely managed pastures (Chapter V and VI).

VII.2 Summary of findings and conclusion

The results from this study strengthen arguments presented in previous studies and bring some new clarifications and research questions with respect to N_2O emissions from intensively managed pasture soils:

- The first focus of this study was to strengthen knowledge around the role of D_p/D_o as a key soil physical variable that describes soil N_2O emissions and to compare it against WFPS across different soil types and compaction factors. This was undertaken in Chapter III and IV, using repacked soil cores, to reduce the variability, and under laboratory conditions that were optimal for the denitrification process to occur with a high concentration of substrates (C and NO_3^-). Balaine *et al.* (2013) showed peak N_2O emissions occurred across a relatively wide range of WFPS and volumetric water content but maximum N_2O emissions occurred at a D_p/D_o value of 0.006 that was independent of soil ρ_b in a repacked Templeton silt loam soil. I expanded upon this assessing different soil types. As expected N_2O-N increased with the decrease in D_p/D_o. While WFPS increased significantly with increases in soil ρ_b and soil water content. The results confirmed that D_p/D_o can be used as a useful measure to predict soil physical conditions where N_2O emissions occurs and confirm recent observations of a critical diffusivity window under 0.02 and close to 0.006, which needs to be avoided when managing pastures if excessive N_2O emissions are to be avoided.

- The results from Chapter III and Chapter IV revealed a decline in N_2O fluxes for D_p/D_o values lower than 0.006 (Figure 30, Figure 41), the causes of which can be explained, by either N_2O entrapped in the soil cores or reduction of N_2O to N_2. Activity of N_2O reductase often lags behind the activity of the other reductases (Zheng and Doskey 2015). Laboratory soil incubations have revealed that the activity of N_2O reductase was initially low but increased in 12–40 h in response to prolonged incubation under anaerobic conditions (Zheng and Doskey 2015). This could also explain the decrease in the N_2O emissions after the peak in day 3 (Figure 41) for $D_p/D_o < 0.006$. However, this hypothesis could not be confirmed due to the low N_2 fluxes measured during the experiment (**Erreur ! Source du renvoi introuvable.**).
- Low N_2 fluxes observed may be explained by the acidic soil pH measured in the experiment. Čuhel *et al.* (2010) showed that for acidic pH (average 5.52), the $N_2O/(N_2O + N_2)$ ratio increased due to changes in the total denitrification activity with acidic pH being unfavourable for N_2O reduction into N_2. Soil pH has also been observed to decrease during the draining phase (Figure 23). In addition, the high soil NO_3^- concentration did not favour N_2O reduction. There was also a clear dilution of the ^{15}N enriched nitrate pools due to the relatively rapid dilution of the ^{15}N pool by organic-N mineralisation which also did not favour N_2 flux detection.
- Soil texture and structure were shown to have an effect on drainage rate as observed in Chapter III and Chapter IV which in turn directly affected D_p/D_o. A recent study of Jayarathne *et al*. (2020b) showed that the peak N_2O flux varied with D_p/D_o dynamics that were in turn a function of inter-aggregate and intra aggregates pore drainage. In this PhD, the loss of macropores (finer texture e.g. Wakanui soil vs Otorohanga soil) is related to an increase in micropores and longer periods of saturation due to a lower

drainage rate which in turn decreases D_p/D_o (< 0.02) stimulating higher N_2O production via denitrification.

- The importance of wetting and draining cycles as a major control of N_2O emissions in irrigated pastures was also highlighted. Irrigation events clearly affect D_p/D_o dynamics and N_2O fluxes. Nitrous oxide peaks were observed after irrigation events. In Chapter V (lysimeter experiment) the optimised irrigation resulted in higher cumulative N_2O emissions. Optimised irrigation minimised soil anaerobic conditions when compared to standard irrigation, identified through higher soil D_p/D_o, which, in turn, increased plant growth and N uptake. Following optimised irrigation events, mineralisation of C due to the "Birch effect" is enhanced (Birch 1958; Bloem *et al.* 1992; Franzluebbers *et al.* 2000) due to rewetting after extended drying periods (reduced in the standard irrigation), resulting in increased substrate for microbial respiration that in turn promotes hypoxia and N_2O generating processes.
- Chapter VI, field experiments, showed a successful reduction of the cumulative N_2O emissions in the optimised irrigation treatment compared to the standard irrigation with no significant impact being made on the growth rate. This study demonstrates the need to adjust irrigation cycles to prevent the soil gas diffusion declining to ≤ 0.006, in the event of subsequent rain.

In recent years, knowledge of processes producing and the occurrence of N_2O fluxes has advanced tremendously. New tools and techniques have allowed studies and thus increased understanding on the microbial processes involved in the production along with the different soil physical characteristics and conditions affecting such fluxes. However, new approaches for up-scaling processes and fluxes from microbial scale to soil micro-sites, fields, entire landscapes and regions are still required, despite the recent progress. Soil relative gas diffusivity appears through this study to be a relevant parameter to predict N_2O

emissions and future implementation into models is conceivable. Moreover, this study demonstrates the need to adjust irrigation cycles to prevent excessive drying of the soil profile between rainfall events while also keeping $D_p/D_o > 0.02$. Management practices which reduce extreme fluctuations in soil water content may consequently reduce N_2O and total denitrification losses. However, irrigation should not be the only concern for N_2O mitigation. This study shows once more that N_2O emissions are enhanced by the urine application or urea application. Consequently, future farming practices should be a chain of mitigation solutions aiming to prevent sub-optimal conditions for both nitrifiers and denitrifiers.

VII.3 The next steps to improving our knowledge on N_2O production in soils and future direction for irrigation management

The work described in this thesis has also identified future opportunities for research, from simple repetitions of experiments to the use of D_p/D_o in future modelling applications for farmers' irrigation systems.

Measurements of D_p/D_o are relatively time consuming but current predictive models are adequate for generating D_p/D_o values that align to and explain N_2O fluxes. However, further consideration should be given to understanding what soil depth should be targeted in relation to modelling D_p/D_o, with respect to minimising N_2O emissions resulting from irrigation. This is because pasture rooting networks which are known to influence N_2O emissions through root exudates (e.g. Langarica-Fuentes *et al*. 2018) and autotrophic respiration can be found at different depths depending on soil types and plant species, and because N_2O reduction to N_2

can occur in the soil profile (e.g. Klefoth *et al*. 2014). The soil surface N_2O flux may be produced from deeper soil layers and transported upward and/or be produced in the topsoil. This is all the more interesting that the production of N_2O flux at deeper depth could enhance its reduction into N_2. Future studies including measures of N_2 and microbial dynamics will be required to evaluate the denitrification losses, although measuring N_2 emissions in situ is always challenging due to the high background level of atmospheric N_2.

Plant growth modelling studies with varying soil moisture conditions (irrigation) are required where soil moistures are modelled to optimise both plant growth and aerobic soil conditions (D_p/D_o values > 0.02). Models should be generating D_p/D_o values to better understand soil O_2 conditions and associated biogeochemistry. Such modelled D_p/D_o data immediately informs of the aerobic/anaerobic status of a soil zone and intrinsically tells us what the likelihood of N_2O formation, emission, consumption potential is regardless of soil bulk density. WFPS does not do this.

This study, and recently published work (Mumford *et al*. 2019), has also found that the 'Birch' effect may potentially exacerbate efforts to mitigate N_2O emissions through reduced irrigation frequency. Explanations given for the Birch effect include disruption of soil aggregates due to drying and the enhanced bioavailability of intra-aggregate carbon upon soil rewetting. Future work should look at irrigation frequency and soil respiration (Birch effect) with respect to both intra-aggregate and inter-aggregate D_p/D_o, both of which can be modelled (Resurreccion *et al.* 2008; Jayarathne *et al.* 2020a). It may be that intra-aggegrate disruption can be avoided through irrigation management which would minimise the Birch effect while also helping to minimise N_2O emissions through reducing the bioavailable C supply for denitrifiers. In the studies performed in this thesis there was no way to determine, based on prior research, the soil D_p/D_o value that would trigger irrigation: instead irrigation was triggered based on the plant's need, when the soil was at 50% PAW and the associated D_p/D_o value was then determined (ca. 0.033

in the field studies). But modelled D_p/D_o was used as a measure to prevent overwatering with the aim of keeping soil at $D_p/D_o > 0.006$ and thus minimise N_2O emissions. In principle, this worked, but the 'Birch effect' was a confounding factor that emerged (e.g. Chapter V - lysimeter experiment) and thus it raises the question of what the irrigation trigger should be in terms of D_p/D_o - which given that D_p/D_o is a variable that accurately describes soil's oxygen status in terms of inter and aggregate boundaries (Jayarathne *et al.* 2020a), and thus the Birch effect, provides a rationale to explore this further using modelling and laboratory studies.

Nitrous oxide emissions were highly episodic in response to the irrigation events and the changes in D_p/D_o. Automated gas sampling chambers provided the necessary high temporal frequency to capture those emission events in real time, ensuring the development of accurate N_2O inventories. This technique could be extended for longer periods and monitor pasture fields over few years instead of over few months. This would allow considering the seasonal effect (more frequent rain events in spring and autumn) but also could also potentially combine farm management techniques which not only influence the soil O_2 supply (irrigation) but also lead to re-structuring of pores, thus affecting the total porosity and pore structure (e.g. tillage and soil compaction).

Systemic changes to current agricultural practices will not occur by themselves. The reduction of agricultural N_2O emissions can only be achieved if there is first a transfer of knowledge from the research outputs into the irrigation practices on the coalface. It is possible to reduce energy costs while improving water use efficiency through comprehensive irrigation management; in this study energy cost seems achievable without significant yield reduction. An economic analysis in terms of water saving and dry matter production should be included in future researches on optimising irrigation based on D_p/D_o. Where necessary, farmers could adopt modifications to their current practices which align with the scientific recommendations made in this research.

Appendices

Appendix 1: Data distribution graphs showing the general distribution of N_2O fluxes over gas diffusivity (A) and the density estimates of D_p/D_o for the 4 different soil types (B) and bulk densities (C) in the second lab experiment (Chapter III). The dashed lines represent the 0.006 threshold (Balaine et al. 2013) and 0.02 threshold (Stepniewski 1981).

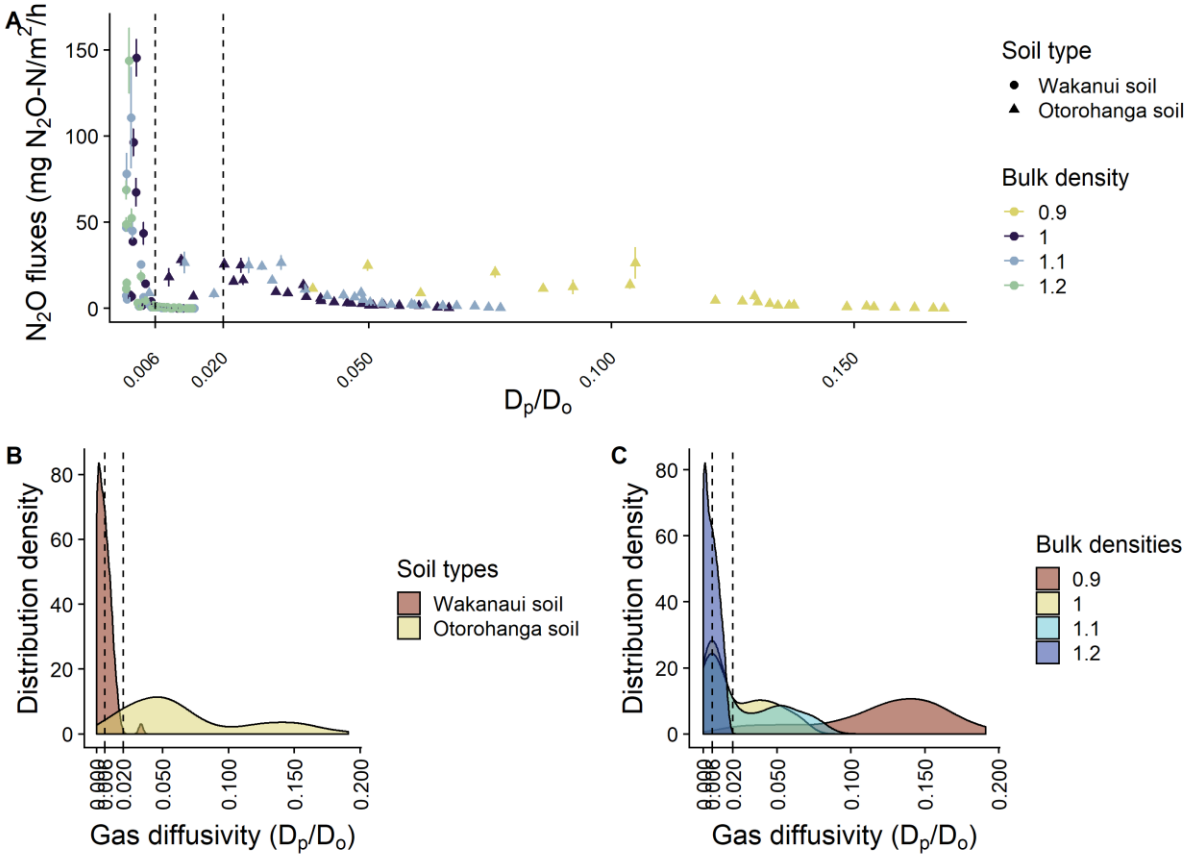

Appendix 2: Data distribution graphs showing the general distribution of N_2O fluxes over WFPS (A) and the density estimates of the WFPS for the 4 different soil types (B) and bulk densities (C) in the second lab experiment (Chapter III).

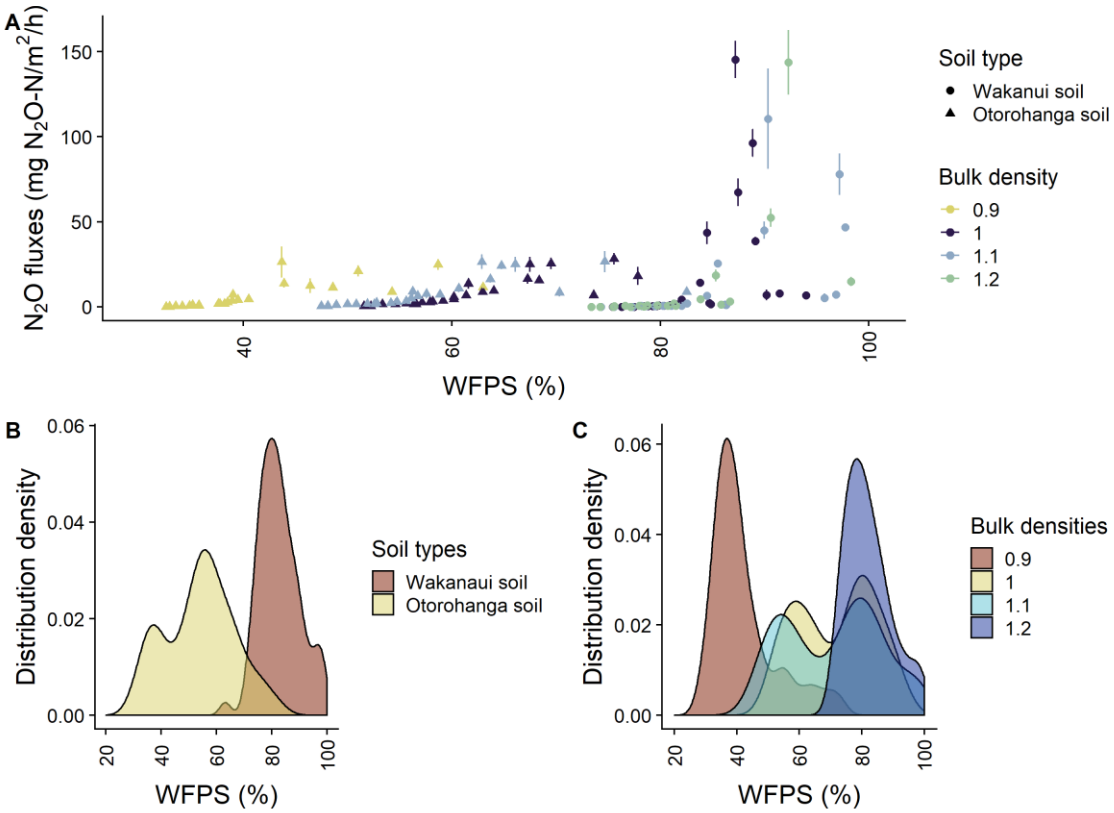

Appendix 3: Hourly N_2O emissions (µg N m^{-2} h^{-1}) from the 11/02/2020 to the 25/03/2020. The red bar represents the urine application, blue triangles and yellow horizontal lines denote the standard (STD) and optimised (OPT) irrigation applications, respectively. Error bars = s.e.m, n=4. Treatment with urine applied (on) or no urine applied (off).

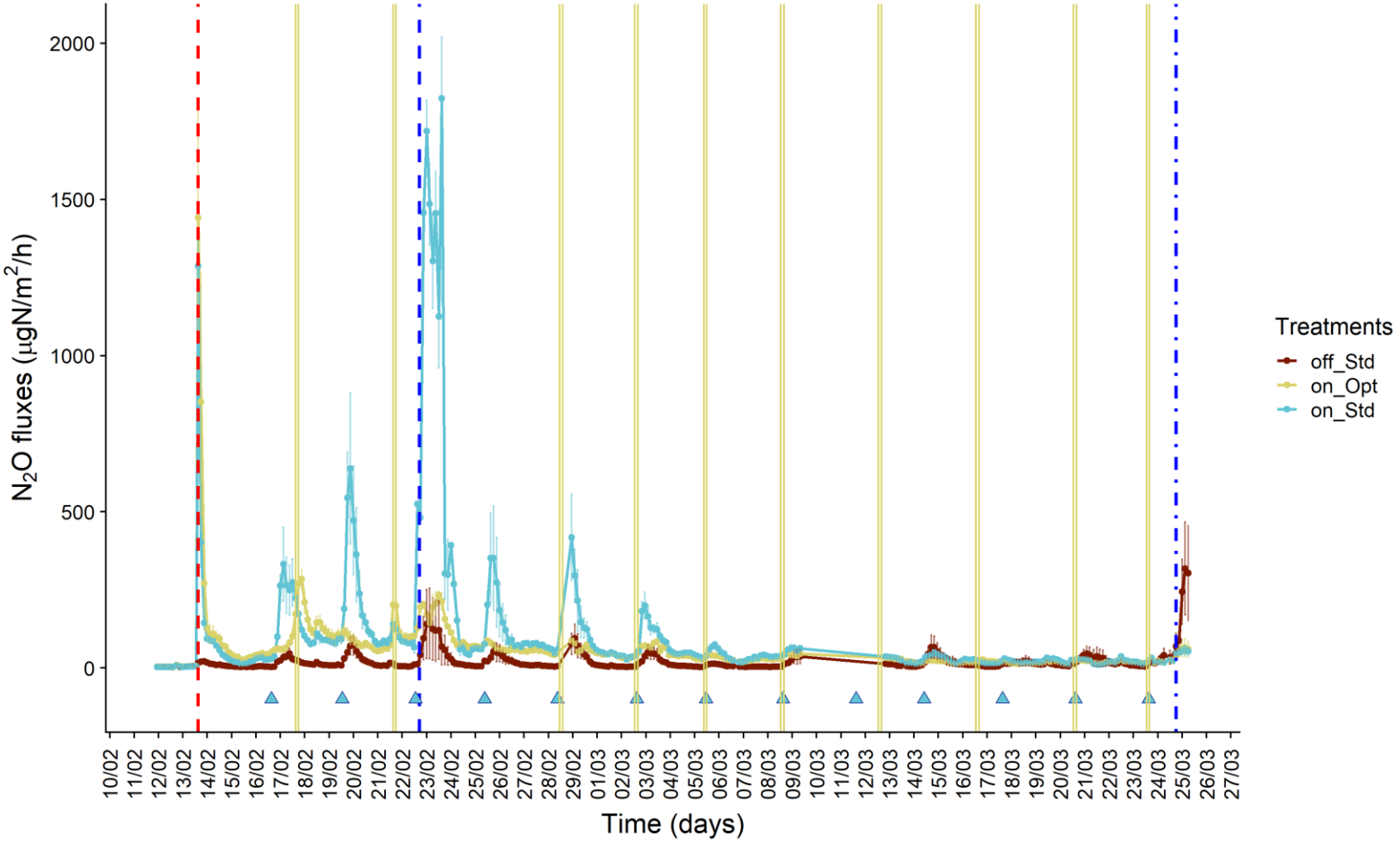

Appendix 4: Explained and explanatory variables used in each chapter for the statistical tests.

Chapters	Explained variables	Explanatory variables	Chapters	Explained variables	Explanatory variables
Chapter III	pH DOC NO_3^- NH_4^+ WFPS D_p/D_o N_2O-N fluxes	Bulk densitty (4 levels) Matric potential (9 levels) Soil type (4 level)	Chapter V	pH DOC NO_3^- NH_4^+ WFPS D_p/D_o N_2O-N fluxes Cumulative N_2O fluxes Cumulative dry biomass ^{15}N recovery Root biomass	Treatments (4 levels) Only urine (2 levels) Only irrigation (2 levels) Days
Chapter IV	pH DOC NO_3^- NH_4^+ WFPS D_p/D_o N_2O-N fluxes Cumulative N_2O fluxes N_2 fluxes	Bulk densitty (4 levels) Days Soil type (2 level)	Chapter V	DOC NO_3^- NH_4^+ WFPS D_p/D_o N_2O-N fluxes Cumulative N_2O fluxes Cumulative dry biomass	Treatments (depending on trial*) Only urine (*) Only irrigation (*) Days

References

Abed RMM, Lam P, de Beer D, Stief P (2013) High rates of denitrification and nitrous oxide emission in arid biological soil crusts from the Sultanate of Oman. *The ISME Journal* **7**, 1862–1875. doi:10.1038/ismej.2013.55.

Allen RG (2006) Evaporation Modeling: Potential. 'Encyclopedia of Hydrological Sciences'. (American Cancer Society) doi:10.1002/0470848944.hsa044.

Amatya IM, Kansakar BR, Tare V, Fiksdal L (2011) Role of pH on biological Nitrification Process. *Journal of the Institute of Engineering* **8**, 119–125. doi:10.3126/jie.v8i1-2.5102.

Andersen AJ, Petersen SO (2009) Effects of C and N availability and soil-water potential interactions on N_2O evolution and PLFA composition. *Soil Biology and Biochemistry* **41**, 1726–1733. doi:10.1016/j.soilbio.2009.06.001.

Austin AT, Yahdjian L, Stark JM, Belnap J, Porporato A, Norton U, Ravetta DA, Schaeffer SM (2004) Water pulses and biogeochemical cycles in arid and semiarid ecosystems. *Oecologia* **141**, 221–235. doi:10.1007/s00442-004-1519-1.

Baggs L, Rees B, Smith K, Vinten A (2006) Nitrous oxide emission from soils after incorporating crop residues. *Soil Use and Management* **16**, 82–87. doi:10.1111/j.1475-2743.2000.tb00179.x.

Balaine N, Clough TJ, Beare MH, Thomas SM, Meenken ED (2016) Soil Gas Diffusivity Controls N O and N Emissions and their Ratio. *Soil Science Society of America Journal* **80**, 529. doi:10.2136/sssaj2015.09.0350.

Balaine N, Clough TJ, Beare MH, Thomas SM, Meenken ED, Ross JG (2013) Changes in Relative Gas Diffusivity Explain Soil Nitrous Oxide Flux Dynamics. *Soil Science Society of America Journal* **77**, 1496–1505. doi:10.2136/sssaj2013.04.0141.

Ball BC (1981) Modelling of Soil Pores as Tubes Using Gas Permeabilities, Gas Diffusivities and Water Release. *Journal of Soil Science* **32**, 465–481. doi:10.1111/j.1365-2389.1981.tb01723.x.

Baral BR, Kuyper TW, Van Groenigen JW (2014) Liebig's law of the minimum applied to a greenhouse gas: alleviation of P-limitation reduces soil N_2O emission. Plant and Soil **374**, 539–548. doi:10.1007/s11104-013-1913-8.

Barton L, Kiese R, Gatter D, Butterbach-Bahl K, Buck R, Hinz C, Murphy DV (2008) Nitrous oxide emissions from a cropped soil in a semi-arid climate. *Global Change Biology* **14**, 177–192. doi:10.1111/j.1365-2486.2007.01474.x.

Barton L, McLay CDA, Schipper LA, Smith CT (1999) Annual denitrification rates in agricultural and forest soils: a review. *Soil Research* **37**, 1073–1094. doi:10.1071/sr99009.

Bateman E, Baggs L (2005) Contributions of nitrification and denitrification to N_2O emissions from soils at different water-filled pore space. *Biology and Fertility of Soils* **41**, 379–388. doi:10.1007/s00374-005-0858-3.

Beauchamp EG, Trevors JT, Paul JW (1989) Carbon Sources for Bacterial Denitrification. 'Soil Restoration'. (Eds R Lal, BA Stewart) Advances in Soil Science. 113–142. (Springer New York: New York, NY) doi:10.1007/978-1-4613-8847-0_3.

Bergaust L, Mao Y, Bakken LR, Frostegård Å (2010) Denitrification Response Patterns during the Transition to Anoxic Respiration and Posttranscriptional Effects of Suboptimal pH on Nitrogen Oxide Reductase in Paracoccus denitrificans. *Applied and Environmental Microbiology* **76**, 6387–6396. doi:10.1128/AEM.00608-10.

Beven K, Germann P (1982) Macropores and water flow in soils. *Water Resources Research* **18**, 1311–1325. doi:10.1029/WR018i005p01311.

Bhandral R, Bolan NS, Saggar S, Hedley MJ (2007) Nitrogen transformation and nitrous oxide emissions from various types of farm effluents. *Nutrient Cycling in Agroecosystems* **79**, 193–208. doi:10.1007/s10705-007-9107-5.

Birch HF (1958) The effect of soil drying on humus decomposition and nitrogen availability. *Plant and Soil* **10**, 9–31. doi:10.1007/BF01343734.

Birendra KC, Mohssen M, Chau HW, Curtis A, Cuenca R, Bright J, Srinivasan M, Hu W, Cameron K (2018) Impact of Rotational Grazing Systems on the Pasture Crop Coefficient for Irrigation Scheduling. *Irrigation and Drainage* **67**, 441–453. doi:10.1002/ird.2210.

Blackmore LC, Searle PL, Daly BK (1987) Methods for chemical analysis of soils. https://digitallibrary.landcareresearch.co.nz/digital/collection/p20022coll2/id/155.

Bloem J, de Ruiter PC, Koopman GJ, Lebbink G, Brussaard L (1992) Microbial numbers and activity in dried and rewetted arable soil under integrated and conventional management. *Soil Biology and Biochemistry* **24**, 655–665. doi:10.1016/0038-0717(92)90044-X.

Bottner P (1985) Response of microbial biomass to alternate moist and dry conditions in a soil incubated with 14C- and 15N-labelled plant material. *Soil Biology and Biochemistry* **17**, 329–337. doi:10.1016/0038-0717(85)90070-7.

Boyd CE (1995) Soil Organic Matter, Anaerobic Respiration, and Oxidation—Reduction. 'Bottom Soils, Sediment, and Pond Aquaculture'. (Ed CE Boyd) 194–218. (Springer US: Boston, MA) doi:10.1007/978-1-4615-1785-6_6.

Boyer EW, Alexander RB, Parton WJ, Li C, Butterbach-Bahl K, Donner SD, Skaggs RW, Grosso SJD (2006) Modeling Denitrification in Terrestrial and Aquatic Ecosystems at Regional Scales. *Ecological Applications* **16**, 2123–2142. doi:10.1890/1051-0761(2006)016[2123:MDITAA]2.0.CO;2.

Brady N, Weil R (2013) 'Elements of the Nature and Properties of Soils: Pearson New International Edition.' *Pearson Education Inc., New Delhi*

Breland TA, Hansen S (1996) Nitrogen mineralization and microbial biomass as affected by soil compaction. *Soil biology and biochemistry* **9**. 655-653. doi:10.1016/0038-0717(95)00154-9

Breuillin-Sessoms F, Venterea RT, Sadowsky MJ, Coulter JA, Clough TJ, Wang P (2017) Nitrification gene ratio and free ammonia explain nitrite and nitrous oxide production in urea-amended soils. *Soil Biology and Biochemistry* **111**, 143–153. doi:10.1016/j.soilbio.2017.04.007.

Bristow AW, Whitehead DC, Cockburn JE (1992) Nitrogenous constituents in the urine of cattle, sheep and goats. *Journal of the Science of Food and Agriculture* **59**, 387–394. doi:10.1002/jsfa.2740590316.

Bryant RH, Snow VO, Shorten PR, Welten BG (2020) Can alternative forages substantially reduce N leaching? findings from a review and associated modelling. *New Zealand Journal of Agricultural Research* **63**, 3–28. doi:10.1080/00288233.2019.1680395.

Buckingham, E (1904) Contributions to our knowledge of the aeration of soils, vol. 25. United States Dept of Agriculture, Bureau of Soil Bulletin, Washington, DC. Retrieved from http://hdl.handle.net/2027/uc1.b3044430.

Buckthought LE, Clough TJ, Cameron KC, Di HJ, Shepherd MA (2015) Fertiliser and seasonal urine effects on N_2O emissions from the urine-fertiliser interface of a grazed pasture. *New Zealand Journal of Agricultural Research* **58**, 311–324. doi:10.1080/00288233.2015.1031405.

Buckthought LE, Clough TJ, Cameron KC, Di HJ, Shepherd MA (2016) Plant N uptake in the periphery of a bovine urine patch: determining the 'effective area'. *New Zealand Journal of Agricultural Research* **59**, 122–140. doi:10.1080/00288233.2015.1134589.

Butterbach-Bahl K, Baggs EM, Dannenmann M, Kiese R, Zechmeister-Boltenstern S (2013) Nitrous oxide emissions from soils: how well do we understand the processes and their controls? *Philosophical Transactions of the Royal Society B: Biological Sciences* **368**, 20130122. doi:10.1098/rstb.2013.0122.

Butterbach-Bahl K, Dannenmann M (2011) Denitrification and associated soil N_2O emissions due to agricultural activities in a changing climate. *Current Opinion in Environmental Sustainability* **3**, 389–395. doi:10.1016/j.cosust.2011.08.004.

Cameron KC, Smith NP, McLay CDA, Fraser PM, McPherson RJ, Harrison DF, Harbottle P (1992) Lysimeters Without Edge Flow: An Improved Design and Sampling Procedure. *Soil Science Society of America Journal* **56**, 1625–1628. doi: 10.2136/sssaj1992.03615995005600050048x.

Canion A, Overholt WA, Kostka JE, Huettel M, Lavik G, Kuypers MMM (2014) Temperature response of denitrification and anaerobic ammonium oxidation rates and microbial community structure in Arctic fjord sediments. *Environmental Microbiology* **16**, 3331–3344. doi:10.1111/1462-2920.12593.

Caranto JD, Lancaster KM (2017) Nitric oxide is an obligate bacterial nitrification intermediate produced by hydroxylamine oxidoreductase. *Proceedings of the National Academy of Sciences* **114**, 8217–8222. doi:10.1073/pnas.1704504114.

Caranto JD, Vilbert AC, Lancaster KM (2016) Nitrosomonas europaea cytochrome P460 is a direct link between nitrification and nitrous oxide emission. *Proceedings of the National Academy of Sciences of the United States of America* **113**, 14704–14709. doi:10.1073/pnas.1611051113.

Carlton AJ, Cameron KC, Di HJ, Edwards GR, Clough TJ (2019) Nitrate leaching losses are lower from ryegrass/white clover forages containing plantain than from ryegrass/white clover forages under different irrigation. *New Zealand Journal of Agricultural Research* **62**, 150–172. doi:10.1080/00288233.2018.1461659.

Carlton AJ, Cameron KC, Edwards GR, Di HJ, Clough TJ (2018) Effect of two irrigation rates on nitrate leaching from diverse or standard forages receiving spring deposited urine. *New Zealand Journal of Agricultural Research* **61**, 440–453. doi:10.1080/00288233.2017.1409243.

Cavagnaro TR, Jackson LE, Hristova K, Scow KM (2008) Short-term population dynamics of ammonia oxidizing bacteria in an agricultural soil. *Applied Soil Ecology* **40**, 13–18. doi:10.1016/j.apsoil.2008.02.006.

Chadwick DR, Cardenas LM, Dhanoa MS, Donovan N, Misselbrook T, Williams JR, Thorman RE, McGeough KL, Watson CJ, Bell M, Anthony SG, Rees RM (2018) The contribution of cattle urine and dung to nitrous oxide emissions: Quantification of country specific emission factors and implications for national inventories. *The Science of the Total Environment* **635**, 607–617. doi:10.1016/j.scitotenv.2018.04.152.

Chamindu Deepagoda TKK, Clough TJ, Jayarathne JRRN, Thomas S, Elberling B (2020) Soil-gas diffusivity and soil-moisture effects on N_2O emissions from repacked pasture soils. *Soil Science Society of America Journal* **84**, 371–386. doi:10.1002/saj2.20024.

Chamindu Deepagoda TKK, Jayarathne JRRN, Clough TJ, Thomas S, Elberling B (2019) Soil-Gas Diffusivity and Soil-Moisture effects on N_2O Emissions from Intact Pasture Soils. *Soil Science Society of America Journal* **83**, 1032–1043. doi:10.2136/sssaj2018.10.0405.

Chen R-P, Liu P, Liu X-M, Wang P-F, Kang X (2019) Pore-scale model for estimating the bimodal soil–water characteristic curve and hydraulic conductivity of compacted soils with different initial densities. *Engineering Geology* **260**, doi:10.1016/j.enggeo.2019.105199.

Chen D, Suter HC, Islam A, Edis R (2010) Influence of nitrification inhibitors on nitrification and nitrous oxide (N_2O) emission from a clay loam soil fertilized with urea. *Soil Biology and Biochemistry* **42**, 660–664. doi:10.1016/j.soilbio.2009.12.014.

Cheng L, Judson HG, Bryant RH, Mowat H, Guinot L, Hague H, Taylor S, Edwards GR (2017) The effects of feeding cut plantain and perennial ryegrass-white clover pasture on dairy heifer feed and water intake, apparent nutrient digestibility and nitrogen excretion in urine. *Animal Feed Science and Technology* **229**, 43–46. doi:10.1016/j.anifeedsci.2017.04.023.

Ciais P, Sabine C, Bala G, Bopp L, Brovkin V, Canadell J, Chhabra A, DeFries R, Galloway J, Heimann M, Jones C, Le Quéré C, Myneni RB, Piao S, Thornton PE (2013) Carbon

and Other Biogeochemical Cycles. The Physical Science Basis. Contribution of Working Group I to the Fifth Assessment Report of the Intergovernmental Panel on Climate Change. Cambridge University Press (Cambridge, United Kingdom)

Clough T, Di H, Cameron K, Sherlock R, Metherell A, Clark H, Rys G (2007) Accounting for the utilization of a N_2O mitigation tool in the IPCC inventory methodology for agricultural soils. *Nutrient Cycling in Agroecosystems* **78**, 1–14. doi:10.1007/s10705-006-9069-z.

Clough TJ, Ray JL, Buckthought LE, Calder J, Baird D, O'Callaghan M, Sherlock RR, Condron LM (2009) The mitigation potential of hippuric acid on N_2O emissions from urine patches: An in situ determination of its effect. *Soil Biology and Biochemistry* **41**, 2222–2229. doi:10.1016/j.soilbio.2009.07.032.

Clough TJ, Rochette P, Thomas SM, Pihlatie M, Christiansen JR, Thorman RE (2020) Global Research Alliance N_2O chamber methodology guidelines: Design considerations. *Journal of Environmental Quality* **49**, 1081–1091. doi:10.1002/jeq2.20117.

Clough TJ, Sherlock RR, Cameron KC, Stevens RJ, Laughlin RJ, Müller C (2001) Resolution of the 15N balance enigma? *Soil Research* **39**, 1419–1431. doi:10.1071/sr00092.

Clough TJ, Sherlock RR, Rolston DE (2005) A Review of the Movement and Fate of N_2O in the Subsoil. *Nutrient Cycling in Agroecosystems* **72**, 3–11. doi:10.1007/s10705-004-7349-z.

Colton GQ (1886) 'Anaesthesia, who made and developed this great discovery?' (New York: AG Sherwood & Co) https://issuu.com/idesigninc/docs/s_abvr.

Čuhel J, Šimek M, Laughlin RJ, Bru D, Chèneby D, Watson CJ, Philippot L (2010) Insights into the Effect of Soil pH on N_2O and N_2 Emissions and Denitrifier Community Size and Activity. *Applied and Environmental Microbiology* **76**, 1870–1878. doi:10.1128/AEM.02484-09.

Currie JA (1984) Gas diffusion through soil crumbs: the effects of compaction and wetting. *Journal of Soil Science* **35**, 1–10. doi:10.1111/j.1365-2389.1984.tb00253.x.

Czyż E (2004) Effects of traffic on soil aeration, bulk density and growth of spring barley. *Soil & Tillage Research* **79**, 153–166. doi:10.1016/j.still.2004.07.004.

Daims H, Lebedeva EV, Pjevac P, Han P, Herbold C, Albertsen M, Jehmlich N, Palatinszky M, Vierheilig J, Bulaev A, Kirkegaard RH, von Bergen M, Rattei T, Bendinger B, Nielsen PH, Wagner M (2015) Complete nitrification by Nitrospira bacteria. *Nature* **528**, 504–509. doi:10.1038/nature16461.

Dairy NZ (2020) "View average pasture growth data for different areas of New Zealand here." Accessed 15/06/2020, https://www.dairynz.co.nz/feed/pasture-management/pasture-growth-data

Dalley DE, Malcolm BJ, Chakwizira E, Ruiter JM de (2017) Range of quality characteristics of New Zealand forages and implications for reducing the nitrogen leaching risk from

grazing dairy cows. *New Zealand Journal of Agricultural Research* **60**, 319–332. doi:10.1080/00288233.2017.1345762.

Davidson EA (2009) The contribution of manure and fertilizer nitrogen to atmospheric nitrous oxide since 1860. *Nature Geoscience* **2**, 659–662. doi:10.1038/ngeo608.

Davidson EA, Kanter D (2014) Inventories and scenarios of nitrous oxide emissions. *Environmental Research Letters* **9**, 105012. doi:10.1088/1748-9326/9/10/105012.

De Catanzaro JB, Beauchamp EG (1985) The effect of some carbon substrates on denitrification rates and carbon utilization in soil. *Biology and Fertility of Soils* **1**, 183–187. doi:10.1007/BF00257635.

Denef K, Six J, Paustian K, Merckx R (2001) Importance of macroaggregate dynamics in controlling soil carbon stabilization: short-term effects of physical disturbance induced by dry–wet cycles. *Soil Biology and Biochemistry* **33**, 2145–2153. doi:10.1016/S0038-0717(01)00153-5.

De Klein CAM, Smith LC, Monaghan RM (2006) Restricted autumn grazing to reduce nitrous oxide emissions from dairy pastures in Southland, New Zealand. *Agriculture, Ecosystems & Environment* **112**, 192–199. doi:10.1016/j.agee.2005.08.019.

Di HJ, Cameron KC, Shen JP, Winefield CS, O'Callaghan M, Bowatte S, He JZ (2009) Nitrification driven by bacteria and not archaea in nitrogen-rich grassland soils. *Nature Geoscience* **2**, 621–624. doi:10.1038/ngeo613.

Ding F, Sun W, Huang Y (2019) Net N_2O production from soil particle size fractions and its response to changing temperature. *Science of The Total Environment* **650**, 97–104. doi:10.1016/j.scitotenv.2018.08.428.

Eagle AJ, Olander LP, Henry LR, Haugen-Kozyra K, Millar N, Robertson GP (2012) Greenhouse Gas Mitigation Potential of Agricultural Land Management in the United States: A Synthesis of the Literature. *Technical Working Group on Agricultural Greenhouse Gases (T-AGG) Report*

Elliott ET, Coleman DC (1988) Let the Soil Work for Us. *Ecological Bulletins* 23–32.

Encyclopedia Britannica (2019) nitrous oxide | Definition, Formula, Uses, Effects, & Facts. *Encyclopedia Britannica*. https://www.britannica.com/science/nitrous-oxide.

Erisman, J.W., Galloway, J., Seitzinger, S., Bleeker, A., Butterbach-Bahl, K., 2011. Reactive nitrogen in the environment and its effect on climate change. *Current Opinion in Environmental Sustainability* **3**, 281-290.

Eysholdt-Derzsó E, Sauter M (2017) Root Bending Is Antagonistically Affected by Hypoxia and ERF-Mediated Transcription via Auxin Signaling1. *Plant Physiology* **175**, 412–423. doi:10.1104/pp.17.00555.

Fangueiro D, Pereira J, Coutinho J, Moreira N, Trindade H (2008) NPK farm-gate nutrient balances in dairy farms from Northwest Portugal. *European Journal of Agronomy* **28**, 625–634. doi:10.1016/j.eja.2008.01.007.

FAO (2014) Area equipped for irrigation. http://www.fao.org/nr/water/aquastat/infographics/Irrigation_eng.pdf.

Farquharson R, Baldock J (2007) Concepts in modelling N_2O emissions from land use. *Plant and Soil* **309**, pages147–167. doi:10.1007/s11104-007-9485-0.

Flint AL, Flint LE (2002) 2.2 Particle Density. 'Methods of Soil Analysis'. *John Wiley & Sons, Ltd* 229–240. doi:10.2136/sssabookser5.4.c10.

Fowler D, Coyle M, Skiba U, Sutton MA, Cape JN, Reis S, Sheppard LJ, Jenkins A, Grizzetti B, Galloway JN, Vitousek P, Leach A, Bouwman AF, Butterbach-Bahl K, Dentener F, Stevenson D, Amann M, Voss M (2013) The global nitrogen cycle in the twenty-first century. *Philosophical Transactions of the Royal Society B: Biological Sciences* **368**. doi:10.1098/rstb.2013.0164.

Franzluebbers A, Haney RL, Honeycutt C, Schomberg H, Hons FM (2000) Flush of Carbon Dioxide Following Rewetting of Dried Soil Relates to Active Organic Pools. *Soil Science Society of America* **64**. doi:10.2136/sssaj2000.642613x.

Freydank K, Siebert S (2008) Towards mapping the extent of irrigation in the last century: time series of irrigated area per country. *University of Frankfurt (Main)*. doi:10.13140/2.1.1743.1687.

Friedl J, De Rosa D, Rowlings DW, Grace PR, Müller C, Scheer C (2018) Dissimilatory nitrate reduction to ammonium (DNRA), not denitrification dominates nitrate reduction in subtropical pasture soils upon rewetting. *Soil Biology and Biochemistry* **125**, 340–349. doi:10.1016/j.soilbio.2018.07.024.

Friedl J, Scheer C, Rowlings DW, McIntosh HV, Strazzabosco A, Warner DI, Grace PR (2016) Denitrification losses from an intensively managed sub-tropical pasture – Impact of soil moisture on the partitioning of N_2 and N_2O emissions. *Soil Biology and Biochemistry* **92**, 58–66. doi:10.1016/j.soilbio.2015.09.016.

Friedl J, Scheer C, Rowlings DW, Mumford MT, Grace PR (2017) The nitrification inhibitor DMPP (3,4-dimethylpyrazole phosphate) reduces N2 emissions from intensively managed pastures in subtropical Australia. *Soil Biology and Biochemistry* **108**, 55–64. doi:10.1016/j.soilbio.2017.01.016.

Galloway JN, Aber JD, Erisman JW, Seitzinger SP, Howarth RW, Cowling EB, Cosby BJ (2003) The Nitrogen Cascade. *BioScience* **53**, 341–356. doi:10.1641/0006-3568(2003)053[0341:TNC]2.0.CO;2.

Galloway JN, Dentener FJ, Capone DG, Boyer EW, Howarth RW, Seitzinger SP, Asner GP, Cleveland CC, Green PA, Holland EA, Karl DM, Michaels AF, Porter JH, Townsend AR, Vöosmarty CJ (2004) Nitrogen Cycles: Past, Present, and Future. *Biogeochemistry* **70**, 153–226. doi:10.1007/s10533-004-0370-0.

Garcia-Pichel F, Belnap J (1996) Microenvironments and Microscale Productivity of Cyanobacterial Desert Crusts1. *Journal of Phycology* **32**, 774–782. doi:10.1111/j.0022-3646.1996.00774.x.

Gardiner C, Clough T, Cameron K, Di H, Edwards G, de Klein C (2016) Potential for forage diet manipulation in New Zealand pasture ecosystems to mitigate ruminant urine derived N 2 O emissions: a review. *New Zealand Journal of Agricultural Research* **59**, 301–317. doi:10.1080/00288233.2016.1190386.

Ghezzehei T (2012) Soil Structure. In Handbook of Soil Sciences: Vol. 1 Properties and Processes Edition: 2nd EdPublisher: CRC Press, Boca Raton, Fla.Editors: P.M. Huang, Y. Li, M.E. Sumner. 1–17

Giles ME, Morley NJ, Baggs EM, Daniell TJ (2012) Soil nitrate reducing processes – drivers, mechanisms for spatial variation, and significance for nitrous oxide production. *Frontiers in Microbiology* **3**. doi:10.3389/fmicb.2012.00407.

Goerig M, Schulte am Esch J (2001) History of nitrous oxide—with special reference to its early use in Germany. *Best Practice & Research Clinical Anaesthesiology* **15**, 313–338. doi:10.1053/bean.2001.0165.

Grace PR, der Weerden TJ, Rowlings DW, Scheer C, Brunk C, Kiese R, Butterbach-Bahl K, Rees RM, Robertson GP, Skiba UM (2020) Global research alliance N 2 O chamber methodology guidelines: Considerations for automated flux measurement. *Journal of Environmental Quality*. doi:10.1002/jeq2.20124.

Graf DRH, Jones CM, Hallin S (2014) Intergenomic Comparisons Highlight Modularity of the Denitrification Pathway and Underpin the Importance of Community Structure for N_2O Emissions. *Plos One* **9**, e114118. doi:10.1371/journal.pone.0114118.

Groffman P, Tiedje J, Robertson GP, Christensen S (1988) Denitrification at different temporal and geographical scales: proximal and distal controls. In J.R. Wilsom, editor. Advances in nitrogen cycling in agricultural ecosystems. 174–192

Gruber N, Galloway JN (2008) An Earth-system perspective of the global nitrogen cycle. *Nature* **451**, 293–296. doi:10.1038/nature06592.

Guo X, Drury CF, Yang X, Reynolds WD, Fan R (2014) The Extent of Soil Drying and Rewetting Affects Nitrous Oxide Emissions, Denitrification, and Nitrogen Mineralization. *Soil Science Society of America Journal* **78**, 194–204. doi:10.2136/sssaj2013.06.0219.

Hallin S, Philippot L, Löffler FE, Sanford RA, Jones CM (2018) Genomics and Ecology of Novel N_2O-Reducing Microorganisms. *Trends in Microbiology* **26**, 43–55. doi:10.1016/j.tim.2017.07.003.

Hansen S, Mæhlum JE, Bakken LR (1993) N_2O and CH_4 fluxes in soil influenced by fertilization and tractor traffic. *Soil Biology and Biochemistry* **25**, 621–630. doi:10.1016/0038-0717(93)90202-M.

Hao X, Ball BC, Culley JLB, Carter MR, Parkin GW (2008) Soil density and porosity. *Soil Sampling and Methods of Analysis* 743–759.

Harrison-Kirk T, Thomas S.M, Clough T.J, Beare M.H, Van der Weerden T.J, Meenken E.D (2015) Compaction influences N_2O and N_2 emissions from 15N-labeled synthetic

urine in wet soils during successive saturation/drainage cycles. *Soil Biology and Biochemistry* **88**, 178-188. doi:10.1016/j.soilbio.2015.05.022

Hayatsu M, Tago K, Saito M (2008) Various players in the nitrogen cycle: Diversity and functions of the microorganisms involved in nitrification and denitrification. *Soil Science and Plant Nutrition* **54**, 33–45. doi:10.1111/j.1747-0765.2007.00195.x.

Haynes RJ, Williams PH (1993) Nutrient Cycling and Soil Fertility in the Grazed Pasture Ecosystem. 'Advances in Agronomy'. (Ed DL Sparks) pp. 119–199. (Academic Press) doi:10.1016/S0065-2113(08)60794-4.

Hazen A (1892) 'Some physical properties of sands and gravels: With special reference to their use in filtration.' (s.n)

Hénault C, Bizouard F, Laville P, Gabrielle B, Nicoullaud B, Germon JC, Cellier P (2005) Predicting in situ soil N_2O emission using NOE algorithm and soil database. *Global Change Biology* **11**, 115–127. doi:10.1111/j.1365-2486.2004.00879.x.

Hénault C, Bourennane H, Ayzac A, Ratié C, Saby NPA, Cohan J-P, Eglin T, Gall CL (2019) Management of soil pH promotes nitrous oxide reduction and thus mitigates soil emissions of this greenhouse gas. *Scientific Reports* **9**, 20182. doi:10.1038/s41598-019-56694-3.

Henry S, Texier S, Hallet S, Bru D, Dambreville C, Chèneby D, Bizouard F, Germon JC, Philippot L (2008) Disentangling the rhizosphere effect on nitrate reducers and denitrifiers: insight into the role of root exudates. *Environmental Microbiology* **10**, 3082–3092. doi:10.1111/j.1462-2920.2008.01599.x.

Hermansson A, Lindgren P-E (2001) Quantification of Ammonia-Oxidizing Bacteria in Arable Soil by Real-Time PCR. *Applied and Environmental Microbiology* **67**, 972–976. doi:10.1128/AEM.67.2.972-976.2001.

Hink L, Gubry-Rangin C, Nicol GW, Prosser JI (2018) The consequences of niche and physiological differentiation of archaeal and bacterial ammonia oxidisers for nitrous oxide emissions. *The ISME Journal* **12**, 1084–1093. doi:10.1038/s41396-017-0025-5.

Horn R, Van den Akker J, Van der Heiligenberg H, Arvidsson J (2000) Subsoil compaction: Distribution, processes and consequences. *Reiskirchen (Germany), Catena, 2000 Adv Geoecol* **32**.

Horton R, Ankeny MD, Allmaras RR (1994) Effects of Compaction on Soil Hydraulic Properties. 'Developments in Agricultural Engineering'. *Elsevier*, 141–165. doi:10.1016/B978-0-444-88286-8.50015-5.

Hutchinson GL, Mosier AR (1981) Improved Soil Cover Method for Field Measurement of Nitrous Oxide Fluxes. *Soil Science Society of America Journal* **45**, 311–316. doi:10.2136/sssaj1981.03615995004500020017x.

IPCC (2007) Climate Change (2007): The Physical Science Basis. Contribution of Working Group I to the Fourth Assessment Report of the Intergovernmental Panel on Climate Change.

Jamali H, Quayle W, Baldock J (2015) Reducing nitrous oxide emissions and nitrogen leaching losses from irrigated arable cropping in Australia through optimized irrigation scheduling. *Agricultural and Forest Meteorology* **208**, 32–39. doi:10.1016/j.agrformet.2015.04.010.

Jamali H, Quayle W, Scheer C, Baldock J (2016) Mitigation of N_2O emissions from surface-irrigated cropping systems using water management and the nitrification inhibitor DMPP. *Soil Research* **54**, 481. doi:10.1071/SR15315.

Jarvis SC, Scholefield D, Pain BF (1995) Nitrogen cycling in grazing systems. 'Nitrogen Fertilization and the Environment'. (Ed P Bacon) pp. 381–419. (Marcel Dekker Inc, New York) https://repository.rothamsted.ac.uk/item/84z54/nitrogen-cycling-in-grazing-systems.

Jayarathne JRRN, Chamindu Deepagoda TKK, Clough TJ, Nasvi MCM, Thomas S, Elberling B, Smits K (2020a) Gas-Diffusivity based characterization of aggregated agricultural soils. Soil Science Society of America Journal **84**, 387–398. doi:10.1002/saj2.20033.

Jayarathne JRRN, Chamindu Deepagoda TKK, Clough TJ, Thomas S, Elberling B, Smits KM (2020b) Effect of aggregate size distribution on soil moisture, soil-gas diffusivity, and N_2O emissions from a pasture soil. *Geoderma* **383**, 114737. doi:10.1016/j.geoderma.2020.114737.

Ji B, Yang K, Zhu L, Jiang Y, Wang H, Zhou J, Zhang H (2015) Aerobic denitrification: A review of important advances of the last 30 years. *Biotechnology and Bioprocess Engineering* **20**, 643–651. doi:10.1007/s12257-015-0009-0.

Kaminsky R, Trouche B, Morales SE (2017) Soil classification predicts differences in prokaryotic communities across a range of geographically distant soils once pH is accounted for. *Scientific Reports* **7**, 45369. doi:10.1038/srep45369.

Kasper M, Foldal C, Kitzler B, Haas E, Strauss P, Eder A, Zechmeister-Boltenstern S, Amon B (2019) N_2O emissions and NO_3^- leaching from two contrasting regions in Austria and influence of soil, crops and climate: a modelling approach. *Nutrient Cycling in Agroecosystems* **113**, 95–111. doi:10.1007/s10705-018-9965-z.

Kelliher FM, Cox N, van der Weerden TJ, de Klein CAM, Luo J, Cameron KC, Di HJ, Giltrap D, Rys G (2014) Statistical analysis of nitrous oxide emission factors from pastoral agriculture field trials conducted in New Zealand. *Environmental Pollution* **186**, 63–66. doi:10.1016/j.envpol.2013.11.025.

Keuter A, Hoeft I, Veldkamp E, Corre MD (2013) Nitrogen response efficiency of a managed and phytodiverse temperate grassland. *Plant and Soil* **364**, 193–206. doi:10.1007/s11104-012-1344-y.

Klefoth RR, Clough TJ, Oenema O, Van Groenigen J-W (2014) Soil Bulk Density and Moisture Content Influence Relative Gas Diffusivity and the Reduction of Nitrogen-15 Nitrous Oxide. *Vadose Zone Journal* **13**, 0. doi:10.2136/vzj2014.07.0089.

Köster JR, Cárdenas L, Senbayram M, Bol R, Well R, Butler M, Mühling KH, Dittert K (2011) Rapid shift from denitrification to nitrification in soil after biogas residue

application as indicated by nitrous oxide isotopomers. *Soil Biology and Biochemistry* **43**, 1671–1677. doi:10.1016/j.soilbio.2011.04.004.

Kozlowski JA, Stieglmeier M, Schleper C, Klotz MG, Stein LY (2016) Pathways and key intermediates required for obligate aerobic ammonia-dependent chemolithotrophy in bacteria and Thaumarchaeota. *The ISME Journal* **10**, 1836–1845. doi:10.1038/ismej.2016.2.

Kroetsch D, Wang C (2008) Particle Size Distribution. In: Carter MR, Gregorich EG (2008) Soil Sampling and Methods of Analysis (Second ed; CRC Press; Taylor & Francis Group, Boca Raton, FL)

Kuypers MMM, Marchant HK, Kartal B (2018) The microbial nitrogen-cycling network. *Nature Reviews Microbiology* **16**, 263–276. doi:10.1038/nrmicro.2018.9.

Langarica-Fuentes A, Manrubia M, Giles ME, Mitchell S, Daniell TJ (2018) Effect of model root exudate on denitrifier community dynamics and activity at different water-filled pore space levels in a fertilised soil. *Soil Biology and Biochemistry* **120**, 70–79. doi:10.1016/j.soilbio.2018.01.034.

Lambers H, Oliveira RS (2019) 'Plant Physiological Ecology.' (Springer International Publishing: Cham) doi:10.1007/978-3-030-29639-1.

Letey J, Valoras N, Hadas A, Focht DD (1980) Effect of Air-filled Porosity, Nitrate Concentration, and Time on the Ratio of N_2O/N_2 Evolution During Denitrification. *Journal of Environmental Quality* **9**, 227–231. doi:10.2134/jeq1980.00472425000900020013x.

Lew V, McKay E, Maze M (2018) Past, present, and future of nitrous oxide. *British Medical Bulletin* **125**, 103–119. doi:10.1093/bmb/ldx050.

Lilburne L, Hewitt A, Trevor W (2012) Soil and informatics science combine to develop S-map: A new generation soil information system for New Zealand. *Geoderma* **170**, 232–238. doi:10.1016/j.geoderma.2011.11.012.

Linn DM, Doran JW (1984) Effect of Water-Filled Pore Space on Carbon Dioxide and Nitrous Oxide Production in Tilled and Nontilled Soils. *Soil Science Society of America Journal* **48**, 1267–1272. doi:10.2136/sssaj1984.03615995004800060013x.

Liu G (2012) 'Greenhouse Gases: Emission, Measurement and Management.' (BoD – Books on Demand)

Liu C, Wang K, Meng S, Zheng X, Zhou Z, Han S, Chen D, Yang Z (2011) Effects of irrigation, fertilization and crop straw management on nitrous oxide and nitric oxide emissions from a wheat–maize rotation field in northern China. *Agriculture, Ecosystems & Environment* **140**, 226–233. doi:10.1016/j.agee.2010.12.009.

MacFarling Meure C, Etheridge D, Trudinger C, Steele P, Langenfelds R, Ommen T van, Smith A, Elkins J (2006) Law Dome CO2, CH4 and N_2O ice core records extended to 2000 years BP. *Geophysical Research Letters* **33**. doi:10.1029/2006GL026152.

Maeda K, Spor A, Edel-Hermann V, Heraud C, Breuil M-C, Bizouard F, Toyoda S, Yoshida N, Steinberg C, Philippot L (2015) N_2O production, a widespread trait in fungi. *Scientific Reports* **5**, 96-97. doi:10.1038/srep09697.

Malcolm BJ, Ruiter JM de, Dalley DE, Carrick S, Waugh D, Arnold NP, Dellow SJ, Beare MH, Johnstone PR, Wohlers M, Brown H, Welten B, Horrocks AJ (2020) Catch crops and feeding strategy can reduce the risk of nitrogen leaching in late lactation fodder beet systems. *New Zealand Journal of Agricultural Research* **63**, 44–64. doi:10.1080/00288233.2019.1704422.

Marchant HK, Holtappels M, Lavik G, Ahmerkamp S, Winter C, Kuypers MMM (2016) Coupled nitrification–denitrification leads to extensive N loss in subtidal permeable sediments. *Limnology and Oceanography* **61**, 1033–1048. doi:10.1002/lno.10271.

Marshall TJ (1959) The Diffusion of Gases Through Porous Media. *Journal of Soil Science* **10**, 79–82. doi:10.1111/j.1365-2389.1959.tb00667.x.

Marshall TJ, Holmes JW, Rose CW (1996) 'Soil Physics.' (Cambridge University Press: Cambridge) doi:10.1017/CBO9781139170673.

Mathieu O, Lévêque J, Hénault C, Ambus P, Milloux M-J, Andreux F (2007) Influence of 15N enrichment on the net isotopic fractionation factor during the reduction of nitrate to nitrous oxide in soil. *Rapid Communications in Mass Spectrometry* **21**, 1447–1451. doi:10.1002/rcm.2979.

McAllister CH, Beatty PH, Good AG (2012) Engineering nitrogen use efficient crop plants: the current status. *Plant Biotechnology Journal* **10**, 1011–1025. doi:10.1111/j.1467-7652.2012.00700.x.

McLaren RG, Cameron KC (1996) 'Soil Science: Sustainable Production and Environmental Protection.' (Oxford University Press: Oxford, New York)

MetService Lincoln Weather Forecast and Observations - MetService New Zealand. *MetService*. https://www.metservice.com/rural/regions/christchurch/locations/lincoln.

Minasny B, McBratney AB (2018) Limited effect of organic matter on soil available water capacity. *European Journal of Soil Science* **69**, 39–47. doi:10.1111/ejss.12475.

Ministry for the Environment (2018) New Zealand's greenhouse gas inventory 1990-2016. https://www.mfe.govt.nz/sites/default/files/media/Climate%20Change/final_greenhouse_gas_inventory_snapshot.pdf.

Ministry of the Environment New Zealand (2019) New Zealand greenhouse gas inventory 2019. https://www.mfe.govt.nz/sites/default/files/media/Climate%20Change/nz-greenhouse-gas-inventory-2019.pdf.

Misselbrook TH, Cardenas LM, Camp V, Thorman RE, Williams JR, Rollett AJ, Chambers BJ (2014) An assessment of nitrification inhibitors to reduce nitrous oxide emissions from UK agriculture. *Environmental Research Letters* **9**, 115006. doi:10.1088/1748-9326/9/11/115006.

Moir J, Cameron K, Di H (2016) Potential Pasture Nitrogen Concentrations and Uptake from Autumn or Spring Applied Cow Urine and DCD under Field Conditions. *Plants* **5**,. doi:10.3390/plants5020026.

Moir JL, Cameron KC, Di HJ, Fertsak U (2011) The spatial coverage of dairy cattle urine patches in an intensively grazed pasture system. *The Journal of Agricultural Science* **149**, 473–485. doi:10.1017/S0021859610001012.

Moldrup P, Chamindu Deepagoda TKK, Hamamoto S, Komatsu T, Kawamoto K, Rolston DE, Jonge LW de (2013) Structure-Dependent Water-Induced Linear Reduction Model for Predicting Gas Diffusivity and Tortuosity in Repacked and Intact Soil. *Vadose Zone Journal* **12**. doi:10.2136/vzj2013.01.0026.

Moldrup P, Olesen T, Schjønning P, Yamaguchi T, Rolston D (2000) Predicting the Gas Diffusion Coefficient in Undisturbed Soil from Soil Water Characteristics. *Soil Science Society of America Journal - SSSAJ* **64**. doi:10.2136/sssaj2000.64194x.

Moser G, Gorenflo A, Brenzinger K, Keidel L, Braker G, Marhan S, Clough TJ, Müller C (2018) Explaining the doubling of N_2O emissions under elevated CO2 in the Giessen FACE via in-field 15N tracing. *Global Change Biology* **24**, 3897–3910. doi:10.1111/gcb.14136.

Mullan B, Porteous A, Wratt D, Hollis M (2005) Changes in drought risk with climate change. NIWA Client Report: WLG2005-23, **69**.

Muller C, Laughlin RJ, Spott O, Rütting T (2014) Quantification of N_2O emission pathways via a 15N tracing model. *Soil Biology and Biochemistry* **72**, 44–54. doi:10.1016/j.soilbio.2014.01.013.

Mulvaney RL, Boast CW (1986) Equations for determination of nitrogen-15 labeled dinitrogen and nitrous oxide by mass spectrometry. *Soil Science Society of America Journal* **50**, 360–363. doi:10.2136/sssaj1986.03615995005000020021x.

Mumford M, Rowlings D, Scheer C, De Rosa D, Grace P (2019) Effect of irrigation scheduling on nitrous oxide emissions in intensively managed pastures. *Agriculture, Ecosystems and Environment* **272**, 126–134. doi:10.1016/j.agee.2018.11.011.

Myhre G, Shindell D, Bréon F-M, Collins W, Fuglestvedt J, Huang J, Koch D, Lamarque J-F, Lee D, Mendoza B, Nakajima T, Robock A, Stephens G, Takemura T, Zhang H (2013) Anthropogenic and Natural Radiative Forcing. Supplementary Material. In: Climate Change 2013: The Physical Science Basis. Contribution of Working Group

New Zealand, Statistics New Zealand (2010) 'New Zealand official yearbook 2010: Te Pukapuka Houanga Whaimana o Aotearoa.' (David Bateman: Auckland, N.Z.)

Niklaus PA, Wardle DA, Tate KR (2006) Effects of Plant Species Diversity and Composition on Nitrogen Cycling and the Trace Gas Balance of Soils. Plant and Soil 282, 83–98. doi:10.1007/s11104-005-5230-8.

NOAA (2020) Global monitoring laboratory, Earth system research laboratories, nitrous oxide (N_2O) combine data set. https://www.esrl.noaa.gov/gmd/ccgg/trends_n2o/.

Noor MA (2017) Nitrogen management and regulation for optimum NUE in maize – A mini review (MT Moral, Ed.). *Cogent Food & Agriculture* **3**, 1348214. doi:10.1080/23311932.2017.1348214.

Norton J, Ouyang Y (2019) Controls and Adaptive Management of Nitrification in Agricultural Soils. *Frontiers in Microbiology* **10**. doi:10.3389/fmicb.2019.01931.

Okano Y, Hristova KR, Leutenegger CM, Jackson LE, Denison RF, Gebreyesus B, Lebauer D, Scow KM (2004) Application of real-time PCR to study effects of ammonium on population size of ammonia-oxidizing bacteria in soil. *Applied and Environmental Microbiology* **70**, 1008–1016. doi:10.1128/aem.70.2.1008-1016.2004.

Owens J, Clough TJ, Laubach J, Hunt JE, Venterea RT (2017) Nitrous Oxide Fluxes and Soil Oxygen Dynamics of Soil Treated with Cow Urine. *Soil Science Society of America Journal* **81**, 289–298. doi:10.2136/sssaj2016.09.0277.

Owens J, Clough TJ, Laubach J, Hunt JE, Venterea RT, Phillips RL (2016) Nitrous Oxide Fluxes, Soil Oxygen, and Denitrification Potential of Urine- and Non-Urine-Treated Soil under Different Irrigation Frequencies. *Journal of Environmental Quality* **45**, 1169–1177. doi:10.2134/jeq2015.10.0516.

Pan Y, Ni B-J, Yuan Z (2013) Modeling Electron Competition among Nitrogen Oxides Reduction and N_2O Accumulation in Denitrification. *Environmental Science & Technology* **47**, 11083–11091. doi:10.1021/es402348n.

Pandey A, Suter H, He J-Z, Hu H-W, Chen D (2019) Dissimilatory nitrate reduction to ammonium dominates nitrate reduction in long-term low nitrogen fertilized rice paddies. *Soil Biology and Biochemistry* **131**, 149–156. doi:10.1016/j.soilbio.2019.01.007.

Parfitt RL, Schipper LA, Baisden WT, Elliott AH (2006) Nitrogen Inputs and Outputs for New Zealand in 2001 at National and Regional Scales. *Biogeochemistry* **80**, 71–88.

Parton WJ, Holland E, Del Grosso S, Hartman M, Martin R, Mosier AR, Ojima D, Schimel D (2001) Generalized model for NO_x and N_2O emissions from soils. Journal of Geophysical Research: Atmospheres 106, 17403–17419.

Pelster DE, Chantigny MH, Rochette P, Angers DA, Rieux C, Vanasse A (2012) Nitrous oxide emissions respond differently to mineral and organic nitrogen sources in contrasting soil types. *Journal of Environmental Quality* **41**, 427–435. doi:10.2134/jeq2011.0261.

Perchlik M, Tegeder M (2017) Improving Plant Nitrogen Use Efficiency through Alteration of Amino Acid Transport Processes. *Plant Physiology* **175**, 235–247. doi:10.1104/pp.17.00608.

Petersen SO, Ambus P, Elsgaard L, Schjønning P, Olesen JE (2013) Long-term effects of cropping system on N_2O emission potential. *Soil Biology and Biochemistry* **57**, 706–712. doi:10.1016/j.soilbio.2012.08.032.

Petersen SO, Schjønning P, Thomsen IK, Christensen BT (2008) Nitrous oxide evolution from structurally intact soil as influenced by tillage and soil water content. *Soil Biology and Biochemistry* **40**, 967–977. doi:10.1016/j.soilbio.2007.11.017.

Petersen SO, Stamatiadis S, Christofides C (2004) Short-term nitrous oxide emissions from pasture soil as influenced by urea level and soil nitrate. *Plant and Soil* **267**, 117-127 doi:10.1007/s11104-005-4688-8

Pierer M, Winiwarter W, Leach AM, Galloway JN (2014) The nitrogen footprint of food products and general consumption patterns in Austria. *Food Policy* **49**, 128–136. doi:10.1016/j.foodpol.2014.07.004.

Pilegaard K (2013) Processes regulating nitric oxide emissions from soils. *Philosophical Transactions of the Royal Society B: Biological Sciences* **368**. doi:10.1098/rstb.2013.0126.

Portmann RW, Daniel JS, Ravishankara AR (2012) Stratospheric ozone depletion due to nitrous oxide: influences of other gases. Philosophical Transactions of the Royal Society B: Biological Sciences 367, 1256–1264. doi:10.1098/rstb.2011.0377.

Powell JM, Gourley CJP, Rotz CA, Weaver DM (2010) Nitrogen use efficiency: A potential performance indicator and policy tool for dairy farms. *Environmental Science & Policy* **13**, 217–228. doi:10.1016/j.envsci.2010.03.007.

Prather MJ, Holmes CD, Hsu J (2012) Reactive greenhouse gas scenarios: Systematic exploration of uncertainties and the role of atmospheric chemistry. *Geophysical Research Letters* **39**. doi:10.1029/2012GL051440.

Prosser JI, Hink L, Gubry-Rangin C, Nicol GW (2019) Nitrous oxide production by ammonia oxidizers: Physiological diversity, niche differentiation and potential mitigation strategies. *Global Change Biology* **26**, 103–118. doi:10.1111/gcb.14877.

Qin SP, Ding K, Clough TJ, Hu C, Luo J (2017) Temporal in situ dynamics of N_2O reductase activity as affected by nitrogen fertilization and implications for the $N_2O/(N_2O+N_2)$ product ratio and N_2O mitigation. *Biology and Fertility of Soils* **53**, 723–727. doi:10.1007/s00374-017-1232-y.

Randhawa G, Bodenham A (2016) The increasing recreational use of nitrous oxide: history revisited. *British Journal of Anaesthesia* **116**, 321–324. doi:10.1093/bja/aev297.

Ravishankara AR, Daniel JS, Portmann RW (2009) Nitrous Oxide (N_2O): The Dominant Ozone-Depleting Substance Emitted in the 21st Century. *Science* **326**, 123–125. doi:10.1126/science.1176985.

Rawls WJ, Pachepsky YA, Ritchie JC, Sobecki TM, Bloodworth H (2003) Effect of soil organic carbon on soil water retention. *Geoderma* **116**, 61–76. doi:10.1016/S0016-7061(03)00094-6.

Resurreccion AC, Komatsu T, Kawamoto K, Oda M, Yoshikawa S, Moldrup P (2008) Linear model to predict soil-gas diffusivity from two soil-water retention points in unsaturated volcanic ash soils. *Soils and Foundations* **48**, 397–406. doi:10.3208/sandf.48.397.

Revell LE, Tummon F, Salawitch RJ, Stenke A, Peter T (2015) The changing ozone depletion potential of N_2O in a future climate. *Geophysical Research Letters* **42**, 47-55. doi:10.1002/2015GL065702.

Ritchie H, Roser M (2017) CO_2 and Greenhouse Gas Emissions. *Our World in Data*. https://ourworldindata.org/co2-and-other-greenhouse-gas-emissions.

Rolston DE, Moldrup P (2002) 4.3 Gas Diffusivity. *Methods of Soil Analysis: Part 4 Physical Methods* 1113–1139.

Rolston, DE (1986) Gas diffusivity. In: Klute, A. (Ed.), Methods of soil analysis, Part 1. Physical and Mineralogical Methods - Agrononomy Monograph no.9 (2nd Edition). Agronomy society of America, Madison, WI, pp. 1089-1102.

Roos D (2015) How Nitrous Oxide Works. *HowStuffWorks*. https://science.howstuffworks.com/nitrous-oxide.htm.

Rousset C, Clough TJ, Grace PR, Rowlings DW, Scheer C (2020) Soil type, bulk density and drainage effects on relative gas diffusivity and N_2O emissions. *Soil Research*. doi:10.1071/SR20161.

RStudio Team (2016) RStudio Team (2016). RStudio: Integrated Development for R. http://www.rstudio.com/.

Ruser R, Schulz R (2015) The effect of nitrification inhibitors on the nitrous oxide (N_2O) release from agricultural soils—a review. *Journal of Plant Nutrition and Soil Science* **178**. doi:10.1002/jpln.201400251.

Ruser R, Sehy U, Weber A, Gutser R, Munch JC (2008) Chapter 2.2 - Main Driving Variables and Effect of Soil Management on Climate or Ecosystem-Relevant Trace Gas Fluxes from Fields of the FAM. 'Perspectives for Agroecosystem Management'. (Eds P Schröder, J Pfadenhauer, JC Munch) pp. 79–120. (Elsevier: San Diego) doi:10.1016/B978-044451905-4.50006-4.

Rutting T, Boeckx P, Müller C, Klemedtsson L (2011) Assessment of the importance of dissimilatory nitrate reduction to ammonium for the terrestrial nitrogen cycle. *Biogeosciences* **8**, 1779–1791. doi:10.5194/bg-8-1779-2011.

Rutting T, Clough TJ, Müller C, Lieffering M, Newton PCD (2010) Ten years of elevated atmospheric carbon dioxide alters soil nitrogen transformations in a sheep-grazed pasture. *Global Change Biology* **16**, 2530–2542. doi:10.1111/j.1365-2486.2009.02089.x.

Ryden JC (1983) Denitrification loss from a grassland soil in the field receiving different rates of nitrogen as ammonium nitrate. *Journal of Soil Science* **34**, 355–365. doi:10.1111/j.1365-2389.1983.tb01041.x.

Saggar S, Giltrap DL, Davison R, Gibson R, de Klein CA, Rollo M, Ettema P, Rys G (2015) Estimating direct N_2O emissions from sheep, beef, and deer grazed pastures in New Zealand hill country: accounting for the effect of land slope on the N_2O emission factors from urine and dung. *Agriculture, Ecosystems & Environment* **205**, 70–78. doi:10.1016/j.agee.2015.03.005.

Sahrawat KL (2008) Factors Affecting Nitrification in Soils. *Communications in Soil Science and Plant Analysis* **39**, 1436–1446. doi:10.1080/00103620802004235.

Samad MS, Bakken LR, Nadeem S, Clough TJ, De Klein CAM, Richards KG, Lanigan GJ, Morales SE (2016) High-Resolution Denitrification Kinetics in Pasture Soils Link N_2O Emissions to pH, and Denitrification to C Mineralization. *Plos One* 11. doi:10.1371/journal.pone.0151713

Scheer C, Grosso SJD, Parton WJ, Rowlings DW, Grace PR (2014) Modeling nitrous oxide emissions from irrigated agriculture: testing DayCent with high-frequency measurements. *Ecological Applications* **24**, 528–538. doi:10.1890/13-0570.1.

Scheer C, Wassman R, Kienzler K, Ibragimov N, Lamers J, Martius C (2008) Methane and nitrous oxide fuxes in annual and perennial land-use systems of the irrigated areas in the Aral Sea Basin. *Global Change Biology* **14**, 2454–2468. doi:10.1111/j.1365-2486.2008.01631.x.

Schimel JP (2018) Life in Dry Soils: Effects of Drought on Soil Microbial Communities and Processes. *Annual Review of Ecology, Evolution, and Systematics* **49**, 409–432. doi:10.1146/annurev-ecolsys-110617-062614.

Schimel JP, Bennett J (2004) Nitrogen Mineralization: Challenges of a Changing Paradigm. *Ecology* **85**, 591–602. doi:10.1890/03-8002.

Schindlbacher A, Zechmeister-Boltenstern S, Butterbach-Bahl K (2004) Effects of soil moisture and temperature on NO, NO2, and N_2O emissions from European forest soils. *Journal of Geophysical Research* **109**. doi:10.1029/2004JD004590.

Schjønning P, Thomsen IK, Moldrup P, Christensen BT (2003) Linking Soil Microbial Activity to Water- and Air-Phase Contents and Diffusivities. *Soil Science Society of America Journal* **67**, 156–165. doi:10.2136/sssaj2003.1560.

Selbie DR, Buckthought LE, Shepherd MA (2015) Chapter Four - The Challenge of the Urine Patch for Managing Nitrogen in Grazed Pasture Systems. 'Advances in Agronomy'. (Ed DL Sparks) 229–292. doi:10.1016/bs.agron.2014.09.004.

Senbayram M, Chen R, Budai A, Bakken L, Dittert K (2012) N_2O emission and the $N_2O/(N_2O+N2)$ product ratio of denitrification as controlled by available carbon substrates and nitrate concentrations. *Agriculture, Ecosystems & Environment* **147**, 4–12. doi:10.1016/j.agee.2011.06.022.

Senbayram M, Chen R, Mühling KH, Dittert K (2009) Contribution of nitrification and denitrification to nitrous oxide emissions from soils after application of biogas waste and other fertilizers. *Rapid Communications in Mass Spectrometry* **23**, 2489–2498. doi:10.1002/rcm.4067.

Sexstone AJ, Revsbech NP, Parkin TB, Tiedje JM (1985) Direct Measurement of Oxygen Profiles and Denitrification Rates in Soil Aggregates. *Soil Science Society of America Journal* **49**, 645–651. doi:10.2136/sssaj1985.03615995004900030024x.

Shcherbak I, Millar N, Robertson GP (2014) Global metaanalysis of the nonlinear response of soil nitrous oxide (N_2O) emissions to fertilizer nitrogen. *Proceedings of the National Academy of Sciences* **111**, 9199–9204. doi:10.1073/pnas.1322434111.

Signor D, Cerri CEP (2013) Nitrous oxide emissions in agricultural soils: a review. *Pesquisa Agropecuária Tropical* **43**, 322–338. doi:10.1590/S1983-40632013000300014.

Sigurdarson JJ, Svane S, Karring H (2018) The molecular processes of urea hydrolysis in relation to ammonia emissions from agriculture. *Reviews in Environmental Science and Bio/Technology* **17**, 241–258. doi:10.1007/s11157-018-9466-1.

Singleton PL, Boyes M, Addison B (2000) Effect of treading by dairy cattle on topsoil physical conditions for six contrasting soil types in Waikato and Northland, New Zealand, with implications for monitoring. *New Zealand Journal of Agricultural Research* **43**, 559–567. doi:10.1080/00288233.2000.9513453.

Sitaula BK, Hansen S, Sitaula JIB, Bakken LR (2000) Effects of soil compaction on N_2O emission in agricultural soil. *Chemosphere - Global Change Science* **2**, 367–371. doi:10.1016/S1465-9972(00)00040-4.

Skiba M, George T, Baggs L, Daniell T (2011) Plant influence on nitrification. *Biochemical Society transactions* **39**, 275–8. doi:10.1042/BST0390275.

Stein LY (2019) Insights into the physiology of ammonia-oxidizing microorganisms. *Current Opinion in Chemical Biology* **49**, 9–15. doi:10.1016/j.cbpa.2018.09.003.

Stein LY, Klotz MG (2016) The nitrogen cycle. *Current biology: CB* **26**, R94-98. doi:10.1016/j.cub.2015.12.021.

Stepniewski W (1981) Oxygen diffusion and strength as related to soil compaction. II. Oxygen diffusion coefficient. *Polish journal of soil science*. https://agris.fao.org/agris-search/search.do?recordID=US201302172215.

Stępniewski W, Przywara G (1992) The influence of soil oxygen availability on yield and nutrient uptake (N, P, K, Ca, Mg, Na) by winter rye (Secale cereale). *Plant and Soil* **143**, 267–274. doi:10.1007/BF00007882.

Stevens RJ, Laughlin RJ (2001) Lowering the detection limit for dinitrogen using the enrichment of nitrous oxide. *Soil Biology and Biochemistry* **33**, 1287–1289. doi:10.1016/S0038-0717(01)00036-0.

Talbot WD, Cameron KC, Di HJ, Malcolm BJ, Whitehead D (2019) Effects of adding readily available carbon to soil on nitrogen losses from cattle urine patches. *New Zealand Journal of Agricultural Research* **63**, 529–550. doi:10.1080/00288233.2019.1581237.

Taylor SA (1950) Oxygen Diffusion in Porous Media as a Measure of Soil Aeration. *Soil Science Society of America Journal* **14**, 55–61. doi:10.2136/sssaj1950.036159950014000C0013x.

Thion CE, Poirel JD, Cornulier T, De Vries FT, Bardgett RD, Prosser JI (2016) Plant nitrogen-use strategy as a driver of rhizosphere archaeal and bacterial ammonia oxidiser abundance. *FEMS microbiology ecology* **92**. doi:10.1093/femsec/fiw091.

Thomas SM, Fraser PM, Hu W, Clough TJ, van der Klei G, Wilson S, Tregurtha R, Baird D (2019) Tillage, compaction and wetting effects on NO_3^-, N_2O and N_2 losses. *Soil Research* **57**, 670. doi:10.1071/SR18261.

Thompson RL, Lassaletta L, Patra PK, Wilson C, Wells KC, Gressent A, Koffi EN, Chipperfield MP, Winiwarter W, Davidson EA, Tian H, Canadell JG (2019) Acceleration of global N 2 O emissions seen from two decades of atmospheric inversion. *Nature Climate Change* **9**, 993–998. doi:10.1038/s41558-019-0613-7.

Thomson AJ, Giannopoulos G, Pretty J, Baggs EM, Richardson DJ (2012) Biological sources and sinks of nitrous oxide and strategies to mitigate emissions. *Philosophical Transactions of the Royal Society B: Biological Sciences* **367**, 1157–1168. doi:10.1098/rstb.2011.0415.

Thorbjørn A, Moldrup P, Blendstrup H, Komatsu T, Rolston DE (2008) A Gas Diffusivity Model Based on Air-, Solid-, and Water-Phase Resistance in Variably Saturated Soil. *Vadose Zone Journal* **7**, 1276–1286. doi:10.2136/vzj2008.0023.

Tian H, Yang J, Lu C, Xu R, Canadell JG, Jackson RB, Arneth A, Chang J, Chen G, Ciais P, Gerber S, Ito A, Huang Y, Joos F, Lienert S, Messina P, Olin S, Pan S, Peng C, Saikawa E, Thompson RL, Vuichard N, Winiwarter W, Zaehle S, Zhang B, Zhang K, Zhu Q (2018) The Global N_2O Model Intercomparison Project. *Bulletin of the American Meteorological Society* **99**, 1231–1251. doi:10.1175/BAMS-D-17-0212.1.

Tobias CR, Macko SA, Anderson IC, Canuel EA, Harvey JW (2001) Tracking the fate of a high concentration groundwater nitrate plume through a fringing marsh: A combined groundwater tracer and in situ isotope enrichment study. *Limnology and Oceanography* **46**, 1977–1989. doi:10.4319/lo.2001.46.8.1977.

Trost B, Prochnow A, Drastig K, Meyer-Aurich A, Ellmer F, Baumecker M (2013) Irrigation, soil organic carbon and N_2O emissions. A review. *Agronomy for Sustainable Development* **33**, 733–749. doi:10.1007/s13593-013-0134-0.

UNESCO (2017) Fact2: Agricultural use. http://www.unesco.org/new/en/natural-sciences/environment/water/wwap/facts-and-figures/all-facts-wwdr3/fact2-agricultural-use/.

UN-Water & FAO (2007), Coping with Water Scarcity. Challenge of the Twenty-first Century, http://www.fao.org/nr/water/docs/escarcity.pdf

US EPA O (2015) Overview of Greenhouse Gases. *US EPA*. https://www.epa.gov/ghgemissions/overview-greenhouse-gases.

Ussiri DAN, Lal R (2013) Soil Emission of Nitrous Oxide and its Mitigation. *Springer* doi:10.1007/978-94-007-5364-8.

Van Cleemput O (1998) Subsoils: chemo- and biological denitrification, N_2O and N_2 emissions. *Nutrient Cycling in Agroecosystems* **52**, 187-194. doi:10.1023/A:1009728125678.

Van Cleemput O, Samater AH (1995) Nitrite in soils: accumulation and role in the formation of gaseous N compounds. *Fertilizer research* **45**, 81–89. doi:10.1007/BF00749884.

Van den Berg EM, Boleij M, Kuenen JG, Kleerebezem R, Van Loosdrecht MCM (2016) DNRA and Denitrification Coexist over a Broad Range of Acetate/N-NO_3^- Ratios, in a Chemostat Enrichment Culture. *Frontiers in Microbiology* **7**. doi:10.3389/fmicb.2016.01842.

Van der Weerden TJ, Kelliher F, De Klein C (2012) Influence of pore size distribution and soil water content on nitrous oxide emissions. *Soil Research* **50**, 125–135. doi:10.1071/SR11112.

Van der Weerden TJ, Manderson A, Kelliher FM, de Klein CAM (2014) Spatial and temporal nitrous oxide emissions from dairy cattle urine deposited onto grazed pastures across New Zealand based on soil water balance modelling. *Agriculture, Ecosystems & Environment* **189**, 92–100. doi:10.1016/j.agee.2014.03.018.

Van der Weerden TJ, Noble AN, Luo J, de Klein CAM, Saggar S, Giltrap D, Gibbs J, Rys G (2020) Meta-analysis of New Zealand's nitrous oxide emission factors for ruminant excreta supports disaggregation based on excreta form, livestock type and slope class. *Science of The Total Environment* **732**, 139235. doi:10.1016/j.scitotenv.2020.139235.

Van der Weerden TJ, Styles TM, Rutherford AJ, Klein CAM de, Dynes R (2017) Nitrous oxide emissions from cattle urine deposited onto soil supporting a winter forage kale crop. *New Zealand Journal of Agricultural Research* **60**, 119–130. doi:10.1080/00288233.2016.1273838.

Van Kessel MAHJ, Speth DR, Albertsen M, Nielsen PH, Op den Camp HJM, Kartal B, Jetten MSM, Lücker S (2015) Complete nitrification by a single microorganism. *Nature* **528**, 555–559. doi:10.1038/nature16459.

Venterea RT, Clough TJ, Coulter JA, Breuillin-Sessoms F, Wang P, Sadowsky MJ (2015) Ammonium sorption and ammonia inhibition of nitrite-oxidizing bacteria explain contrasting soil N 2 O production. *Scientific Reports* **5**, 12153. doi:10.1038/srep12153.

Venterea RT, Coulter JA, Clough TJ (2020) Nitrite accumulation and nitrogen gas production increase with decreasing temperature in urea-amended soils: Experiments and modeling. *Soil Biology and Biochemistry* **142**, 107727. doi:10.1016/j.soilbio.2020.107727.

Vogeler I, Cichota R, Thomsen IK, Bruun S, Jensen LS, Pullens JWM (2019) Estimating nitrogen release from Brassicacatch crop residues—Comparison of different approaches within the APSIM model. *Soil and Tillage Research* **195**, 104358. doi:10.1016/j.still.2019.104358.

Waddell JT, Gupta SC, Moncrief JF, Rosen CJ, Steele DD (2000) Irrigation- and Nitrogen-Management Impacts on Nitrate Leaching under Potato. *Journal of Environmental Quality* **29**, 251–261. doi:10.2134/jeq2000.00472425002900010032x.

Wang M, Hu R, Ruser R, Schmidt C, Kappler A (2020) Role of Chemodenitrification for N_2O Emissions from Nitrate Reduction in Rice Paddy Soils. *ACS Earth and Space Chemistry* **4**, 122–132. doi:10.1021/acsearthspacechem.9b00296.

Weier KL, Doran JW, Power JF, Walters DT (1993) Denitrification and the Dinitrogen/Nitrous Oxide Ratio as Affected by Soil Water, Available Carbon, and Nitrate. *Soil Science Society of America Journal* **57**, 66–72. doi:10.2136/sssaj1993.03615995005700010013x.

Wrage N, Velthof GL, van Beusichem ML, Oenema O (2001) Role of nitrifier denitrification in the production of nitrous oxide. *Soil Biology and Biochemistry* **33**, 1723–1732. doi:10.1016/S0038-0717(01)00096-7.

Wrage-Mönnig N, Horn MA, Well R, Müller C, Velthof G, Oenema O (2018) The role of nitrifier denitrification in the production of nitrous oxide revisited. *Soil Biology and Biochemistry* **123**, A3–A16. doi:10.1016/j.soilbio.2018.03.020.

Wu L, Rees RM, Tarsitano D, Zhang X, Jones SK, Whitmore AP (2015) Simulation of nitrous oxide emissions at field scale using the SPACSYS model. *The Science of the Total Environment* **530**, 76–86. doi:10.1016/j.scitotenv.2015.05.064.

Yin SX, Chen D, Chen LM, Edis R (2002) Dissimilatory nitrate reduction to ammonium and responsible microorganisms in two Chinese and Australian paddy soils. *Soil Biology and Biochemistry* **34**, 1131–1137. doi:10.1016/S0038-0717(02)00049-4.

Zaman M, Nguyen ML, Matheson F, Blennerhassett JD, Quin BF (2007) Can soil amendments (zeolite or lime) shift the balance between nitrous oxide and dinitrogen emissions from pasture and wetland soils receiving urine or urea-N? *Soil Research* **45**, 543–553. doi:10.1071/SR07034.

Zheng J, Doskey P (2015) Modeling Nitrous Oxide Production and Reduction in Soil Through Explicit Representation of Denitrification Enzyme Kinetics. *Environmental science & technology* **49**. doi:10.1021/es504513v.

Zhu X, Burger M, Doane TA, Horwath WR (2013) Ammonia oxidation pathways and nitrifier denitrification are significant sources of N_2O and NO under low oxygen availability. *Proceedings of the National Academy of Sciences* **110**, 6328–6333. doi:10.1073/pnas.1219993110.

Zhu-Barker X, Cavazos A, Ostrom N, Horwath W, Glass J (2015) The importance of abiotic reactions for nitrous oxide production. *Biogeochemistry* **126**. doi:10.1007/s10533-015-0166-4.

Zumft WG (1997) Cell biology and molecular basis of denitrification. *Microbiology and Molecular Biology Reviews* **61**, 533–616.